

INFORMATION TO USERS

This manuscript has been reproduced from the microfilm master. UMI films the text directly from the original or copy submitted. Thus, some thesis and dissertation copies are in typewriter face, while others may be from any type of computer printer.

The quality of this reproduction is dependent upon the quality of the copy submitted. Broken or indistinct print, colored or poor quality illustrations and photographs, print bleedthrough, substandard margins, and improper alignment can adversely affect reproduction.

In the unlikely event that the author did not send UMI a complete manuscript and there are missing pages, these will be noted. Also, if unauthorized copyright material had to be removed, a note will indicate the deletion.

Oversize materials (e.g., maps, drawings, charts) are reproduced by sectioning the original, beginning at the upper left-hand corner and continuing from left to right in equal sections with small overlaps.

Photographs included in the original manuscript have been reproduced xerographically in this copy. Higher quality 6" x 9" black and white photographic prints are available for any photographs or illustrations appearing in this copy for an additional charge. Contact UMI directly to order.

**Bell & Howell Information and Learning
300 North Zeeb Road, Ann Arbor, MI 48106-1346 USA
800-521-0600**

UMI[®]

**Patterns, Mechanics and Geomorphic Effects of
Wood Debris Accumulations in a Forest River System**

by

Timothy Best Abbe

Doctor of Philosophy

University of Washington

2000

Department of Geological Sciences

UMI Number: 9964236

Copyright 2000 by
Abbe, Timothy Best

All rights reserved.

UMI[®]

UMI Microform 9964236

Copyright 2000 by Bell & Howell Information and Learning Company.

All rights reserved. This microform edition is protected against
unauthorized copying under Title 17, United States Code.

Bell & Howell Information and Learning Company
300 North Zeeb Road
P.O. Box 1346
Ann Arbor, MI 48106-1346

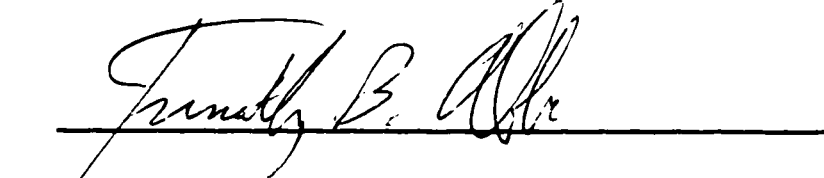
© Copyright 2000

Timothy Abbe

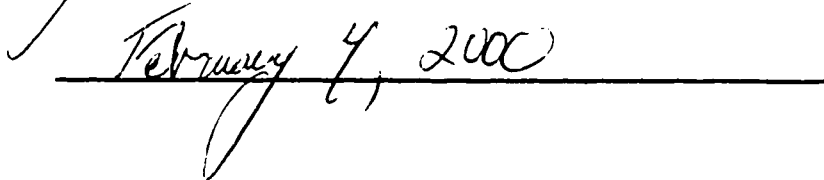
Doctoral Dissertation

In presenting this dissertation in partial fulfillment of the requirements for the Doctoral degree at the University of Washington, I agree that the Library shall make its copies freely available for inspection. I further agree that extensive copying of the dissertation is allowable only for scholarly purposes, consistent with "fair use" as prescribed in the U.S. Copyright Law. Requests for copying or reproduction of this dissertation may be referred to Bell and Howell Information and Learning, 300 North Zeeb Road, P.O. Box 1346, Ann Arbor, MI 48106-1346, to whom the author has granted "the right to reproduce and sell (a) copies of the manuscript and microform and/or (b) printed copies of the manuscript made from microform."

Signature

A handwritten signature in cursive script, appearing to read "Timothy B. Allen", written over a horizontal line.

Date

A handwritten date "February 4, 2000" written in cursive script over a horizontal line.


University of Washington
Graduate School

This is to certify that I have examined this copy of a doctoral dissertation by

Timothy Best Abbe

and have found that it is complete and satisfactory in all respects,
and that any and all revisions required by the final
examining committee have been made.

Chair of Supervisory Committee:

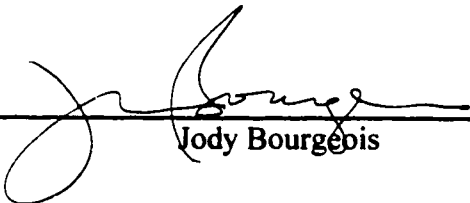


David Montgomery

Reading Committee:



Derek Booth



Jody Bourgeois



Catherine Petroff

Date: 2/4/2000

University of Washington

Abstract

Patterns, Mechanics, and Geomorphic Effects of
Wood Debris Accumulations
in a Forest River System

by Timothy Best Abbe

Chairperson of the Supervisory Committee
Associate Professor David Montgomery
Department of Geological Sciences

Field surveys in the forested Queets River basin of northwestern Washington, revealed that wood debris (WD) entering the fluvial system accumulates in distinctive patterns dependent on the physical characteristics of the WD, recruitment mechanisms, and channel morphology. Eleven fundamental types of WD accumulation or jams are identified based on patterns of WD deposition and its geomorphic effects. WD jams decrease channel radius of curvature and increase pool and forested island frequency. WD jams can persist for centuries within migration zones that are recycled in less than 88 years, thereby creating hard points within the floodplain that allow patches of old-growth forest to develop despite frequent disturbance. Accumulations of WD can also be a principal mechanism for forming terrace-like surfaces by episodically raising the channel and floodplain over 10 meters. Stable WD jams influenced both channel reach and floodplain terrace morphology throughout the Queets River system.

Two basic models were developed to investigate the principal factors controlling the stability of individual WD or logs. Where resistance is primarily provided by pre-existing boundary conditions, such as headwater channels where log length equals or exceeds channel width, stability is linked to material-strength. In large alluvial channels, where log length tends to be less than the channel width, the principal source of resistance is

attributed to how the log itself alters boundary conditions, which is primarily as a function of the log's shape. Both models and empirical data indicate both that rootwads are critical to log stability large channels and that log diameter affects stability and longevity throughout a channel network. This study demonstrates that WD can result in spatially and temporally complex fluvial land forms unique to forest regions.

Table of Contents

List of Figures	iii
-----------------------	-----

List of Tables	xi
----------------------	----

CHAPTER 1: PATTERNS AND PROCESSES OF WOOD DEBRIS

ACCUMULATION IN FORESTED BASINS	1
1.1 Introduction	1
1.2 Study Area	3
1.3 Methods	5
1.4 Wood Debris Recruitment	6
1.5 A Classification of Wood debris Accumulations	8
1.5.1.1 Bank Input Deposits	9
1.5.1.2 Log Steps	11
1.5.2 Combination Wood debris	12
1.5.2.1 Valley Jams	13
1.5.2.2 Flow Deflection Jams	16
1.5.3 Transport Jams	18
1.5.3.1 Debris Flow Jams	19
1.5.3.2 Flood-Peak Jams	20
1.5.3.3 Bankfull Bench Jams	24
1.5.3.4 Bar-Apex Jams	24
1.5.3.5 Meander Jams	26
1.5.3.6 Unstable Debris: Bar Top Jams and Bank Edge Jams ..	29
1.5.3.7 Rafts	30
1.5.4 Summary of Jam Types	32
1.6 Wood Debris Jam Frequency	33
1.7 Wood Debris Stability	34
1.8 Discussion	36
1.9 Summary	40

CHAPTER 2: LARGE WOOD DEBRIS JAMS, CHANNEL HYDRAULICS, AND HABITAT FORMATION IN LARGE RIVERS

2.1 Wood Debris Accumulations In Streams	70
2.2 Study Area and Methods	71
2.3 Types and Distribution of Wood Debris Jams	73
2.3.1 Alluvial Bedforms and Riparian Forest Patches	75
2.4 Hydraulic Effects of Debris Jams	77
2.4.1 Effect of Obstructions on Flow	80
2.5 Influence of Debris Jams on Channel Morphology	81
2.5.1 Pool Depths	83
2.5.2 Historical Jam Stability	85

2.6	Discussion	86
	2.6.1 Channel Habitat Structure	86
	2.6.2 Riparian Forest Development and Management	87
2.7	Conclusion	88
CHAPTER 3: MECHANICS OF WOOD DEBRIS STABILITY IN A FLUVIAL NETWORK		
	3.1 Introduction	101
	3.2 Methods	102
	3.3 Stability in Large Channels: Friction Limited	104
	3.3.1 Buoyancy	105
	3.3.2 Friction and a Deformable Bed	112
	3.3.2.1 Friction	116
	3.3.2.2 Effect of Flow and a Deformable Bed	118
	3.4 Stability in Small Channels: Strength Limited	129
	3.4.1 Beam Model	130
	3.5 Discussion	135
	3.5.1 Stabilizing Factors Associated With A Root Mat	136
	3.5.2 Physical Properties of Wood	137
	3.5.3 Additional Factors Affecting Stability	139
	3.6 Conclusion	140
CHAPTER 4: A NEW MECHANISM OF FLOODPLAIN AND TERRACE FORMATION IN FORESTED REGIONS		
	4.1 Introduction	180
	4.2 Study Site	181
	4.3 Methods	182
	4.4 Floodplain Development	184
	4.5 Terrace Development	186
	4.6 Complementary Evidence of Historical Observation	190
	4.7 Conclusions	191
	List of References	201

List of Figures

- Figure 1- 1. Queets River watershed upstream of Clearwater River confluence, northwest Washington. Shaded relief map by based on USGS 1981 30m digital elevation (courtesy of Harvey Greenberg, University of Washington Department of Geological Sciences) . 42
- Figure 1- 2. Distribution of forest zones and dominant tree species in Queets River basin, within Olympic National Park (based on Buckingham et al. 1995) 43
- Figure 1- 3. Definition sketch of channel (a), wood debris measurements (b), and classification of in-situ and transport wood debris accumulations (c) 44
- Figure 1- 4. Cross-sectional illustration of in-situ WD deposits associated with blow-down events (wind disturbance). Cluster of trees (a) is knocked over essentially simultaneously by severe wind gust (b), some of the effected trees are partially introduced into channel with no initial change in bank position (c). Flow constriction due to initial WD recruitment can accelerate bank erosion and introduce additional WD (d). The wind controls the direction of tree-fall, thus trees enter the channel in a wide range of orientations. Since trees enter the channel at the same time, there is a relatively uniform age distribution of new trees colonizing the fallen trees. 45
- Figure 1- 5. Cross-sectional illustration of in-situ WD deposits associated with bank erosion; riparian forest stand (a) is locally disturbed as individual trees are recruited to the channel by progressive retreat of the stream bank (b-c). Trees tend to fall 180° to the direction of maximum bank retreat, usually deposited orthogonal to flow (c). Initial WD constricts flow, accelerates erosion and subsequent recruitment of additional trees (d). Successive tree recruitment through time can result in a corresponding age distribution of colonizing trees. 46
- Figure 1- 6. Photograph of large oblique log step in Dante Creek, a steep headwater tributary to Queets River (a). Schematic plan view of oblique log steps in steep headwater channels (a) and photograph of normal log steps typical of low gradient channels (b) . . 47
- Figure 1- 7(a,b,c). Location of principal valley jams in active channel of Alta Creek in 1993 and 1994 (a). Schematic plan view of valley jam no.1 (b) and channel profile change upstream of valley jam no.2 from 1993 to 1994 (c) 48
- Figure 1-7(d,e). Photograph illustrating aggradation of Alta Creek upstream of valley jam no.2 in Figure 1-7a, elevating stream bed above old growth forest terrace surface (d). Flows occurring much more frequently than the “bankfull event,” now spread out across the terrace surface which had been over 2-5 m above the creek (e). 49

Figure 1- 8. Map (a) and cross-section (b) of flow deflection jam along south bank of Queets River at RK 66.2 (RM 41.1) as surveyed in 1993. Photographic sequence from 1985 (c) to 1993 (d) to 1997 (e) illustrating process of bank erosion and local recruitment of large old growth *Picea sitchensis* to create a flow deflection jam. This jam is located at Queets RK 50.9 (RM 31.6) opposite the Tshletshy Creek confluence and persisted through at least 10 annual peak flows with a recurrence interval greater than 2 years between 1985-1997, including two flows with recurrence intervals of 20 and 21 years.. 50

Figure 1- 9. Flood peak jam along Alta Creek, site location (a) and plan-view map (b) 51

Figure 1- 10. Example of large bankfull bench jam in Dante Creek (a), tributary to Alta Creek, Queets RM 41. Bankfull bench jam in Kokopelli Creek, tributary to Harlow Creek (Queets RM 34): plan-view sketch map (b) and cross-section A-A' (c). These jams create elevated surfaces composed of alluvium and WD in steep headwater channels where floodplains do not occur. 52

Figure 1- 11. Plan-view schematic illustrating basic structure of bar apex jams (a). Schematic profile illustrating tree age structure reflecting progressive downstream sedimentation. Bar apex jam in mainstem Queets River, RK 43.5 (RM 27) in 1993 (c). 53

Figure 1- 12. Schematic plan-view map showing basic structure of meander jams with inset illustrating reach-scale setting (a). Oblique photograph of meander jam along north bank of Queets River at RK 27.4 (RM 17) in 1994 (b). Schematic channel cross-sectional, looking downstream into meander jam (c) and photograph with similar perspective of meander jam along south bank of Queets at RK 24 (RM 15) in 1994 (d) 54

Figure 1- 13. Channel radii of curvature for Queets River meanders associated with unobstructed channels, bedrock outcrops, meander jams, and flow deflection jams as a function of river kilometer 55

Figure 1- 14. Simple model of channel planform changes associated with meander jams. Location of initial key member is arbitrary (a) but appears to occur most commonly just downstream of the thalweg cross-over between meanders, just upstream and on the same side as the downstream point bar. Meander jams don't necessarily begin with a single tree; sometimes they begin with the deposition of several trees during the same flow event. The migrating channel flows around the ever-enlarging jam (b), leading to a reduction in radius of curvature and distinct asymmetry in channel planform (c). If the jam increases in size enough, it may precipitate a channel avulsion around the jam (d). 56

Figure 1- 15. Unstable wood debris deposits: plan view of bar top accumulation shows wide distribution in log orientations (a), bank edge (jam height < channel depth) and bank revetment jams (jam height ≥ channel depth) are composed of logs with similar orientations approximately parallel to flow (b). Cross-sections illustrate difference between unstable jams deposited on a pre-existing bank (b) and stable jams which pre-date the bank (c) . 57

Figure 1-16 (a). Large wood debris jam or “raft” diverted lower Nooksack River completely around the Lummi peninsula so the river discharged into Bellingham Bay instead of Lummi Bay (War Department 1892) 58

Figure 1- 16 (b,c). Historical maps of wood debris rafts in large rivers entering Puget Sound in northwest Washington state: (b) Lower Stillaguamish River (Shoecraft 1875) and (c) Lower Skagit River (War Department 1898) 59

Figure 1- 17. Frequency distribution of wood debris accumulation types as a function of drainage area for the Queets River 60

Figure 1- 18. Dimensionless size plot of log stability thresholds for key, racked and loose pieces in 32 jams located in five study reaches representing different portions of the Queets channel network. Ratio of log basal diameter to bankfull depth, D_1/h_{bkt} , is plotted versus ratio of log length, L , to bankfull width, w_{bkt} . If D_1 is replaced with the rootwad diameter, D_0 , the domain of key members is further separated from that of racked members and distinguish key members occurring in large channels versus those in smaller channels . 61

Figure 1- 19. Rose plot illustrations of wood debris orientation normalized to total volume of wood in a particular type of accumulation, showing differences among types 62

Figure 1- 20. Summary chart of wood debris accumulation types and their location within a drainage network 63

Figure 2-1. The Queets River watershed, Olympic Peninsula 90

Figure 2-2. Example of WD jams in a large alluvial channel: a) March 7, 1985 aerial photograph of Queets River Reach km 50.58 - km 52.12 and Tshletshy Creek Reach km 0 - km 1.12 illustrating complex channel and forest patch patterns of an old-growth river system. b) Selected examples of three types of WD jam types observed in the area: unstable Bar Top Jams (BTJ); stable Bar Apex Jams (BAJ) and stable Meander Jams (MJ). General patterns in the forest-patch structure are illustrated 91

Figure 2-3. Frequency distribution of the depth of pools associated and not-associated with WD jams between Queets RK 41 and RK 66; surveyed in August 1994 92

Figure 2-4. Features associated with Bar Apex Jams. a) key member (BAJ Q5993), b) crescentic pool (BAJ Q5022), c) arcuate bar (BAJ Q5291), d) associated riparian forest patch (BAJ Q6749) 93

Figure 2-5. Composite sketch of physical attributes of the Bar Apex jam type showing characteristic patterns in channel-bed topography, WD structure, and riparian forest age structure 94

Figure 2-6. General flow patterns showing relative flow velocity vectors upstream of a BAJ. a) plan view of idealized near-bed flow field, point 1 delineates zone of vortex initiation, 2 is the saddle-point where flow goes to zero, 3 is the point of flow separation and 4 is boundary of separation envelope downstream of jam; b) plan view of measured near-bed flow velocities at BAJ Q5993 during low flow; c) profile of idealized flow field upstream of BAJ, illustrating horizontal and vertical velocity components, point 1 corresponding to the development of a downward acceleration in flow initiating vortex flow, 2 is the saddle point, and 3 and 4 delineate the zone of vortex scour; d) profile of measured flow field; upstream of BAJ Q5993 95

Figure 2-7. Field survey of BAJ Q5993, flow is right to left; a) pool and bar topography, shaded area delineates closed depression defining pool, b) median grain size of bed surface 96

Figure 2-8. Maps illustrating development of a bar apex jam and associated alluvial morphology and riparian forest development, Queets RK 51.52 - 52.3. Flow is from left to right. a) 1931 - active channel boundaries from U.S. Geological Survey plane table map (1:32,630, 1.52 m contours); b) 1939 - channel outline from 1:62,500 black and white aerial photograph (U.S. Army); c) 1985 - channel, bar, and forest boundaries from a 1:12,000 black and white aerial photograph shows deposition of several Bar Apex jams and colonization of forest vegetation occurred within the active channel sometime between 1939 and 1985; d) 1993 - channel, bar, and forest boundaries from a 1:12,000 color infrared aerial photograph shows each of the BAJs visible in 1985 are still present and island forest patches have continued to mature 97

Figure 2-9. Morphologic stages in alluvial topography associated with construction of a Bar Apex jam (key to geomorphic surfaces identical to Figure 2-5): a) deposition of the key member; b) formation of an upstream arcuate bar, a crescentic pool upstream and adjacent to the key member rootwad and/or normal members, and a downstream central bar along the axis of the key member bole; c) island development along central bar; and d) eventual integration into the floodplain development 98

Figure 3-1 Basic Tree Bole Structure and Force Definitions 145

Figure 3-2 Simple Form Models of Tree Boles: Uniform Cylinder (a), Fustrum (b), and Power-law Taper Model 146

Figure 3-3 Bole and Canopy Form of Common Pacific Northwest Trees 147

Figure 3-4 Free-body Diagram of Ideal Tree Bole Resting on Channel Bed 148

Figure 3-5 Centroids of Circle Segments 149

Figure 3-6 Effect of Bole Taper on Draft or Buoyant Depth (a), and Dimensionless Buoyant Depth as a Function of Specific Gravity and Bole Taper	150
Figure 3-7 Comparison of tree geometry models to estimate weights of trees with measured weights. Field density of trees computed from tree cores	151
Figure 3-8 WD orientation with respect to ground surface slope and differences between rolling and sliding friction. Adapted from Onda and Matsuleura 1997	152
Figure 3-9 Simple model of WD foot print and depth (a). Conical approximation for estimating sediment volume which must be overridden or plowed in profile (b). Simple cylindrical model of decreasing log footprint area on stamp depth (e)	153-154
Figure 3-10 (a,b,c) Empirical estimates of static friction by dragging tree boles with and without rootwads across gravel bar. Tree boles were weighed (a), rigged up to drag with a scale between skidder and bole (b). The skidder slowly accelerated until the tree bole began to slide (c). The scale recorded the maximum force necessary to initiate sliding. Drag repeated at least 3 times for each orientation of tree bole and substrate composition. Tree boles were rotated to change the plow length and effective surface area in contact with the ground surface (i.e., normal stress)	155
Figure 3-10 (d) Force necessary to initiate sliding plotted as a function of tree weight for different normal stresses. Regression excludes outlier point ($F_i = 1043$ kg) which occurred when the crown of one tree bole became embedded in the ground	156
Figure 3-10 (e) Incipient motion force as function of plow depth	157
Figure 3-11 Drag coefficients derived by Gippel et al (1992) for different tree forms and orientations	158
Figure 3-12 General flow structure around a bluff body and sediment accumulation within separation Envelope or eddy (a). Flow structure summary illustrating sediment flux into eddy region (b)	159
Figure 3-13 (a,b,c) Anchoring of a snag (tree bole) in an alluvial bed. Graphic description of tree bole with rootwad penetrating bed surface (a). Sediment buttressing downstream of rootwad could result from either sedimentation in the lee of a stable snag or from sediment pushed up as a tree moves along the bed with its rootwad acting like a bulldozer blade (b). Tree bole taper will directly influence the relative magnitude of sediment buttressing (c)	160
Figure 3-13 (d) Settling of bole associated with scour directly upstream and beside of rootwad and sediment buttressing downstream of rootwad (a)	161

Figure 3-14 Anchor analogy for snag stability demonstrating the significance of shape on holding power (data from Myers et al., 1969)	162
Figure 3-15 Flow chart presentation of factors and processes associated with wood debris stability in low-gradient channels	163
Figure 3-16 Definition sketch of simple beam model of log barriers or steps in low-order, steep headwater channels. Log is assumed to be a uniform cylinder (no taper) securely anchored on either end and oriented normal to flow	164
Figure 3-17 (a) Diameter of a log beam fixed at both ends necessary to withstand a uniformly distributed load due to a debris flow with a density of 2000 kg/m ³ and moving at 10 m/s, plotted as a function of channel width (assumed coincident with flow width). Critical diameters for <i>Pseudotsuga menziesii</i> (PSME), <i>Alnus rubra</i> (ALRU), <i>Picea sitchensis</i> (PISI), <i>Thuja plicata</i> (THPL), and <i>Populus trichocarpa</i> (POTR) are plotted as a function of channel width (assumed coincident with beam length)	165
Figure 3-17 (b) Diameter of a log beam fixed at both ends necessary to withstand an impact by a boulder 1/4 the beam's length (i.e., channel width). Boulder is assumed to have a density of 2600 kg/m ³ and moving at 10 m/s. Critical diameters for <i>Pseudotsuga menziesii</i> (PSME), <i>Alnus rubra</i> (ALRU), <i>Picea sitchensis</i> (PISI), <i>Thuja plicata</i> (THPL), and <i>Populus trichocarpa</i> (POTR) are plotted as a function of channel width (assumed coincident with beam length)	166
Figure 3-17 (c) Diameter of a log beam fixed at one end and pinned at the other end necessary to withstand a uniformly distributed load due to a debris flow with a density of 2000 kg/m ³ and moving at 10 m/s, plotted as a function of channel width (assumed coincident with flow width). Critical diameters for <i>Pseudotsuga menziesii</i> (PSME), <i>Alnus rubra</i> (ALRU), <i>Picea sitchensis</i> (PISI), <i>Thuja plicata</i> (THPL), and <i>Populus trichocarpa</i> (POTR) are plotted as a function of channel width (assumed coincident with beam length)	167
Figure 3-17 (d) Diameter of a log beam fixed at one end and pinned at the other end necessary to withstand an impact by a boulder 1/4 the beam's length (i.e., channel width). Boulder is assumed to have a density of 2600 kg/m ³ and moving at 10 m/s. Critical diameters for <i>Pseudotsuga menziesii</i> (PSME), <i>Alnus rubra</i> (ALRU), <i>Picea sitchensis</i> (PISI), <i>Thuja plicata</i> (THPL), and <i>Populus trichocarpa</i> (POTR) are plotted as a function of channel width (assumed coincident with beam length)	168
Figure 3-18 Plot illustrating the maximum range of wood densities found several species native to the Pacific Northwest. Note that once saturated, the specific gravity of wood debris can exceed unity. Even in regions where most of the trees have low densities, such as the PNW, it is not uncommon to find sunken log resting on the channel bottom ...	169

Figure 3-19 Hypothetical graph illustrating the effect of regional climates and seasonal precipitation on the stability of wood debris. In catchments on the west slope of the Cascade and Olympic mountains in Washington State, almost all of the annual precipitation occurs during the 9 months of Fall, Winter, and Spring. The summers are characterized by long, sunny, warm days and extremely low flows in streams and rivers. By the end of the summer, wood debris situated above the water table reaches its lowest moisture content of the year and its greatest potential buoyancy. Wood debris in this region will generally be most susceptible to transport early in the Fall. By November or December, wood moisture contents may be near saturation due to the frequent rain and high flows, low rates of evaporation, and short days. If two identical logs are placed in streams of similar size in two different climates and the logs subjected to identical flow conditions, the log in the more arid region will be the first to move, thus suggesting a lower frequency of stable wood debris accumulations in arid regions 170

Figure 3-20 Effects of decay on wood strength. Bending strength and especially toughness, experience a rapid reduction with respect to mass loss. Based on effect of fungus *Chaetomium globosum* on bending strength and toughness of beech (*Fagus sylvatica*) (from Armstrong and Savory 1959) 171

Figure 3-21 Application of simple decay model using decay constants of $k=0.006$ (old-growth conifers) and $k=0.031$ (black cottonwood) to estimate % mass remaining and diameter relative to initial diameter with time. Diameter predictions based on decay progressing from the perimeter of a cylinder to its center. Decay coefficients based on Sollins (1982), Means et al. (1986), Ceylonese et al. (1987), Hyatt (1998) 172

Figure 3-22 Illustration summarizing additional factors that influence debris stability: surcharge (alluvium and vegetation), additional debris accumulation (sealing and deflecting flow), root cohesion (adding cohesion to cohesionless sediments downstream and on top of debris); and overlying canopy (shade can reduce drying rates of wood, maintaining greater moisture contents but accelerating decay) 173

Figure 4-1. Drainage basins of Queets River drainage basin and adjacent catchments, southwestern portion of the Olympic Peninsula. Along the most of its length, the Queets River channel actively migrates across its valley, portrayed by the river's position in 1932 and 1985 193

Figure 4-2. Distribution of recurrence intervals which the Queets River moves across its floodplain over approximately 65% of the river's length from RM 7.5 to 38.5 (RK 12- 62), drainage areas ranging from 673 to 137 km², respectively. Within these reaches, the Queets River moves across its floodplain in 200 years or less. The mean and median time it takes the river to recycle its floodplain within these reaches are 103 and 90 years, respectively 194

Figure 4-3. Bar Apex jam in Queets River at Sam’s River confluence, Queets RM 24.6 (RK 39.6). Drainage area at site is 410 km² 195

Figure 4-4. Floodplain channel and forest patch mosaic along Queets River mainstem channel, RM 20.2 (RK 32.5). Drainage area at site is approximately 435 km² 196

Figure 4-5. Calibrated radiocarbon dates and tree ages for buried jams distributed throughout the Queets River network 197

Figure 4-6. Map illustrating positions of mainstem Queets River channel, recent wood debris accumulations, and relict jams in reach extending from RM 28.3-29.0 (RK 45.6-47). Coarse channel cobbles in abandoned positions of 1932 channel indicate the river bed was about 2.6-3.0 m higher than its current elevation. Note coincidence of old-growth forest patches above buried log jams, of which had wood over 1000 years old 198

Figure 4-7. Channel profiles of Alta Creek in 1993 and 1994 showing aggradation upstream of valley jams. The profile of the terrace along the channel’s eastern margin (river right bank) is also plotted (surveyed in 1994) . Note the step-like form of the profiles created by the wood debris jams that results in surfaces that converge upstream and clearly evident in terrace profile. This profile morphology is most pronounced in smaller channels such as Alta (drainage area of about 23 km²), but identical patterns were found throughout the Queets River basin 199

Figure 4-8. Large buried log jam beneath 8 m terrace adjacent to Queets River at RM 16 (RK 25.8). The remaining terrace surface had a slope of approximately 0.0003, compared to the active river’s slope of 0.0025. Drainage area at site is approximately 552 km² . 200

List of Tables

Table 1-1. Recruitment processes introducing wood debris into a fluvial channel network	64
Table 1-2. Log dam characteristics in selected channel reaches of the Queets River watershed.	65
Table 1-3. Changes in the Red River, LA from 1886 to 1980 after removal of the "great raft" in 1873	66
Table 1-4a. General Characteristics of Wood Debris Accumulation Types: In-situ Jams	67
Table 1-4b. General Characteristics of Wood Debris Accumulation Types: Combination Jams	68
Table 1-4c. General Characteristics of Wood Debris Accumulation Types: Transport Jams	69
Table 2-1 Channel Characteristics of Example Study Reaches	99
Table 2-2 Shear stress derivations for Pelton Reach based on bed surface texture	99
Table 2-3 Estimates of mean horizontal flow velocity for the Pelton Reach	100
Table 2-4 Scour predictions for two example Bar Apex jams discussed in text	100
Table 3-1 Alluvial substrate bearing capacities	174
Table 3-2 Best-fit empirical models for estimating drag coefficients	175
Table 3-3 Bulk densities and friction angles as a function of grain size	176
Table 3-4 Physical characteristics of common Pacific Northwest trees	177
Table 3-5 Specific Gravity, Modulus of Rupture and Modulus of Elasticity Values . for Common Pacific Northwest Trees	178
Table 3-6 Variables influencing force balance analysis for in-stream wood debris ...	179

Acknowledgments

I am grateful for the funding support I received from The Washington State Timber, Fish, and Wildlife Program, U.S. Environmental Protection Agency, Washington Forest Protection Association, the Watershed Science Institute of the Natural Resources Conservation Service (U.S.D.A.), and the University of Washington Department of Geological Sciences. Olympic National Park authorized the field work and generously allowed access to historical records and images. I would like to thank all the wonderful individuals who have lent their support and believed in me. Completing this dissertation has been the biggest challenge of my life. Foremost, I'd like to thank David Montgomery. I couldn't have asked for a better and more understanding advisor; he always supported and encouraged me through some very difficult times. I am sincerely grateful to my wonderful partner, Laurie Best Mann, and all she did to help finish this. I am forever indebted to my dear friend Donna Ortiz de Anaya for the time she took to help me finish my first drafts of this dissertation. I made significant improvements to this manuscript based on the advice and encouragement of my committee members, Catherine Petroff, Jody Bourgeois, and Derek Booth. Special thanks to Pat and Jean Mann for being there for me on many, many occasions and to my own parents, Harriette and Whip Abbe. I'm grateful to my brother Dan Abbe, Carolyn Adams, Harvey Greenberg, Bernie Anderson, Jill Silver, George Pess, Rolf Aalto, and Kevin Fetherston. I benefitted from outstanding field assistance provided by the UW students who spent their summers working with me in the Queets. I dedicate this dissertation to the very special Queets River, and to my daughter Carmen River Abbe for her patience, support and inspiration.

CHAPTER 1: PATTERNS AND PROCESSES OF WOOD DEBRIS ACCUMULATION IN FORESTED BASINS

1.1 Introduction

Wood debris (WD) is a significant component of the matter contributed to stream channels in forested landscapes around the world, yet few attempts have been made to establish whether or not physically distinct types of WD accumulations or jams occur within channel networks. If distinct types of WD jams exist, what physical attributes distinguish them, and are there differences in how they are distributed through the channel network of a drainage basin? This chapter identifies and describes physical characteristics of distinct WD jam types, factors influencing WD jam formation and stability, distribution of WD jam types throughout a large channel network, and some of the associated geomorphic effects of WD jam types.

Observations that wood debris had significant effects on the morphology and processes of streams and rivers in North America were relatively common during exploration and settlement of the late 1800s and early 1900s (e.g., Lyell 1830, Shoecraft 1875, Russell 1909, Day 1921; see also Tarzwell 1934, Dorsey 1941, Kanes 1970, McCall 1984). Scientific study of wood debris in fluvial systems, however, has grown rapidly only in the last several decades as it has become increasingly apparent that wood debris is a significant ecological and physical component in channels draining forested landscapes (e.g., Zimmerman et al. 1967, Heede 1972, Swanson and Lienkaemper 1978, Bilby 1979, Tally 1980, Marston 1982, Sedell and Frogatt 1984, Triska 1984, Gregory et al. 1985, Lisle 1986b, Harvey et al. 1988, Nakamura and Swanson 1993, Rice 1994, Richmond 1994, Gippel et al. 1996).

Despite recognition that wood debris is often a principal part of the channel bed material, observed patterns of wood debris accumulation in different sized channels of a drainage basin have largely been limited to general descriptions of a progression of channel-spanning accumulations in small channels to accumulations at the margins of large channels (e.g., Vannotte et al. 1980, Bisson et al. 1987). While systematic relationships

among distinct sedimentary bedforms, channel characteristics, and flow conditions are well established (e.g., Kennedy 1969, Southard 1971, Allen 1985), research into analogous relationships for fluvial wood debris accumulations is still in its infancy.

Several studies have shown systematic changes in the characteristics of WD accumulations as a function of channel size. Zimmerman et al. (1967) found that the presence and effect of WD and tree roots in and along small headwater streams of Vermont changed as a function of drainage area. Hogan developed a nomenclature for log jams based on their size relative to the channel and effect on channel sedimentation (Church 1992). Keller and Swanson (1979) found a reduction in WD loading from first through sixth order channels in old-growth *Pseudotsuga menziesii* forests of the McKenzie River watershed in western Oregon. Wallerstein et al. (1997) describe six types of WD accumulation found in different parts of low-order channels of northern Mississippi. Nakamura and Swanson (1994) discuss the effect of WD length, channel width, and channel radius of curvature on WD deposition and the formation of stable WD accumulations. Other studies have reported a correlation between channel width and the length and diameter of stable WD (e.g., Seno et al. 1984, Bilby and Ward 1989, Ishikawa 1989).

Descriptions of WD accumulations commonly refer to the presence of large “key logs” anchoring debris jams (Gillespie 1881, Deane 1888, Russell 1909, Keller and Tally 1979, Nakamura and Swanson 1994), but little has been done to investigate the relationship between log diameter and flow depth, or to consider other factors such as buttressing geometry, intact rootwads, or multiple boles or stems. The orientation of individual tree boles and jams has been noted to change from relatively random positions at high angles to flow in small channels, to arrangements parallel to flow in larger channels (Triska and Cromack 1979, Bisson et al. 1987). Hogan (1987) reported that smaller WD was most likely to have its bole aligned with flow, whereas the orientations of larger pieces and accumulations ranged from about 20 to 90 degrees to flow.

General types of in-stream WD throughout a channel network based on physical characteristics of the WD and channel have been identified only in relatively small basins

(channel bankfull widths ≤ 40 m, catchments < 100 km²). Yet, published data are limited to correlations of bole length and diameter to channel bankfull widths, or estimates of WD volume per unit channel length or area (Bilby 1979, Swanson and Lienkaemper 1984, Harmon et al. 1986, Bisson et al. 1987).

1.2 Study Area

The Queets River watershed on the Olympic Peninsula of Washington was selected for this study because it is a watershed with: (a) a relatively large channel network, (b) a large range in the size and shape of riparian trees, (c) a relatively constant climate through the Holocene, and (d) a relatively pristine forest subject to negligible human disturbance.

On the west slope of the Olympic Peninsula in northwest Washington, preserved within Olympic National Park, remains one of the largest continuous tracts of old-growth montane forest in the continental United States. The largest intact old-growth watershed on the west slope is located within the Queets River drainage basin (Figure 1-1). The headwaters of the Queets River begin below Mount Olympus (2,430 m) and the river flows approximately 86 km to the Pacific Ocean. The Queets River near its mouth (river km 7.4) has a drainage area of 1163 km² and an average annual flow of 121 m³/s. The 397 km² Clearwater River watershed and the Queets River below its confluence (11 km from the Pacific) were not included as part of this study because they have been intensively logged. Most of the Queets River valley in the 754 km² above the Clearwater confluence lies within Olympic National Park, and much of the watershed is still mantled with old-growth. The study area was separated into the upper and lower Queets at the river's confluence with Sam's River, based on differences in current and past land management (Figure 1-1).

Portions of the Queets valley were affected by homesteaders prior to inclusion in the park (Morgan 1955). Although tributaries to the lower Queets are subject to logging, essentially all of the mainstem river valley lies within Olympic National Park, and negligible alteration of the channel or riparian forests has occurred in the last sixty years. The upper Queets is a rare example of a large, unmanaged, and relatively low-gradient forested

alluvial river valley. The Queets watershed offers a wide size range of channel and tree dimensions: bankfull channel widths, w_{bf} , exceed 100 m, and trees can reach over 70 m in height and attain diameters greater than 3 m. Study reaches for small and moderate channels ($w_{bf} < 80$ m) are all located in the 334 km² pristine area upstream of the Sam's River confluence.

The Olympic Mountains resulted from a complex convergence of the Juan de Fuca and North American plates that began sometime in the Miocene. The Queets basin consists of highly folded marine sandstones and shales accreted to North America in the late Miocene (Tabor and Cady 1978, Tabor 1987). The Pacific Northwest experienced several major glaciations during the Pleistocene; only alpine glaciations affected the west slope of the Olympics. Despite major climatic variations, several studies have shown that forest cover on the west slope of the peninsula has been relatively consistent for at least 17,000 years (Florer 1972, Heusser 1972, 1974, Buckingham et al. 1995).

The west slope of the Olympic Peninsula has a humid maritime climate associated with some of the highest levels of precipitation in North America. Precipitation ranges from approximately 2500 mm at the coast to over 6000 mm near the summit of Mount Olympus (U.S. Army 1947, Philips and Donaldson 1972, Buckingham et al. 1995), with eighty percent of the annual precipitation falling between October and March (Philips and Donaldson 1972, NOAA 1978). The majority of winter precipitation falls as rain, with fog drip from trees contributing several centimeters to the total precipitation; these characteristics are typical of temperate rainforests (Buckingham et al. 1995).

Winds are the principal climatic disturbance influencing forest cover (Franklin and Hemstrom 1981, Henderson et al. 1986). Windstorms are almost always associated with onshore circulation from west to east; wind-throw is common in east-west trending valleys and east-facing slopes. Disturbance processes on steep hillslopes and streams include landslides and avalanches in the higher elevations (>1,500 m). Fires are extremely rare within the Queets basin, and those recorded in historical times were small and due either to lightning high in the basin or to human activities.

The western slope of the Olympic mountains is mantled by temperate rainforest (e.g., Franklin and Dryness 1988, Henderson et al. 1986, Norse 1990, Weigand et al. 1992), and has one of the highest rates of biomass production per unit area in North America (Franklin and Waring 1979, Harmon et al. 1986). Forest communities on the Olympic Peninsula vary with elevation and precipitation and have been classified into coastal, lowland, montane, and subalpine forest zones (Buckingham et al. 1995) (Figure 1-2).

1.3 Methods

Field observations and literature reviews were used to define different types of WD accumulations and to characterize the processes influencing their formation and geomorphic effects. Interpretation of 1:12,000 color IR aerial photos taken during low-flow conditions in August of 1993, together with field surveys during the summers of 1993-95 were used to investigate WD jams in approximately 75 km of the mainstem Queets River and 16 km of tributary channels, whose widths range in size from 2 m to over 150 m. Channel morphologies of the Queets basin differ markedly, ranging from steep, single-thread bedrock, cascade, and step-pool channels in confined valleys, to relatively simple unconstricted plane bed reaches, to complex anastomosing pool-riffle channel reaches (see Montgomery and Buffington, 1997, for explanation of channel types). Bankfull channel characteristics were obtained by measuring channel reaches exhibiting as little influence from WD structures as possible.

During the summer of 1993, patterns of WD accumulations were documented in relation to recruitment processes. A description of recurring jam types were developed in recognition of these recurring patterns. During three summers of field work (1993-95), surveys cataloged the types and sizes of WD jam types and channel characteristics for different portions of the Queets watershed. Channel profiles, cross-sections, and individual pieces of WD were measured at each study reach (Figure 1-3). The identification of stable WD was based on interpretation of field observations and historical evidence. For example, a minimum estimate of WD residence time and whether the material had been

subjected to a large flood could be made using the age of vegetation growing on top of WD, or the presence of the WD in historical aerial photos, together with historical gage records. In addition, I distinguished stable WD based on its apparent effect on the channel. WD that significantly altered channel morphology was assumed to be stable.

Topographic surveys of channel cross-sections, profiles, and floodplain maps were made with an optical auto-level and a laser theodolite. Measures of channel morphology are defined in Figure 1-3a. Channel reaches extended from 8 to 20 bankfull widths in length. Bankfull channel widths, w_{bf} , and depths, h_{bf} , of the study reaches ranged from 2 to 130 m and 0.3 to 2.2 m, respectively. Reach-averaged channel gradients, S , ranged from 0.001 to 0.26. Geomorphic sketch maps of each study site included the location of WD, bed-material characteristics, bars, and vegetation. All measured WD was greater than 1 m in length and 0.1 m in diameter (Bisson et al. 1987). There is nothing physically or biologically unique about this size criteria, which appears to have been based on the size of wood an adult human could be expected to remove from a channel for purposes of channel clearing, common earlier this century in the Pacific Northwest (J.R. Sedell, pers. comm. 1993).

Measurement of WD was done with tapes or laser range-finders and included measuring the root-mass or "rootwad" diameter, D_1 , the basal diameter of a bole measured 1.4 m from the top side of the rootwad, D_b , the crown diameter at the end of the bole, D_n , the total bole length, L_n , and the bole orientation relative to the channel axis (Figure 1-3b). Log measurements were used to estimate log volume and weights. Individual pieces of debris were classified relative to their function in a jam: *key members* anchor other debris, *racked members* lodge against a channel obstruction (e.g., boulder, key member, or other debris) and divert flow, and *loose members* fill interstitial space, but add little physical integrity to the jam.

1.4 Wood Debris Recruitment

The formation of WD jams is influenced by recruitment processes and the characteristics of the WD entering the channel. Debris can be recruited from external

sources or from upstream channels. Recruitment can occur either by tree fall proximal to the channel, through fluvial processes, or through external processes associated with landscape disturbance (Table 1-1). Fluvial processes responsible for recruitment include bank erosion and large flood events. Recruitment processes external to the fluvial system include wind throw and mass failures such as debris flows and landslides (e.g., Keller and Swanson 1979, Bisson et al. 1987, Swanston 1991). Other disturbance processes, such as fire, can indirectly contribute large quantities of debris to a channel system (e.g., through high winds associated with fire or subsequent loss of root strength and wind-throw after a fire). Mechanical break-down and downstream routing of WD in a channel is controlled by in-stream processes such as debris flows and flood flows.

The strong dependence of particular disturbance processes on topography results in a relatively systematic pattern of potential recruitment mechanisms throughout the channel network. Wood debris recruitment to unconfined, low-to-moderate gradient alluvial channels is dominated by bank erosion. Channel migration is the principal mechanism of bank erosion in large pool-riffle channels. In channels that are less likely to move laterally, such as plane bed and step-pool channels, flow obstructions introduced to the channel can account for much of the bank erosion. Local obstructions can constrict, divert, and accelerate flow leading to bank erosion. More extensive, channel-spanning obstructions can decrease channel gradient, aggrade the channel, and initiate bank erosion as the channel widens to compensate for the decrease in depth and gradient. Bank erosion mines both alluvium and wood debris from the valley bottom (i.e., floodplains and terraces), and can initiate landsliding along the valley hillslopes through toe erosion and oversteepening.

In confined headwater channels with inherently stable banks, the orientation of a tree bole at the time of recruitment has a significant effect on the amount of material that enters the channel. Trees that fall perpendicular to the channel are commonly found suspended over channels with widths less than the trees' bole length, leaving a small portion of the tree volume lying within the channel. In contrast, trees that fall perpendicular to a slope are more likely to roll down into the channel in confined headwater channels, which can result in full tree-length recruitment. Tree-fall, wind-throw

and landsliding deliver WD to channels throughout the Queets basin, but these processes are most significant in confined, steep channels.

In steep tributary valleys, shallow landsliding and colluvial debris flows deliver large rocks, colluvium, and wood debris to channels. In steep headwater channels examined in the Queets river basin (e.g., Coal Creek, Upper Harlow Creek, Alta Creek, Dante Creek), most of the WD was delivered to the channel by small shallow landslides which appear to have the most pronounced effect where they enter the channel. A catastrophic deposit observed in the Queets basin was found in riparian areas downstream of where the torrent left the active channel. Upstream, in the portion of the channel which the torrent had passed, the channel appeared to be scoured and cleared of all WD, or simply relocated around stubborn pre-existing WD (i.e., Alta Creek). Based on this site and observations from other sites impacted by similar events in other western Washington watersheds, torrents associated with debris flows or dam break events appear to reduce the number and distribution of WD flow obstructions in the portion of the channel through which the torrent passes. Torrents leave a large concentration of WD where they come to rest, either in the channel or in riparian forests outside the channel. Thus, torrents appear to be more of a WD export mechanism than recruitment mechanism. No compelling evidence of debris flows was found in the Queets. Only one site was found with gradients over 6%, and which exhibited strong evidence of a catastrophic flow.

1.5 A Classification of Wood debris Accumulations

Stable WD accumulations were observed in all parts of the Queets basin and they showed significant differences in their characteristics. Three fundamental categories of WD accumulations, or “jams,” are differentiated by whether or not the WD moved downstream once entering the channel. *In-situ* jams are made of WD that has not moved from the point where it first entered the channel, although it may have rotated, or the channel may have moved. *Combination* jams consist of substantial quantities of both in-situ and transported wood debris. *Transport* jams are made of WD that has moved some distance downstream by fluvial processes.

Within these three categories, recognition of nine basic types of WD accumulation in the Queets basin provides a nomenclature and process-based model that illustrates systematic ways in which WD accumulations influence alluvial landforms and riparian habitat. Two additional types of WD accumulations have been identified based on data from managed rivers, and from historical data and observation. Each of these WD jam types has additional characteristics which are identified and described in the following sections.

1.5.1 In-Situ Wood debris

In-situ debris includes those pieces of WD that remain where initially introduced, and which subsequently form stable roughness elements that significantly affect a channel's hydraulic geometry. These tree boles have sufficient size and mass to prevent their hydraulic transport downstream during high flows. Scour resulting from constricted flow around the rootwad of a fallen tree can allow the rootwad to settle into the substrate until the bole is flush with the channel bed, creating a log step in smaller channels. In large channels the same process can occur, but the tree bole is more likely to rotate parallel to flow and incline 10-20° out of the river bed, with the rootwad settled even deeper into the bed. Wood debris stability is also directly influenced by mechanical breakdown, since any reduction in size will tend to decrease WD's potential resistance to transport downstream. In-situ jams may lie partially or completely within the channel. Fallen trees of sufficient size relative to the channel may remain in the place where they entered a channel for many years (e.g., Keller and Tally 1979, Bryant 1980, Nakamura and Swanson 1994, Hogan et al. 1995). Bank input and log steps are two distinct varieties of in-situ jams which can be identified based on the orientation, position, and number of key-members forming the jam. Each of these jam types also exhibits different influences on channel characteristics.

1.5.1.1 Bank Input Deposits

Bank input deposits consist of tree boles situated partially or completely within the channel where they first entered the channel. Only a small volume of bank input debris is

situated within the bankfull channel; most of its weight, however, is imparted onto the channel bed space. In confined channels this can be due to steep hill slopes adjacent to the channel. In unconfined channels, multiple stems, large branches, or an attached root-wad can elevate a significant portion of the debris mass above the water surface even though the debris sits entirely on the channel bed. Trees falling into unconfined channels are more likely to have some of their weight supported on banks above bankfull elevation. This effect increases debris stability because buoyant and drag forces are reduced relative to gravitational forces. By forming only a partial obstruction of flow, bank input deposits tend to exert localized effects on channel morphology such as pool and bar formation proximal to the structure. Over time, however, the original bank input structure can obstruct larger portions of the channel cross-sectional area, A_c , as increased quantities of WD enter the channel. The degree of flow obstruction is defined as the channel blockage coefficient, $B_c = A_d/A_c$, where A_d is the area of in-stream WD projected normal to flow. As B_c increases, so does the probability of trapping additional WD and sediment, potentially leading to growth of a channel-spanning impoundment or debris dam. Bank erosion and bed scour associated with the portion of bank input debris within the channel can allow portions situated on banks to settle into the channel and form a single log step.

Bank input deposits forming in the Queets watershed are predominantly associated with wind-throw events or bank erosion. Wind-throw is an external process independent of channel processes, but bank erosion depends on channel processes. Differences between bank input deposits formed from wind-throw and bank erosion are summarized in Figures 1- 4 and 1-5. Wind-throw usually affects clusters of trees knocked down parallel to one another and coincident with the responsible wind gust; different wind-throw events can result in a wide range of tree orientations relative to the channel. As wind-throws are not restricted to streamside trees, only some of the affected trees are introduced to the channel (Figure 1- 4a-b). In contrast, only streamside trees are recruited through bank erosion; they are usually deposited normal to flow (Figure 1-5a -b). In either case, once in the channel, the debris can accelerate bank erosion by diverting flows to unobstructed areas

which often will be toward the base of the recently recruited tree (Figures 1- 4c-d and 1-5c-d).

The stability of smaller WD appears to be partially a function of growth position relative to other trees and partially to the temporal pattern of recruitment. The deposition of large stems upstream can dissipate and divert flow; deposition downstream provides a trap for smaller debris, and debris recruited at a later time can stabilize material in the channel by accumulating on top of it.

1.5.1.2 Log Steps

A log step forms when a tree bole spans a channel with each end locked in place along the channel margins by rock, boulders, WD, or sediments. Once deposited, sediment accumulates upstream of the bole and water flows over the top, forming a distinctive step. Though tree boles that create steps are generally oriented normal to flow, they can have a wide range of orientations. Larger accumulations of WD forming step-like structures are described in the valley jam section. The mean diameter of tree boles that form steps ranges from about one-half to 8 times the bankfull flow depth, but the height of steps commonly exceeds the log diameter due to the scour pools that form on the downstream side. Similar structures documented in small channels can account for up to 80% of the elevation loss in steep mountain streams (e.g., Heede 1972, Keller and Swanson 1979, Keller and Tally 1979, Marston 1982). Similar percentages were documented in profiles of both high-gradient, first-order and low-gradient, third-order channels of the Queets watershed, with up to 77% of the low-flow head loss attributed to log steps (Table 1-2). Accumulations of small organic debris with diameters less than 3 cm were observed occasionally to form steps up to 30 cm in height and 3 meters wide (normal to flow) within small aggrading channels. But such accumulations rarely extended across the channel and are assumed to have negligible consequences due to their rapid decay.

Log steps can be sub-divided into two types based on log orientation relative to the channel axis: oblique and orthogonal. Log orientation, in turn, appears to be influenced by channel gradients. Oblique steps occur most commonly in low-order, steep semi-confined

channels (Figure 1-6). Log steps in three study reaches with gradients of 0.40 to 0.69 had orientations 18° to 64° to the channel axes. These channels were confined by relatively steep hill slopes and the majority of log orientations were more parallel than perpendicular to flow. Because WD is more readily transported down steeper hill slopes, the potential source distance for WD recruitment increases with hillslope gradient. In channel reaches with negligible lateral migration, bank input debris and log-step frequency tend to decrease proportional to channel gradient, as shown in the occurrence of log steps forming in three steep channels and three low-gradient channels (Table 1-2).

In unconfined low-gradient channels there is a distinct increase in the number of steps oriented nearly orthogonal to the channel, and an increased variance in log orientation (29° - 120°). In moderate gradient ($0.03 < S < 0.10$) channels the majority of elevation loss along a channel profile commonly occurs in bedrock, boulder, or log steps (e.g., Marston 1982). Such steps are uncommon in lower gradient channels ($S < 0.02$). In our study reaches with bankfull widths of 15 meters or less, log steps accounted for a significant quantity, sometimes the majority, of the elevation loss (Table 1-2). Log steps in moderate to low-gradient channels tend to occur less frequently than oblique steps found in the steeper channels, but can account for a greater proportion of the total elevation drop (Table 1-2).

The higher variance of bole orientations in low-gradient channels may reflect the diminished influence that adjacent hillslopes have on the direction a tree will fall. In contrast, wind throw of trees growing on a relatively flat bank will result in orientations independent of the channel course. Low-gradient channels lack recruitment due to mass-wasting processes and are subjected more to lateral bank erosion of the stream, usually resulting in log steps orthogonal to the channel axis or flow.

1.5.2 Combination Wood debris

Combination debris accumulations initiate when deposits of stable in-situ debris obstruct a channel and trap large quantities of transported debris. The combination of in-situ and transported debris forms an effective barrier, deflecting flows around the structure

or completely impounding the channel. The presence of significant quantities of transported WD distinguish combination jams from in-situ debris.

1.5.2.1 Valley Jams

Valley jams are stable log structures that occur across a wide range of channel gradients. Such jams can initiate with the local recruitment of a single key member log to the channel, or with the massive debris deposits associated with landsliding or wind throw. Regardless of the recruitment process, key members experience insignificant movement once in the channel. Key members form stable in-stream structures that constrict a large portion of the bankfull cross-sectional area and deflect flow around the log, especially around its rootwad. This can result in a period of rapid bank erosion, channel widening, and recruitment of additional key members (Figure 1-5). Additional WD racks up on these key members during high flows, further constricting the channel until it is completely impounded. The valley jam thus forms an effective sediment reservoir that can bury much of the WD comprising the initial structure. This process further drives channel widening or even avulsion by elevating the river bed upstream of the jam. Russell (1909) recognized that large log jams in the Teanaway River, WA, formed in a similar process linked to the local recruitment of one or more large trees over several years or flood events, rather than during a single flood. In the Sierra Nevada mountains of California, Muir (1878) noted that individual boles of *Sequoiadendron giganteum* effectively impounded small stream valleys, elevated flood plains, and resulted in landforms resembling terraces. Valley jams can form in both confined and unconfined channels, but my observations indicate they are limited to channels with gradients between 0.02 and 0.20. The geomorphological influences of these jams can affect the morphology of the entire valley floor.

Field observations suggest a simple model for valley jam creation. Valley jams form when bank-input jams block enough of the channel to impound debris (or sediment) moving down the channel. Formation of a valley jam depends on the introduction of WD with sufficient size and mass to remain immobile within the channel. These stable key members form the structural foundation of the jam and are therefore a necessary condition

for valley jams to form. Bank erosion is the most common mechanism of key member recruitment for valley jams, but landsliding, windfall, and tree throw contribute key members that can go on to form valley jams. In narrow, steep valleys in the Queets basin, landslides deliver trees that extend across the valley floor and are the dominant mechanism initiating valley jams. Hogan et al.(1995) describe similar WD accumulations in small headwater channels in British Columbia.

Valley jams do not necessarily form catastrophically. In unconfined channels, valley jams form when one or more trees create an obstruction that deflects the channel into adjacent banks. When trees falling into the channel along the eroding bank are large, they extend the width and are integrated into the jam. Through this process, a jam can expand across the valley floor, attaining much greater than the bankfull channel widths. The active channel delivers WD which racks up onto the fallen trees, raising the jam's height and creating a barrier effective at impounding and aggrading the channel. The key member trees in valley jams are usually oriented approximately perpendicular to the channel and less than 30 degrees off the horizontal. The development of valley jams is reflected in the trend among tree seedlings that colonize the jam: the oldest are found toward the center of the jam where bank erosion occurs on both sides of the channel, or one side of the jam where channel widening occurs on only one side. The progressive age distribution of these colonizing seedlings also indicates a gradual rather than the catastrophic process of a debris flow or dam-break jam.

Repeated mapping (1993-95) of several valley jams in lower Alta Creek provided additional evidence supporting this gradual process of jam growth. At Alta Creek valley jam #1, sixteen additional key members were recruited and the channel increased in width by over 14 m from 1993 to 1995 (Figure 1-7a,b).

The vertical relief of individual valley jams is limited by channel confinement, composition of channel banks, forest characteristics, and the structural integrity of the jam. Confined jams are defined as those with width-to-height ratios of less than 10, whereas unconfined jams can have width-to-height ratios ranging from 10 to 200. In unconfined systems, vertical relief will be a function of tree diameter, stand density, and tree length.

Increased stand density results in more trees per unit area and thus, a potentially higher jam. Increased tree heights will also correspond to higher jams since there will be greater potential for bole overlap. Because lateral expansion is restricted, confined channels tend to respond to large obstructions, such as valley jams, through vertical aggradation. Because a stream channel cannot go around a confined valley jam, these structures rarely have vegetation growing on them and are more susceptible to catastrophic failure than unconfined valley jams. A *Pseudotsuga menziesii* (Douglas Fir) found growing on a fluvial terrace upstream of a confined valley jam on lower Dante Creek (17 m wide, slope = 0.19) in 1995 was 77 years old (DBH = 0.18m), suggesting that some portion of the valley jam had been present since 1918 or before (tree age and species provided by K. Fetherston).

During the lifetime of a valley jam, several peak flow events may occur in which racked and loose debris forming a portion of the jam collapses and releases a wave of water and sediment in a dam-break type flood. A dam-break type of event occurred during the winter of 1993-94 at a large valley jam in the east channel of lower Alta Creek, which washed out approximately 3.5 hectares of 20-30 year-old *Alnus rubra* (Red Alder) up to 230 m downstream of the jam. Yet there was no perceivable change in the position or condition of the key members in the affected valley jam. The failure instigating the dam-break flow was limited to racked debris comprising about 4% of the jam's cross-sectional area. Although headward erosion associated with the failure extended 87 m upstream of the jam, the vast majority of sediment and WD retained by the jam remained intact.

While expansion of a valley jam's width across the valley floor can take years, vertical rates of sedimentation upstream of a structure can be extremely rapid. A large *Thuja plicata* (Western Red Cedar) bole present in Alta creek during my initial survey in 1993 initiated a small valley jam that formed during the winter of 1993-94, resulting in up to four meters of sedimentation and a three-fold reduction in slope upstream of the jam, from 0.062 to 0.019 (Figure 1-7c).

Channel aggradation resulting from the formation of valley jams can result in a topographic inversion where the channel bed is elevated above adjacent terraces; the

terraces are subsequently transformed into active floodways. Old-growth forest stands on these terrace surfaces can become partially buried as bed material is deposited on these surfaces with increasingly frequent flows. Active valley jams have been found in mainstem portions of the Queets River with bankfull widths of 50 m and valley widths of 500 m. A relic jam buried in fluvial gravel and which exhibited attributes of a valley jam, was found at RK 26.3, in the mainstem Queets River, where the bankfull width is over 100 m and valley width about 1600 m. Even though the height of valley jams tends to decrease downstream through a network as the valley floors widen, this relic jam was 8 m in height. Trees growing on surfaces above valley jams buried in fluvial gravel of Alta Creek and the Queets River indicate these structures can last more than 300 years.

In summary, valley jams result in two fundamental geomorphological changes: (i) at the channel reach scale they increase width, decrease depth and slope, and form major obstructions, creating anabranching channels where a single-thread channel previously existed; and (ii) at the valley scale they create large sediment and debris reservoirs and elevate large sections of the channel bed, inducing flows to inundate older surfaces with greater frequencies and to initiate new channels elsewhere on the valley floor.

1.5.2.2 Flow Deflection Jams

In large alluvial channels, the incremental recruitment of stream-side trees through bank erosion can result in distinct debris structures that deflect flow nearly orthogonal to the channel axis. Unlike valley jams, flow-deflection jams do not completely span a channel. Flow-deflection jams consist of in-situ key members and substantial quantities of raked and loose debris delivered during high flows (Figure 1-8a).

Flow-deflection jams contribute to channel complexity and local floodplain development in nearly all portions of the Queets drainage network excluding steep headwater channels. Formation of a flow-deflection jam typically begins when a key member tree falls into the channel. Trees usually enter the channel perpendicular to flow since bank erosion tends to proceed perpendicular to the channel axis. Once in the channel, the tree constricts flow around its rootwad and thereby accelerates bank erosion

and the recruitment of additional trees, a phenomenon noted in previous studies (e.g., Swanson and Lienkaemper 1978, Bisson et al. 1987, Nakamura and Swanson 1993). As this process proceeds, the channel widens, and the jam structure grows by further recruitment of trees from the eroded bank to occupy a larger portion of the bankfull cross-sectional area. Due to their position in the channel, key members recruited first are subject to the most severe drag during high flows and can rotate downstream to orientations of 20° - 45°.

The age structure of trees colonizing the key member stems often records this chronological sequence of jam development and is similar to valley jams except that the jam doesn't impound the channel. The oldest colonizing trees are found on the key members recruited first, and are thus located farthest from the bank (Figure 1-8b). Jam development decelerates when a major channel avulsion or cut-off occurs on either side of the jam or when debris racking onto the jam plugs the area between the eroding bank and recently recruited key members. Flow-deflection jams can develop into valley jams if their expansion impounds the channel.

As a flow-deflection jam continues to accumulate debris it can dramatically affect channel morphology. Large pools form directly upstream of the jam and extend along most or all of the jam's width measured normal to the channel. Slack water or eddies downstream of the jam results in sedimentation and bar development. Much of this sediment can originate from bank erosion associated with key member recruitment. The area downstream of the jam forms an arcuate wedge in plan-view that is bounded by the eroding bank on one side and by the jam on its upstream and channel margins (Figure 1-8a). The elevations of these depositional surfaces tend to correspond to floodplain elevations. Tree colonization on the depositional surface downstream of the jam appears to occur after it has reached elevations corresponding to the local floodplain and outside the wetted perimeter of the channel. Based on the similar age structure of forest patches growing on these surfaces, sedimentation appears to occur at the same rate over most of the surface. The dominant species colonizing the bar area is *Alnus rubra*, though conifers are common on key-member nurse logs.

Based on the age of the oldest trees on flow-deflection jams observed in the Queets watershed, flow deflection jams generally are abandoned after 5-15 years as the active channel migrates away from the jam. The structure is subsequently buried and incorporated into the river's floodplain where it remains until re-exposed by channel migration. Because key members are deposited in the channel bed, they can lie at relatively low elevations relative to in-stream flows and can remain saturated throughout much of the year and experience extremely low rates of decay. In such situations, a jam can repeatedly form a hydraulic control and natural revetment for long periods of time, allowing the associated forest patches to mature into large trees that eventually provide a recruitment source for key members.

1.5.3 Transport Jams

The third fundamental category of wood debris consists of material that subsequently experienced some hydraulic transport within the channel. Transport jams are the most diverse category of jam types. Observations in the field (Abbe and Montgomery 1996, Diehl 1997) and in laboratory flumes (Braudrick et al. 1997) have found that WD transport is coincident with the flow-line of maximum depth and velocity, and that deposition occurs at points where this flow-line is obstructed. Wood debris deposits typically occur where this streamline splits (i.e., upstream of obstructions and bars), upstream of bars where flow depth decreases, or on the outside of bends.

Although transport jams usually form the dominant WD structure in the mainstem channel of a large alluvial river, in-situ and combination jams can occur in smaller floodplain channels (i.e., side channels) within the same reach. Stable jams that initially formed in the main stem channel are often incorporated into the floodplain and thus, reflect previous positions of the river. Jams that were stable in the mainstem channel will be stable in any secondary floodplain channel, frequently influencing the locations of these smaller channels. Conversely, jams that form in a floodplain channel may not remain intact when the mainstem channel reoccupies the site.

1.5.3.1 Debris Flow Jams

Debris flow jams result from catastrophic deposition of WD entrained in debris flows initiated by shallow landsliding (e.g., Swanson and Lienkaemper 1978, Swanston 1991). No studies specifically address the structural characteristics of WD deposited by a debris flow, but several studies describe general characteristics (Swanson and Lienkaemper 1978, Keller and Swanson 1979, Benda 1990, Johnson 1991, Swanston 1991, Coho and Burges 1994). Ishikawa (1989) presents the most detailed description of WD accumulations associated with debris flows. These descriptions are summarized here because no debris flow jams were found in the surveyed channels of the Queets watershed. There is little doubt that debris flows occasionally occur within the Queets drainage network, but apparently they do not generally travel far downstream. This is not surprising when one recognizes that the abundant, stable WD structures within steep low-order channels of the Queets watershed likely retard the downstream propagation of debris flows, probably in the manner described by Swanson and Lienkaemper (1978, p.6). Also, although catastrophic disturbances such as landslides and debris flows occur naturally throughout forested mountain regions, studies in the Pacific Northwest have shown that their frequency increases dramatically in clearcut regions (e.g., Swanston 1991). Evidence of these events in channels draining old-growth regions (i.e., areas undisturbed by roads or other land use) has rarely been observed (e.g., Swanson and Lienkaemper 1978, Coho and Burges 1994).

Debris flow jams can grossly resemble valley jams because they commonly span the channel and retain large volumes of sediment upstream. In contrast to valley jams, however, debris flow jams lack key members and have a chaotic assemblage of WD with many different horizontal and vertical orientations. Whereas few of the tree boles which form the key members of a valley jam tend to be oriented such that the bole axis forms an angle greater than 45 degrees with the horizontal, vertical orientations of boles and bole fragments are common in debris flow jams. The key members of a valley jam are relatively dispersed, laying in the position in which they were recruited. The turbulent accumulation of WD at the snout of a debris flow jam may explain the chaotic structure

and tight packing. Debris flow jams can be very large structures, measuring several meters in height and over a hundred meters in length (e.g., Swanson and Lienkaemper 1978, Keller and Swanson 1979, Swanston 1991).

Sedimentation associated with the structures when they initially form is expected to have characteristics typical of debris flows, such as matrix-supported clasts and coarse-grained deposits along the margins of the flow. If a debris flow passed through a channel, some of the following evidence is usually seen: scour trails, run-up scour or deposition lines associated with super-elevation around channel bends, or the unique characteristics of debris flow deposits (e.g., poorly sorted, matrix supported, absence of grain imbrication). In the channels I hiked, I found no clear evidence that a debris flow had occurred. Evidence that some sort of catastrophic flow may have occurred was found in several locations, but never affecting more than 100 m of channel.

The presence or absence of stable wood accumulations in a channel subject to debris flows can influence the development and downstream propagation of debris flows by influencing their mass and velocity. Valley jams and log steps provide three mechanisms of reducing the momentum and run-out distance of debris flows and dam-break flood torrents: (i) material capture (trapping sediment and debris), (ii) flow deceleration due to slope reduction, and (iii) drag and flow dispersion imposed by obstructions.

1.5.3.2 Flood-Peak Jams

Large quantities of WD mobilized during high flows can become congested and form flood-peak jams. Such jams initiate under two distinct mechanisms: the gradual hydrograph rise typical of most flood waves, or the sharp step-like hydrographs characteristic of dam-breaks. Descriptions of debris deposits associated with debris flows and dam-break floods are almost entirely from regions that have been logged; the characteristics of these processes and deposits are poorly documented in old-growth regions (e.g., Swanson and Lienkaemper 1978, Coho and Burges 1994). Factors influencing the formation and attributes of WD jams associated with each of these

processes have been developed based on one structure deposited during the winter of 1994-95 in Alta Creek. This jam was the only one found that could be confidently associated with a dam-break flood in the 74 km of surveyed channels of the Queets basin.

The size range of WD entrained and transported through a channel will be a function of channel flow velocity, depth, and width. The size of debris susceptible to transport will be proportional to flow depth and flood stage. Floating debris will experience the least frictional resistance if suspended completely above the riverbed. As an example, assume an ideal channel free of obstructions, where the mean cross-sectional flow velocity reaches a maximum coincident with the maximum water elevation (stage), and where WD is advected no faster than the flow velocity. In this situation, the debris entrained during the rising limb of the flood hydrograph will accelerate to a maximum velocity limited by the flood wave celerity, and will result in maximum debris concentrations coincident with the flood crest.

Wood debris can move through a channel as either individual pieces or as congested accumulations (Braudrick et al. 1994, 1997). The velocity of individual pieces of WD is a function of their specific gravity, shape, size relative to the depth and width of flow, and channel boundary conditions; factors that influence the frictional resistance that a piece encounters. Wood debris moving at slower velocities is generally larger, denser, and distinctly tapered (i.e., bole with rootwad). This large, slower moving debris obstructs more rapidly moving smaller WD and can lead to congested accumulations. Debris accumulations are likely to be routed downstream until the flood peak has sufficiently diffused or the material comes to rest on channel obstructions, on the floodplain, or at the outside of channel bends. When debris accumulations become large enough and A_w approaches A_c , the debris mass will begin to decelerate under its own frictional resistance. At this point the debris can begin to reduce the flood wave celerity thereby causing water upstream of the accumulation to rise, and the flood hydrograph to take on a step-like form atypical of most floods (e.g., Costa and Schuster 1988). Elevated water levels can then result in buoyant forces sufficient to dislodge the jam, and will continue transporting it downstream. It is through this process of temporary impoundment of the river and

catastrophic failure that dam-break events occur (Coho and Burges 1994). Backwater effects of a jam elevate the water surface elevation upstream, which can allow additional WD accumulation at higher elevations and increase the jam's height and stability. In the process of "hanging up," a jam can also break apart and be routed downstream as smaller accumulations. Whether a jam will diffuse or break-up into small stable structures, or stabilize en-masse, or continue to route downstream depends on the presence or supply of key members. In-stream WD not entrained by the flood crest can form major obstructions that trap mobile debris upstream and thereby diffuse material that otherwise would have contributed to the formation of a flood peak jam or debris torrent. A series of stable structures can also diffuse and retard a flood wave through local backwater effects that increase the storage capacity in those channel reaches (Gregory et al. 1985).

The perception that debris in transport during floods accumulates into massive congregations was challenged by Chang and Shen (1979) who found that debris was rarely observed floating in large accumulations in large rivers. In contrast, they claim that massive debris accumulations entering a stream all at once (e.g., from debris flows, landsliding, bank slumping), broke up or untangled and floated freely. Though Chang and Shen (1979) compiled observations primarily from managed river systems, they do imply that large accumulations such as those associated with dam-breaks (Coho and Burges 1994) do not travel far in large channels before breaking up or coming to rest along the channel margins.

Flood-peak jams can form channel-spanning structures that remain intact after the flood recedes (Johnson 1991, Coho and Burges 1994). The flood-peak jam surveyed in Alta Creek was composed of relatively small debris characterized by stem fragments and small trees with no attached rootwads. Previous studies have also found that the debris associated with catastrophic events (i.e., flood torrents, debris flows) tends to be relatively small, such as waste left behind by logging operations (e.g., Swanson and Lienkaemper 1978, Swanston 1991). Wood debris structures composed of relatively small logs and lacking key members are more susceptible to decay and catastrophic failure that could trigger dam-break flood events.

The flood-peak jam observed along Alta Creek left the creek and cut a 65-m swath through a young stand of *Alnus rubra* before being deposited on a pre-existing valley jam (Figure 1-9). Observations of similar types of jams associated with dam-breaks (Coho and Burges 1994) suggest that these jams commonly avulse into adjacent forests where the debris becomes deposited against standing trees. When a flood-peak WD accumulation enters a channel bend, angular acceleration and momentum of the flow can drive the material into adjacent forest stands. If riparian vegetation is of sufficient size it can form a barrier where debris is deposited and floodwaters are dispersed over the floodplain. If not, the flow and debris can cut a new channel through the riparian forest. The resistance of standing trees to such catastrophic flows will depend on whether their root cohesion and bole strength is greater than the external moments and shear imposed by the flow (e.g., Ishikawa 1989, Coho and Burges 1994). In addition to riparian trees, other types of obstructions can play a significant role in limiting the downstream propagation of flood-peak debris. The Alta Creek flood-peak jam was deposited against a valley jam that had formed at least 40 years earlier (Figure 1-9). The key members of the valley jam were readily distinguished by their large size, intact rootwads, orientation normal to valley axis, and the heavy coats of moss, shrubs, and trees growing on top of them, as well as the alluvium in which some were buried.

Similar to debris-flow jams, flood-peak jams have a distinctive “snout” composed of two distinct WD populations differentiated by bole orientation relative to the direction of flow when deposited: orthogonal WD is deposited about the centerline of flow, and is flanked by deposits of oblique WD (Figure 1-9).

Flood-peak jams differ from debris flow jams in several ways. Sediment deposition associated with a flood-peak jam typically consists of well imbricated clasts, negligible fines, fining-up sorting, and an absence of levee deposits. In addition, fewer of the stems comprising the flood peak jam are inclined at a high angle relative to the bed, as commonly found in the debris flow jam.

1.5.3.3 Bankfull Bench Jams

Bankfull bench jams occur most frequently in headwater channels with gradients of 0.06 - 0.20; they form the dominant WD structure in steep tributaries of the Queets River. Log structures in these accumulations consist of one or more key members oriented oblique to flow and wedged into irregularities or obstructions in the margins of the channel, such as bedrock outcrops or boulders (Figure 1-10). A substantial portion of the cross-sectional area of the channel is left unobstructed because the jams form along the margins of the channel. Deposition of key members creates a structural barrier or natural revetment resulting in low shear stress areas along the channel. These hydraulically sheltered areas accumulate both fine sediments and WD, leading to development of benches at or above the elevation of bankfull flows. Smaller WD racks up on the key members and loose pieces collect on the bench surface. Vegetation patterns associated with bankfull bench jams appear to correspond with substrate; grasses and shrubs dominate sediment-covered surfaces and trees colonize WD. Bankfull bench jams have a significant effect on alluvial morphology and riparian ecology by effectively extending the upstream limits of floodplain deposits and communities. In all of the moderately to highly confinement study reaches ($S > 0.06$), forested floodplains were commonly associated with bankfull bench jams and occasionally with active or relic valley jams.

1.5.3.4 Bar-Apex Jams

Bar-apex jams are one of the most common stable log structures in large pool-riffle channels. These distinctive structures typically occur at the upstream end of mid-channel bars and forested islands. Unlike unstable WD accumulations deposited on existing bars, bar-apex jams play an integral role in the formation of the associated bars and islands. Bar-apex jams can initiate formation of a bar in the thalweg of a channel or accelerate the development of a pre-existing bar. Although most of the WD is only visible at the upstream head of the bar, the structure may consist of one or more key members that extend through much of the bar's length. Bar-apex jams can form the principal boundary roughness component in a reach, and these jams can also dominate the morphology and

pattern of aquatic and riparian habitat in large pool-riffle channels (Abbe and Montgomery 1996b).

Bar-apex jams consist of three distinct structural members. The jam initiates when a key member deposits in the channel thalweg, on a mid-channel bar or the toe of a point bar. This key member is always parallel to flow and usually has an attached rootwad facing upstream (Figure 1-11a). The second structural component of the jam consists of racked members that are deposited against the key member root wad and oriented with their bole axes normal to flow. Wood debris that extends into the unobstructed portion of the flow will likely experience considerable torque that will either break or rotate the tree bole. The third structural component is debris that has rotated and deposited along the flanks of the key member, referred to as oblique members. These structural components can be distinguished by the WD orientation (Figure 1-11a). The resulting form can be likened to an upstream pointing arrowhead. A more complete description of these jams and their evolution is presented by Abbe and Montgomery (1996).

Deep pools form beside the jam apex, and deposition of fine sediments occurs immediately downstream of the apex. These morphologic features result from changes in flow due to the jam's presence. Three distinct alluvial features are formed by bar apex jams: flow divergence and deceleration upstream of the jam results in deposition of an arcuate bar; flow convergence and acceleration into the bed, vortex flow, and lateral acceleration of flow around the upstream margins of the jam create a crescent shaped pool; and deceleration within the flow-separation envelope in the lee of the racked members creates a central bar composed of relatively fine sediments along the bole of the key member (Figure 1-11a). In wide pool-riffle reaches of the mainstem Queets River, bar apex jams are a principal factor in pool formation, accounting for the majority of pools and the largest range of pool depths.

Although vegetation can rapidly obscure WD accumulations, the age structure of riparian forest patches can sometimes be used to recognize the jams. Vegetation colonization corresponds to the deposition of substrate sufficiently elevated above the bed (i.e., approaching bankfull or floodplain elevations) and protected from frequent

disturbance. Thus, trees initially colonize the protected and elevated areas immediately on and around the basal portion of the key member. Colonization proceeds downstream along the key member bole as deposition of sediment and WD progressively enlarges the central bar. The resulting age structure of the associated forest patch progressively decreases downstream and normal to the bole axis of the key member (Figure 1-11b). Bar-apex jams appear to be the principal mechanism of island formation within pool-riffle reaches of the mainstem Queets River: they are associated with 72% of the forested islands surrounded by channels > 24 m in width. Within this same 52.6 km section of the Queets River, 98% of the bar-apex jams associated with islands in 1985 remained in 1993. Island development increases the stability of a bar-apex jam by adding root cohesion and the additional mass of overlying trees to the structure.

1.5.3.5 Meander Jams

A variety of WD accumulations occur along the outer margins of meander bends in large alluvial channels. Many of these accumulations are simply unstable debris deposited in shallow portions of a channel, but some are stable structures (e.g., flow deflection jams, see 1.5.2.2). Meander jams form another type of stable structure that, unlike flow deflection jams, are composed of debris that underwent downstream transport (Figure 1-12). The name “meander jam” was chosen because these structures are commonly found along the outer, downstream bank of channel bends or meanders, though the jams do not necessarily form at bends. Meander jams establish local (sub-reach scale) hard points within alluvial valleys that limit channel migration and influence meander curvature.

Meander jams can initiate in several different parts of an alluvial channel, but subsequent development of the jam and channel tends to produce similar conditions, making it difficult to determine the initial conditions at a particular site without detailed geomorphic and historical analysis. Field observations from 1993 to 1995 and aerial photos (1968, 1976, 1985, 1993, 1996, and 1997) were used to assemble a conceptual model of meander jam development. Initial deposition of two or more adjacent key members parallel to flow (when deposited) with their rootwads aligned along a transect 70-

90° to flow (Figure 1-12). A meander jam introduces a local flow deflection that can allow the jam to accumulate additional debris and significantly decrease the channel's radius of curvature (Figure 1-13). Early in jam development, flow between the key members adds additional sediment and debris to the jam. Sediment accumulates along the key member boles and initiates bar formation. Debris accumulates against key member rootwads. Racked members generally have bole orientations 90° +/-20°. Racked debris progressively restricts the flow area between the key members, diverting the principal streamline parallel toward the opposite bank along the axis of racked debris. Flow obstruction leads to an increase in water surface elevation (wsel) upstream of the meander jam, allowing debris to be deposited at higher elevations, and increasing the size, mass, and stability of the jam. The hydraulic gradient set up by this local increase in wsel re-directs the principal streamline along the upstream plane of the jam and can also lead to overbank flow across the adjacent floodplain and possible channel avulsion (e.g., Miller 1995).

After a jam has initiated, it remains stable, but the channel can continue to migrate. The outer margin of the meander is held in place at the jam while continuing to migrate upstream of the jam. The result is a progressive decrease in the channel's radius of curvature and increase in meander amplitude, contributing to additional increases in wsel upstream of the jam (Figure 1-14).

Eventually the increased wsel upstream of a meander jam can lead to either one or a combination of the following: an avulsion in which part or most of the flow bypasses the jam through what had previously been the floodplain adjacent to the jam (Figure 1-14); or a channel cutoff across the point bar or the recently formed floodplain left behind by channel migration since the jam formed. This process can re-position the principal streamline to bypass the meander jam entirely, though a side channel and pool often are commonly maintained along the jam margins.

The width of a meander-jam, measured orthogonal to key member orientation, commonly exceeded 200 m for jams observed along the lower Queets River. Meander-jam widths can exceed the bankfull width of the channel and can obstruct 20% or more of the valley floor, and thus are likely to influence overbank as well as within channel flows

(Figure 1-12). Even though meander jams form entirely within the bankfull channel, only the upstream margin of the jam, consisting of racked WD and part of a key member rootwad, will usually remain within the active channel. This sometimes gives the impression that WD is piled up against a pre-existing bank. Meander jams, just like bankfull bench jams (see 1.5.3.3), actually form the bank along channel bends.

The distributions of bankfull bench and meander jams can overlap, although bankfull-bench jams are primarily found in headwater streams and meander jams in large, low-gradient alluvial channels. The principal means of distinguishing these two jam types is the composition of their foundations. Bankfull bench jam stability depends on the strength of the WD and the resisting forces provided by obstructions or irregular boundaries (i.e., boulders, banks) upon which key members are deposited. In contrast, the stability of meander jams depends on the resistance provided by key members, sediment deposition around the key member boles, and the quantity of racked debris.

As a meander jam grows, erosion accelerates along the opposite bank due to the deflection and constriction of the flow, which initiates changes in channel planform downstream. Channel curvature is exaggerated upstream of the jam, concentrating flow along the same side of the channel as the jam. Bank erosion increases the amplitude of the upstream meander and decreases its radius of curvature. Channel meanders adjacent to static features or “hard points” such as bedrock and stable WD jams have reduced radii of curvature when compared to free-formed, unobstructed meanders (Figure 1-13).

Meander jams influence the local water surface topography and energy gradient of a river through several mechanisms. Backwater conditions can occur upstream of the jams due to an increase in boundary roughness, drag imposed on the flow by the jam, and constriction of flow around the jam. The reduction in the channel’s radius of curvature, r_c , upstream of the jam increases the transverse head gradient across the channel.

Large pools are associated with every active meander jam observed in the Queets and other rivers of western Washington. The pools are located along the upstream and lateral margins of the jams due to local vortex flow that scours along the upstream margin of the structure, with maximum scour usually observed near the channel edge of racked

debris. Surveys of pools in the Queets River in 1993, 1994, and 1995, all found the deepest pools to occur along the margins of meander jams (Abbe and Montgomery 1996b).

1.5.3.6 Unstable Debris: Bar Top Jams and Bank Edge Jams

Stable jams store a vast quantity of organic debris and to some degree regulate the flux of WD in the Queets River system, but large quantities of mobile WD are also deposited along channel banks and on the floodplain during high flows, and on bar tops as flood peaks recede. These deposits have negligible impact on channel morphology or bed texture because the debris in unstable deposits is likely to continue downstream with the next bankfull event. Bar top jams refer to such unstable accumulations found on bars within the bankfull channel. These deposits commonly consist of a chaotic assemblage of racked and loose WD with a large variance in orientations (Figure 1-15a). They may be slightly more hospitable to colonizing vegetation than areas with no wood because of their nutrients and moisture retention, but they do not offer the structural protection provided by stable jams. Because they initiate in areas of flow deceleration already associated with sediment deposition, they are commonly buried and incorporated into alluvial stratigraphy. From the small size of WD comprising these deposits and their deposition at higher elevations (where debris is unlikely to remain saturated) rapid decay and breakdown are predicted when compared to the larger WD deeply buried near or below the baseflow water table (such as found in stable jams).

Bank-edge jams are associated with bankfull or greater flows that inundate the upper margins of a channel. Loose, mobile debris can accumulate along the bank edge and rack up against stream-side vegetation (Figure 1-15b). These deposits tend to consist of WD parallel to channel flow, although material racked onto trees can introduce a wide range of orientations. These deposits rarely influence channel or floodplain morphology, although Kochel et al. (1987) document that similar log accumulations (bank edge jams) racked up along trees adjacent to a gravel-bedded stream in Virginia acted locally to retain bed material that elevated the channel bed by up to 1.50 m. Similar wood accumulations

racking up against riparian trees have been observed after extreme floods in the Oregon Cascades (G. Grant, pers. comm., 1997). Unstable WD deposits lack key members. In a stable jam, racked WD accumulates against the key member as if it were a bank and in fact precedes development of an alluvial bank (Figure 1-15c).

Bank edge jams can become very large. When these deposits attain vertical dimensions exceeding the bankfull depth of the channel, they can form effective bank revetments that limit channel migration. Examined from upstream, these “bank revetment jams” are indistinguishable from meander jams or flow deflection jams. The critical difference is that downstream of all the racked WD, meander jams and flow deflection jams have key members. With time, key members become buried under alluvium, WD and vegetation, and can be difficult to find. Bank revetment jams have no key members and are simply racked up against a pre-existing bank. A change in the channel’s alignment can rip apart the racked WD, destroying a revetment jam and eroding the banks it had protected. The key members in flow deflection or meander jams can be sufficient to limit erosion and collect new racked WD. Revetment jams are also more susceptible to decay because they are composed entirely of racked debris smaller than key members.

1.5.3.7 Rafts

Historical references from early exploration and land surveys describe the presence of extensive floating accumulations of WD, commonly referred to as “rafts,” that completely blocked large lowland rivers in forested regions of the world (e.g., Lyell 1830, Gillespie 1881, War Department 1898, Lowrey 1968, Clay 1949, Philips and Holder 1991). Raft accumulations could have a significant influence on the morphology, planform characteristics, gradient, and sediment-transport capacity of large alluvial river valleys (e.g., Triska 1984, Harvey et al. 1988), and even on the development of coastal deltas (e.g., Shepard and Moore 1960, Kanen 1970, Hartopo 1991). Because I observed no mainstem rafts in the Queets, I have constructed a conceptual model of these rafts based on historical mapping and descriptions (Figure 1-16).

The historical accounts of mainstem rafts are primarily from large rivers with much wider valley bottoms (channel migration zones) and with lower gradients than the Lower Queets River. The absence of rafts on the Lower Queets may be in part due to human impacts. Much of the Queets Valley bottom within 30 km of the Pacific was cleared by homesteaders in the late 1800s and early 1900s, removing old growth that would have certainly contributed key members, based on the subsequent erosion of many homesteads. The higher gradient and relatively narrow valley bottom of the Queets probably also inhibits raft formation.

The first recorded observation of a large channel-spanning wood accumulation or raft in the lower Colorado River, Texas (drainage area = 110,190 km²), was by Spanish explorers in 1690 (Clay 1949). Prior to removal of this WD jam by the U.S. Army in 1927, the shoreline at the river's confluence into Matagorda Bay exhibited no protruding delta. Directly after removing the jam, a pronounced delta began to extend into and eventually across the bay (Kanes 1970, Hartopo 1991). Based on the difference between topographic maps of the site, approximately 14×10^6 m³ of sediment was introduced to Matagorda Bay over a 29-year period after raft removal. Dramatic geomorphic change after WD raft removal also has been described in the Red River, LA, where a complex of massive WD rafts was documented in the earliest records of European exploration, and Native Americans could not recall a time when jams did not block the river (Lowrey 1968, Triska 1984). Prior to its removal at the end of the nineteenth century, the Red River Raft complex of channel-spanning jams extended 257 km from Shreveport, Louisiana to Fulton, Arkansas, and created a vast mosaic of anastomosing channels and large lakes within the Red River valley.

Veatch (1906) reported that a 24-km reach of the Red River upstream from Shreveport incised its channel from one to five meters in the 19 years after the last log jam had been removed (1873-1892). Beginning with initial conditions 13 years after final jam removal (therefore underestimating the influence of the jams), Harvey et al. (1988) examined the geomorphic changes experienced by the Red River over the next 92 years (1886-1980), and estimated that the river's sediment transport capacity increased by a

factor of six (Table 1-3). The increase in channel width may have been due to the conversion from a system of numerous anastomosing channels to a single channel.

Massive WD accumulations and rafts were recorded in many of the large, low-gradient rivers of Oregon and Washington, and often blocked the channel and exhibited similar effects to those in the southeastern U.S. (e.g., Gillespie 1881, War Department 1898, Russell 1909, Sedell and Frogatt 1984). Removal of these large wood accumulations had dramatic effects on flood routing and the frequency of floodplain inundation. A raft jam spanning the width of the Skagit River over a length of 1.21 km (6.4 km downstream of the town of Mount Vernon, WA) caused “the river to overflow its banks annually, flooding 150 mi²” (Habersham 1881, p.2606). The Skagit floodplain was inundated up to 0.30 - 0.61 m several times a year prior to raft removal, but after removal even a record spring flood failed to over-top the river banks (Habersham 1881).

1.5.4 Summary of Jam Types

I have attempted to distinguish jam types using three basic conditions: (i) where in a drainage basin they tend to be found; (ii) the principal mechanism by which they remain in place; and (iii) unique characteristics of the WD and jam dimensions relative to channel width (Tables 1-4a, b, c). WD jam types can be identified by the orientation and size of individual pieces. Plotting these two characteristics in a rose diagram reveals distinct differences among different jam types (Figure 1-19). Using the same rose plot, but defining the magnitude of each orientation range based on the number of pieces, will tend to over emphasize the significance of racked and loose debris. Many jams will only have 1-4 key members and 10-100 times as many racked pieces. While key members often account for a small fraction of the individuals in a jam, they can compose most of the jam’s wood volume (see valley jam, flow deflector jam, and meander jam examples in Figure 1-19).

Jam types can be difficult to distinguish in the field because the most visible portion of the jam is usually racked debris, which cannot by itself distinguish a jam type. To identify jam types, the presence and characteristics of key members, which are often buried

and covered by vegetation, must be identified. For example, it would be difficult to distinguish the differences between some flow deflection, meander, and bank revetment jams by looking at their racked WD. Flow deflection and meander jams are distinguished by the orientation of their key members; bank revetment jams have no key members, and the racked WD accumulates along a pre-existing bank.

1.6 Wood Debris Jam Frequency

My observations from the Queets River indicate that WD accumulations are abundant and can significantly affect the channel and floodplain morphology of an old-growth-forest mountain-river network. Because the lower portions of the Queets were affected by homesteading and logging from 1880 to the 1930's, the current distribution of stable WD provides minimum estimates of pre-settlement extent of WD accumulations. Wood debris has accumulated in channels throughout the upper Queets basin, but was sparse in two types of channels: confined, steep bedrock reaches with few flow obstructions, and large bedrock and plane-bed reaches with significantly greater slope and flow depth (i.e., stream power) than pool-riffle reaches with similar drainage areas. The frequency of log steps and jams in bedrock and plane-bed channels decreases with increasing drainage area. The frequency of jams increases with drainage area up to about 300 km², above which they gradually decrease. Valley jam frequency peaks at drainage areas of about 20-30 km² where the channel gradient is about 0.04 and there is a transition from confined channels with bedrock exposure to unconfined alluvial channels.

The frequency of different types of stable jams varies at different points of the Queets drainage network, suggesting that there are specific types of jams that are associated with different channel conditions (Figure 1-17). The frequency of different types of WD accumulations varies systematically downstream through the watershed (Figure 1-17), although anomalies in jam frequency occur in association with significant changes in channel conditions due to geological controls (e.g., hanging valleys, bedrock confinement, geological contacts, or glacial moraines). In-situ jams occur most frequently in headwater channels, but my surveys of mainstem channels do not include side channels within the

alluvial floodplains of the Queets, where in-situ jams were common. In channels where in-situ debris forms most of the key members, combination jams form the majority of stable jam types. Transport jams are found in channels where flows are sufficient to move trees entering the channel. The mobility of individual pieces of WD appears to depend on their size and shape, as well as the depth, curvature, and unobstructed width of the channel.

1.7 Wood Debris Stability

Stability refers to the ability of something to remain intact and in-place over time. Bisson et al. (1987) defined stable logs as those not susceptible to frequent movement. I consider “stable” WD pieces to be those which have a significant effect on channel bed morphology and/or trap additional WD and that are unlikely to move downstream during a bed-mobilizing flow. By controlling flow conditions, stable WD influences both the deposition and scour of the channel bed and bank (e.g., pools, bars, bed textures) and ecological attributes (e.g., nutrient reservoirs, cover).

Log size has been repeatedly reported as the principal factor controlling log stability in a given channel (e.g., Swanson and Lienkaemper 1978, Toews and Moore 1982, Bryant 1980, Bilby 1979, Grette 1985, Bilby and Ward 1989, Nakamura and Swanson 1994). Tree bole geometry has been treated as either a simple cylindrical or conical model. Wood debris transport is also related to its submerged cross-sectional area for a given flow event (i.e., bankfull flow). Boles with lengths greater than one-half the channel bankfull width appear to define stable logs in small streams of the Pacific Northwest (Swanson and Lienkaemper 1984, Bilby and Ward 1989).

A dimensionless plot of the ratio of basal bole diameter, D_b , to bankfull depth, h , versus the ratio of total tree or log length, L , to bankfull width, W , reveal distinct domains for loose, racked, and stable WD measured in the Queets watershed (Figure 1-18). Excluding large channels (i.e., $W > 50\text{m}$), ratios of $D_b/h > 0.5$ and $L/W > 0.5$ offer a rough approximation for delineating key members. This relationship changes for different locations in the channel network. In small channels, the lower limit of L/W for key members approaches unity while D_b/h remains at 0.5, and in larger channels D_b/h

increases toward unity while L/W approaches zero. Rootwads have a dramatic effect on WD stability by effectively increasing D_r/h . The importance of rootwads is described in chapter 3.

The flow depth at which a cylindrical bole will float if situated entirely in an unobstructed channel is controlled by the diameter and specific gravity, and is independent of the length of the bole. In geometric models more representative of natural WD (e.g., boles with rootwads), such as tapered cones, tree length can have a secondary effect on the centroid elevation, which is primarily controlled by the maximum diameter (Abbe et al. 1997, see chapter 3). In contrast to length, diameter serves as a proxy for WD strength (i.e., internal bending moment $= f(D^3)$ and decay longevity $(\propto D)$). Observations from the Queets watershed show that WD stability depends on diameter, especially in large channels where bankfull widths tend to exceed the maximum length of in-stream debris.

The shape of WD can significantly affect log stability, but remains a poorly understood aspect of WD in fluvial systems. Swanson et al. (1984) reported that unstable debris generally consisted of stem fragments less than half the bankfull width in length and lacking rootwads, whereas large stems with attached rootwads observed in the same channels had remained in place over 70 years. Other observations that boles with intact branches and rootwads are likely to increase stability (e.g., Bisson et al. 1987) are supported by data collected in the Queets watershed. Several key members had bole diameters $\leq 0.5h$, but consisted of two or more stems attached to a single rootwad and estimated centroid elevations $>0.5h$. The mechanical breakdown of tree boles and limbs creates a lot of logs lacking a rootwad or significant taper. The presence of rootwads and multiple boles effectively increases the ratio of D/w and increases piece stability. Eighty-two percent of the 319 key members cataloged in the Queets watershed had attached rootwads; in channels greater than 40 meters in bankfull width, ninety-nine percent (112 key members) had attached rootwads. The influence of log diameter, log shape, and rootwads on log stability remains one of the most poorly explored aspects of in-stream WD.

1.8 Discussion

The Queets River watershed offers a rare opportunity to examine patterns of WD accumulation in a channel network which has received substantial quantities of WD representative of a wide range of sizes throughout the last 10,000 years. Observations from the Queets may be representative of many forested regions prior to human disturbance. Geographic differences in the spatial distribution of WD accumulations within a channel network would be expected due to changes in tree distribution and size, channel size, and fluvial processes (e.g., debris flows, channel migration). I suspect that additional types of WD jams occur in regions with distinct differences in trees (size, taper and distribution), channel characterization, climate, or fluvial processes (e.g. ice flows). But examples of particular jam types described above have been observed in rivers draining the western and eastern Cascades, the Bitterroot Mountains of western Montana, the Canadian Rockies, the Rio Beni in eastern Bolivia, and the New Zealand Alps. Each of these regions is characterized by distinctly different runoff hydrology and forest communities.

The position of a tree bole when it first enters a channel can have a significant influence on its own stability and how it effects the channel. Once deposited in the channel, WD is subjected to stresses proportional to the submerged area normal to flow, and the fluid density and velocity. Stable debris must withstand the impact of material moving downstream and static loads of debris and sediment accumulation. Wood debris that succumbs to these forces and moves downstream can either go on to rack onto other jams or form a different type of jam. The relative orientation of key and racked WD within a channel can distinguish different types of WD jams characteristic of different parts of a drainage network.

Topography adjacent to the channel will influence the orientation at which a tree falls into the channel. Trees are more likely to fall down-slope as hillslope gradient increases, and thus trees no farther from a stream than their height will tend to land orthogonal to the channel (Van Sickle and Gregory 1990). This provides one possible explanation for WD commonly observed suspended over small confined channels. If unobstructed, a fallen tree will move down a steep hillslope either by rolling, with its bole

axis 90° to slope, or by sliding with its bole axis aligned down the slope. A cylinder encounters less friction over a relatively smooth slope when rolling as opposed to sliding (Onda and Matsukura 1997). But trees which fall over with their roots largely intact are not cylinders, and behave quite differently. The rootwad is the point of maximum friction, and thus tends to align the tree with its crown pointed downslope. Fallen trees on steep hillslopes in the Queets basin, both with and without rootwads, were usually oriented parallel to slope, and those normal to slope were often held in place, at least partially, by standing trees. Most of the large logs observed in steep tributaries of the Queets were oriented slightly oblique to the channel, probably because they couldn't fit otherwise. Despite being oblique to the channel, these logs frequently formed step structures between banks or between pre-existing obstructions. Similar-sized logs suspended over the channel rarely exceeded the number in the channel except in confined low gradient channels (i.e. gullies) where the suspended WD sometimes was the only WD observed.

Along an eroding bank, trees fall into the channel into the direction from which erosion is proceeding. Since an eroding bank usually retreats normal to flow, trees enter the channel oriented nearly orthogonal to flow ($\theta = 90^\circ$ or 270°). Wind-throw deposits will tend to be oriented at angles representing the difference between the direction (compass azimuth) which the dominant wind is blowing, ω , and the direction the channel is flowing, ζ . Thus, for sites where the principal winds blow east down into the valley of a south flowing channel such as Harlow Creek (Figure 1-1), $\omega \approx |\theta - \zeta| \approx |90^\circ - 180^\circ| \approx 90^\circ$. Where Harlow Creek enters the Queets valley, the two valleys are nearly orthogonal, so for this portion of the Queets, wind throw would result in distinctly different initial WD orientations, $\omega \approx |\theta - \zeta| \approx \zeta |90^\circ - 80^\circ| \approx 10^\circ$. Once in the channel, the tree might remain as it fell, rotate, or be carried downstream. Stable jams depend on the recruitment of trees capable of forming stable snags, which are referred to as key members.

Key members comprise a small percentage of the WD recruited to channels, yet they govern the occurrence, construction, and effects of WD jams in the channel network. The diversity and frequency of jams depends on the presence of key members. The supply of key members capable of transforming channel morphology and even the type of channel

(Montgomery, et al. 1996) are dependent on the extent and characteristics of riparian forests both upstream and adjacent to a site. Thus the elimination or reduction in the number of large trees in a forest can significantly affect a channel's hydraulic geometry, planform characteristics, gradient, texture, and floodplain development.

In-stream WD accumulation will therefore depend on the size and distribution of riparian trees. In turn, the distribution in tree species, age, and size in a riparian forest are directly influenced by fluvial processes, especially along alluvial channels with floodplains. Bedrock, cascade, step-pool, and plane-bed channels typical of headwater streams generally experience little lateral migration, and were usually flanked by old growth forests. Riparian forest disturbance in these headwater regions of the Queets drainage network is typically associated with infrequent mass wasting events (e.g., landsliding or debris flows), which allow mature forest stands to develop. WD recruitment in headwater channels thus tends to be infrequent, localized inputs relatively concentrated with trees sufficiently large to form key members. In contrast, recruitment along a large, migrating channel occurs much more frequently along much of the channel, but the WD recruited includes few trees sufficient to form key members.

Low gradient floodplain forests primarily consist of early-seral-stage deciduous communities dominated by *Alnus rubra* (e.g., Fonda 1974, McKee et al. 1984). The deciduous trees in these early seral stages rarely attain the sizes found in late-seral-stage conifer communities. Wood debris recruitment from these early-seral-stage forests accounts for the majority of drift or mobile WD that goes on to form the racked and loose members found in jams or in overbank deposits on the flood plain. Occasionally, a group of several *Alnus rubra* or *Acer macrophyllum* boles attached to the same rootwad were observed forming key members in locations where the individual tree's chance to form a stable snag was negligible. But even when small trees team up to successfully form a stable snag, they will be subjected to more rapid bio-chemical and mechanical decay than the single bole key member within the same reach, and are thus less-likely to persist as long.

Channel surveys in the Queets drainage network show that the recruitment of large trees is responsible for most of the flow obstructions occurring throughout the watershed.

Local exceptions occur, principally consisting of bedrock channels and large boulder plane bed channels where big trees rarely fall into the channel and the channel's transport capacity is greater due to high gradients and flow depths. Any WD entering these reaches from upstream will pass through the reach, since it has already moved through a reach with a lower transport capacity. The key members formed by large trees are the principal mechanism of retaining and diffusing mobile WD, especially in large channels where the quantity of mobile WD far exceeds that forming key members. If the number of key members is reduced, the corresponding reduction in stable obstructions will decrease the number of secondary channels, increase the size of the mainstem channel, and decrease the channel curvature. All these changes diminish the system's complexity and increase its transport capacity, thus destabilizing WD. Due to the low percentage of large trees capable of forming key members, large river channels are most sensitive to these changes. Despite making up a small percentage of riparian trees on the Queets River floodplain, large trees have a significant effect on the river. Big trees entering the Queets River form natural revetments that protect small areas of the flood plain that make it possible for similar trees to again occur in frequently disturbed environments. Through this process of creating forest refugia, log jams ultimately ensure a future source of key members.

The reduction in key members will also have significant effects on small headwater channels where stable jams are responsible for much of the sediment storage. Key members create jams, converting channels from bedrock to alluvial. Conversely, a loss of key members will reduce the extent of alluvial channels within a network (Montgomery et al. 1996). Since recruitment of large trees along these headwater channels appears to occur on time-scales associated with mass wasting events (several thousand years), channel incision could further reduce the chances of WD entering or staying in the channel. This interpretation clearly implies that forest clearing can have irreversible consequences to the physical landscape and biological communities.

The dearth of wood debris in channels today reflects the human legacy of channel alteration driven by expansion of agricultural and industrial development, navigation, and flood control. Historical observations of large, pristine rivers clearly elucidate that wood

debris in the form of snags, planters or chicots, jams, and rafts were ubiquitous river features. In a description of the abundant snags in the Mississippi River and its tributaries McCall (1984, p.181) noted: "It is difficult today to picture the size of those underwater trees, for today's forest trees do not compare with the first-growth giants that became snags in rivers, many of them three to six feet (1-2 m) in diameter and imbedded in the channels to a depth of ten to fourteen feet (3 - 4.3 m)." Sycamore trees forming snags in rivers of the southern U.S. were commonly 1.5 to 3.6 m in diameter (Dorsey 1941). Prior to the 1800s, many of the deciduous trees of Vermont commonly reached diameters of 1.2 to 1.5 m and heights of 60 m; some common pines were even larger (Outwater 1996). Clearly, old growth forests across much of North America contained abundant trees capable of forming key members in a large range of channels and initiating the massive WD jams common in North American Rivers (Lyell 1830, Russell 1909, Veatch 1906, Keller and Swanson 1979, Sedell and Froggatt 1984).

1.9 Summary

In-stream WD exhibits patterns of systematic accumulation within a channel network that result in distinct structures or jams that reflect characteristics of the WD and the channel. Observations from the Queets River watershed have been used to identify nine distinct types of WD accumulation that occur systematically through an old-growth channel network. Two additional types of WD accumulation have been identified based on data from managed watersheds (debris flow jams) and based on historical records (rafts). Each of these eleven WD accumulation types falls into one of three basic categories of WD jams defined by key member movement: in situ, combination, and transport (Figure 1-20, Table 4). Different types of WD accumulations reflect local forest conditions, physical processes, and physiography. These factors both influence jam development and also are subsequently affected by jam formation. Wood debris jam types are distinguished by patterns of WD deposition, morphologic changes to the channel, and characteristics of associated forest patches. The size and type of WD accumulations found in the channel vary in frequency as a function of drainage area and channel type.

Prediction of how landscape disturbance and change may affect WD jams and forested river systems can be based on a better understanding of WD accumulation, stability and longevity. Sufficiently large trees are capable of forming stable flow obstructions that alter the fundamental character of a fluvial system by increasing morphological complexity and dissipating energy. Channel change attributed to WD can set-up a positive feedback system that tends to increase WD recruitment and reduce the channel's capacity to move WD.

Forest cover can significantly affect fluvial processes and landform throughout montane channel networks. I believe rehabilitation of channels and riparian corridors involving in-stream structures can be significantly enhanced by designing structures that emulate natural analogs such as those described here. The diversity and productivity of riparian and aquatic habitat depend on a plentiful and sustained supply of key members capable of initiating WD jams and perpetuate the presence of large trees in riparian forests. In addition, stable log jams significantly enhance the ability of a river system to buffer the impacts of disturbance, such as elevated sediment loads. Eliminating or reducing the supply of the largest and therefore potentially most stable WD can have significant geomorphic consequences, can result in deleterious impacts to aquatic and riparian communities, and can have potential long-term physiographic effects.

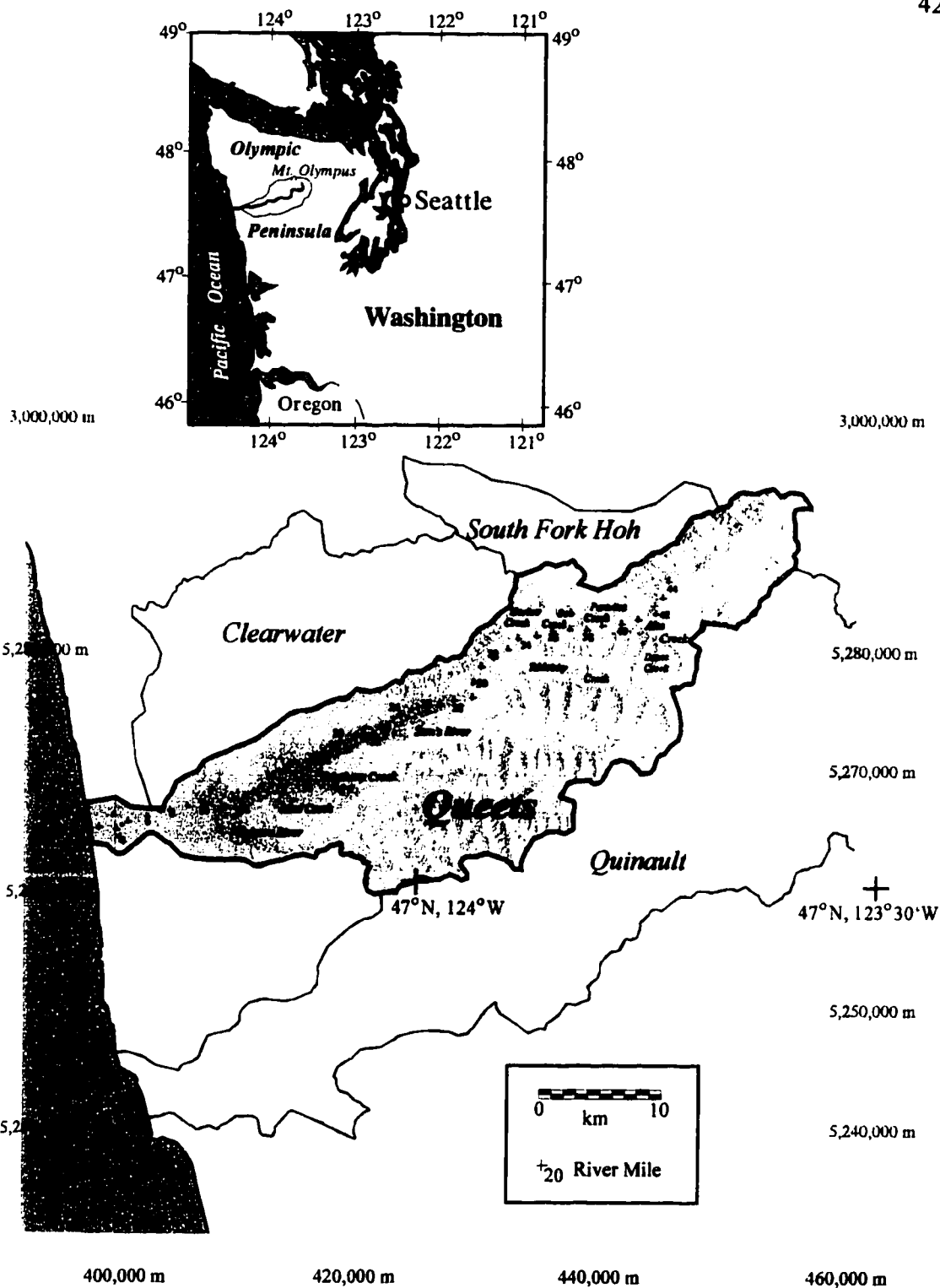
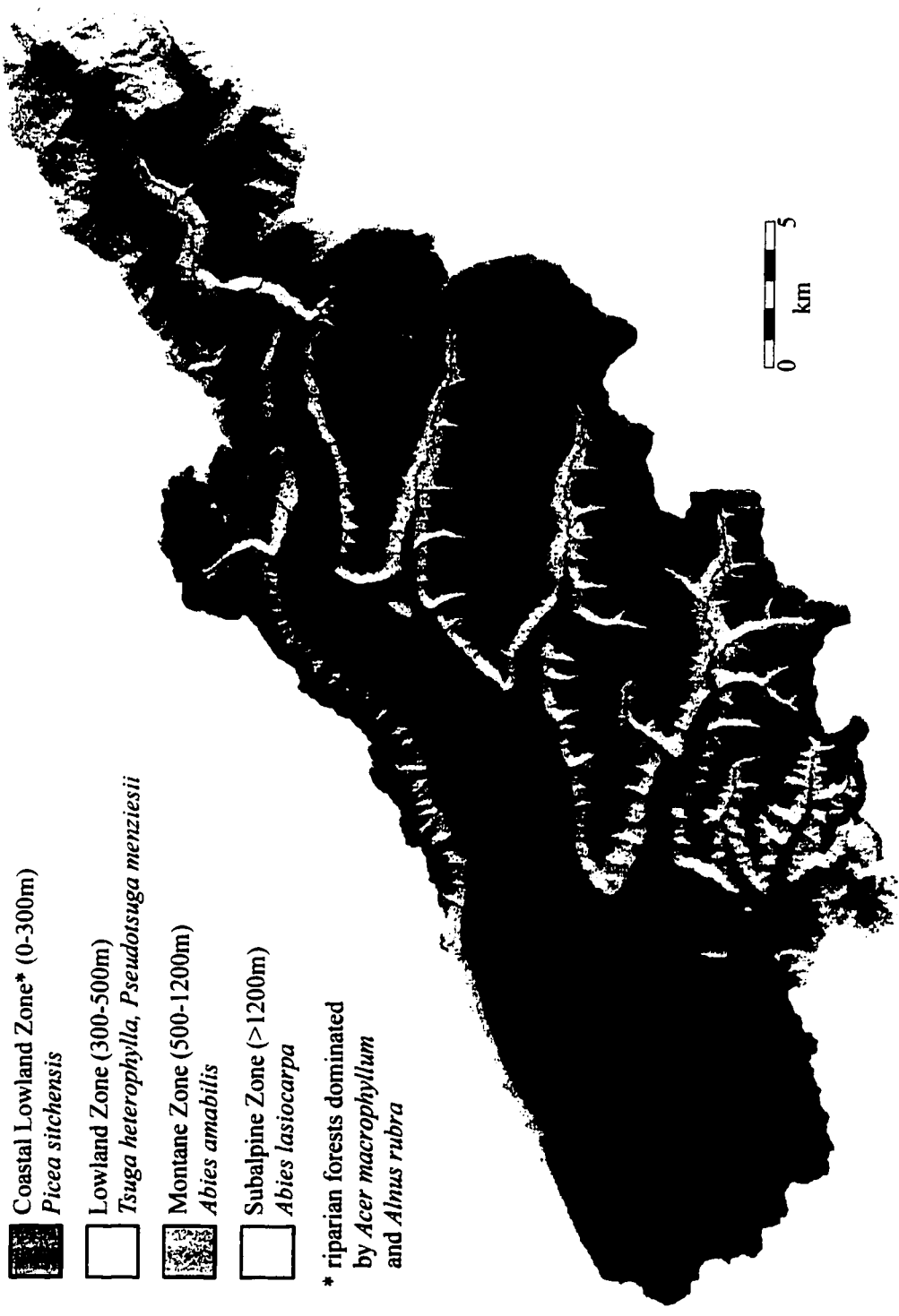






Figure 1- 1. Queets River watershed upstream of Clearwater River confluence, northwest Washington. Shaded relief map by based on USGS 1981 30m digital elevation (courtesy of Harvey Greenberg, University of Washington Department of Geological Sciences)



-  Coastal Lowland Zone* (0-300m)
Picea sitchensis
-  Lowland Zone (300-500m)
Tsuga heterophylla, Pseudotsuga menziesii
-  Montane Zone (500-1200m)
Abies amabilis
-  Subalpine Zone (>1200m)
Abies lasiocarpa

* riparian forests dominated by *Acer macrophyllum* and *Alnus rubra*

Figure 1 - 2. Distribution of forest zones and dominant tree species in Queets River basin, within Olympic National Park (based on Buckingham et al. 1995).

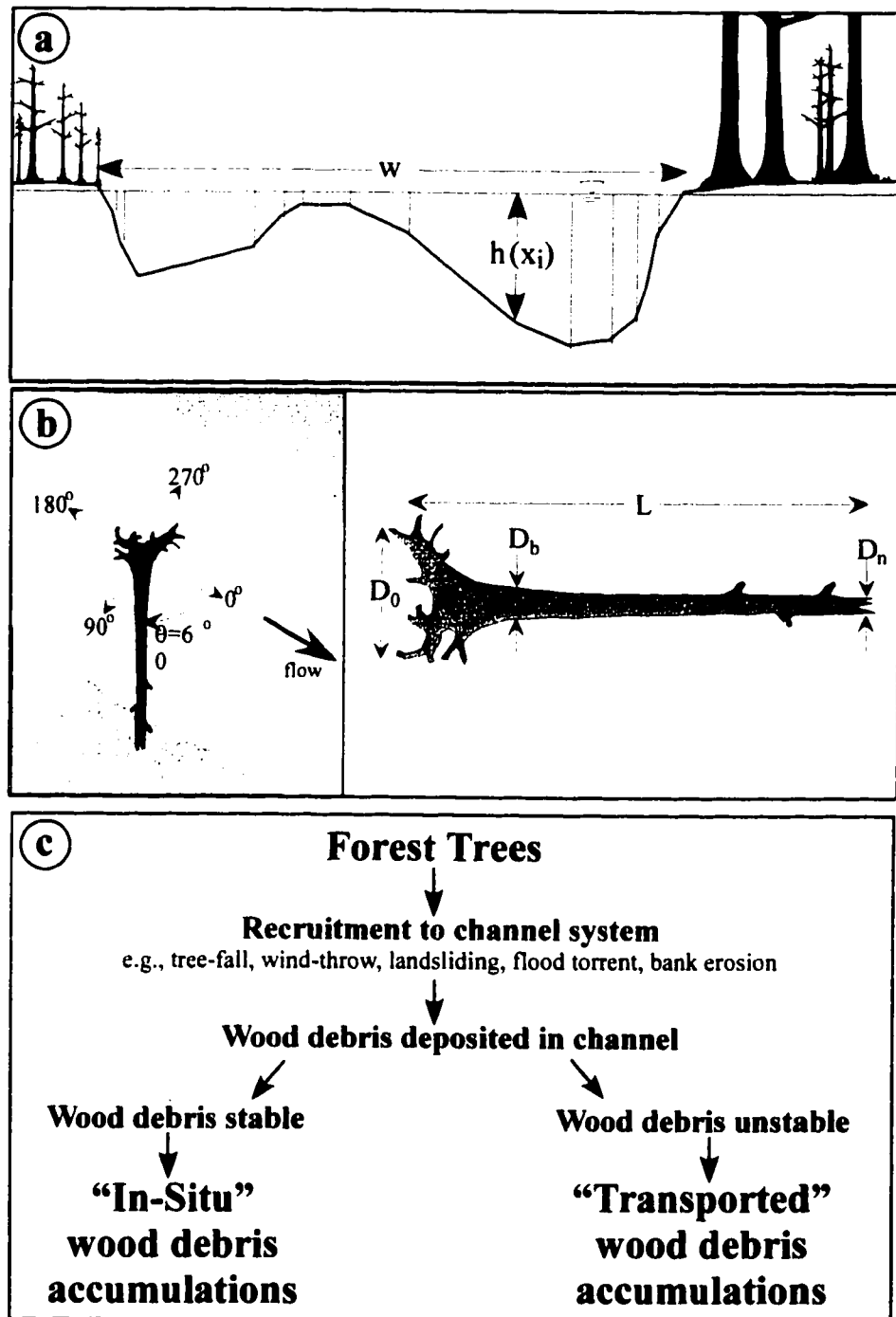


Figure 1- 3. Definition sketch of channel (a), wood debris measurements (b), and classification of in-situ and transport wood debris accumulations (c)

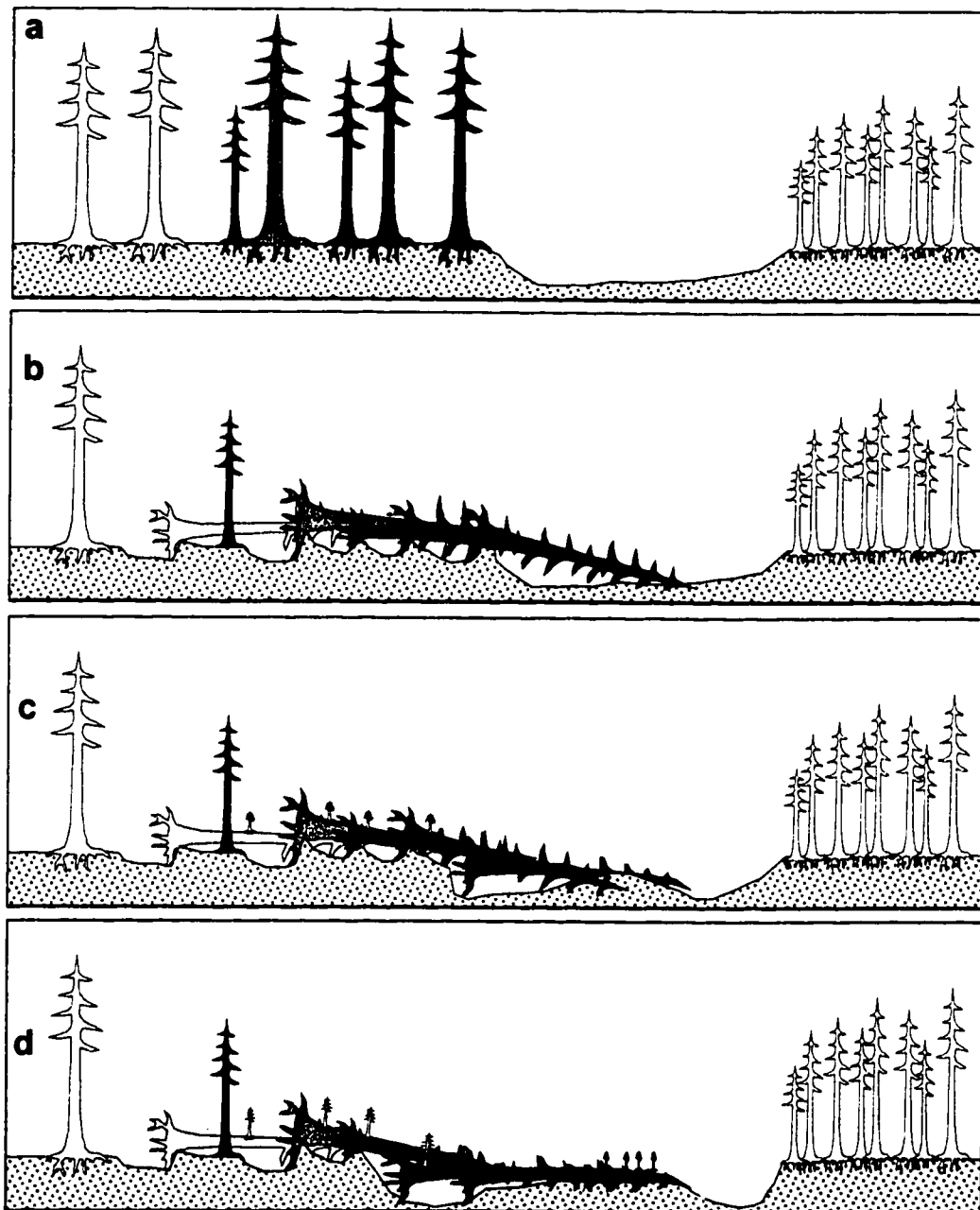


Figure 1- 4. Cross-sectional illustration of in-situ WD deposits associated with blow-down events (wind disturbance). Cluster of trees (a) is knocked over essentially simultaneously by severe wind gust (b), some of the effected trees are partially introduced into channel with no initial change in bank position (c). Flow constriction due to initial WD recruitment can accelerate bank erosion and introduce additional WD (d). The wind controls the direction of tree-fall, thus trees enter the channel in a wide range of orientations. Since trees enter the channel at the same time, there is a relatively uniform age distribution of new trees colonizing the fallen trees.

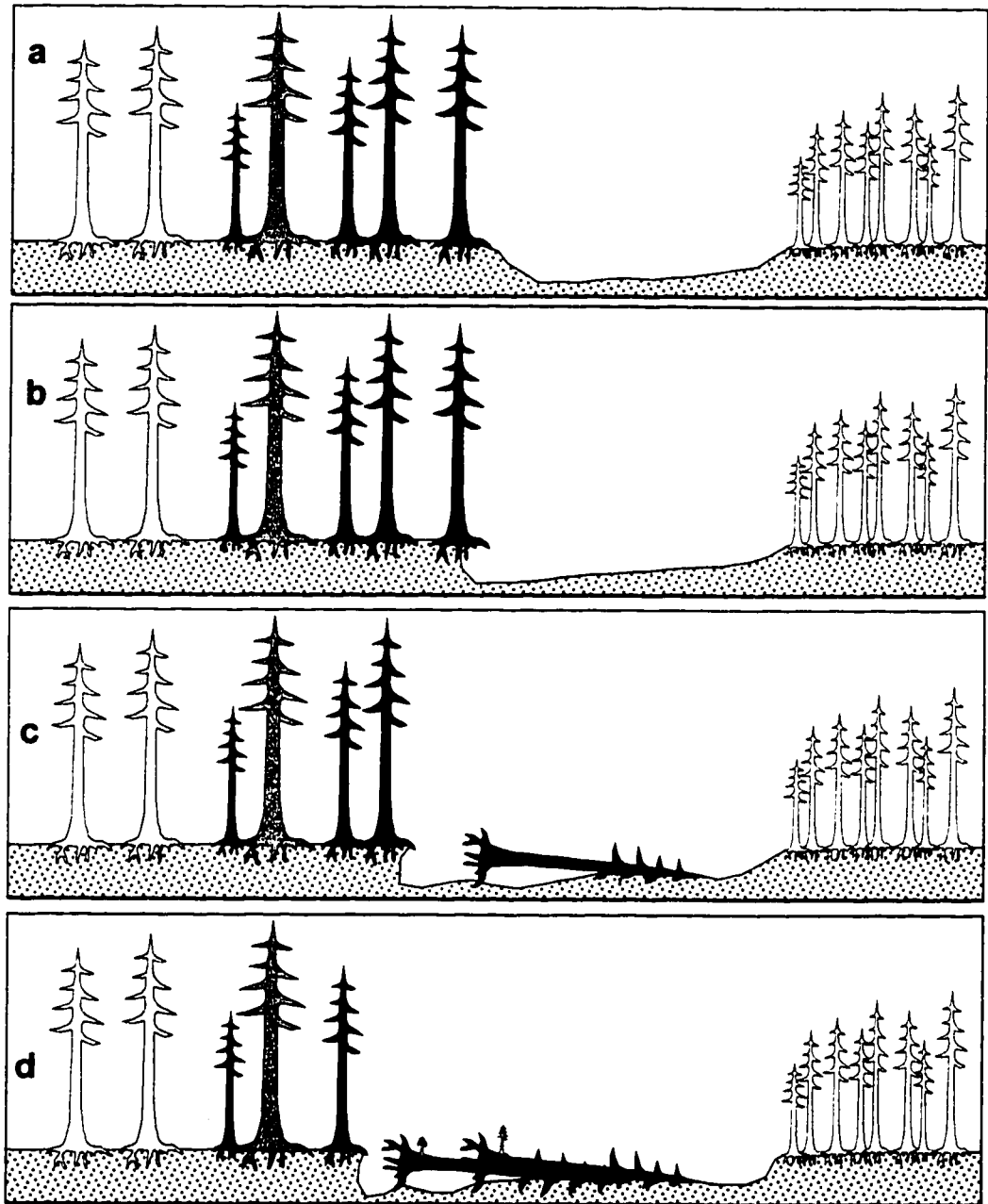


Figure 1- 5. Cross-sectional illustration of in-situ WD deposits associated with bank erosion; riparian forest stand (a) is locally disturbed as individual trees are recruited to the channel by progressive retreat of the stream bank (b-c). Trees tend to fall 180° to the direction of maximum bank retreat, usually deposited orthogonal to flow (c). Initial WD constricts flow, accelerates erosion and subsequent recruitment of additional trees (d). Successive tree recruitment through time can result in a corresponding age distribution of colonizing trees.

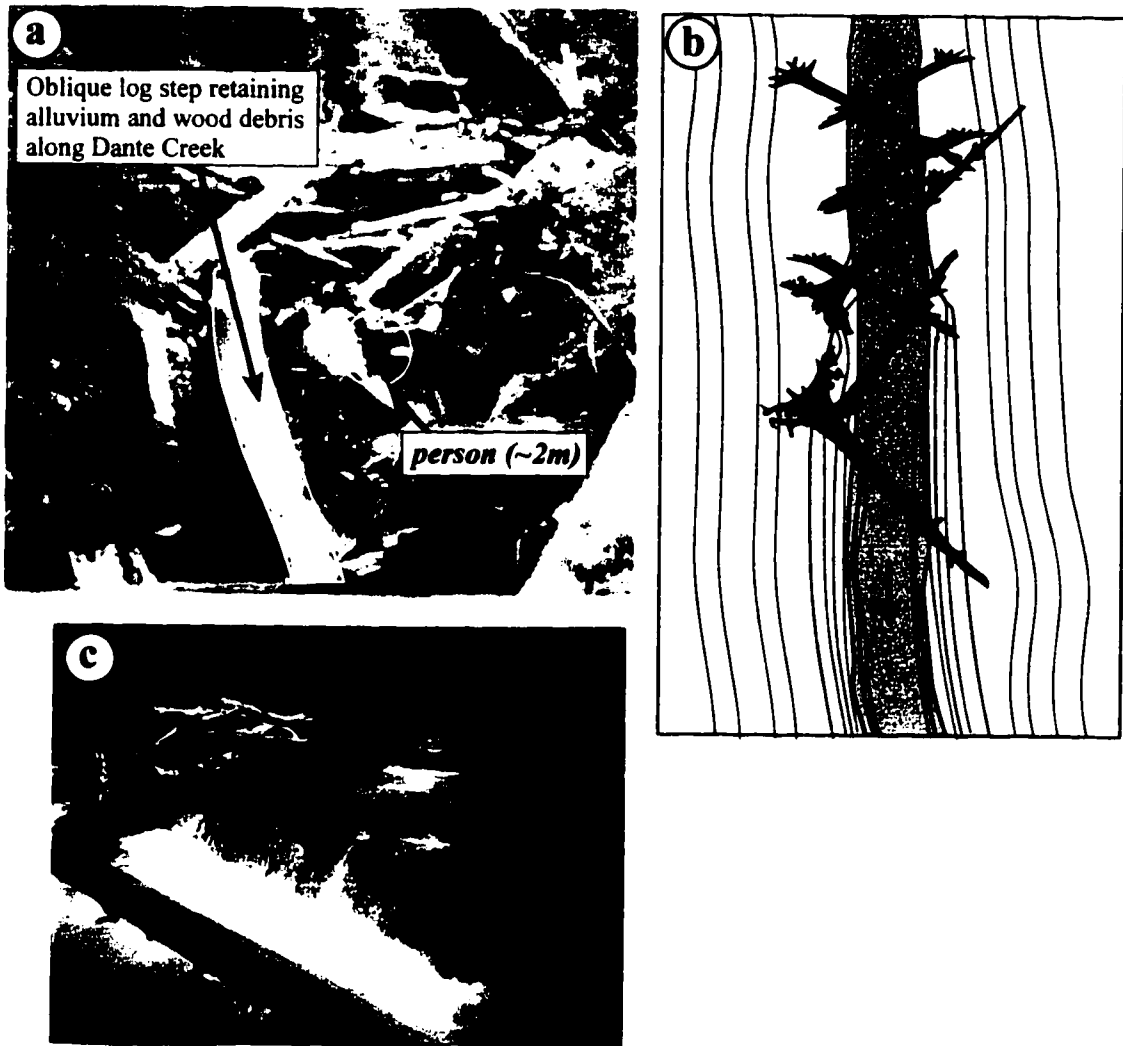


Figure 1- 6. Photograph of large oblique log step in Dante Creek, a steep headwater tributary to Queets River (a). Schematic plan view of oblique log steps in steep headwater channels (a) and photograph of normal log steps typical of low gradient channels (b).

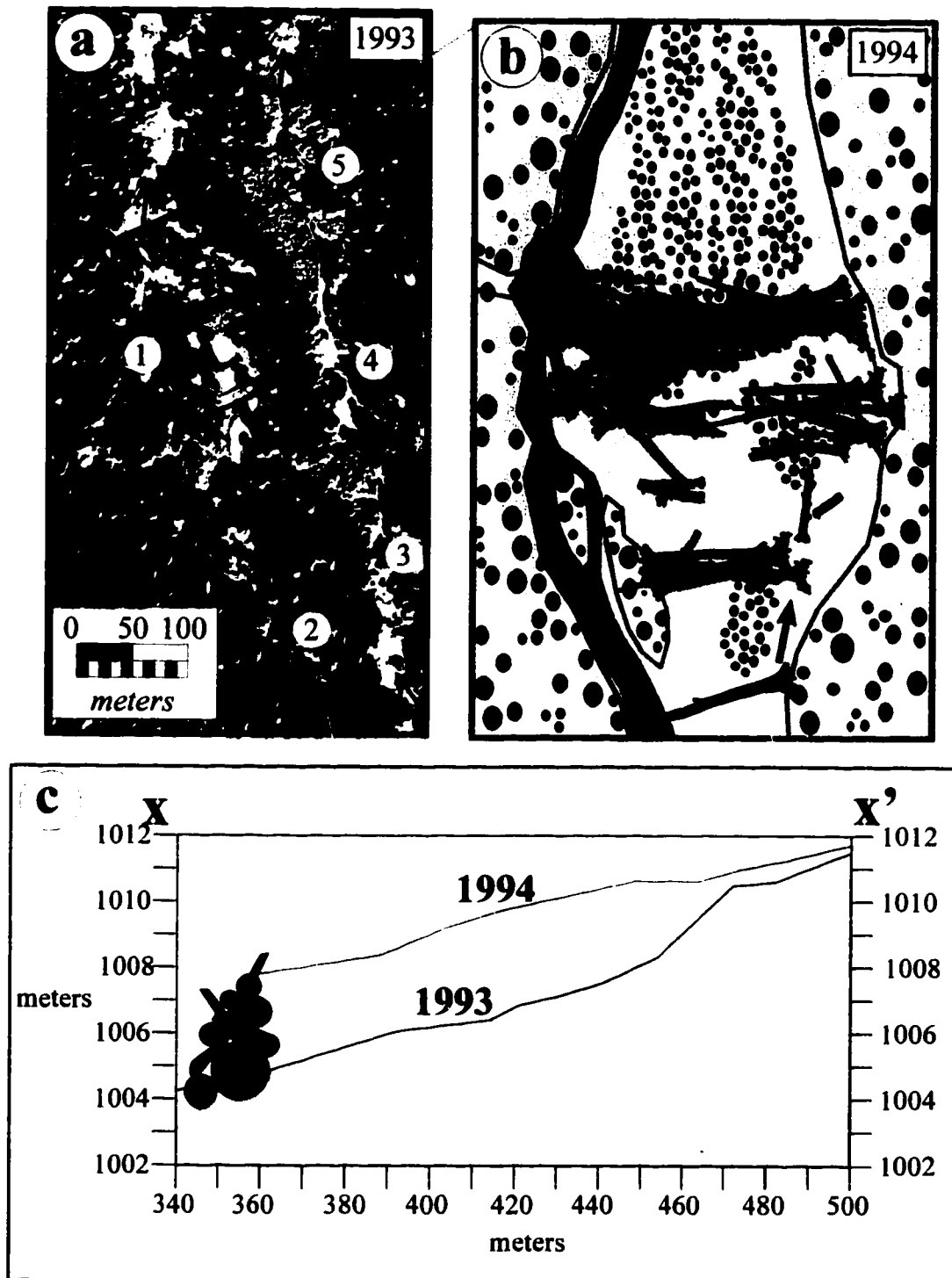


Figure 1- 7(a,b,c). Location of principal valley jams in active channel of Alta Creek in 1993 and 1994 (a). Schematic plan view of valley jam no.1 (b) and channel profile change upstream of valley jam no.2 from 1993 to 1994 (c).

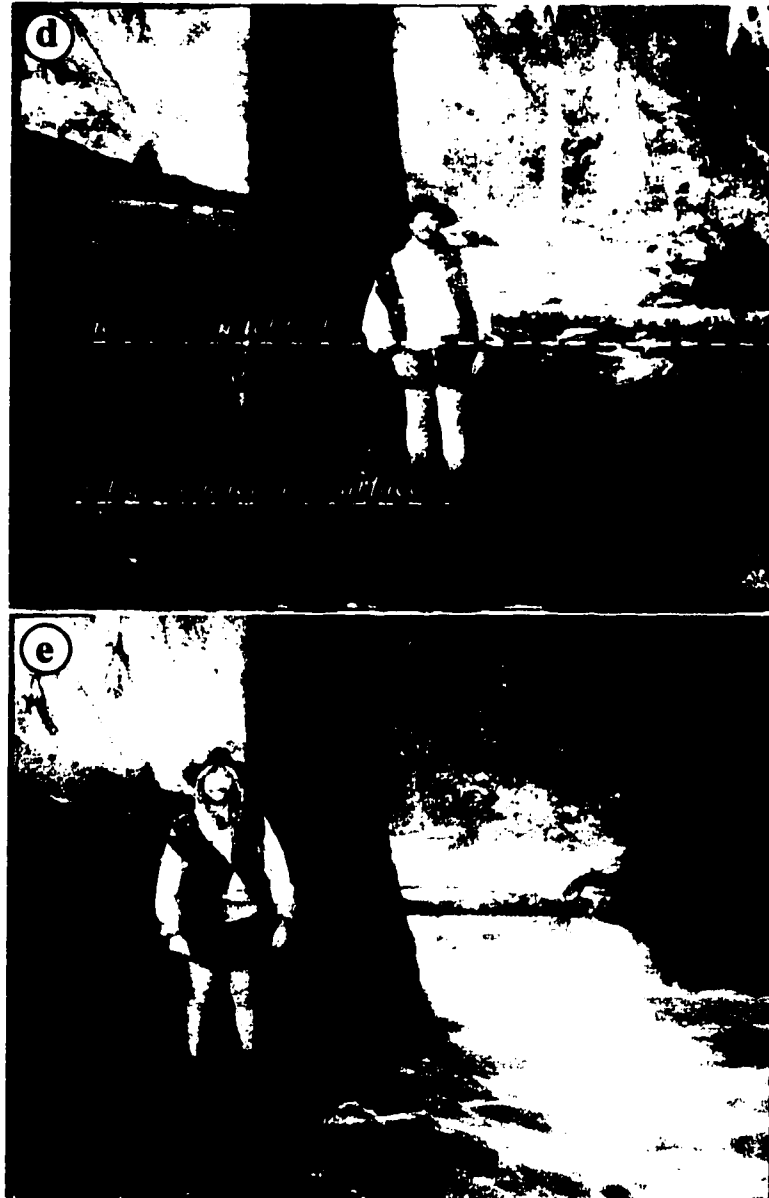


Figure 1-7(d,e). Photograph illustrating aggradation of Alta Creek upstream of valley jam no.2 in Figure 1-7a, elevating stream bed above old growth forest terrace surface (d). Flows occurring much more frequently than the “bankfull event,” now spread out across the terrace surface which had been over 2-5 m above the creek (e).

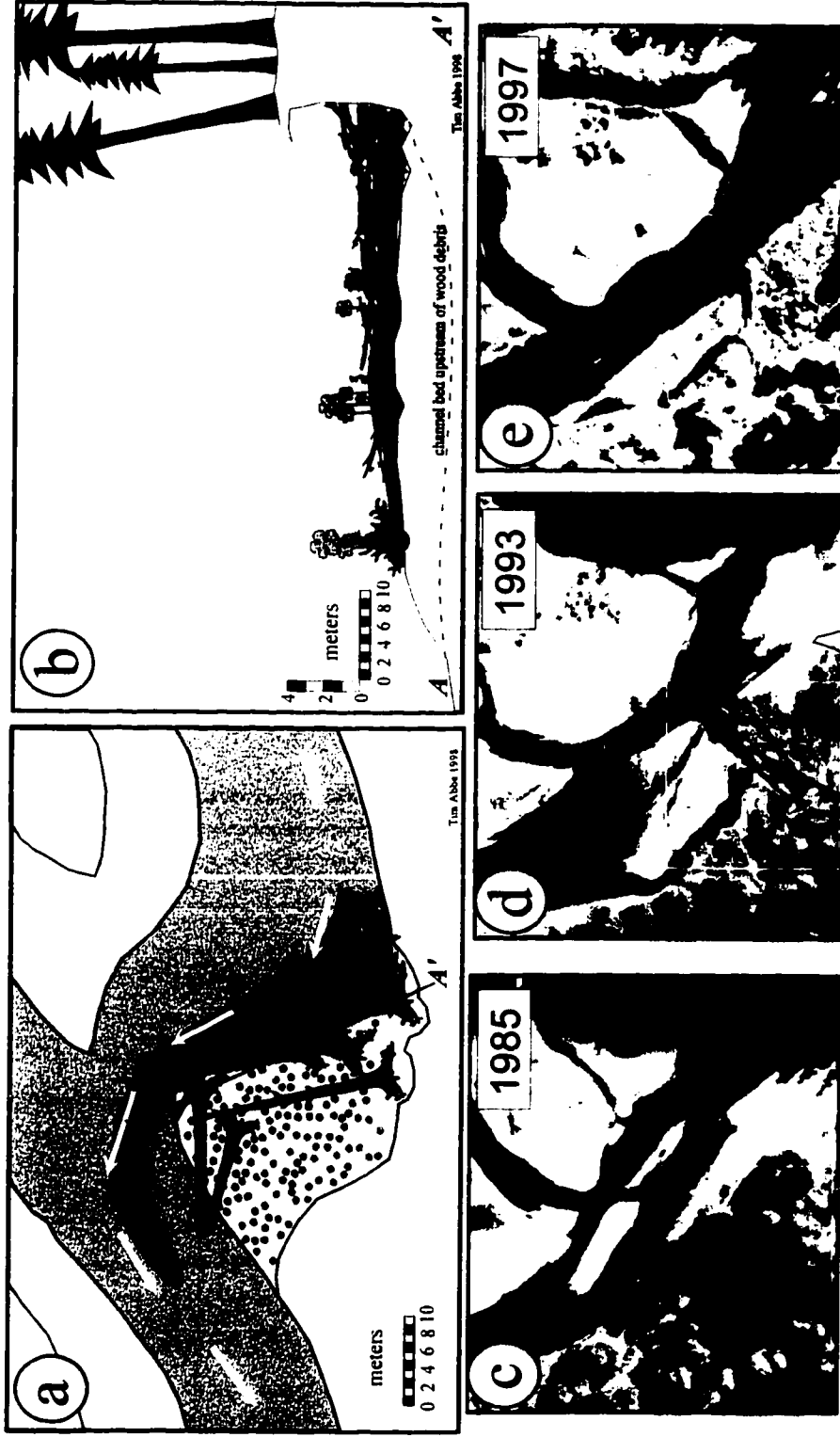


Figure 1-8. Map (a) and cross-section (b) of flow deflection jam along south bank of Queets River at RK 66.2 (RM 41.1) as surveyed in 1993. Photographic sequence from 1985 (c) to 1993 (d) to 1997 (e) illustrating process of bank erosion and local recruitment of large old growth *Picea sitchensis* to create a flow deflection jam. This jam is located at Queets RK 50.9 (RM 31.6) opposite the Tshletshy Creek confluence and persisted through at least 10 annual peak flows with a recurrence interval greater than 2 years between 1985-1997, including two flows with recurrence intervals of 20 and 21 years.

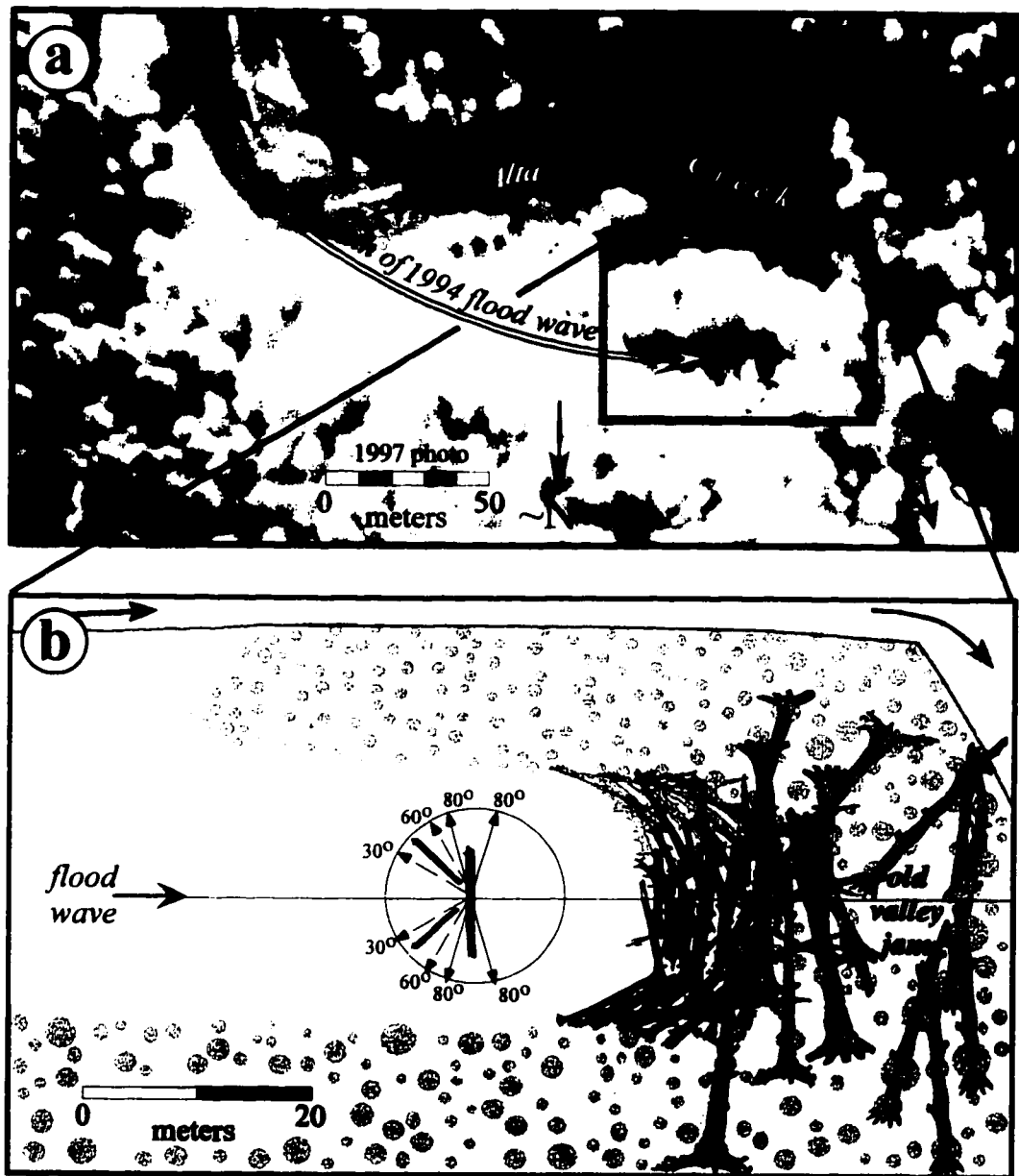


Figure 1- 9. Flood peak jam along Alta Creek, site location (a) and plan-view map(b).

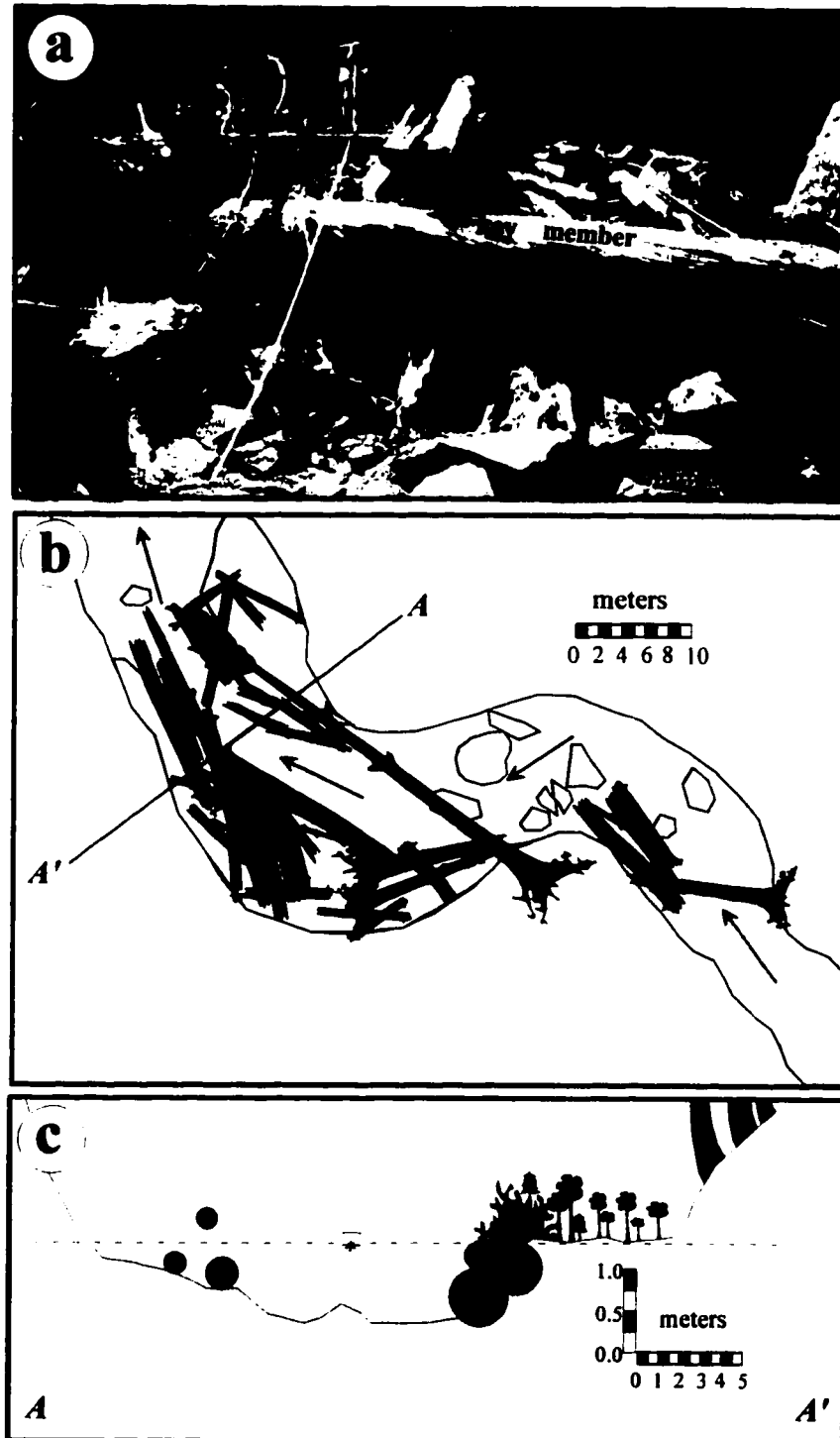


Figure 1- 10. Example of large bankfull bench jam in Dante Creek (a), tributary to Alta Creek, Queets RM 41. Bankfull bench jam in Kokopelli Creek, tributary to Harlow Creek (Queets RM 34): plan-view sketch map (b) and cross-section A-A' (c). These jams create elevated surfaces composed of alluvium and WD in steep headwater channels where floodplains do not occur.

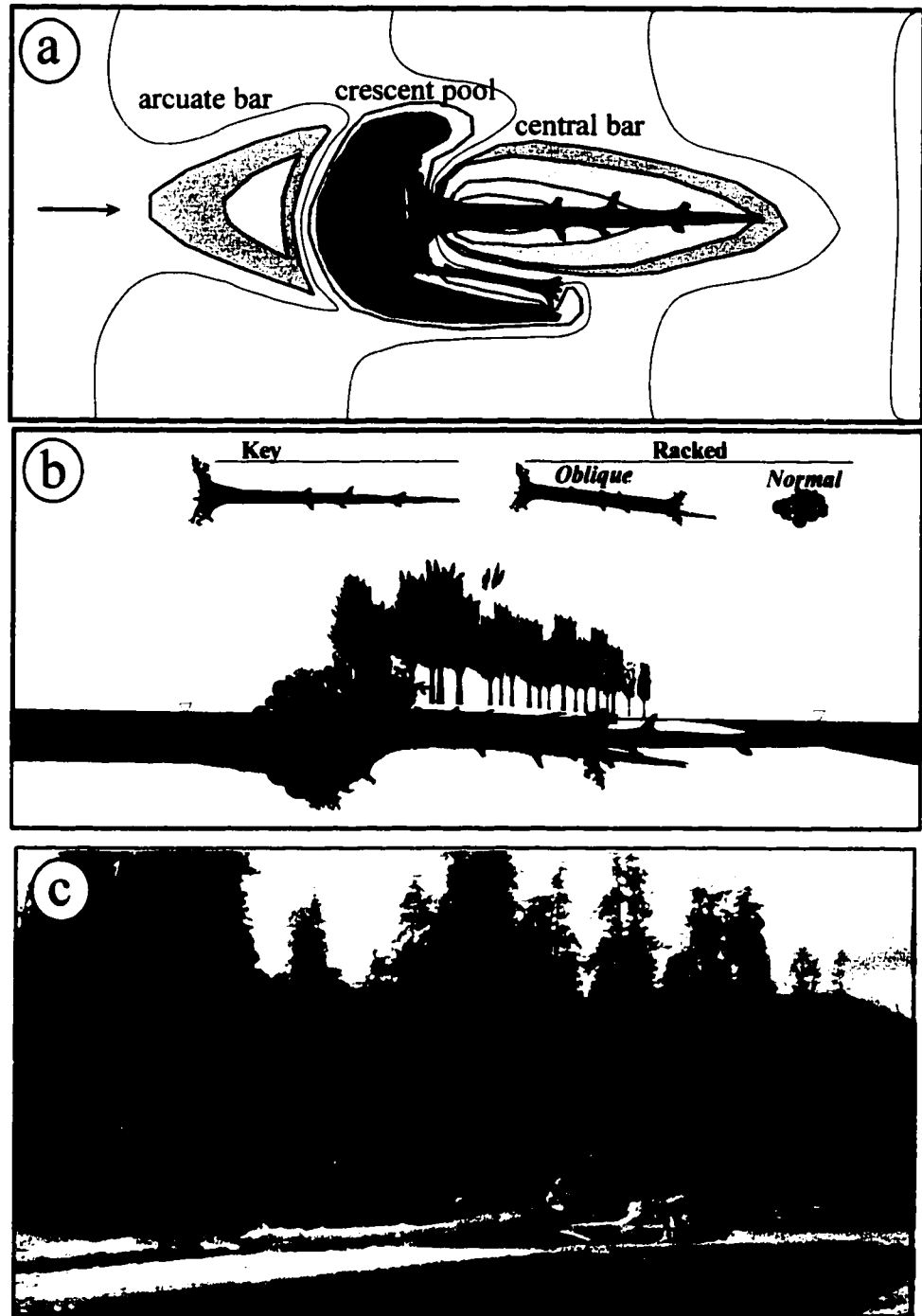


Figure 1- 11. Plan-view schematic illustrating basic structure of bar apex jams (a). Schematic profile illustrating tree age structure reflecting progressive downstream sedimentation. Bar apex jam in mainstem Queets River, RK 43.5 (RM 27) in 1993 (c).



Figure 1-12. Schematic plan-view map showing basic structure of meander jams with inset illustrating reach-scale setting (a). Oblique photograph of meander jam along north bank of Queets River at RK 27.4 (RM 17) in 1994 (b). Schematic channel cross-sectional, looking downstream into meander jam (c) and photograph with similar perspective of meander jam along south bank of Queets at RK 24 (RM 15) in 1994 (d)

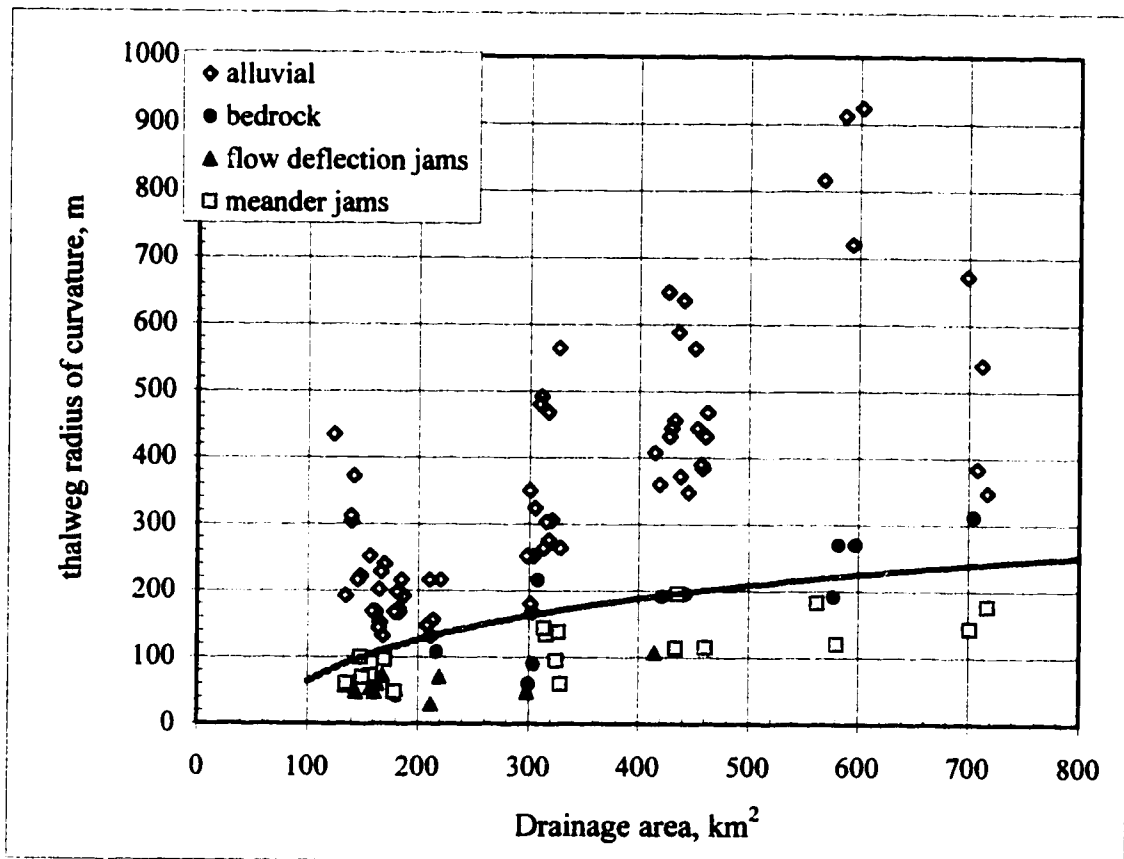


Figure 1- 13. Channel radii of curvature for Queets River meanders associated with unobstructed channels, bedrock outcrops, meander jams, and flow deflection jams as a function of river kilometer.

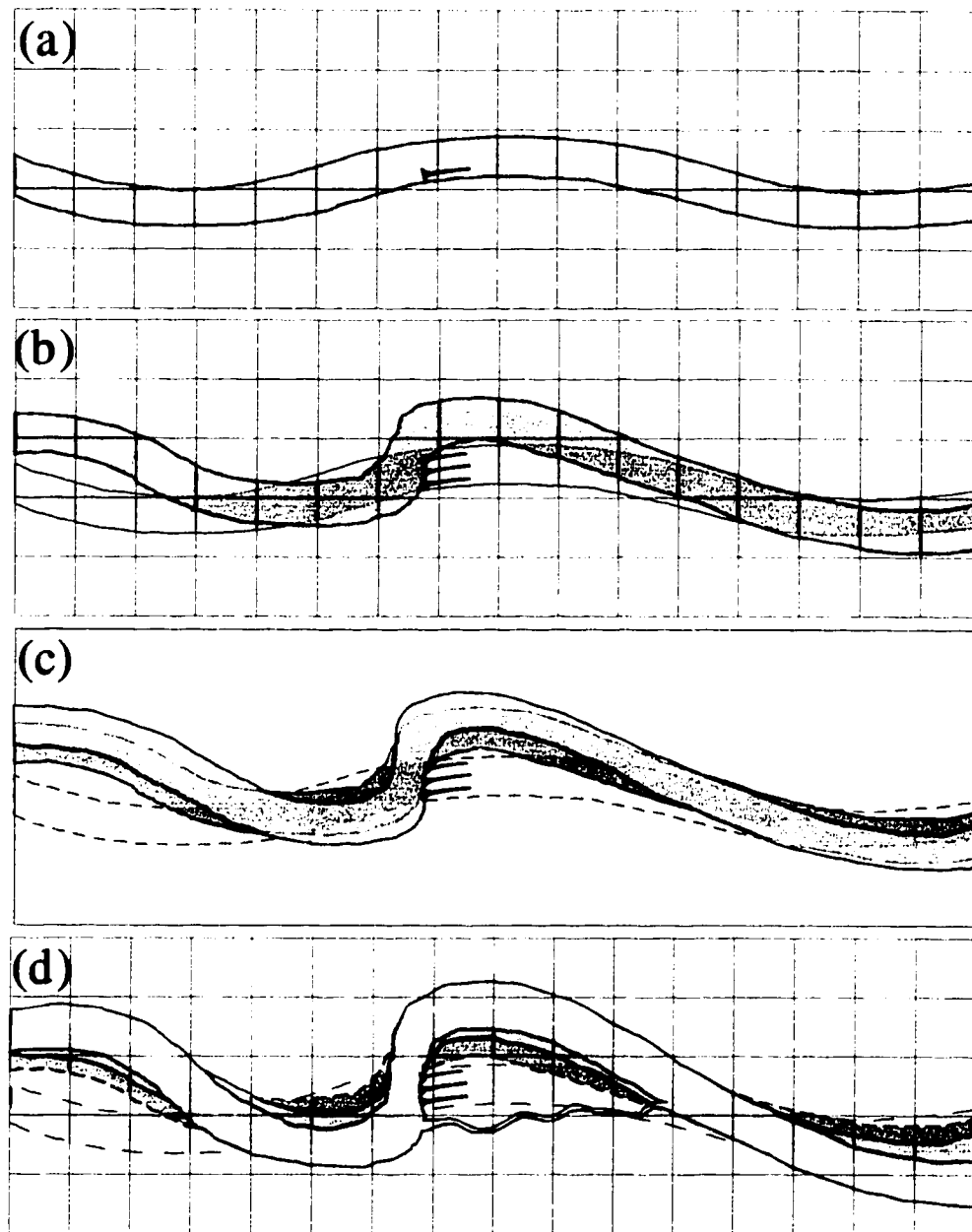


Figure 1- 14. Simple model of channel planform changes associated with meander jams. Location of initial key member is arbitrary (a) but appears to occur most commonly just downstream of the thalweg cross-over between meanders, just upstream and on the same side as the downstream point bar. Meander jams don't necessarily begin with a single tree; sometimes they begin with the deposition of several trees during the same flow event. The migrating channel flows around the ever-enlarging jam (b), leading to a reduction in radius of curvature and distinct asymmetry in channel planform (c). If the jam increases in size enough, it may precipitate a channel avulsion around the jam (d).

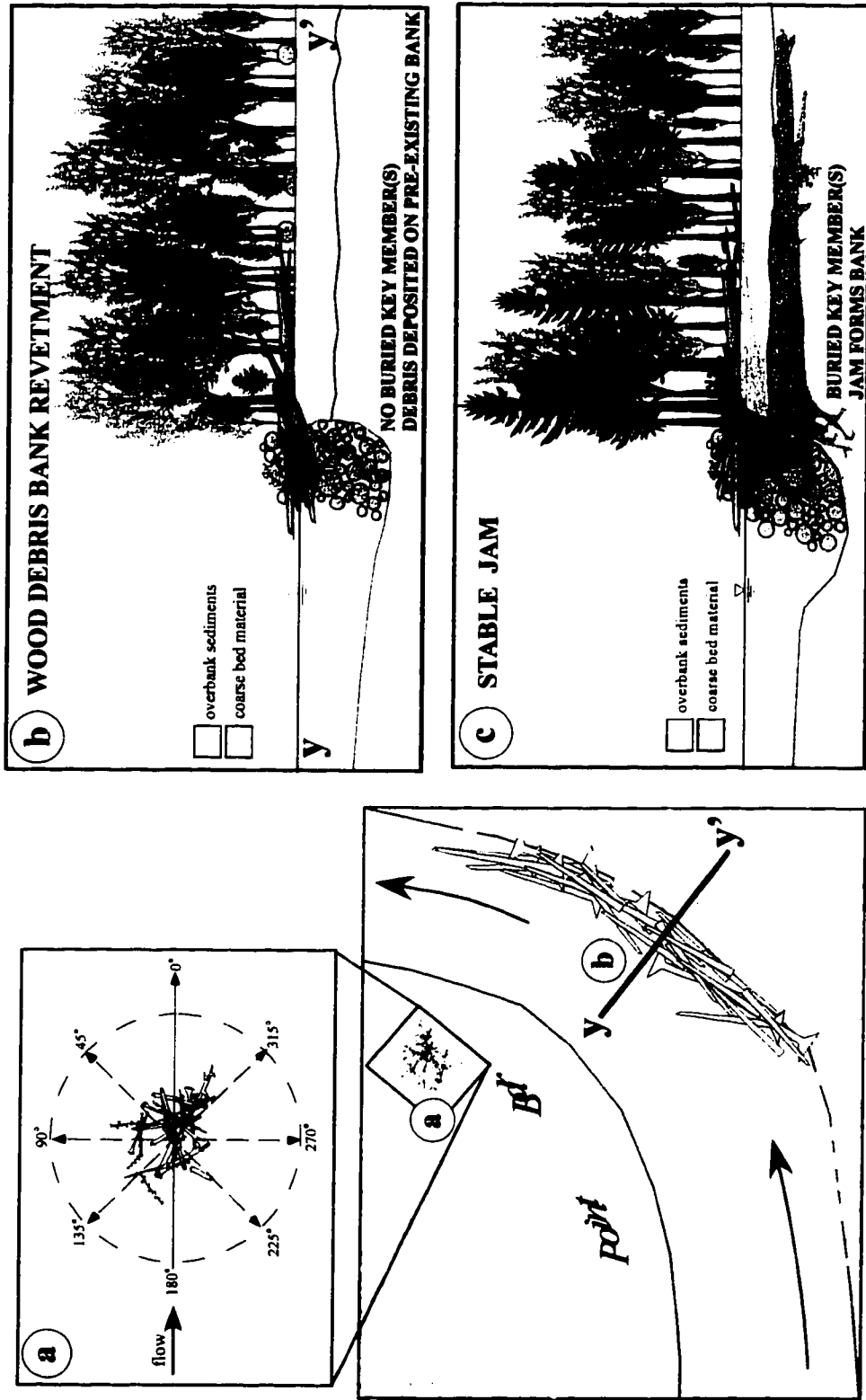


Figure 1-15. Unstable wood debris deposits: plan view of bar top accumulation shows wide distribution in log orientations (a), bank edge (jam height < channel depth) and bank revetment jams (jam height > channel depth) are composed of logs with similar orientations approximately parallel to flow (b). Cross-sections illustrate difference between unstable jams deposited on a pre-existing bank (b) and stable jams which pre-date the bank (c).

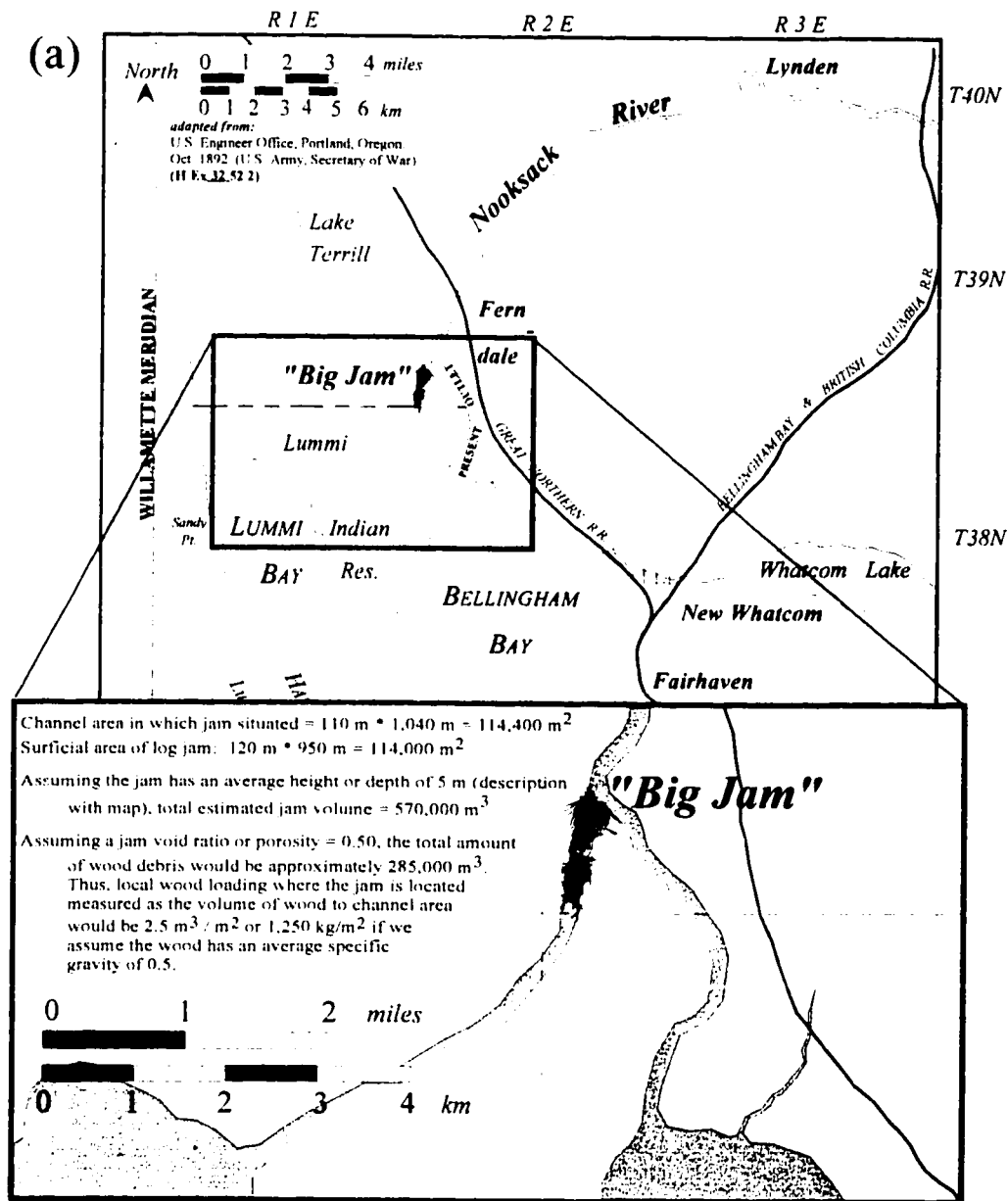


Figure 1-16 (a). Large wood debris jam or "raft" diverted lower Nooksack River completely around the Lummi peninsula so the river discharged into Bellingham Bay instead of Lummi Bay (War Department 1892).

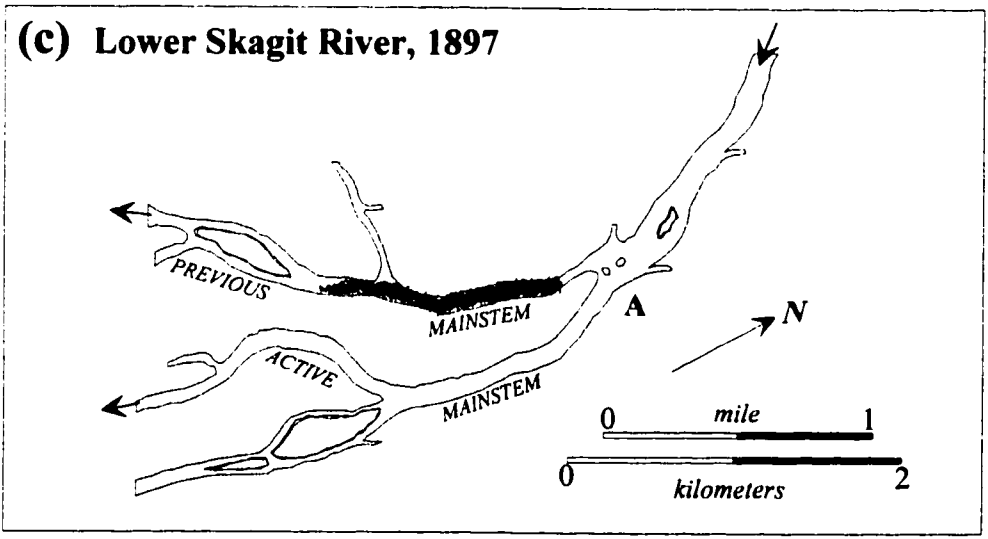
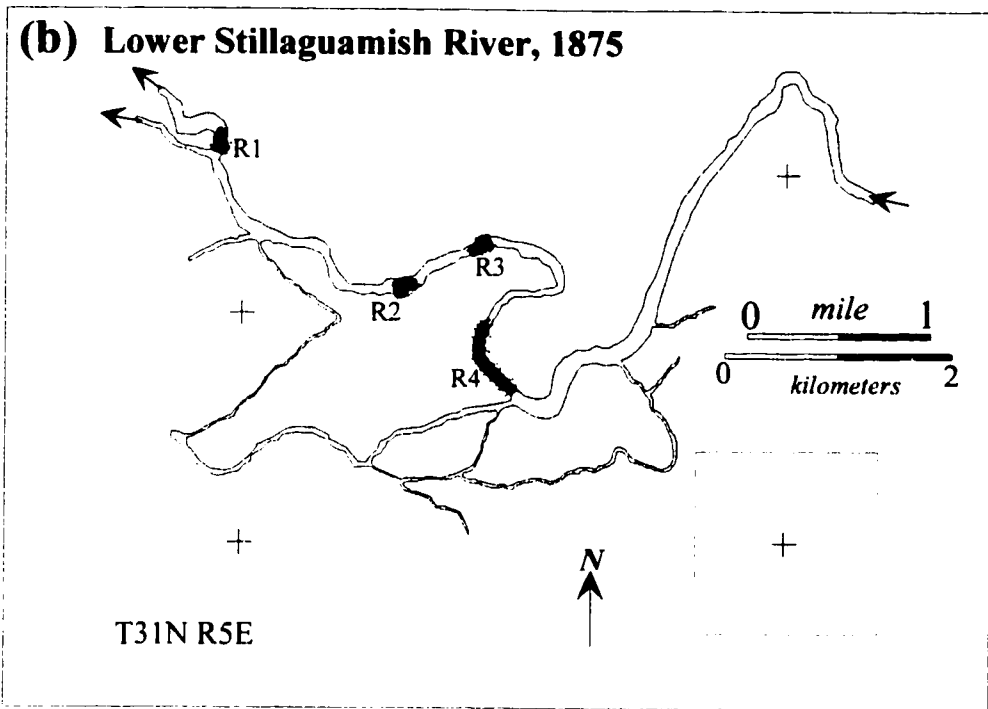


Figure 1- 16 (b,c). Historical maps of wood debris rafts in large rivers entering Puget Sound in northwest Washington state: (b) Lower Stillaguamish River (Shoecraft 1875) and (c) Lower Skagit River (War Department 1898).

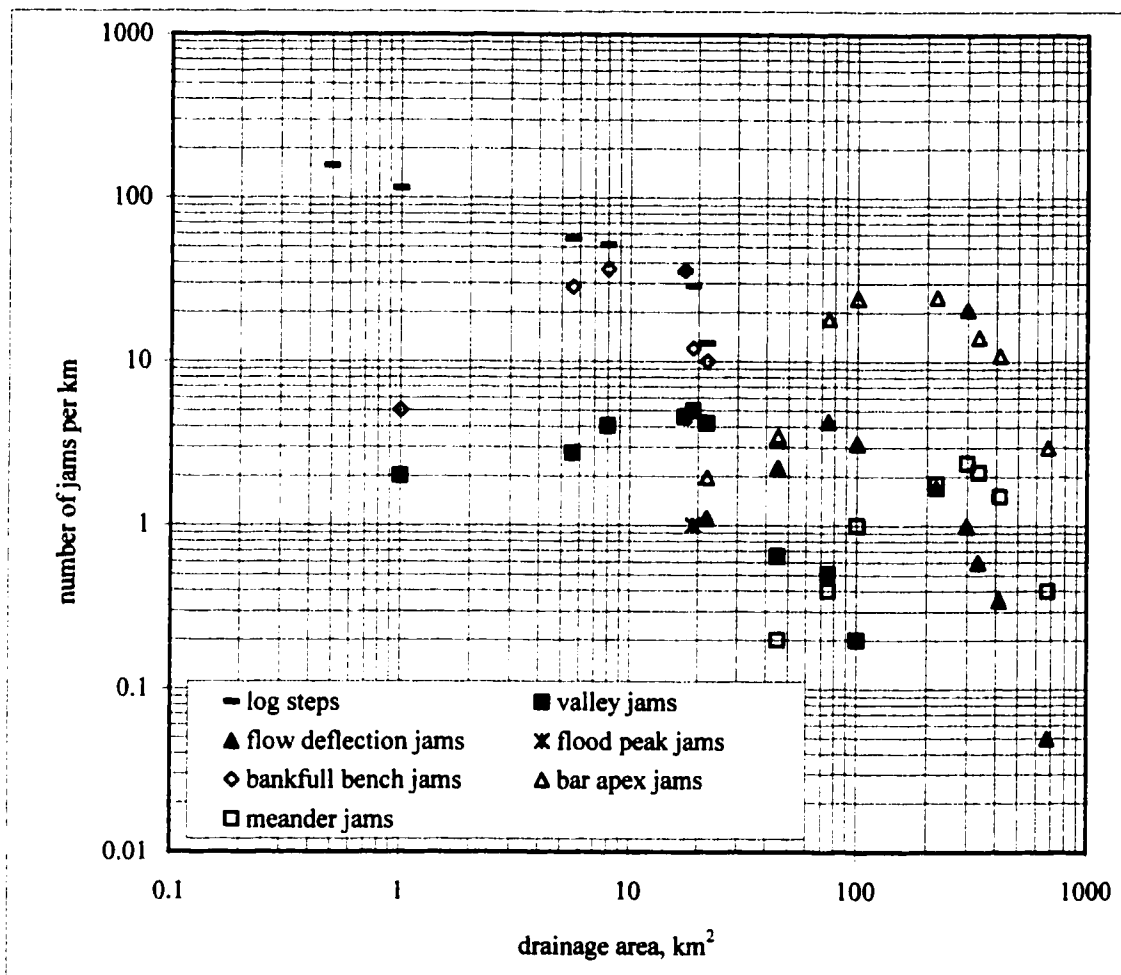


Figure 1-17. Frequency distribution of wood debris accumulation types as a function of drainage area for the Queets River.

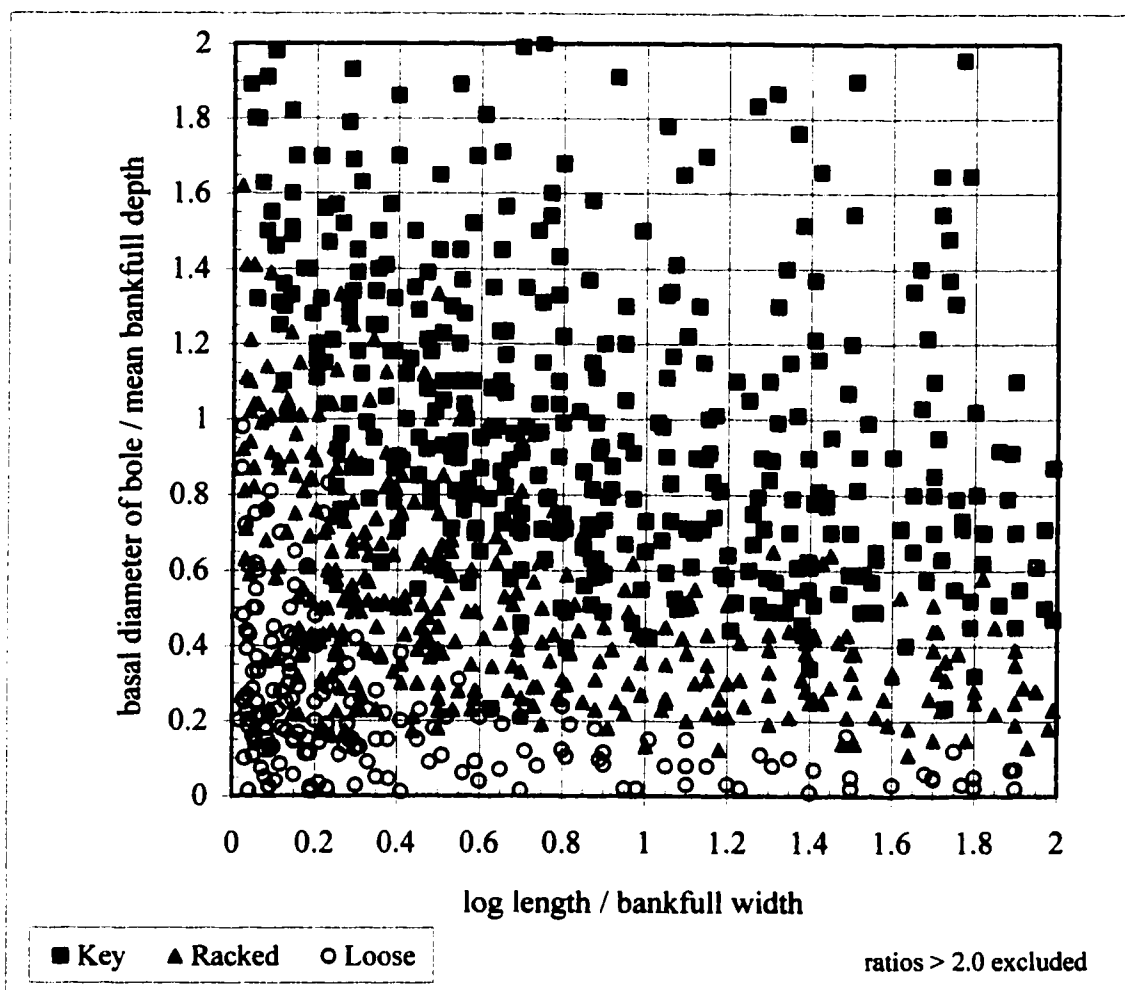


Figure 1- 18. Dimensionless size plot of log stability thresholds for key, racked and loose pieces in 32 jams located in five study reaches representing different portions of the Queets channel network. Ratio of log basal diameter to bankfull depth, D_1/h_{bkf} is plotted versus ratio of log length, L , to bankfull width, w_{bkf} . If D_1 is replaced with the rootwad diameter, D_0 , the domain of key members is further separated from that of racked members and distinguish key members occurring in large channels versus those in smaller channels.

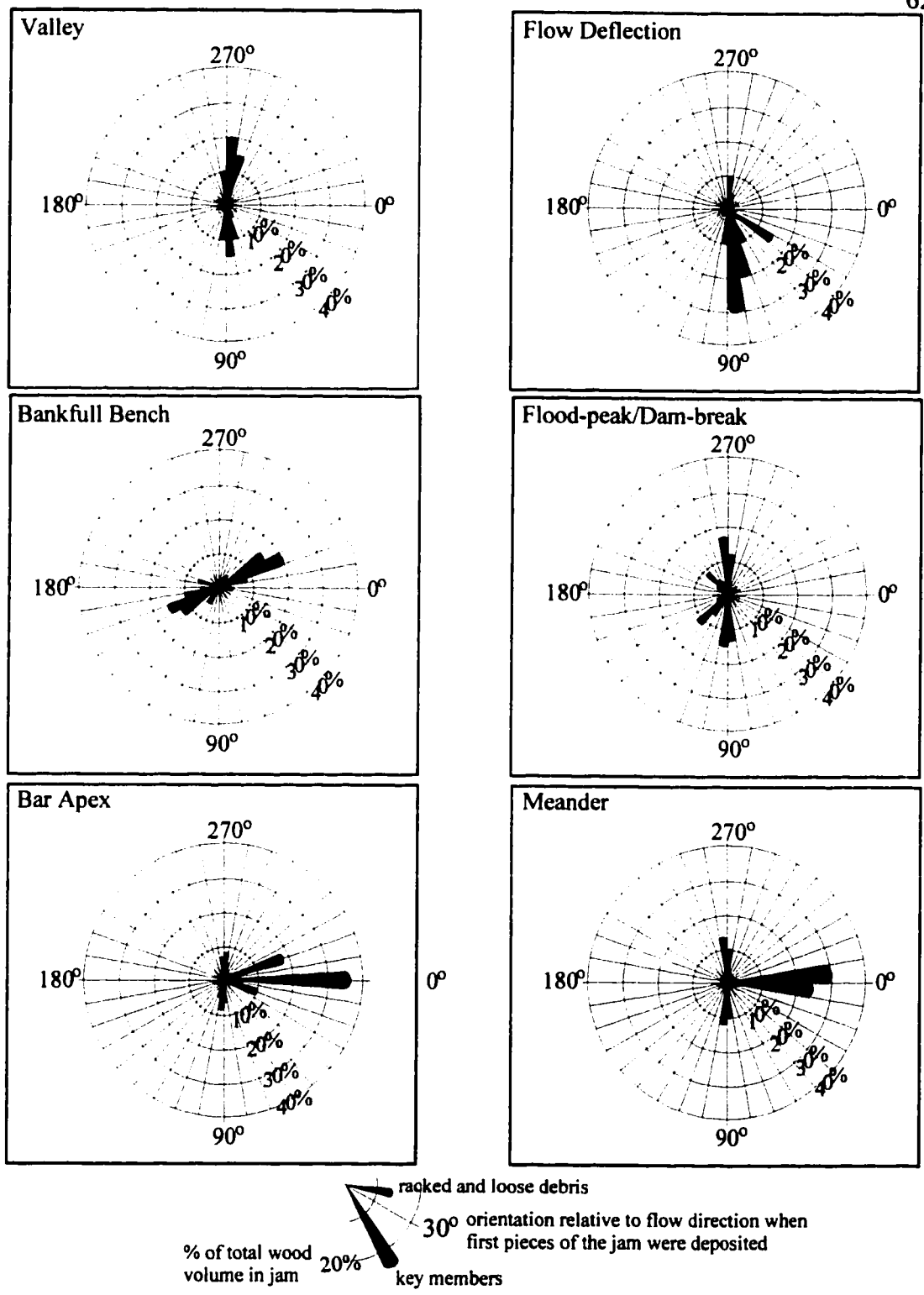


Figure 1- 19. Rose plot illustrations of wood debris orientation normalized to total volume of wood in a particular type of accumulation, showing differences among types.

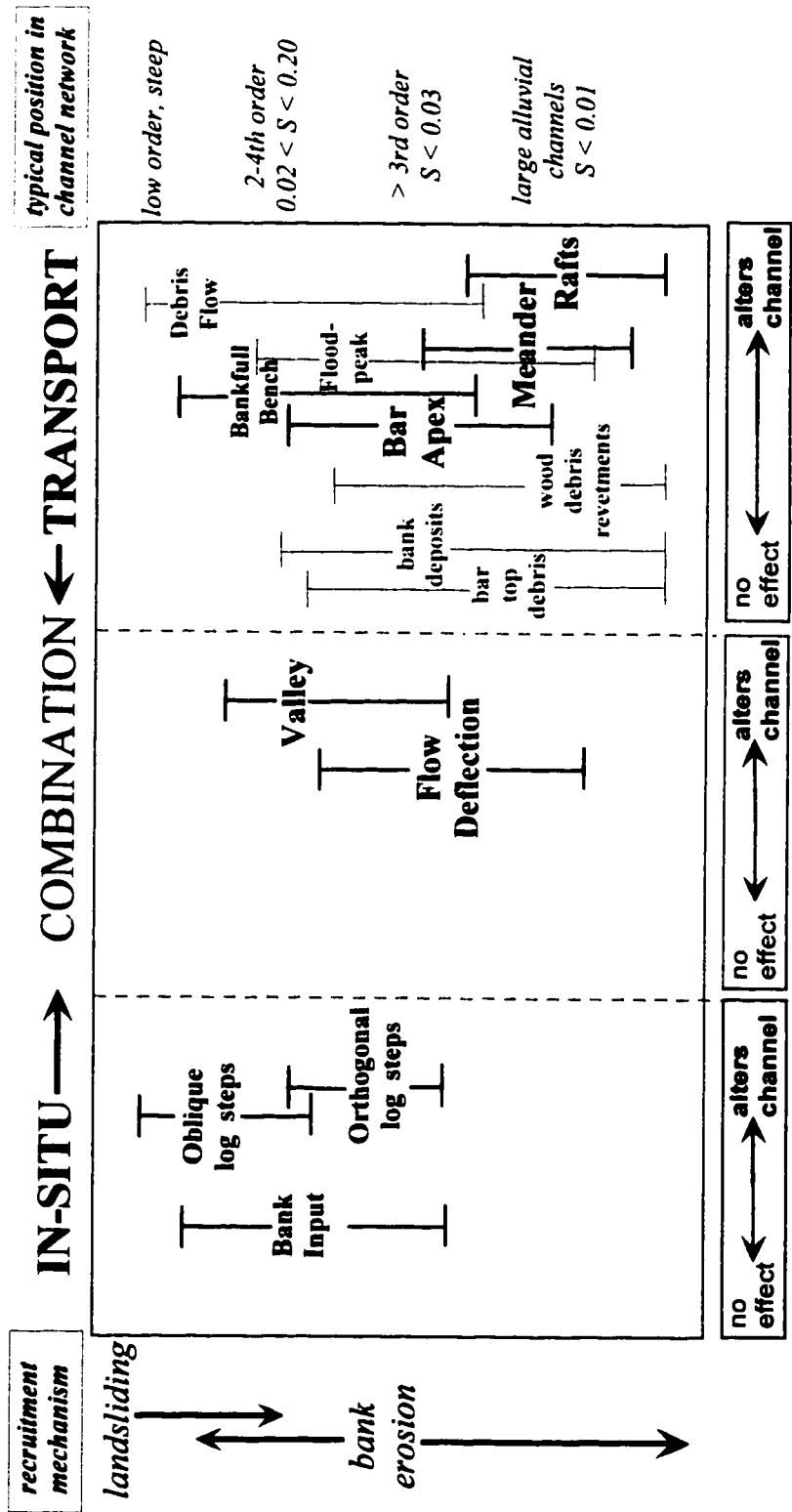


Figure 1-20. Summary chart of wood debris accumulation types and their location within a drainage network.

<p style="text-align: center;">Table 1-1 Recruitment processes introducing wood debris into a fluvial channel network</p>	
Recruitment Process	Applicable Portions of Drainage Basin
Tree fall	All portions of basin, though more frequent in areas where substrate is commonly saturated and steeper slopes.
Wind-throw	All portions of basin are susceptible, especially higher elevations, burn areas, hillslopes in lee of incident wind, and confined valleys aligned with wind direction.
Colluvial hollow failure	Zero-order colluvial channels in steep convergent topography of hillslopes. Deposition usually in close proximity to confluence with perennial channel.
Landsliding	Shallow and deep-seated failures from valley hillslopes often associated areas of subsurface flow convergence, elevated hydraulic gradients, and oversteeping due to toe excavation of hillslopes by channel incision (confined headwater reaches) or channel migration (unconfined alluvial reaches).
Stream bank erosion	Primarily unconfined alluvial reaches.
Flood recruitment	All areas where over-bank flows can potentially recruit debris from riparian forests, other than through bank erosion. Floods can also remove significant quantities of WD and deposit them on floodplains outside the bankfull channel.
Debris Flows	Debris flows can route significant quantities of WD downstream where they occur (i.e., disturbed landscapes) and tend to be a much more important mechanism of removing WD and depositing it outside the channel against streamside trees along outside bends of the channel.

Table 1-2 Log dam characteristics in selected channel reaches of the Queets River watershed						
Channel Reach	reach length meters	reach gradient	No. of log steps	% elev. loss attributed to log steps	range in log angles (degrees)	mean log angle (degrees)
High Gradient Channels						
1st-order tributary to Dante Creek	50	0.69	12	27	23 - 61	41
1st-order tributary to Queets RK 62.8	60	0.55	17	45	38 - 71	50
1st-order tributary to Queets RK 45.9	65	0.33	14	56	37 - 75	57
Low Gradient Channels						
Lower Pelton Creek (2nd order stream)	135	0.016	3	68	71 - 111	93
Lower Bob Creek (3rd order stream)	160	0.015	5	77	79 - 120	89
Lower Paradise Creek (3rd order stream)	180	0.013	3	74	78 - 118	87

Table 1-3
 Changes in the Red River, LA from 1886 to 1980
 after removal of the "great raft" in 1873
 (Harvey et al. 1988)

channel	1888	1938	1980
mean width, m	173 +/- 80	425 +/- 146	unchanged from 1938
mean depth, m	12.4 +/- 2.2	13.6 +/- 2.9	13.2 +/- 1.6
length, m	304,000	---	198,000
mean slope	0.00009 +/- 0.0001	---	0.00014 +/- 0.0001

Table 1-4a
General Characteristics of Wood Debris Accumulation Types: In-situ Jams

Type	Location in Drainage Basin	Principal Resisting Force	Jam/Channel Characteristics
Bank-input	1-5th order, alluvial, unconfined, ($S < 0.06$)	Wood debris	$w_{jam} / w > 0.5$ $w_{jam} > l_{jam}$
Oblique Log Steps	0-4th order, bedrock or alluvial channels, $S > 0.02$	channel boundary conditions	steps oriented oblique to flow, $w_{jam} / w > 1.0$ $w_{jam} > l_{jam}$
Normal Log Steps	0-4th order, bedrock or alluvial channels, $S < 0.02$	channel boundary conditions	steps oriented normal to flow $w_{jam} / w > 1.0$ $w_{jam} > l_{jam}$
WD = wood debris w_{jam} = width of jam measured normal to flow l_{jam} = length of WD accumulation measured parallel to flow w = width of bankfull channel undisturbed by jam			

Table 1-4b General Characteristics of Wood Debris Accumulation Types: Combination Jams			
Type	Location in Drainage Basin	Principal Resisting Force	Jam/Channel Characteristics
Valley confined	2 - 4 th order, bedrock or alluvial $0.04 < S < 0.20$	channel boundary conditions	$w_{jam} / w > 1$ $w_{jam} \leq l_{jam}$
Valley	2 - 6 th order, bedrock or alluvial $0.01 < S < 0.06$	wood debris	$w_{jam} / w \gg 1$ $w_{jam} \gg l_{jam}$
Flow-Deflection	3 - 7 th order bedrock or alluvial $0.01 < S < 0.03$	wood debris	$W_{jam} / w > 0.2$ $w_{jam} \geq l_{jam}$
WD = wood debris w_{jam} = width of jam measured normal to flow l_{jam} = length of WD accumulation measured parallel to flow w = width of bankfull channel undisturbed by jam			

Table 1-4c General Characteristics of Wood Debris Accumulation Types: Transport Jams			
Type	Location in drainage basin	Principal source of resistance	Jam/channel characteristics
Debris Flow	1 - 3 rd order, $S > 0.04$, diffuse rapidly downstream in channels with abundant obstructions	channel margins, bank, floodplain, & riparian trees	$w_{jam} / w_{jam} \approx 1$ $w_{jam} < l_{jam}$
Flood Peak	> 3 rd order, $S < 0.06$ bedrock or alluvial	channel margins, bank, floodplain, & riparian trees	$0.5 < w_{jam}/w < 10$ $w_{jam} \geq l_{jam}$
Bankfull-Bench	2 - 4 th order, $0.02 < S < 0.25$, bedrock, cascade, plane-bed	channel boundary & key wood debris	$0.2 < w_{jam}/w < 1.0$ $w_{jam} < l_{jam}$
Bar Apex	> 3 rd order, $S < 0.03$, alluvial pool-riffle, unconfined	key member(s)	$w_{jam}/w < 0.5$ $w_{jam} \leq l_{jam}$
Meander	> 4 th order, $S < 0.03$, unconfined alluvial pool-riffle, regime	key members	$0.3 < w_{jam}/w < 3.0$ $w_{jam} \geq l_{jam}$
Rafts*	large alluvial regime channels, $S < 0.01$, $w > 200$ m	key pieces, WD input from upstream	$w_{jam}/w \approx 1.0$ $w_{jam} \ll l_{jam}$
Unstable Debris <i>bar-top</i> <i>bank-</i> <i>revetments</i>	>2 nd ord. alluvial channels mantle pre-existing banks	unstable	$w_{jam} / w < 0.5$ $w_{jam} \approx l_{jam}$ (a) $w_{jam} \ll l_{jam}$ (b)
WD = wood debris w_{jam} = width of jam measured normal to flow		l_{jam} = length of WD accumulation measured parallel to flow w = width of bankfull channel undisturbed by jam	
* based on historical descriptions, but modern examples do exist (e.g., Tye & Yakima Rivers, WA; reports from Kansas and Mississippi)			

CHAPTER 2: LARGE WOOD DEBRIS JAMS, CHANNEL HYDRAULICS, AND HABITAT FORMATION IN LARGE RIVERS

2.1 Wood Debris Accumulations In Streams

The manner in which large wood debris (WD) accumulates and influences large alluvial channels is poorly understood despite important implications to hydrologic, geomorphic, and ecological processes in forested watersheds. Forests can contribute prodigious quantities of WD to a channel network and WD exerts a first-order control on channel morphology in small forest channels (e.g., Keller and Tally, 1979; Lisle, 1986; Sedell *et al.*, 1988; Nakamura and Swanson, 1993). Pool frequency, for example, is strongly correlated with WD loading in small to moderately sized gravel-bed channels (Montgomery *et al.*, 1995). Historical records reveal that massive accumulations of WD were a significant channel-altering mechanism in large rivers, directly influencing channel avulsion, lake development, and floodplain formation (e.g., Lyell, 1990; Triska, 1984). WD jams sometimes completely filled channels hundreds of meters in width for tens of kilometers. In addition to historical evidence, sedimentological studies recognize an apparent correspondence between WD deposition and bar formation in larger channels (e.g., Becker and Schirmer, 1977; Nanson, 1981; Green, 1982; Hickin, 1984), though it is unclear from such studies whether bar formation triggers WD deposition or the opposite occurs. Aggressive de-snagging efforts for navigation and flood protection during the past two centuries removed almost all evidence of how WD jams affected fluvial environments in many regions of the world (e.g., Sedell and Luchessa 1982, Sedell and Frogatt 1984, Shields and Nunnally 1984, Triska 1984, Gippel *et al.*, 1992).

Distinctive structural patterns to WD accumulations vary systematically through channel networks (e.g., Abbe *et al.*, 1993; Nakamura and Swanson, 1993), even though WD accumulations in a channel often appear chaotic or even random. This paper discusses processes governing systematic WD deposition and accumulation into structurally distinctive "jams" studies along the Queets River, Washington. Construction of these jams results in distinctive patterns of alluvial channel morphology, which modifies in-stream

habitat and influences local riparian forest succession. Jam types referred to as the "Bar Apex Jam" (BAJ) and "Meander Jam" (MJ) provide examples of WD structures that initiate and accelerate the formation of pools, bars, islands, and side-channels that define major in-channel habitat and riparian zones. Field observations and simple models describe the physical characteristics of BAJs and associated channel topography and forest patches. Channel geometry and bed textures provide estimates of background flow conditions. Models of flow fields and bed scour around a BAJ are compared to field measurements at two BAJs. The persistence of BAJs in the channel and their influence on riparian forest structure is examined and discussed.

2.2 Study Area and Methods

The 1164 km² Queets River basin lies on the west slope of the Olympic Mountains in northwest Washington State (Figure 2-1). Thirty years of U.S. Geological Survey (USGS) gauging station records at river kilometer (RK) 7.41 define the 1.5 year recurrence flood event as a flow of 1,824 m³/s. Steep glaciated terrain in the headwaters of the basin reach 2438 m in elevation; heavily forested terrain below 1200 m drains into a broad, low-gradient alluvial valley. Bedrock geology of the basin is characterized by Tertiary marine sandstones and shales that underwent low-grade metamorphism as a fore-arc accretionary prism (Tabor, 1987; Tabor and Cady, 1978). Extensive glacial till records recurrent alpine glaciation in the Queets valley during the Pleistocene (Crandell, 1965). The majority of the basin is mantled by temperate rainforest vegetation (e.g., Franklin and Dyrness, 1988; Kirk and Franklin, 1992) associated with extraordinary precipitation averaging about 5 meters annually, primarily contributed by rainfall from October to May. Upland forest communities are dominated by Sitka Spruce (*Picea sitchensis*), Douglas Fir (*Pseudotsuga menziesii*), Western Hemlock (*Tsuga heterophylla*), and Western Red Cedar (*Thuja plicata*). Species commonly associated with floodplain forest communities include Red Alder (*Alnus rubra*), Bigleaf Maple (*Acer macrophyllum*), and Black Cottonwood (*Populus trichocarpa*). In-channel WD includes each of these tree species, although individual species abundance depends primarily on the local recruitment population.

Potentially recruitable WD in the Queets River basin includes trees with basal diameters (at breast height) greater than 5 m and lengths in excess of 70 m.

The abundance of large and high quality timber found in the forests of the Olympic Peninsula sustained an intensive resource-based economy over the last century. On touring the region in 1937 and witnessing the rapidly changing landscape, President Franklin D. Roosevelt resolved to protect a significant portion of the Olympic Peninsula. President Roosevelt signed into law the formation of Olympic National Park in 1938, encompassing the upper 335 km² of the Queets River basin, which is now accessible only by foot or pack animal. Of particular interest to river management was Roosevelt's mandate to preserve at least one river valley in its entirety. In 1940 President Roosevelt authorized federal acquisition of a two mile (3.22 km) wide corridor down the lower 40 km of the Queets River Valley (Morgan, 1955). This unique addition to the park extends to within 11.5 km of the river's confluence with the Pacific Ocean, draining an area of 674 km². Field work has been conducted entirely within the park boundaries.

This study was part of a larger investigation in which mapping of channel reaches representative of different portions of the Queets River documented channel morphology, sediment textures, and WD accumulations. Study reaches extended from low-order ephemeral channels with gradients exceeding 0.25 to large mainstem channels with gradients < 0.01. This paper presents results from pool-riffle reaches (Montgomery and Buffington, 1993) of the mainstem Queets in which BAJs were observed. Topographic surveys upstream, downstream, and proximal to BAJs document associated variations in channel morphology. Surveys were conducted with a tripod-mounted autolevel from July through September of 1993 and 1994. Reach surveys recorded floodplain and thalweg elevations, channel and water surface slopes, and bankfull widths and depths. Surveys documented both the geometry of obstructed and unobstructed portions of each study reach and pool and bar topography.

A pool survey recording depth and pool type was conducted along a 25 km section of the active Queets River channel between RK 41 to 66 during August of 1994. Pools were defined as closed topographic depressions with residual depths (Lisle, 1989) greater

than 0.1 m. Pools were divided into those associated with WD, which were further classified by the WD jam type, and other pools, which were either free-formed or related to bedrock or boulders. Bed surface grain textures both representative for each study reach and proximal to jams were documented using pebble counts of at least 100 clasts (Wolman 1954). In-stream flow velocities proximal to a BAJ at RK 59.93 were point sampled with a electro-magnetic velocity probe. Horizontal and vertical velocity components were measured near the bed and at 0.2 and 0.8 of the flow depth. Vertical velocity components were made by attaching a 90° extension to the probe fitting.

Vegetation colonization constrained minimum age estimates for some jams and provided chronologies of topographic and forest patch development following jam formation. The distribution of BAJs was measured both in the field and from 1:12,000 scale color infrared aerial photographs shot during field surveys of August 1993. Comparison of 1993 images and 1985 1:12,000 scale black and white aerial photographs document jam persistence and illustrate changes in channel planform and forest patch development.

2.3 Types and Distribution of Wood Debris Jams

The WD accumulations in large channels display distinctive structural patterns that distinguish jam types formed by different processes (Abbe *et al.*, 1993). The Queets River system exhibits spatial patterns typical of large alluvial rivers in old-growth forest environments: a meandering channel frequently divided by bars and islands, abundant WD deposition, and a complex assemblage of riparian forest patches. These features are illustrated in Figure 2-2a, a 1985 aerial photograph of the confluence of Tshletsby Creek (flowing north) with the Queets River (flowing northeast to southwest). Examples of three WD jam types commonly observed along the mainstem Queets River, the Bar Top jam (BTJ), Bar Apex jam (BAJ), and Meander jam (MJ) are highlighted in Figure 2-2b. All jams cataloged in the study are recorded by channel name and river kilometer (RK), e.g., the BAJ on the Queets at RK 59.93 is designated as BAJ Q5993. Characteristics of four example study reaches are presented in Table 2-1.

A random accumulation of logs with little vertical stacking characterize BTJ's, which form a loose mat deposited on a bar top during receding flows. Although logs in a BTJ are oriented in all directions relative to the depositing flow, the majority are oblique. Two of the numerous BTJs visible in Figure 2-2a are highlighted in 2b. Bar top jams are relatively unstable as they are mobilized at discharges approaching bankfull. Hence they have little appreciable effect on channel morphology.

The more stable bar apex jam (BAJ) has a distinctive architecture characterized by three primary structural components; a key member nearly parallel to flow, normal members orthogonal to flow, and oblique members oriented 10-30° to flow. In the Queets River, key members appear to be invariably a large log with an attached rootwad facing upstream. Deposition of a key member significantly reduces the effective width of flow within a channel. WD that otherwise might be flushed through that portion of the channel is deposited, usually by racking up against the key member and contributing to a further reduction in the effective channel width. Normal members rack up against the key member rootwad orthogonal to flow, whereas oblique members deposit along the flanks of the key member. Sequential deposition of normal and oblique members commonly results in vertical stacking of five or more interwoven layers. Formation of a jam introduces a local control on channel hydraulics that leads to distinctive changes in channel morphology and riparian forest structure.

Stable WD structures such as the BAJ provide a barrier to high velocity flows, creating sites of sediment aggradation that can lead to floodplain formation. Stable WD structures also resist channel migration, thereby providing refugia for forest development. Jams buried in the Queets River floodplain are associated with anomalous forest patches significantly older than stands of floodplain forest surrounding them (Figure 2-2b). Only two of over 20 BAJs apparent on Figure 2-2a are identified in Figure 2-2b. Neither of these jams mobilized during an approximately 20-year flood November 23, 1990. Reaches of the Queets River containing BAJs have slopes, S , ranging from 0.003 to 0.03; widths from 30 to 100 m; and mean bankfull depths, h_b , ranging from approximately 1 to 3 m.

Meander jams become the most common of the stable jams with increasing channel size. Unlike the BAJ, MJs have only two principal structural components: key members and racked members. A MJ has two or more key members that are initially deposited at the upstream head of a point bar and oriented nearly parallel to bankfull flows. Key members usually have rootwads facing upstream and are within approximately one rootwad diameter of one another. Racked members of various sizes accumulate normal to key member rootwads, stacking on top of one another to heights of 6 m or more (several MJs are visible in Figure 2-2a). As the river migrates laterally, a stable MJ forms a revetment halting local bank erosion, often measurably compressing the river's radius of curvature and changing the orientation of the flow relative to the jam. Meander Jams are visible both on the Queets River and Tshletshy Creek in Figure 2-2a. The MJ identified on the Queets River in Figure 2-2b was constructed shortly before 1985. Field observations and aerial photographs from 1993 indicate the Queets channel migrated to the southwest after 1985, except at the MJ, which currently resembles the MJ identified on the north bank of Tshletshy Creek in Figure 2-2b. These jams eventually armor the concave outer bank of a meander and harbor riparian forest patches proportional in size to the size of the jam.

2.3.1 Alluvial Bedforms and Riparian Forest Patches

Field surveys indicate that WD jams strongly influence formation of scour pools and bars in large alluvial channels. Our survey of pool depths and probable formative mechanisms along the mainstem Queets channel documents the relative importance of WD jams for habitat formation in a large alluvial channel. WD jams are associated with 70% of all observed pools. Pools associated with jams on average are deeper and exhibit greater variance in depth than free-formed pools (Figure 2-3). While these observations illustrate that WD jams strongly influence pool abundance and morphology in alluvial channels, WD-associated pools also provide other habitat values (e.g., complex cover and nutrient trapping) not associated with pools formed by other mechanisms.

Pool characteristics differ for pools associated with different WD jam types. The BTJs have little or no influence on pool and bar formation. A BAJ is associated with several alluvial bedforms, each of which appears to form after deposition of the key member (Figure 2-4a). A crescentic pool (Figure 2-4b) forms directly upstream of and adjacent to the jam in an area of vortex development and flow acceleration. A region of flow deceleration upstream of this pool and centered along the axis of the jam results in deposition of an arcuate bar (Figure 2-4c). The largest pools associated with WD jams occur directly upstream of MJs. These pools tend to be long, narrow, and curve around the channel side of the MJ. The deepest pools surveyed were also adjacent to MJs.

Distinctive riparian forest patches develop in association with these jam types. Flow separation around the BAJ, for example, results in an elliptical area of low-velocity flow and sediment deposition along the axis of the key member. Progressive downstream colonization of a riparian forest patch occurs on this bar, displaying a distinctive downstream-decreasing profile of tree height (Figure 2-4d). A composite sketch of the BAJ and the associated alluvial topography and forest patch structure is presented in Figure 2-5. The region on the backside of the MJ, anchored by the boles of key members becomes incorporated into the floodplain and is characterized by spatially coeval tree colonization. Riparian forest patches associated with MJs thus tend to exhibit more uniform age structure and lack the more streamlined patches associated with BAJs. The time over which jams could potentially offer refugia for forest development can be deduced from dendochronology, historical data, and sedimentological evidence.

Analysis of U.S. Geological Survey maps of the Queets from 1931 and 1985, together with aerial photographs, indicates that large low-gradient alluvial reaches of the Queets actively migrate within the valley floor. Comparison of channel planforms from 1931 and 1985 digitized and referenced to UTM coordinates reveals long-term channel migration rates exceeding 10 m/yr. Assuming a simple model of progressive channel migration of 10 m/yr across a 1 km floodplain (i.e., ignoring avulsions often associated with WD jams) that riparian forests should rarely attain an age over 100 years. Yet anomalous forest patches within the floodplain reach ages in excess of 300 years.

Association of these patches with WD jams indicates that stable WD jams can provide hydraulic refugia over century time scales in extremely dynamic forested floodplains.

2.4 Hydraulic Effects of Debris Jams

Analyzing the influence of WD jams on local hydraulics and channel morphology requires modeling jams as simplified flow obstructions. Estimates of channel flow depths and velocities are necessary to determine whether a log is likely to be stable under particular flow conditions. Bed surface textures and topographic surveys allow back-calculation of channel flow conditions for a range of flows associated with the initiation of active bedload transport.

Grain size distributions on the active channel surface in a section of the study reach lacking other significant roughness elements allow quantitatively estimating the minimum critical shear stress required to initiate motion of the bed material, c , the associated flow depth, h , and mean channel flow velocity, U . This allows estimating the stability and local hydraulic effects of a log through analysis of buoyancy and flow drag (Abbe and Montgomery, in preparation). If the channel bed is mobile during bankfull events, then the basal shear stress, θ , exceeds c . Estimates of c and θ therefore can be used to evaluate a range of possible flow depths and velocities frequently occurring within the study reach.

The bed of most gravel-bed channels mobilizes at near-bankfull flow (see review in Buffington, 1995). The shear stress back-calculated from the size of the bed material depends on a dimensionless shear stress parameter, τ_c^* (Shields, 1936). Pitlick (1992) recommends using $\tau_c^* \approx 0.06$ and the median grain size, D_{50} , of the bed surface material to estimate the τ_c necessary to maintain bed material transport on a gravel bed. Buffington (1995) reviewed studies of τ_c^* and concluded that 0.032 provides the most appropriate estimate for τ_c^* in gravel-bed streams with bed material of mixed grain size. Several other studies, however, found that the best estimate of the τ_c necessary to initiate motion of a gravel bed of mixed grain sizes uses both the D_{50} and the coarsest fraction of the bed surface material (e.g., Parker and Klingeman, 1982; Wiberg and Smith, 1987; Pitlick, 1992). Wiberg and Smith (1987) demonstrate in theory that τ_c increases non-linearly as

the bed roughness length, k_s , increases relative to the median grain size. Komar (1987) derived an empirical expression for the transport of a particular size fraction of bed material, d_i , in gravel beds of mixed grain sizes assuming $\tau_c^* = 0.045$.

Critical shear stress values derived using these approaches (Table 2-2) allow the estimation of flow depths associated with active bedload transport by assuming $\tau_c = \tau_o = \rho_w g R S$, where $h \approx R$ and $S \approx$ hydraulic gradient. Together with calculated bedform roughness (Nelson and Smith, 1989) values of 0.05 - 0.10 τ_c for the low-amplitude, long-wave length bar forms in the Pelton reach, this implies significant excess shear stress during bankfull events.

Background flow velocities are needed to estimate the drag and alterations to the local flow field imposed by a WD structure. A logarithmic velocity profile as expressed in the Prandtl-von Karman equation (*law of the wall*) describe velocity profiles in natural channels where flow depth, h , is much greater than the boundary roughness:

$$\frac{u}{u_*} = \frac{1}{\kappa} \ln\left(\frac{z}{z_0}\right)$$

where u is the time averaged velocity at elevation z above the bed, u_* is the shear velocity $[(ghS)^{0.5}]$, κ is the von Karman constant (0.4), and z_0 is the boundary roughness length scale or height above the bed where velocity, u , goes to zero. Assuming the law of the wall adequately describes the velocity profile, integration of (1) over the depth of flow yields the average cross-section flow velocity, U ,

$$U = u_* \left(6.00 + 5.75 \log \frac{h}{30z_0} \right)$$

where h = flow depth. Nikuradse (1933) demonstrated that $z_0 = k_s / 30$ in hydraulically rough or high Reynolds number flow where k_s equals the equivalent sand roughness. Thus the roughness scale measure, either z_0 or k_s , becomes the only unknown in solving for U .

The Darcy-Weisbach expression provides an additional estimate for the mean flow velocity, $[U = (8ghS/f)^{0.5}]$, where f = Darcy-Weisbach friction factor (proxy of roughness scale). Limerinos (1970) found k_s in gravel-bedded rivers to be a function of D_{84} , such that

$$f = \left(1.16 + 2.03 \log \frac{h}{D_{84}} \right)^{-2}$$

an expression similar to the derivation of Leopold *et al.* (1964). This also yields a Nikuradse's sand roughness, k_s , of $3(D_{84})$, a value corresponding to derivations of $z_0 = 0.1(D_{84})$ presented by Whiting and Dietrich (1990). This, in turn, allows calculating the flow velocity from h and D_{84} (Table 2-3). Flow velocities associated with the initiation of bedload transport also can be derived from Equation (2) using flow depths computed from the three estimated values of τ_c (Table 2-3). Alternatively, Ferro and Giordano (1992) also used the D_{84} to experimentally derive an expression for the Chezy roughness coefficient, C , in gravel-bed rivers:

$$C = g^{0.5} \left[7.85 \log \left(\frac{h}{D_{84}} \right) + 1.41 \right]$$

which allows the estimation of C for bankfull conditions using estimates of τ_c in the Chezy formula, $U_b = C (RS)^{0.5}$ (Table 2-3). Estimates of bankfull flow conditions imply that BAJ Q6617 frequently experiences flow velocities of at least 0.8 to 2.9 m/s (Table 2-3).

Buoyancy analyses (see Chapter 3) indicate that key members with large rootwads float only at stages well above bankfull and thus the mobility of such logs is principally a function of the drag imposed by the flow. Analytical techniques in open-channel hydraulics for describing flow past bridge piers offer crude analogs to simple WD models. A model of uniform turbulent flow past a rectangular obstruction attached to a static boundary presents an analog to flow around a stable rootwad.

2.4.1 Effect of Obstructions on Flow

Assuming conservation of mass and no energy losses from upstream to downstream of an obstruction, flow will accelerate due to the associated with the decrease in cross-sectional area. Static pressure increases directly upstream of an obstruction in response to a reduced velocity and dynamic pressure of the approaching fluid mass. In an ideal non-viscous fluid, the energy exchange between dynamic and static pressure upstream of the obstruction occurs downstream and there is no drag. But the presence of factors such as viscous friction along the boundary, flow separation, and high pressure in front and low pressure behind an obstruction generate a pressure deficit defining a pressure drag force, F_D , empirically described as:

$$F_D = \frac{1}{2} \rho_w C_D U_1^2 A_{SW}$$

where A_{SW} is the submerged area of the obstruction normal to the incident flow, ρ_w is the fluid mass density, U is the mean incident flow velocity, and C_D is the drag coefficient of the obstruction.

Mobilization of WD requires that the drag force must exceed the normal and frictional forces resisting motion. Modeling the rootwad as a solid disk, the key member of BAJ 6617 would have a submerged area of 4.27 m² normal to flow during bankfull conditions ($h_b = 1.2$ m). Estimating the drag coefficient is less straight forward. Assuming channel banks impose no boundary effects on the obstruction suggests $C_D = 1.55$ (Rouse, 1946; Hoerner, 1965). Rootwads, however, are rarely solid, instead consisting of a radial network of roots. Petryk and Bosmajian (1975) recommended setting $C_D = 1.0$ for flows through living (standing) vegetation. Boundary conditions influencing flow around the obstruction strongly effect C_D . The magnitude of accelerations around bluff bodies proximal to separation points depends on the blockage ratio, Br , defined as the width of the obstruction to the channel width. Ramamurthy and Ng (1973) found that for Reynolds numbers of $10^4 - 10^5$ C_D remains relatively constant when $Br \ll 0.10$, but when $Br > 0.10$, C_D increases as a function of Br . Gippel *et al.* (1992) suggest that the effect on C_D

becomes significant with regards to flow conveyance and backwater affects when $Br \gg 0.05$. Drag is also affected by the surface boundary of the obstruction itself, the jagged edges of a rootwad, for example, would increase the length scale of the turbulent boundary layer, thereby reducing C_D . Assuming an estimate of $C_D \approx 1.55$, the resulting drag force imposed on the key member during a bankfull flow of ≈ 3 m/s is approximately 29.8 kN. For bankfull flow depths the resisting force stabilizing the example key member (Q6617) exceeds 600 kN (Abbe and Montgomery, in preparation), an order of magnitude greater than the estimated drag. At the bankfull flow depth of 1.2 m, (5) predicts the log would become unstable when the flow reached an unrealistic velocity of 42 m/s. Hence, mobilization of this BAJ key member requires flows greatly exceeding bankfull stage.

2.5 Influence of Debris Jams on Channel Morphology

Changes in channel hydraulics due to the presence of stable WD alter channel topography and surface textures. A simplified description of WD jam form, initial channel geometry, and particular flow conditions can be used to predict possible channel response to the jam. Although flow around obstructions in natural channels with deformable boundaries is extremely complex, experimental work provides a range of qualitative and empirical models for predicting channel response around obstructions, especially for bed scour.

Channel topography and bed surface textures provide evidence that WD jams do effect local hydraulics in ways that appear to reflect jam structure or type. The development of null points, vortex flow, separation, and flow acceleration around a BAJ resembles a conceptual model of flow past a simple obstruction by Raudkivi (1990). Modeling a BAJ as a rectangular plate extending through the water column, one would expect a zone of flow deceleration upstream of the jam, acceleration adjacent to the jam, and vortex development due to the translation of predominantly horizontal flow to vertical flow directly upstream of the jam (Figure 2-5). If a simple rectangular or circular obstruction is introduced orthogonal to a spatially uniform flow, than the flow pattern in the horizontal (x, y) plane (plan view) upstream of the obstruction are assumed to

symmetrical about its central axis. A hypothetical near-bed (x,y) flow field upstream of a BAJ modeled as a simple obstruction on a static bed is presented in Figure 2-6a. This interpretation was compiled based on Eckerle and Langston's (1986) conceptual model of vortex flow around a cylindrical pile, Lai and Makomaski's (1989) numerical modeling results of three-dimensional upstream of a rectangular obstruction, and Kwan and Melville's (1994) flow visualization experiments for scour around bridge abutments. Accumulation of static pressure directly upstream of an obstruction leads to flow reversal near the bed and formation of a "saddle" or null point at some distance upstream of the obstruction (Figure 2-6a). For an ideal flow, near-bed horizontal velocity components directly upstream of an obstruction are characterized by two distinct null points, (points 1 and 2) and flow reversal. Flow constriction and acceleration occurs adjacent to the obstruction and flow separation occurs downstream (points 3 and 4). Measured flow patterns exhibit similar characteristics around an actual BAJ during low-flow conditions (Figure 2-6b, photograph of site in Figure 2-4a). The measured flow field displays a distinct asymmetry mirroring that of the channel; higher flow velocities correspond to the channel thalweg north of BAJ Q5993 and the lower velocities toward the point bar south of the jam. Null points identified in Figure 6a correspond to areas in which the principal velocity components are transformed from horizontal to vertical, as illustrated along profile A-A' in Figure 2-6c. Downward flow acceleration adjacent to the obstruction (between points 1 and 4) and upstream accelerations (between points 4 and 3) are strongly associated with vortex formation partially responsible for local scour contributing to the formation of the concentric pool upstream of the jam. These flow patterns and resulting scour and deposition are illustrated in profile B-B' of the measured flow field upstream of BAJ Q5993 (Figure 2-6d). Flow patterns around BAJ Q5993 illustrated in Figures 2-6b and 2-6d are reflected in channel topography and bed surface textures (Figures 2-7a and 2-7b). Flow in Figure 2-7a is right to left and topography mirrors the asymmetry of flow presented in Figure 2-6b. Figure 2-7a also illustrates formation of the arcuate bar, crescentic pool, and downstream bar outlined in Figure 2-5. In addition to topographic effects, BAJs introduce significant local variation in bed surface textures, most notably

coarsening of the bed in the crescentic pool and deposition of fines on the downstream bar (Figure 2-7b). Field observations reveal that sediment deposition forming the downstream bar commonly buries the bole of the key member.

2.5.1 Pool Depths

The flow field around a WD jam not only affects its stability, but the bedform characteristics around the jam. Pools due to flow scour are commonly associated with channel constrictions or obstructions such as bedrock outcrops, boulders, and WD (e.g., Bisson *et al.*, 1982; Lisle, 1986). Pool frequency is directly correlated to WD loading in plane-bed, pool-riffle, and forced pool-riffle channels in Alaska and Washington (Montgomery *et al.*, 1995). Channel obstructions not only introduce constrictions to channel flow, but generate vortex flow which can influence bed scour.

Raudkivi (1990) discusses three general types of bed scour: (i) *general scour* occurs irrespective of an obstruction's presence; (ii) *constriction scour* occurs due to a reduction in channel cross-sectional area; and (iii) *local scour*, which is attributed directly to an obstruction's effect on flow patterns and can be super-imposed on either general or constriction scour. Local scour is estimated based on either "clean water" or "live-bed" active sediment transport conditions. Vortex flow is attributed to the downward acceleration of flow directly upstream of an obstruction (Baker, 1979; Raudkivi, 1990). The envelope of flow separation and re-attachment downstream of an obstruction define the region in which bar formation is likely due to rapid flow deceleration. The point of flow separation is a function of the obstruction's form and surface roughness and the Reynolds number of the flow. The high surface roughness of WD would tend to reduce the area of separation by increasing the flux of momentum from the outer high-velocity zone into the boundary layer by the transfer of turbulent kinetic energy. This reduces the pressure gradient on either side of the obstruction, thereby reducing pressure drag or forces tending to move the object. It would also reduce the potential scour due to vortex development.

Estimation of bed scour around channel constrictions and obstructions relies primarily on empirical relationships largely based on experimental results from small-scale physical models (Raudkivi, 1990). Models for local scour around an abutment provide a first-order estimate of scour depths around a BAJ structure. Liu *et al.* (1961) derive an equation for dimensionless clean-water scour, (d_{ls} / h), as a function of abutment length, L_A , flow depth, h , and flow Froude number, $Fr = U/(gh)^{0.5}$ using dimensional analysis and laboratory tests:

$$\frac{d_{ls}}{h} = 2.15 \left[\frac{L_A}{h} \right]^{0.4} Fr^{0.33}$$

Liu *et al.* (1961) and later Tey (1984), found observed values for maximum scour to be 30% greater than those predicted by the above expression. Bar Apex jam Q6617 in the Pelton reach is about 10 m wide with scour occurring on either side (e.g., Figure 2-5). Scour predictions made by modeling the structure as an abutment projecting 5 m into a 25 m wide channel for Q6617 and Q5993 (Figures 2-4a, 2-6b, 2-6d, 2-7a, and 2-7b) are presented in Table 2-4. The predicted clean water scour for Q6617 of 4.41 m is significantly greater than the observed pool depth of 1.35 m. This discrepancy may partially reflect bed material characteristics resulting in bed armoring during scour. Raudkivi and Ettema (1977) found that sediment grading is a significant control on the equilibrium clear-water scour depth. They found the ratio of d_{ls} in graded sediments to that in uniform sediments to be function of the geometric standard deviation of the sediment population, $s_g = (D_{84}/D_{16})^{0.5}$. Using the graphical solution presented by Raudkivi (1990, p.251) and the Pelton reach $s_g = 4.0$, a correction factor of 0.25 is obtained and the predicted local scour depth is reduced from 4.41 to 1.15 m (Table 2-4).

Laursen (1963) presented an empirical expression based on experimental results to estimate constriction scour (Raudkivi, 1990, p.245),

$$d_{cs} = h \left[\left(\frac{\tau_o}{\tau_c} \right)^{0.429} \left(\frac{w_{b1}}{w_{b2}} \right)^{0.857} - 1 \right]$$

where h = flow depth, w_{b1} = unobstructed flow width and w_{b2} = constricted flow width. The predicted constriction scour depth for Q6617, where $w_{b1} = 50$ m and $w_{b2} = 40$ m, is 0.62 m (Table 2-4). Applying the correction factor of 0.25 due to bed armoring, $d_{cs} = 0.15$ m. Combining constriction scour and local scour from the abutment analysis, total predicted scour is within 3% of the observed pool depth (Table 2-4). Similar analysis for the BAJ Q5993 example yields a 17% difference between predicted and observed scour (Table 2-4). It seems, therefore, that in some cases experimentally derived expressions can provide approximate analogs for estimating the size of scour pools associated with natural WD structures in alluvial channels.

2.5.2 Historical Jam Stability

Sequential reconstructions based on historical mapping and aerial photographs of the Queets river at RK 52 illustrate channel characteristics before and after deposition of several BAJs (Figure 2-8a - 8d, flow is from left to right). A topographic map of the area completed by a USGS plane-table crew in 1931 shows a single-thread channel (Figure 2-8a). The reach widened by 1939, developing a bar at the downstream end of the field-of-view (Figure 2-8b). A reduction in channel depth likely accompanied this widening, increasing the potential for deposition of key members. Development of the first bar in the reach may reflect the deposition of a BAJ key member, but cannot be confirmed from the image resolution. Aerial photographs from 1985 and 1993 (Figures 2-8c and 2-8d) had the resolution to distinguish general forest cover characteristics not possible from the 1931 map or 1939 photograph. Sometime between 1939 and 1985, several key members were deposited in the upstream end of the reach (Figure 2-8c), well above the initial bar visible in 1939. The BAJ farthest upstream exhibits the distinctive upstream arcuate bar and downstream central island in the process of being colonized by riparian forest vegetation.

The same site eight years later in 1993 (Figure 2-8d) records riparian forest structural development on streamlined islands in the lee of BAJs. By 1993 the islands associated with separate BAJs in 1985 (Figure 2-8c) coalesced into one large island with a small interior back channel (Figure 2-8d). Gage-discharge data for the lower Queets at RK 7.4 indicate that between water years 1985 - 1992 the site was subjected numerous flows above bankfull, including an approximately 20 year flood. Hence, the key members forming these BAJs remained stable through several large flow events.

2.6 Discussion

The development of BAJs provides a dramatic illustration of the morphologic influence of WD jams in large rivers. The process of BAJ development involves the initial deposition of a key member after hydraulic transport. The deposition of a key member alters the local flow patterns, initiating bar growth and potentially island formation. Changes in channel morphology due to BAJs can be synthesized into four morphological stages (Figure 2-9). Stage I consists of the initial recruitment of a key member and the basic flow disturbance it introduces (Figure 2-9a). Stage II involves modification of the alluvial landscape into a distinctive set of bars and pools (Figure 2-9b). Aggradation on the central bar can eventually lead to island development when the sediment surface reaches or exceeds bankfull elevation, Stage III (Figure 2-9c). Additional recruitment of racked WD and/or channel migration unrelated to the original BAJ can close off one of the channels. Subsequent deposition in the abandoned channel can re-attach the island to the floodplain, represented in Stage IV (Figure 2-9d). The entire BAJ site thus can be incorporated into the floodplain environment; such cases appear to result in anomalous forest patches within more recent riparian forests that colonized the abandoned channels.

2.6.1 Channel Habitat Structure

Alteration of in-channel flows due to the formation of a BAJ results in three important geomorphic features directly affecting the quality of aquatic and terrestrial riparian habitat: pools, bars, and islands. The deepest pools in a 25 km section of the

Queets River are associated with WD jams. Pools are an integral physical component for the life stages of many aquatic organisms, such as providing refugia and rearing habitat to anadromous fish. The rate at which jams and their associated bars grow is likely to be a function of the size and rate of WD recruitment to the channel upstream of the BAJ and sediment transport through the reach.

Tarzwel (1934) recognized that natural in-channel WD structures enhance fish habitat and presented designs for constructing hydraulic control structures to restore habitat where natural structures had been eliminated. Despite such early work, natural WD structures in the Pacific Northwest were aggressively removed from the 1950's to 1980's to "improve" fish habitat (Sedell *et al.*, 1984). Recognition of the ecological importance of WD as an in-channel element during the last several decades led many to advocate re-introducing WD to channels and leaving riparian buffers to provide future WD recruitment (e.g., Harmon *et al.*, 1986; Gregory and Davis, 1992; National Research Council, 1992). Recognition and modeling of natural WD structures provide a guide for the design of effective channel restoration schemes.

2.6.2 Riparian Forest Development and Management

Riparian forests along large alluvial channels generally have been characterized as relatively young and homogenous tree communities that reflect frequent disturbance (e.g., Fonda, 1974). Swanson and Lienkaemper (1980), however, noted the presence of isolated forest patches over 250 years in age on relatively low floodplain surfaces dominated by trees only several decades old. Observations along the Queets River (e.g., Figure 2-2a) show a diverse riparian forest structure and anomalous old-growth patches that attain ages in excess of 300 years within the riparian corridor. Three primary factors facilitate riparian forest colonization downstream of the BAJ: i) local flow deceleration and decreased basal shear stresses, ii) sediment deposition, and iii) an abundant accumulation of organic matter on the surface. The formation of natural WD structures creates distinctive alluvial topography that can persist for at least as long as the structure remains stable. Observation of old-growth riparian forest patches within the zone of active channel migration suggests

that some WD structures remain stable despite repeated integration into the active channel. The potential for excellent preservation of WD in fluvial gravels (e.g., Becker and Schmirer, 1977) indicates that a jam buried in floodplain sediments could continue to function as a hydraulic structure even after being re-exposed. Hence these structures may provide long-term refugia for floodplain riparian communities, forming anomalous old-growth riparian forest patches in an alluvial terrain characterized by frequent disturbance.

Our surveys reveal that WD structures are a principal mechanism for the formation of deep pools and islands in large channels in forested environments. In particular, formation of BAJs and the associated habitats depends on recruitment of key members from among the largest trees in channel-margin forests. Moreover, it is the largest trees in a population that are most likely to topple and retain their rootwad instead of snapping above the ground (Putz *et al.*, 1983). Thus if land managers desire preservation of physical habitat features associated with old-growth riparian systems, management activities must ensure adequate recruitment of the largest WD from channel-margin forests. Hence, selective removal of the largest trees from riparian and floodplain forests will have major impacts on in-channel habitat characteristics.

2.7 Conclusion

Although much is known about the influence of WD on small channels, substantial effort is necessary to understand the processes influencing the remaining large pristine forest channels of the world. Evidence from the Queets River Watershed of northwest Washington together with historical studies documents that distinct types of WD jams are an integral structural element in large alluvial channels in forested environments. In particular, WD jams are a principal mechanism controlling reach-level habitat diversity through the formation of scour pools, bars, and riparian forest refugia. Jams can act as local hydraulic controls over several decades and possibly centuries. The initiation and development of Bar Apex jams illustrates the importance of recruiting the largest components of WD from channel-margin forests for the formation of aquatic and riparian

habitat in large alluvial rivers. The large size of the individual trees necessary to initiate formation of stable jams has important implications for riparian forest management.

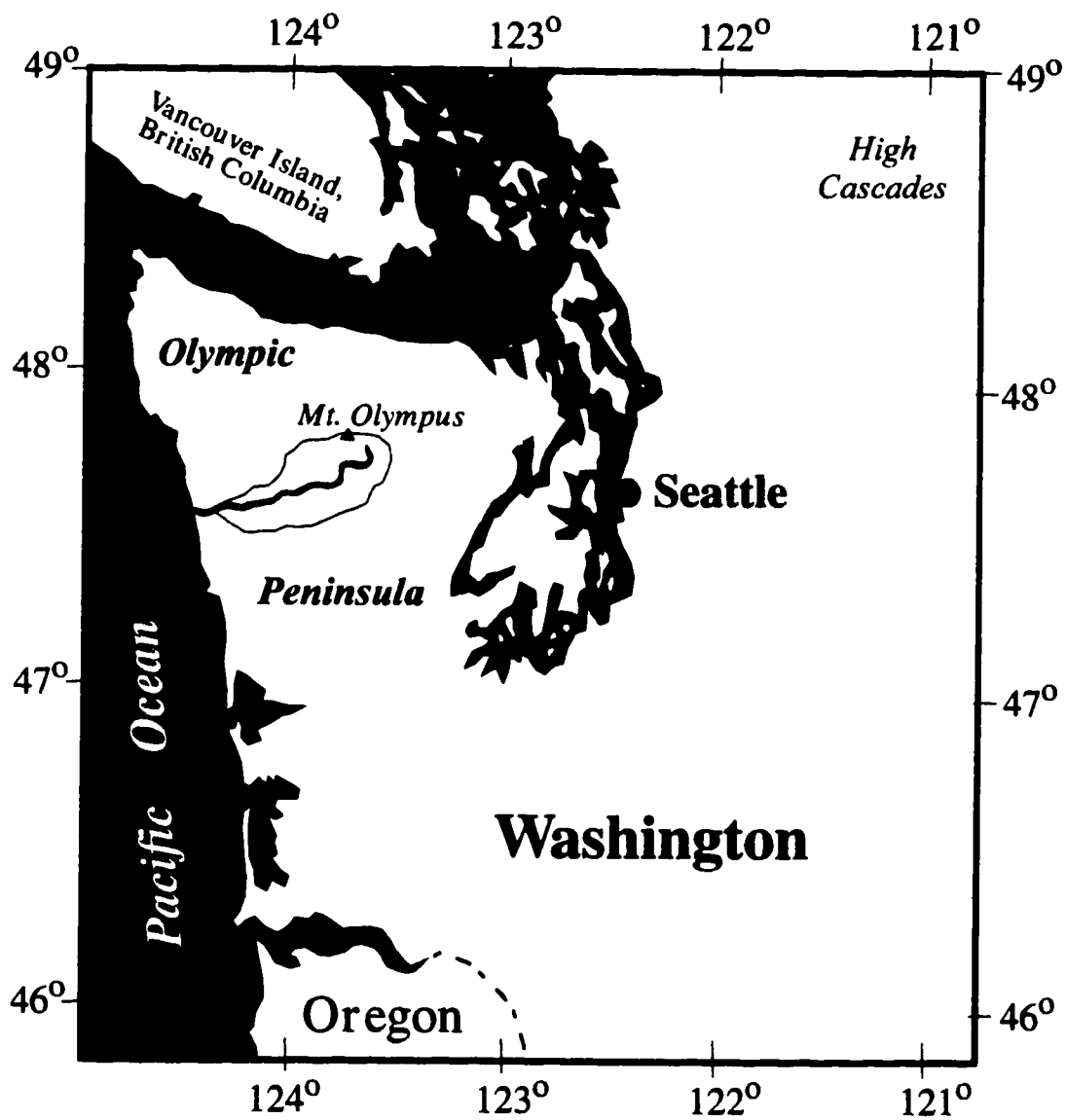


Figure 2-1. The Queets River watershed, Olympic Peninsula.

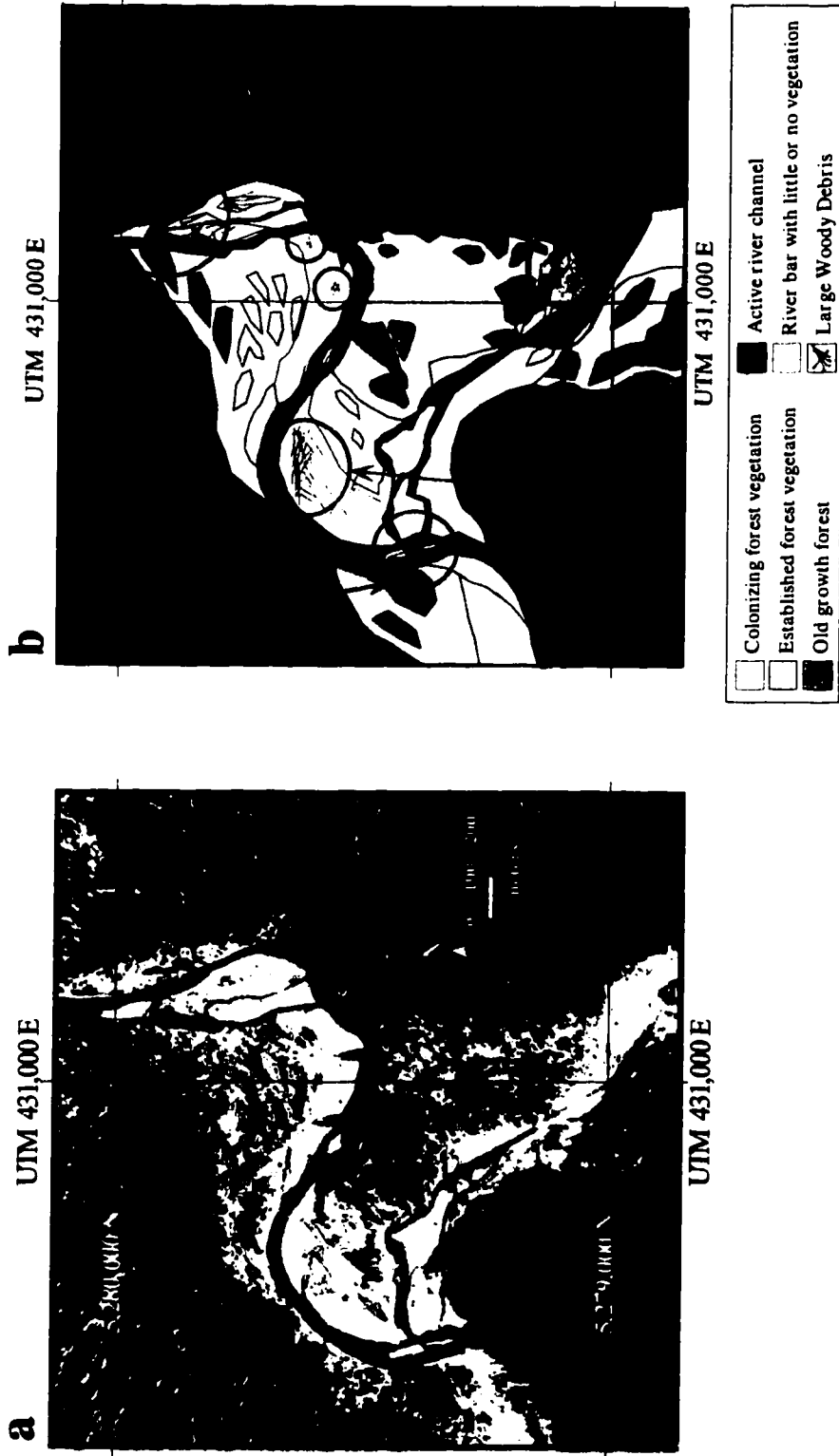


Figure 2-2. Example of WD jams in a large alluvial channel: a) March 7, 1985 aerial photograph of Queets River Reach km 50.58 - km 52.12 and Tshletshy Creek Reach km 0 - km 1.12 illustrating complex channel and forest patch patterns of an old-growth river system. b) Selected examples of three types of WD jam types observed in the area: unstable Bar Top Jams (BTJ); stable Bar Apex Jams (BAJ) and stable Meander Jams (MJ). General patterns in the forest-patch structure are illustrated.

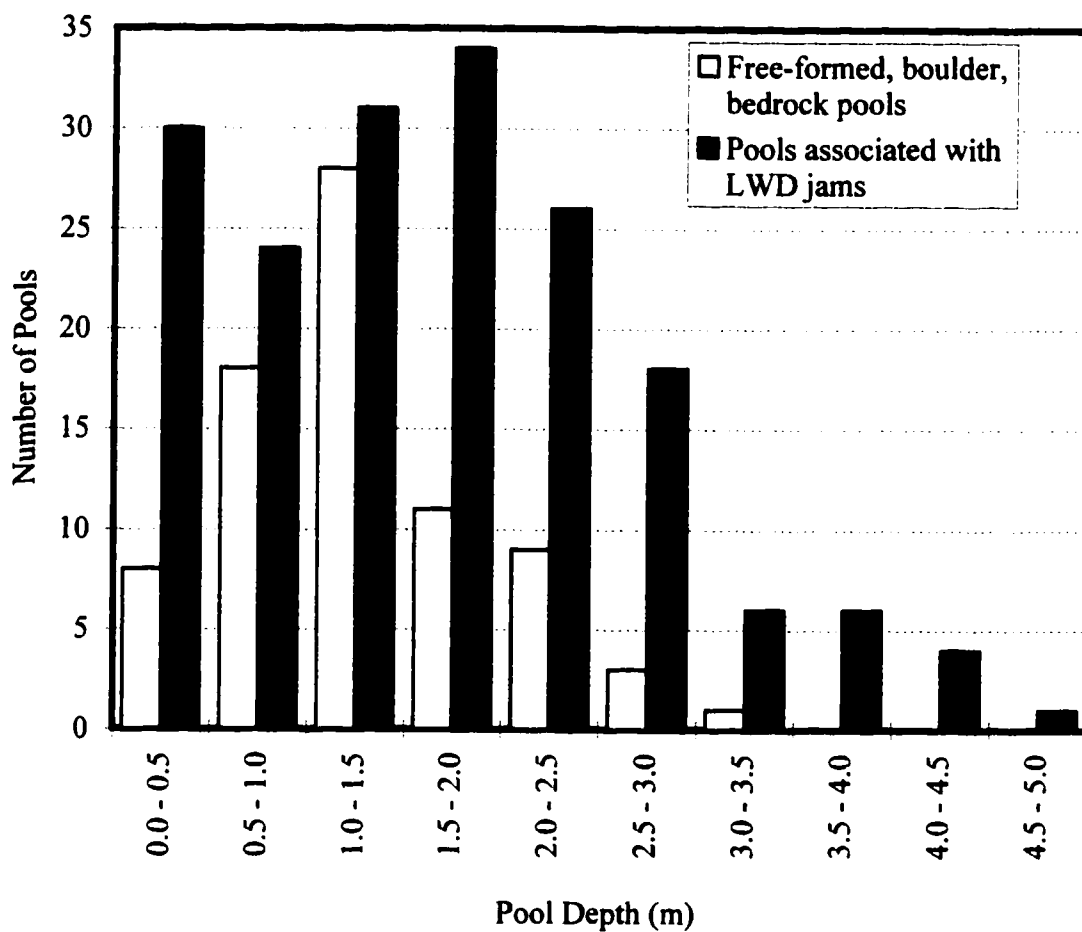


Figure 2-3. Frequency distribution of the depth of pools associated and not-associated with WD jams between Queets RK 41 and RK 66; surveyed in August 1994.



Figure 2-4. Features associated with Bar Apex Jams. a) key member (BAJ Q5993), b) crescentic pool (BAJ Q5022), c) arcuate bar (BAJ Q5291), d) associated riparian forest patch (BAJ Q6749).

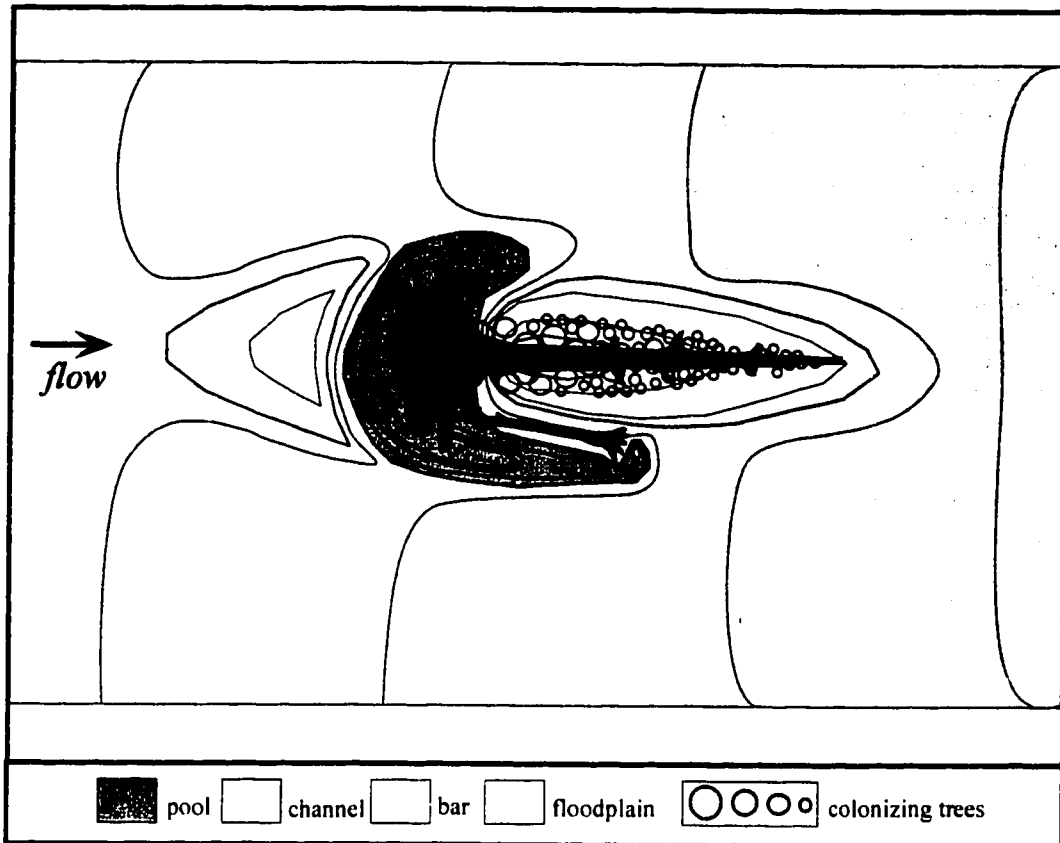


Figure 2-5. Composite sketch of physical attributes of the Bar Apex jam type showing characteristic patterns in channel-bed topography, WD structure, and riparian forest age structure.

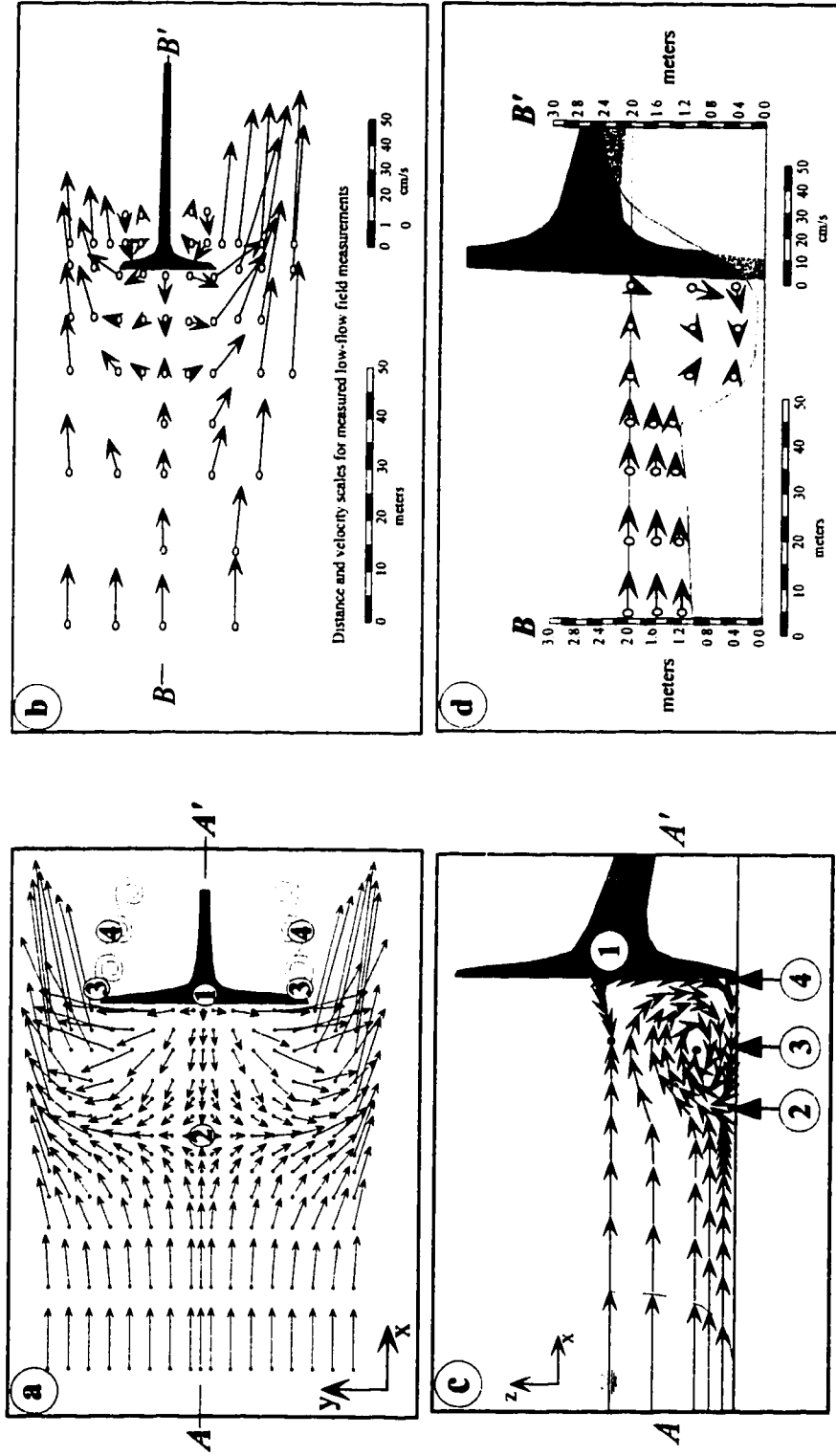


Figure 2-6. General flow patterns showing relative flow velocity vectors upstream of a BAJ. a) plan view of idealized near-bed flow field, point 1 delineates zone of vortex initiation, 2 is the saddle-point where flow goes to zero, 3 is the point of flow separation and 4 is boundary of separation envelope downstream of jam; b) plan view of measured low-flow field measurements, point 1 corresponding to the development of a downward acceleration in flow initiating vortex flow, 2 is the saddle point, and 3 and 4 delineate the zone of vortex scour; d) profile of measured flow field; upstream of BAJ Q5993.

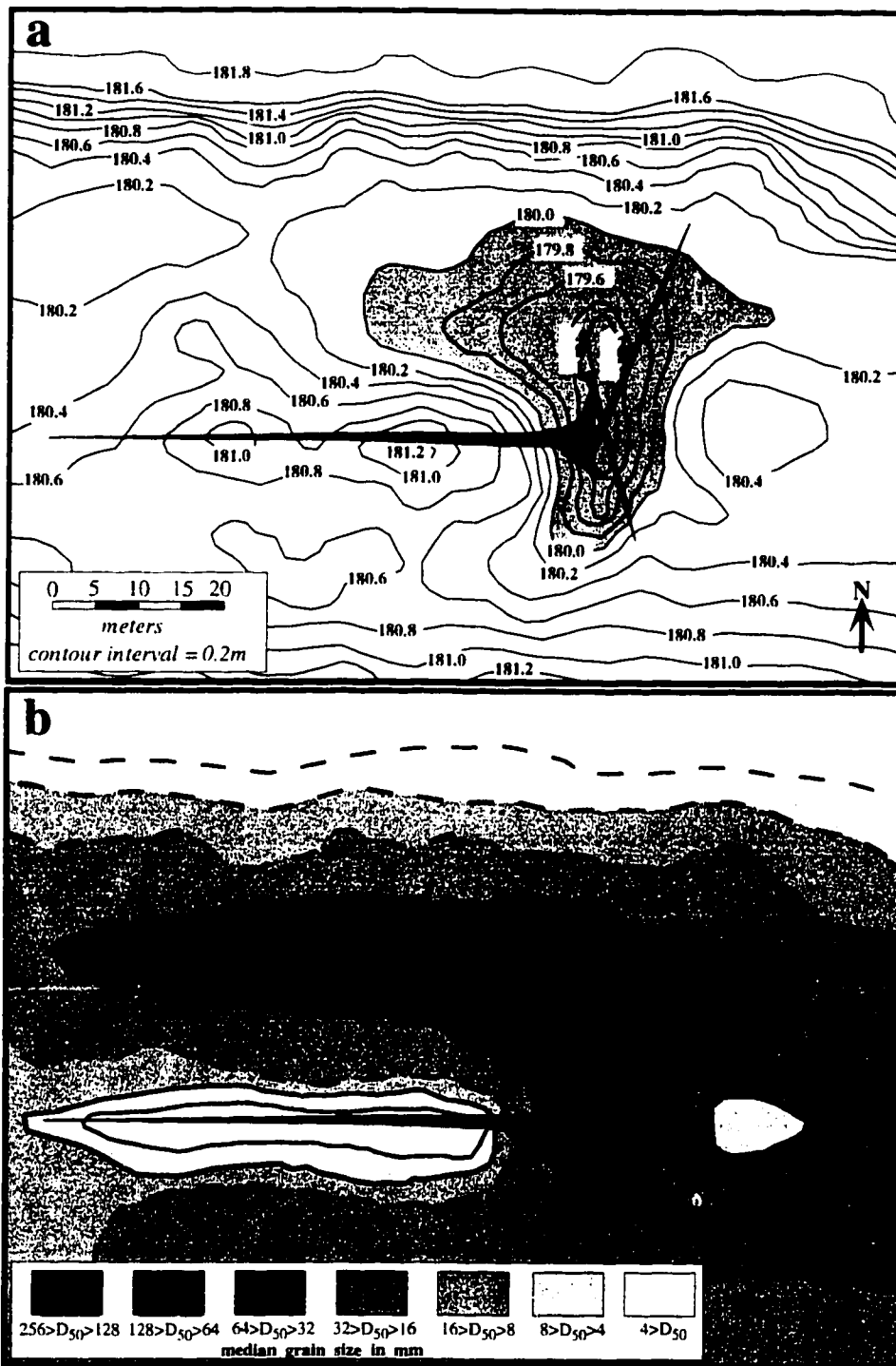


Figure 2-7. Field survey of BAJ Q5993, flow is right to left; a) pool and bar topography, shaded area delineates closed depression defining pool, b) median grain size of bed surface.

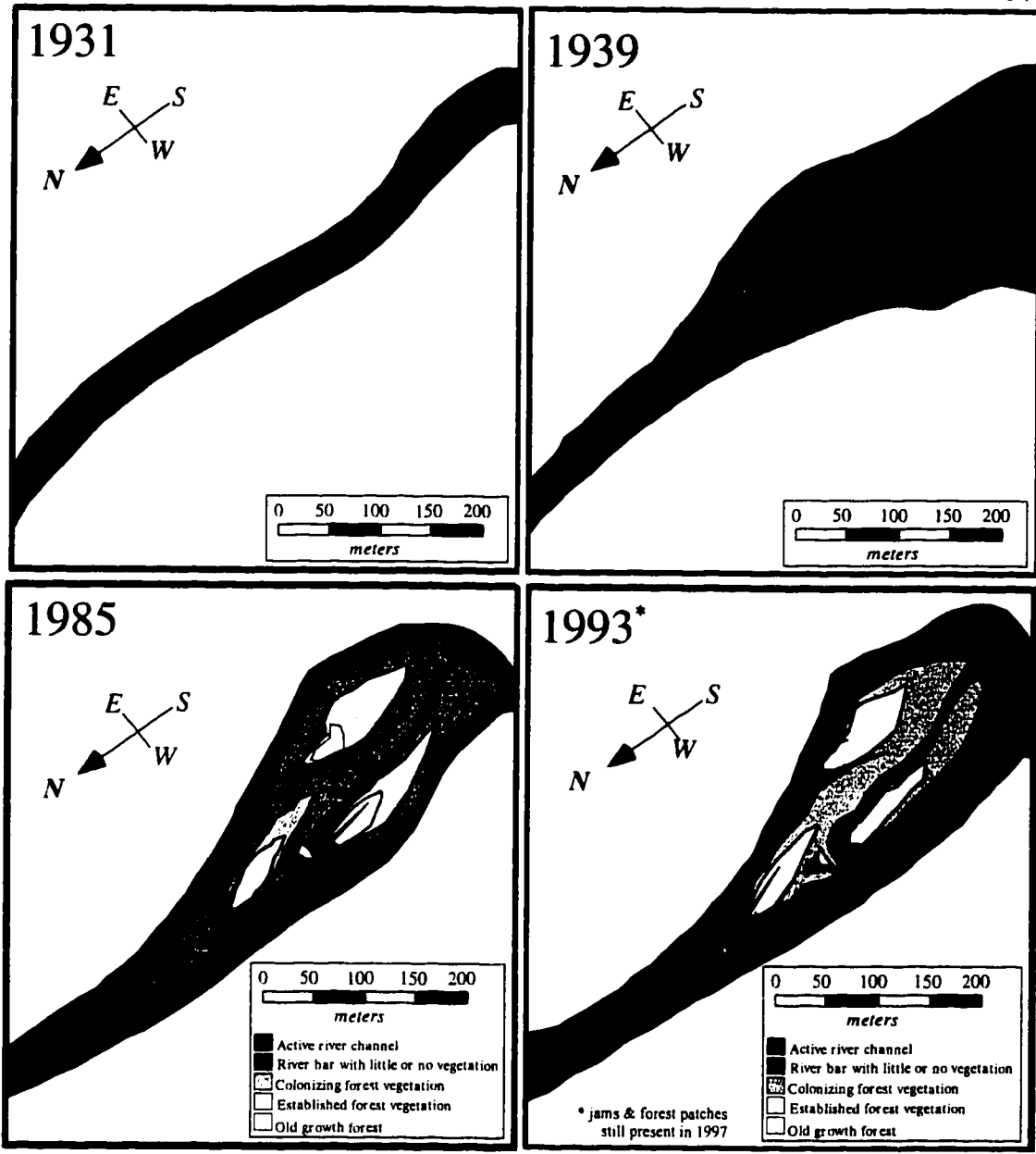


Figure 2-8. Maps illustrating development of a bar apex jam and associated alluvial morphology and riparian forest development, Queets RK 51.52 - 52.3. Flow is from left to right. a) 1931 - active channel boundaries from U.S. Geological Survey plane table map (1:32,630, 1.52 m contours); b) 1939 - channel outline from 1:62,500 black and white aerial photograph (U.S. Army); c) 1985 - channel, bar, and forest boundaries from a 1:12,000 black and white aerial photograph shows deposition of several Bar Apex jams and colonization of forest vegetation occurred within the active channel sometime between 1939 and 1985; d) 1993 - channel, bar, and forest boundaries from a 1:12,000 color infrared aerial photograph shows each of the BAJs visible in 1985 are still present and island forest patches have continued to mature.

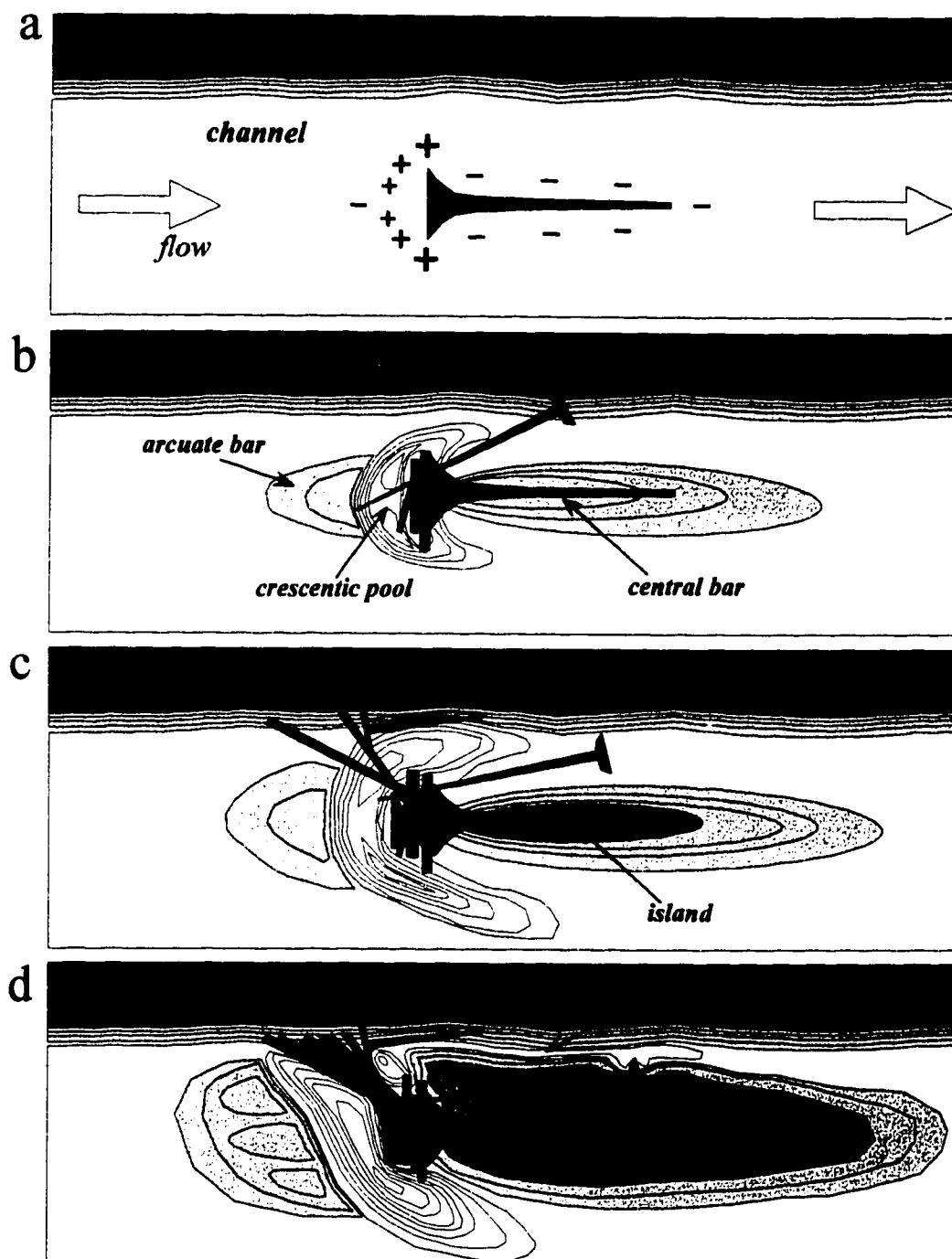


Figure 2-9. Morphologic stages in alluvial topography associated with construction of a Bar Apex jam (key to geomorphic surfaces identical to Figure 2-5): a) deposition of the key member; b) formation of an upstream arcuate bar, a crescentic pool upstream and adjacent to the key member rootwad and/or normal members, and a downstream central bar along the axis of the key member bole; c) island development along central bar; and d) eventual integration into the floodplain development.

Example Study Reach	Drainage Area (km ²)	Bankfull		Slope (m/m)	D ₅₀ (m)	D ₈₄ (m)
		Width (m)	Depth (m)			
T 0.0-1.12 ^a	74.40	30	0.91	0.0112	0.063	0.117
Q 50.58-52.12 ^b	224.72	83	1.42	0.0050	0.022	0.079
Q 59.02-60.31 ^c	178.97	66	1.29	0.0059	0.047	0.087
Q 65.40-66.49 ^d	154.63	50	1.20	0.0095	0.068	0.161

- a Figure 2-2, Tshletshy Creek at confluence with Queets River
b Figure 2-2, Queets River at confluence with Tshletshy Creek
c Figure 2-7, Queets River RK 59.93
d Queets River Pelton Reach

Assumed dimensionless critical shear stress, τ_c^*	Derivation for estimating critical shear stress at initiation of bedload transport	Computed critical shear stress, τ_c (Pa)	Minimum flow depth ^a (m)
0.032 (Buffington, 1995)	$\tau_c = \tau_c^* (\rho_s - \rho_w) g D_{50}$	35.0	0.38
0.060 (Pitlick, 1992)	$\tau_c = \tau_c^* (\rho_s - \rho_w) g D_{50}$	65.6	0.70
0.045 (Komar, 1987)	$\tau_c = \tau_c^* (\rho_s - \rho_w) g D_{50}^{0.6} D_i^{0.4}$	69.5	0.75

a $R = \tau_0 / (\rho g S)$

Estimated basal shear stress (Pa)	Shear velocity u^* (m/s)	Mean velocity using law of the wall (m)	Darcy-Weisbach friction factor, f	Mean velocity using f (m/s)	Chezy roughness coefficient, C	Mean velocity using C (m/s)
35.0 ^a	0.187	1.41	0.272	1.02	13.59	0.82
65.6 ^a	0.256	2.32	0.166	0.77	20.11	1.64
69.5 ^a	0.264	2.44	0.158	0.88	20.85	1.76
111.8 ^b	0.334	2.73	0.110	2.85	25.86	2.76

a Computed critical shear stress, see Table 2-2

b Computed from $\tau_0 = \rho_w gRS$, using the bankfull depth.

Bed scour predictions	BAJ Q6617	BAJ Q5993
Estimated clean-water scour depth, d_{ls} (m) ^a	4.41	4.18
Estimated constriction scour depth ^b , d_{cs} (m) ^b	0.62	0.56
Bed grain size standard deviation, $\sigma = (D_{84}/D_{16})^{0.5}$	3.17	3.11
Bed armouring correction factor, k_g ^c	0.26	0.27
Corrected clean water scour depth (m)	1.15	1.13
Corrected constriction scour depth (m)	0.16	0.15
Total estimated scour depth (m)	1.31	1.28
Observed pool depth (m)	1.35	1.09
Percentage difference	3	17

a Liu *et al.* (1961)

b Laursen (1963)

c Raudkivi (1990, p.251)

CHAPTER 3: MECHANICS OF WOOD DEBRIS STABILITY IN A FLUVIAL NETWORK

“A close study of conditions shows that in every instance the current was first deflected by an accumulation of drift, the huge timber of this section serving readily in its formation.”

- H.H. Wolff (1916, p.2062) from a description of the White River east of Tacoma, Washington

3.1 Introduction

It is well documented that wood debris (WD) can form stable obstructions that significantly alter the physical characteristics of forest streams and rivers. Published reports indicate that in-stream WD can remain stable for decades or even longer in channels ranging from small streams (Bryant 1980, Tally 1980, Nanson et al. 1995) to large lowland rivers (Veatch 1906; Guardia 1927, 1933; Sedell and Luchessa 1982; Phillips and Holder 1991; Nakamura and Swanson 1993; Gippel et al. 1996). Those factors that enable only certain WD to form stable obstructions, however, have not been identified. The objective of this chapter is to present several quantitative models to better understand principal factors influencing the stability of WD and its deposition throughout a channel network. These simple models provide preliminary physical explanations of WD stability that are consistent with field observations presented in Chapters 1 and 2. This chapter will also explore several theoretical explanations for the role of bole shape, which is typically overlooked when interpreting the stability of natural in-stream WD.

Tree boles become embedded in a wide range of alluvial rivers around the world. In North America these flow obstructions are commonly referred to as snags, planters, sawyers or chicots (French for "river teeth"). Snags in the Mississippi and its tributaries have been found buried more than 7 meters in sand or silty channel beds (e.g., Day 1921, Dorsey 1941). Snags observed in gravel bedded rivers of the Pacific Northwest are found embedded up to 5 meters, based on channel bed excavations done for bank protection projects and on snags exposed in scour pools. Embedded snags tend to have similar orientations in the channel: the bole is oriented parallel to flow, the rootwad is at least

partially buried along with the basal portion of the bole, and the trunk or bole of a buried snag typically extends upward at angles of 10-30° from the horizontal. Once embedded, snags can be extremely difficult to dislodge, forming significant navigational hazards on large rivers and the nuclei for large WD accumulations or jams.

In-stream WD once was widely distributed throughout forest drainage basins. Even in large rivers, WD commonly formed stable obstructions that presented a serious hazard to navigation. The presence of several snags could also lead to large accumulations of WD capable of obstructing the entire channel, increasing the frequency and magnitude of flooding, initiating major and unpredictable changes in channel form and location, and transforming a single-thread channel into an anastomosing system of perennial and ephemeral channels spanning the width of a valley bottom (Shoecraft 1875, Ruffner 1886, War Department 1898, Guardia 1927, 1933). Snags posed a significant hazard to navigation and an impediment to land development associated with colonization and industrial expansion.

3.2 Methods

To understand better how stable snags form, simple quantitative models of tree boles were used to investigate the role of shape, size, density and strength in WD stability. Spatial properties in wood are defined using three axes: tangential, longitudinal, and normal (Figure 3-1). Wood debris (WD) shape is modeled as a cylinder with differing taper or change in radius along the longitudinal axis of symmetry. Only models of single tree boles with or without intact root wads were examined. Complex forms with irregular boles, multiple boles, or branches were not examined in this study. Density and strength were assumed to be uniform throughout the tree bole. Realistically, these properties can vary a great deal throughout a tree.

Wood debris shape has most commonly been represented as a truncated cone or fustrum having a linear taper defined by the diameter at either end (Figure 3-2). The rapid increase in tree bole radius near the ground is referred to as buttressing (Putz et al. 1983). The fustrum model does not provide a realistic representation of the majority of snags and

key pieces, which have retained the roots and the lower portion of the bole. As will be shown here, the basal portion of a tree and its rootwad can account for a large percentage of the tree's total mass, significantly affecting the tree's shape, and increasing the trees maximum radius by up to a factor of five.

To compare hypothetical models with actual trees, field measurements of tree forms were used to evaluate the models. A maximum radius was taken at the rootwad, if present. I measured the basal radius of the bole, R_b , at the appropriate inflection point of the bole's curvature or taper. The distance along the bole axis from the rootwad radius to the bole radius was recorded, as was total length and the crown radius at the small end of the bole. Where no rootwad was present, R_b represented the maximum tree radius. Weights for thirty-one trees (not all with rootwads) were obtained using a large crane. An increment borer was used to take 2.5 mm diameter cores from each of the weighed trees. These cores were used to determine densities, after which the tree weights were estimated using each tree geometry model. Estimated weights were compared to measured weights. A moment and force balance analysis was used to investigate the effect of shape on weight distribution and buoyance for different models of tree geometry.

The shape of snags found in Pacific Northwest rivers depends on the original tree structure, which is generally a function of species. Conifers are characterized by a single straight large bole with a narrow, conical canopy structure of branches significantly smaller than the bole. Deciduous trees exhibit a wide variety of bole and branch configurations ranging from Black Cottonwood (*Populus trichocarpa*), which has a structure more similar to conifers with a single, tall dominant bole and narrow canopy, to Big Leaf Maple (*Acer macrophyllum*), which displays an expansive branch structure (Figure 3-3).

Stable snags observed in the Queets River and other Western Washington rivers are characterized by single boles with large rootwads. Rarely are branches preserved, and usually only on trees that entered the channel within the last year. Branches on most conifers have relatively small diameters in comparison to the trees' bole diameters. On some deciduous trees, such as *Acer macrophyllum*, the bole usually forks into large branches. Once in the river, branches don't last long and even snags are left with just the

bole(s) and rootwad. The absence of branches observed in Pacific Northwest (PNW) rivers is not unique. In the Eastern United States, which is dominated by deciduous trees with extensive branch structure, snags tend to be trimmed so that only the bole and root wad remains (Diehl 1997a). These field observations suggest that branch structure may be a secondary factor in snag stability.

Field observations also suggest that WD stability fell into two fundamentally different cases that tend to represent two different parts of the channel network. In large channels, flow obstructions other than WD are rare, and logs are unconstrained by pre-existing boundary conditions. Stability is thus a function of buoyancy, friction, flow and a deformable bed. In small headwater channels where log length equals or exceeds channel width, it is assumed that log resistance will be provided by pre-existing boundary conditions (e.g. banks, boulders). It is assumed that a log spanning a headwater channel will not move unless broken, therefore buoyancy is not relevant. Under these assumptions, it is the material strength of the log that controls stability.

The principle driving force acting to destabilize or move a log is assumed to be fluid drag in all channels. Stability in large channels where logs are unconstrained by pre-existing boundary conditions is investigated by first using a hydrostatic model to examine buoyancy and then a friction and flow limited model is used to delineate static and dynamic factors influencing resistance. Stability in headwater channels, where logs are constrained by pre-existing boundary conditions, is investigated using a strength limited beam model to predict the type of logs capable of withstanding exceptional flows.

3.3 Stability in Large Channels: Friction Limited

Field observations suggest that stable WD jams have the most significant effect on channel morphology. I therefore assume that WD must remain in place when subjected to bed mobilizing flows to effectively alter channel morphology and thus provide a quantitative definition of stability. For WD to remain stable, the sum of resisting forces, F_R , must exceed the driving forces, F_D , acting on it:

$$\frac{\sum F_R}{\sum F_D} > 1.0$$

Resisting forces will depend on forces the tree imposes on the channel bed. To examine how the tree's shape can affect these forces, different models of tree geometry were examined under hydrostatic conditions, beginning with the assumption that the tree rested on a level bed.

To describe how particular characteristics of the WD, channel, and flow each influence WD stability, in this chapter I demonstrate how WD form plays a crucial role in its stability both under hydrostatic and hydrodynamic conditions. If a bole becomes fully buoyant and floats off the channel bed, the bole no longer experiences frictional resistance. A fully buoyant tree bole can still remain in place only if buttressed against pre-existing channel boundaries or obstructions; otherwise, it will move downstream. I develop a dimensionless representation of the buoyant depth for different bole forms as a function of their specific gravity. The same model for determining buoyant depths provides a means to estimate the gravitational forces a bole exerts on the channel bed for water depths less than the buoyant depth.

3.3.1 Buoyancy

Wood debris with a specific weight less than water will float when the water displaced by the WD is equivalent in weight to the WD. The buoyant force acting on the WD (F_B) equals the weight of water displaced by the WD. The difference between F_B and the weight of the WD (F_G) is the force the WD imposes on the channel bed. A force balance analysis must account for resultant forces acting at the bed and upward buoyant forces associated with submerged portions of the WD. The buoyant force, F_B , is a function of the submerged volume of the object, V_s , and is expressed as, $F_B = \rho_f g V_s$, where ρ_f = water density and g = acceleration of gravity. The net gravitational force is thus a function of an object's 3-D geometry and its intersection with the water surface.

Real tree trunks exhibit a rapid increase in diameter close to the ground, a feature commonly referred to as taper or buttressing. A simple power-law expression in which the base of the rootwad or bole is set at $x=1$ was used to represent tree boles. The bole axis is parallel to the x -axis and extends to $x = L+1$, where L =bole length:

$$R(x) = R_0 x^t \quad (x \geq 1)$$

where,

R_0 = maximum bole radius (rootwad radius, if present), and

t = exponent defining the tree's taper or buttressing.

To keep the entire tree bole above $z = 0$, $R(x) = R_1 \pm R_1 x^t$. The species, age, and physical degradation of a tree can effect its taper (Gray 1956, Zimmerman and Brown 1971, Garay, 1979). The tree's volume is estimated by integrating the chosen function about the x -axis (Figure 3-4).

Bole geometry is described using a taper coefficient, t , estimated by a best-fit correlation to actual tree measurements. The model of bole geometry is numerically integrated to estimate total volume and define the bole's center of mass. The need to accurately estimate volume for standing timber has led to considerable efforts to derive quantitative models of bole taper beginning where the tree was cut and extending to the crown (Newaham 1965, Bruce et al. 1968, Garay 1979, Bruce 1982, Biging 1984). Historical timber harvest practice was to cut trees with significant buttressing high above the ground because of the practical problems associated with moving and handling. Most taper models exclude the portion of a tree close to the ground and the tree's rootwad. An entire tree bole, from its root mat to its crown, was described as either: i) a simple power function, $R(x) = R_0 x^t$, for the entire bole, or ii) a power function to describe the tree's buttressing close to its root mat, from $R(x=1)$ to $R_b(x=1)$, and a linear function to describe the remaining portion of the bole, from $R_b(x=1)$ to $R_n(x=n=L+1)$. Linear taper corresponds to a fustrum or truncated cone and has commonly been used to estimate WD volumes in the literature (Lienkaemper and Swanson 1987, Harmon et al. 1986). Linear taper is described by:

$$R(x) = R_0 + |mx_b|$$

$R(x)$ = bole radius at distance x along its axis

x_b = location of butt diameter (above rootwad) on x -axis

R_0 = projected bole radius at $x = 0$

m = taper or slope of bole in linear model, dR/dx

To simplify the moment analysis and force balance, the coordinate system used to describe tree geometry is rotated so the tree's longitudinal axis appears horizontal. Thus the x and z axes are rotated to axes x' and z' to model the tree. The channel bed on which the tree rests is assumed to be horizontal when plotted in x and z , and thus appears inclined in x' and z' . The transformed channel slope, S' is thus defined by the radii at either end of the bole and the bole length (Figure 3-4):

$$S' = \tan \beta = [R_1 - R_n / L]$$

The water surface is assumed parallel to the channel bed, its intersection with the z -axis is defined as $c_1 = h/\cos S'$ where h = water depth. As the water depth increases, buoyant forces acting about the tree's centroid can lift the crown of a bole off the channel bed, and S' decreases to represent the change. Assuming symmetry about the x -axis, the total volume of tree bole, V_{wd} , with a simple power-law taper is:

$$V_{wd} = \iiint f(y, z, x) dydzdx$$

$$V_{wd} = \int_1^n \int_0^{2\pi} \int_0^R (R) dRd\theta dx$$

$$V_{wd} = \int_1^n \int_0^{2\pi} \frac{R^2}{2} d\theta dx$$

$$V_{wd} = \int_1^n 2\pi \frac{R^2}{2} dx$$

since $R = R_1 x^t$, where

x = the coordinate along the transformed x -axis

R_0 = radius at basal end of bole (root wad if present)

t = taper exponent, and therefore:

$$V_{wd} = \pi R_0 \int_1^n (x^t)^2 dx$$

$$= \frac{\pi R_0^2}{2t + 1} (x_n^{2t+1} - 1)$$

To estimate the moments and the resultant forces acting about the tree's centroid for a given flow depth, the submerged portions of the bole must be determined by integrating the volume of the bole below its intersection with the water surface plane (Figure 3-4):

$$V_s = \int_{s'x+c_0}^{s'x+c_1} A_{wd}(x) dx$$

where,

A_{wd} = cross-sectional area of bole at x

dx = interval along x to compute incremental volume of bole

$s'x + c_1$ = line representing plane of water surface

$s'x + c_0$ = line representing plane of ground surface

s' = water surface and ground slope in model

c_1, c_0 = z intercepts for water and bed surfaces, respectively (constant along y -axis)

x, z = coordinates relative to transformed axes, x' and z' , defined below.

A force balance analysis provides a means of estimating the ultimate forces, if any, the tree imposes on the channel bed. Moments and the resultant forces depend on the magnitude and distribution of the tree's mass above and below the water. A bole with none of its volume submerged imposes a force equivalent to its weight into the bed, which in turn imposes an equal and opposite resisting force (F_R) on the tree under static conditions. The force balance is solved by summing the moments acting about the tree's centroid (center of mass) until the resultant forces are equivalent and static conditions established. When no resultant forces are imposed on the channel bed, the tree has become fully buoyant. For the tree to remain static while floating (keep from constantly pitching or rolling), buoyant forces must still be balanced about the tree's centroid

Since mass is assumed to be symmetrical about the bole axis, the tree can be presented as a 2-dimensional profile in the x-z plane (Figure 3-4). The bole's centroid coordinates, z_c and x_c , are functions of the first moment about the z-axis (M_z) and x-axis (M_x).

$$x_c = \frac{M_z}{V} = \frac{\int x dV}{V} = \frac{\pi \int x [f(x)^2] dx}{\pi \int [f(x)^2] dx}$$

$$z_c = \frac{M_x}{V'} = \frac{\int z dV}{V'} = \frac{\pi \int z [f(x)^2] dz}{\pi \int [f(x)^2] dx}$$

Substituting $R(x) = R_0 x^t$, the moments are:

$$M_z = \pi R_0^2 \int_1^n x^{2t+1} dx = \frac{\pi R_0^2}{2(t+1)} (x_n^{2(t+1)} - 1)$$

$$\therefore x_c = \frac{(x_n^{2t+2} - 1)(2t+1)}{(x_n^{2t+1} - 1)(2t+2)}$$

Assuming the bole density does not vary in space, $z'_c = R_0$, for the transformed axis z' . The actual elevation of the centroid in the original coordinate system is equivalent to the orthogonal from (x_c, z_c) to the channel bed surface ($s'x + c_0$). The actual centroid elevation will be a function of the bole's tilt, defined by its radius at either end, and its length:

$$z_c = \left\{ R_n \left(\frac{R_o - R_n}{x_n - 1} \right) x_n - x_c \right\} \sin \left\{ \tan^{-1} \left(\frac{R_o - R_n}{x_n - 1} \right) \right\}$$

where,

variables on the right side of the equation are transformed coordinates (x' , z')

$x_n = x'$ coordinate corresponding to the end of the bole

$R_n =$ radius at the end of the bole.

Buoyancy is estimated using a numerical integration to compute moments acting about the bole's centroid (center of mass) generated by the bole's submerged volumes. The resultant forces between the bole and the channel bed are than balanced. The area of a submerged segment of a circle when less than one-half the bole is submerged is:

$$A_s = 0.5R(x)^2(2\theta - \sin 2\theta)$$

where,

$\theta =$ angle subtending the submerged arc of the bole and the vertical distance of the centroid above the bole axis is

$$dz_{cs}(x) = \frac{2}{3}R(x) \left[\frac{\sin^3 \theta}{\theta - \sin \theta \cos \theta} \right]$$

If more than one-half of the bole is submerged at x , then the submerged area centroid is computed from the centroid of one-half the bole (semi-circle) and the centroid of the submerged portion of the bole's upper half (in cross section, Figure 3-4). The centroid elevation of a semi-circle relative to the center of the circle is

$$dz_{cs}(x) = \frac{4R(x)}{3\pi}$$

where dz_{cs} is the centroid elevation measured from the center. The centroid of the entire submerged area when the water surface lies above the bole axis (measured from bole axis at x) is:

$$dz_c(x) = (A_{S2}dz_{S2}) + [(A_Tdz_T) - (A_{S1}dz_{S1})]$$

where,

$A_{S1} =$ area of submerged semi-circle

$A_T =$ area of sub-aerial bole segment

$A_{S2} =$ difference between A_{S1} and A_T

dz_{S1} = centroid submerged semi-circle (A_{S1})

dz_T = centroid of sub-aerial bole segment (A_T)

dz_{S2} = centroid of submerged segment A_{S2}

dz_C = centroid of entire submerged cross-sectional area of bole at x .

Based on the water surface intercept with the bole, submerged areas are numerically defined at increments dx' (along bole axis or x' -axis) and thus solves for the total submerged volumes and their centroids (Figures 3-4 and 3-5).

In the case of a simple cylinder (Figure 3-2a), mass is distributed uniformly along the length of the bole where the fustrum or power law taper is greatest at its basal end. A force balance analysis reveals that the bole will develop a tilt with respect to the water surface proportional to its taper, reaching a maximum at its buoyant depth. From Archimedes principle we know that concentrating mass at one end of the bole results in the greatest draft at the same end. Boles with more pronounced taper have more of their mass elevated above the channel bed and require a greater water depth before they experience the same buoyancy as a bole with more linear taper (Figure 3-6). The buoyant depth of WD can thus increase several-fold if a rootwad is present. The accuracy of tree geometry models was evaluated by using the models to predict tree volume. Using densities determined from increment curves, tree weight was then predicted and compared to measured tree weights (Figure 3-7). The best correlation was achieved using a power-law taper for the rootwad up to the basal radius, and a fustrum for the bole from the basal radius to the crown radius. Using just the power-law taper function for the entire tree was the next best model.

Broken fragments of a tree bole, branches, or sawed logs may be adequately described as simple cylinders or fustrums (e.g., Swanson and Lienkaemper 1978, Bilby and Ward 1989, Braudrick et al. 1997), but this does not apply for tree boles with intact rootwads which are responsible for stable WD accumulations throughout a channel network (Bryant 1980, Nakamura and Swanson 1993, Abbe and Montgomery 1996b). Modeling the effect of WD shape provides insight on the significance of bole geometry (i.e., taper), particularly the presence of a rootwad, and why the length of logs is an

insufficient criteria if used alone to evaluate log stability. For a perfectly uniform cylindrical log, the center of mass will lie half way between either end. The centroid of a tapered cylinder is more representative of natural WD, especially because a "key member" can be moved much closer to its larger end.

3.3.2 Friction and a Deformable Bed

Bed resistance or friction depends on the normal force acting on the channel bed and a friction coefficient defined by the channel slope at which the WD will begin to slide. For the simple case of a block resting on a uniform surface, resisting force F_R is

$$F_R = C_f F_N$$

where:

F_N = force acting normal to bed surface = $(F_G - F_B) \cos \alpha_c$

F_R = force acting tangential (shear) to bed surface = $(F_G - F_B) \sin \alpha_c$

C_f = coefficient of static friction = $\tan \alpha_c$

F_G = weight of WD

F_B = buoyant force acting on WD

α_c = critical bed slope at which log begins to slide (degrees)

A cylinder resting on a smooth, inclined bedrock plane will move either by rolling or sliding. Cylindrical shapes on a smoothly inclined plane will experience the least friction by rolling about their longitudinal axis so the friction coefficient for rolling is less than for sliding (Onda and Matsukura 1997)(Figure 3-8). For a simple cylindrical bole in an unobstructed smooth channel, maximum drag occurs when the bole is normal to flow (90°) and minimum drag occurs when the bole is parallel to flow (0°). A simple log would most likely come to rest in an orientation parallel to flow if it doesn't encounter any obstructions.

Friction also depends on an object's footprint or area over which it comes in contact with the bed and supports the object's weight; in other words, the normal stress on the bed.

The weight of a simple cylindrical bole (log) is distributed along its entire length. The width of this area is the arc length of its perimeter in contact with the bed, $dS = r\theta$ (Figure 3-9a). A tapered bole will distribute its weight over a smaller bed area, increasing the normal stress for the same weight. Any sufficient increase in the normal stress can result in a portion of the tree bole digging into the bed, a phenomenon that can significantly increase both static and dynamic friction. The slope of the plane of contact between a piece of WD and the channel can diverge dramatically in a natural channel due to particle roughness, bed forms, or obstructions. The stability of a tree bole resting on the stoss side of a dune or bar would be enhanced by a gravitational component of shear in the upstream direction (downslope direction). The slope of a steep headwater stream would tend to reduce stability by increasing the downstream contribution of gravity.

The presence of a rootwad can dramatically reduce the WD footprint area, thus increasing the normal and shear stresses acting on the bed surface. The components of stress are expressed as

$$\sigma = F_N A_{wd}^{-1}$$

$$\tau = F_R A_{wd}^{-1}$$

where,

$$\tau = \text{shear stress} \quad [N/m^2 = kP_a]$$

$$\sigma = \text{normal stress} \quad [N/m^2 = kP_a]$$

$$A_{wd} = \text{footprint area of debris on channel bed} [m^2]$$

When a tree bole rests on unconsolidated sediments such as alluvial channels, the shear stress necessary to move the bole downstream will be affected by the depth to which the bole penetrates the bed surface. When a portion of the tree bole (e.g. rootwad) extends into the bed, the bole must either move upward out of the bed prior to moving downstream or it must plow or push through the bed material it has sunk into. At incipient motion, the shear stress necessary to move the tree bole must overcome the internal angle of friction of

the bed material and the submerged weight of bed material buttressing the downstream side of the bole (Figure 3-9b).

I use several simple hypothetical models to investigate the potential influence of normal stress and stamp depth (depth to which WD penetrates bed) on frictional resistance (i.e., stability) and how these factors are influenced by WD shape. The ability of the ground to support the weight of an object, or its bearing capacity, is fundamental to geotechnical engineering. As an example, changing tire pressure of a wheeled vehicle (e.g. bicycle) can be used to compensate for changes in ground bearing capacity (e.g. muddy trail) by increasing or decreasing the area or footprint over which the vehicle's weight is distributed.

The stamp depth to which a tree bole sinks into an unconsolidated bed is a function of its weight, size and shape, and the bearing capacity of the bed material. If the normal stress exerted by an object on a bed surface exceeds the bearing capacity of the bed material, the object will sink. The object reaches equilibrium when the bearing capacity is equal or greater than the normal stress. Assuming the object's weight is constant, the normal stress it exerts on the bed will only decrease as the area in which it comes in contact with the bed increases with its penetration into the bed. As an object sinks, the bearing capacity of the bed material can increase due to compaction and lateral friction due to the static load of sediment flanking the object. For a cylindrical object lying on a level bed, the normal stress it exerts on the bed would be:

$$\sigma = W_{wd}/A_f$$

where,

W_{wd} = weight of wood debris (tree bole) accounting for buoyancy

A_f = footprint or bearing area [m²]

The footprint area is equivalent to the surface area of an object (i.e., WD) that is in contact with the ground (i.e., alluvial bed) and is a function of the ground's bearing capacity and the weight and shape of the object. The footprint area on which a load is imposed is equal to load divided by the bearing capacity (Nichols 1976):

$$A_f = W / \Phi$$

where: A_f = footprint area [m^2]

W = WD (log) weight [kg]

Φ = bearing capacity [kg/m^2]

Bearing capacities for several alluvial substrates are given in Table 3-1. Given sufficient information on the object's shape, the depth to which an object sinks into the ground (bed) or stamp depth, z_s , can be estimated. For example, assuming a simple cylindrical log resting length-wise on a level bed:

$$A_f = \lambda_s \Delta x$$

where: A_f = footprint area based on log's contact area with bed [m^2]

$\lambda_s = R \theta$ = arc length of log's perimeter in contact with bed

$$\theta = 2 \cos^{-1}[(R - z_s) / R]$$

Δx = length along cylinder's axis over which it comes in contact with bed

R = radius of cylinder, assumed constant with respect to x

Assuming a cylindrical log of uniform density rests on a level bed of uniform composition, then $dl/dx = 0$ (λ_s will be constant along the log's length), $\Delta x = L$, and the log's stamp depth z_s , will be constant. Based on these simple conditions, z_s can be derived for a particular bed material by setting $A_{f^*} = A_f$ and then substituting the appropriate variables above:

$$W / \Phi = \lambda_s \Delta x = R \theta \Delta x$$

setting $\Delta x = L$ (length of log):

$$\frac{W}{\Phi} = 2 R L \cos^{-1} \left(\frac{R - z_s}{R} \right)$$

$$z_s = R \left[1 - \cos \left(\frac{W}{2 R L \Phi} \right) \right]$$

A tree bole with a rootwad that has the same weight as a cylindrical log will have a substantially smaller footprint, thereby increasing the normal stress imposed on the bed and increasing the stamp depth. Several roots with radii less than that of the tree bole (at its butt end) usually are capable of supporting the tree's weight. Assuming the roots are oriented vertically into the bed, the foot print of each supporting root is approximately πr^2 where r = root radius. The total footprint, A_r , of this simplified rootwad consisting of n number of roots in contact with the bed would be:

$$A_r = \sum_{i=1}^{i=n} \pi r_i^2$$

To investigate the effect of reducing the footprint area, I modified the cylindrical log model by simply reducing the log length in contact with the bed, thus replacing L with Δx in the previous expression for z_s . The simple cylindrical model was applied to estimate stamp depth into a substrate of loose gravel and sand as a function of footprint areas (Figure 3-9).

The gravel sand substrate is assumed to have a bearing capacity = 24,400 kg/m² (CABO 1989). A large rootwad on a bole with little taper (similar to the cylinder model used here) can concentrate much of the tree mass on a very small foot print. To further investigate the effect of reducing the footprint area, several experiments were carried out by dragging small tree boles with and without rootwads across a gravel bar to measure the effect of footprint area on resistance.

3.3.2.1 Friction

The force necessary to move several logs was measured to investigate frictional resistance of sliding logs. A logging skidder cable was attached to a scale capable of measuring up to 1,134 kg (2500 lbs), and the scale was then attached to the top (crown)

end of the tree bole. The scale recorded the maximum force exerted by the skidder to initiate sliding of the tree bole (Figure 3-10a-c). Different orientations of the same tree bole and rootwad and different trees were used to vary the relative plow size of the rootwad. Coefficients of static sliding friction were then estimated from the experiments.

Test logs were chosen to evaluate the effect of rootwads on frictional resistance. Test cases were based on the relative size of the rootwad (i.e., plow size) and each case was repeated three times. A sliding friction coefficient of 1.22 with an $R^2 = 0.93$ was estimated based on 21 tests using 5 bole configurations (Figure 3-10d). The outlier point in Figure 3-10d represents a case when the crown of the test log became embedded and the resisting force rapidly increased beyond the limit of the scale with further motion. The resistance or ratio of force necessary for incipient motion to log weight was found to be a logarithmic function of the rootwad sizes (i.e., plow length/log length), as illustrated in Figure 3-10e. Plow length is defined as the height of the trunk above the ground surface due to its rootwad. The results of the drag tests suggest that resistance is directly affected by the plow length and thus the size and shape of the tree. The force necessary to initiate motion normalized to tree weight was correlated to a measure of relative rootwad size referred to as plow length (Figure 3-10e). The plow length is the difference between the rootwad radius directed into the ground and the bole basal radius divided by the tree length:

$$\frac{F_i}{F_G} = 10^{[0.163 \log(n+0.3496)]} \quad R^2 = 0.70, N = 22$$

where,

$n = PL / L$

F_i = force necessary for incipient motion

F_G = weight of tree bole

PL = plow length = $R_{rw} - R_b$

L = length of log

The hydrostatic analysis demonstrated that tree shape and density significantly influence the buoyant force acting on a tree at particular water depths and the depth at which maximum buoyancy occurs. Tree shape was also found to affect the frictional resistance the tree encounters along a level bed of unconsolidated sediment. Snags must have sufficient resistance to overcome the drag and lift forces imposed by flowing water.

3.3.2.2 Effect of Flow and a Deformable Bed

Wood debris that enters a channel is subjected to dynamic conditions of flow and changing boundary conditions. How do these factors influence tree stability and the development of snags? Are changes in bed topography likely to increase or diminish resistance of natural snags? The flow of water around a fallen tree will exert a drag force that will move it downstream if the resisting forces are insufficient. Force balance models are developed to examine direct effects of flow, such as drag, and indirect effects, such as changing the boundary conditions around a snag. Flow around an obstruction can result in predictable patterns of scour and sedimentation. The effect of some of these changes in bed topography on snag stability is examined.

Logs exposed to flowing water experience drag and shear just like other stream bed sediments. Flow drag imposed on the wood debris is given by:

$$F_D = C_d A_c [\rho_f U_0^2] / 2$$

where

C_d = drag coefficient (function of an obstruction's form)

A_c = submerged cross-sectional area of the obstruction orthogonal to flow

ρ_f = fluid density, and

U_0 = incident flow velocity upstream of obstruction.

The velocity of uniform steady flow through a reach will be a function of the energy gradient of the flow (water surface gradient), the effective flow depth (hydraulic radius of

channel), and roughness coefficient accounting for energy loss between the flow and included in Mannings's equation.

The shape of WD directly influences how it will be transported through streams; there are specific orientations within a flow that either minimize or maximize drag. If a log is advected down a channel at the same velocity as the flow, the velocity of water past the log goes to zero, eliminating drag and making log orientation irrelevant. This condition is illustrated by the relatively random orientation of a stick moving within a flow of much larger dimensions. As the wood debris dimensions approach the flow dimensions, the debris will decelerate due to frictional resistance along the channel bed or banks.

Estimating an appropriate drag coefficient is necessary to derive the driving force imposed on WD by the flow. Drag associated with WD in streams and rivers primarily depends on the shape or form of the WD, its orientation relative to flow and its size relative to the cross-sectional flow area. Skin drag, or that due to the surface roughness of an obstruction, becomes negligible relative to form drag (due to the shape of the obstruction) at high Reynold number flows (e.g., Rouse 1946, Chow 1959, Hoerner 1951, Bearman and Morel 1984, Roshko 1993). Just as with the case of frictional resistance, there has been little published regarding the complex fluid dynamics of flow around snags (Smith 1990, Beebe 1997). Consequently, I have drawn on relevant work in aero and hydrodynamics. Research into the fluid dynamics of parachutes indicates that drag produced by a flow approaching a porous disk (e.g. a rootwad) is a function of the disk porosity and a Reynolds number based on the characteristic length of the disk and a Reynolds number relating to the pore size (Roberts 1980). The drag coefficient for a solid disk can actually increase by introducing a nominal porosity.

Gippel et al. (1996) found that for simple tree trunks and trunks with branches, a relatively symmetrical relationship existed between orientations from 0° to 90° and 90° to 180° to the flow. The bole and butt form (tree bole with rootwad) had significantly different drag coefficients at 0° and 180° (Figure 3-11). Best fit equations predict C_D for orientations between 0° and 90° presented in Table 3-2 (Gippel et al. 1996). The percentage of the cross-sectional flow area (plane normal to flow direction) occupied by

the WD or blockage coefficient, B , can have a significant influence on drag. Gippel et al. (1996) found that drag is a function of B , thus small blockage coefficients ($B \leq 0.05$) have little effect but drag increases dramatically for larger blockage coefficients.

Stable snags are usually found with their rootwads at least partially buried in the channel bed, and the bole oriented downstream and inclined approximately 10-30°. Snags are often associated with a distinctive topographic pattern in the bed of alluvial channels (Abbe and Montgomery 1996b). Directly upstream and flanking the rootwad is a crescent or horseshoe shaped pool. Downstream of the rootwad along the axis of the bole, aggradation leads to a narrow elliptical bar. This bar forms a downstream buttress against the rootwad and adds surcharge above the debris.

The fluid dynamics of flow around bluff bodies (Roskho 1993, Williamson et al. 1995) provides some insight into the flow structure and processes associated with snags. Flow separation around a bluff body obstruction such as a large rootwad creates a zone of recirculation or an eddy immediately downstream of the rootwad at the base of the tree's bole (Figure 3-12a). The pressure difference between the upstream and downstream sides of the rootwad leads to flow reversal within the separation envelope. The eddy is separated from downstream flows by a turbulent shear layer. This shear layer is characterized by a train of vortices that increase in diameter downstream and is referred to as the Von Karman vortex street (Best 1996). These vortices transfer momentum and sediments from the high velocity flow into the low velocity region of recirculating flow (Figure 3-12b). The rapid deceleration of flow within the separation envelope allows entrained sediments to settle out.

The volume of potential sedimentation within the separation envelope is limited by its width, the depth of the channel across the shear layer, and the saturated angle of repose of the aggrading sediment (Figure 3-12c). The width of the separation envelope will be controlled by the width (diameter) and shape of the obstruction, and the incident flow conditions (Roskho 1993, Williamson 1995). The maximum width of sediment accumulation in the eddy is limited by the width of the separation envelope between the

vortex streets on either side (Figure 3-12c). Sedimentation within the eddy of a snag can buttress the downstream side of the rootwad and add surcharge on top of the bole.

While sedimentation can occur in the lee of an obstruction, scour along its upstream toe can lead to settling, lowering the rootwad of a snag (Figure 3-13a). If part of the rootwad extends above the water surface, settling can increase buoyant force, but even if the additional buoyancy allows the snag to move, it may only be pushed up against a slope extending from the scour pool to the top of its leeward bar. Natural river snags are often observed with their rootwads deeply buried in the river bed and their boles emerging from bars inclined 10-30° with their tips pointed upward and downstream.

Patterns of sediment scour and deposition around a snag can significantly affect the snag's stability. The flow conditions controlling these patterns are in turn influenced by the size and form of the snag's upstream end (root wad and any raked debris). Assuming initial conditions in which a snag rests on a level bed (i.e., snag has not yet influenced bed topography), bed alteration will only occur if the snag remains stable under flow conditions in which basal shear stresses exceed the critical shear stress for bedload transport. If a snag remains stable after this threshold has been exceeded I predict the snag will alter bed topography. Because a snag obstructs some portion of the channel's cross-sectional area, localized acceleration of flow adjacent to the snag can be expected. This localized effect on flow suggests that incipient bedload transport occurs proximal to the snag before it would otherwise occur in the channel if the snag were absent. It is thus assumed that flow conditions necessary for bedload transport in an unobstructed channel to evaluate snag stability provides a conservative estimate of whether the snag will alter bed topography.

Flow depths associated with bedload initiation can be computed from values of dimensionless critical shear stress estimated from bed surface texture. The minimum flow depths and velocities at which wood debris or a snag must be stable can be estimated by computing the critical shear stress necessary to initiate bedload transport. If a snag remains in place after bed load transport has begun, then it can be assumed that changes in bed topography around the debris resulting from scour and sedimentation will occur in an

alluvial channel. Critical shear stress necessary to initiate bedload transport using the Shields parameter is derived as follows:

$$\tau_c = \tau_c^* (\rho_s - \rho) g D_m.$$

where,

τ_c = critical shear stress [N/m²]

τ_c^* = dimensionless critical shear stress or Shields parameter

ρ_s = sediment density [kg/m³]

ρ = fluid density [kg/m³]

g = acceleration of gravity [m/s²]

D_m = grain size [m]

When the basal shear stress, τ_o , exceeds τ_c , bedload transport is predicted.

For high critical Reynolds numbers and low relative roughness representative of gravel bedded rivers, visually based estimates of τ_c^* range from 0.03 to 0.073 (Buffington and Montgomery 1997). Reported values of τ_c^* for the median grain size of bed surface sediment in the White River of western Washington range from 0.031 (Fahnestock 1963) to 0.047 (Ferguson et al. 1989). Assuming that shear stress must equal or exceed the critical shear stress, flow condition initiating bedload transport can be estimated. Assuming a value of $\tau_c^* = 0.04$ and that the energy slope is constant and analogous to the channel slope, the critical flow depth, h_c , is

$$h_c = 0.04 \gamma D S^{-1}$$

where $\gamma = (\rho_s - \rho) / \rho$,

and the critical shear velocity, u_{*c} , is:

$$u_{*c} = \sqrt{g h_c S}$$

where,

R_c = Reynolds number = $u \cdot D \nu^{-1}$ (where ν = kinematic viscosity [cm²/s], ≈ 0.010)

u = shear velocity = $(\tau_o / \rho)^{1/2} = (g h S)^{1/2}$ [m/s]

$$\tau_o = \text{basal shear stress} = \rho ghS \text{ [N/m}^2\text{]}$$

h = flow depth [m]

S = energy gradient

These values of flow depth and velocity can now be used to define the minimum values at which a tree must be stable in order to evaluate how changes in the bed can also affect stability.

Patterns of bed morphology similar to those described by Abbe and Montgomery (1996b) have been observed around stable snags in many western Washington rivers. Flow acceleration into the bed, and vortex development, result in bed scour upstream of an obstruction. Constriction and downstream accelerations in flow result in scour beside an obstruction.

The initiation of bedload transport around a snag will alter boundary conditions and can subsequently affect the snag's stability. Once the rootwad becomes partially embedded in the channel bed, it becomes more difficult to move. A sediment buttress downstream of a rootwad can form in-situ by the accumulation of sediment in the leeward eddy, or if the rootwad penetrates the bed under its own weight. If the rootwad penetrates the bed and begins to move downstream it will push up a mound of sediment on its downstream side, similar to a bulldozer, making further movement downstream increasingly difficult (Figure 3-13b). The cumulative effect of sediment buttressing downstream of a rootwad has a resistance described using the derivation of Wislicki (1969) for bulldozer blade resistance² (Figure 3-13b) or by using an analysis of passive earth pressure such as described by D'Aoust and Millar (1999).

Rootwads of natural snags are commonly observed to be at least partially embedded in the channel bed. If an embedded rootwad is "pushed downstream" by flowing water, it will immediately encounter resistance due to the alluvium buttressing the rootwad. Assuming a cohesionless substrate, the magnitude of resistance will be dependent on the depth the rootwad extends into the substrate, the surface area of the embedded portion of the rootwad projected downstream (normal to flow), and the submerged weight of the alluvium. D'Aoust and Millar (1999) estimate the resisting force associated with

embedded rootwad from theoretical passive earth pressure, P_p , defined in the Canadian Foundation Engineering Manual (2nd Edition, Canadian Geotechnical Society 1985) as:

$$P_p = K_p \frac{\gamma_{sa} h^2}{2}$$

where,

P_p = passive earth pressure (force per unit width of rootwad) [N/m],

$K_p = (1 + \sin\phi)/(1 - \sin\phi)$ = coefficient of lateral passive earth pressure,

ϕ' = effective angle of internal friction of alluvium = ϕ [degrees], and

γ_{sa} = submerged specific weight of alluvium [N/m³].

Passive earth pressures allow can sufficient resistance to stabilize a snag. For example, assume the substrate alluvium is composed of moderately rounded coarse gravel with a median grain size of 36 mm, $\phi' = 35^\circ$, $K_p = 3.7$, and $\gamma_{sa} = 1200$ N/m³. Dividing up the embedded rootwad area into vertical slices with heights $h(y)$ and widths $w(y)$, the resistance (F_p) contributed by the embedded rootwad is simply:

$$F_p = \sum (P_p w)$$

The snag has a rootwad 4.0 m in diameter that extends 1.2 m into the substrate, the total resisting force due to passive earth pressures would be 69,484 N. If the snag is exposed to a flow moving at 3 m/s and a depth of 1.6 m, and the rootwad has a drag coefficient of 1.5, the total drag would be 42,053 N, resulting in a net resistance of 27,431 N. Since the depth of flow extends from the bed and the rootwad extends 1.2 m into the bed, 2.8 m of the rootwad would be underwater, as would most of the tree. But even if the snag's submerged weight was negligible, it would hold fast in the position described.

Sediment deposition on a tree bole can add substantial surcharge and thus increase the stability of a snag. Field observations show that sediment commonly accumulates downstream of the rootwad and buries part or all of the tree bole. In some cases the entire rootwad becomes buried deep within the bed. Fluvial sediments composed of coarse sand

and gravels have dry bulk densities of 1,400-2,200 kg/m³ (Table 3-3) that are over twice those of most woods, so overburden depths of half the bole diameter can be sufficient to negate positive buoyancy. The volume of alluvium overlying a truncated cone (fustrum) laying horizontally can be derived as the difference between one-half the fustrum's volume and the volume of the encompassing trapezoid. The trapezoid height is equal to the maximum fustrum radius, end widths equal to the end diameters of the fustrum, and a length equal to the fustrum length. Using this simple geometry, the overburden volume of alluvium is:

$$V_a = \frac{L_b}{4} \left[D_b(D_b + D_t) - \frac{\pi}{4} (D_b^2 + D_t^2) \right]$$

where,

V_a = volume of overburden alluvium

L_b = length of bole (fustrum)

D_b = basal (maximum) end diameter of bole

D_t = top (minimum) end diameter of bole

The submerged weight of the overlying alluvium, W_{as} is:

$$\text{where, } W_{as} = (V_a \rho_a) - \left(V_a \frac{\rho_a}{\rho_s} \rho \right)$$

ρ_a = bulk density of alluvium

ρ_s = density of sediment comprising alluvium

ρ = density of water

Assuming the bole itself (no rootwad) has a linear taper, the formula for estimating the volume of a fustrum can be used to estimate bole volume, V_b , as given below.

$$V_b = \frac{\pi}{8} (D_b^2 + D_t^2) L_b$$

Using the model above, the weight of alluvium due to the taper in a tree bole can be estimated assuming the bole is lying horizontally and buried to a depth equal to its largest diameter (D_b). To estimate the surcharge associated with any additional burial, take the

bole area projected into the horizontal plane, $(D_b + D_t) \cdot L_b$, and multiply it by the height of alluvium above the bole and then add it to the previous quantity, the weight of alluvium associated with taper. To estimate alluvial surcharge for a tree that includes its rootwad, calculate the alluvium situated above the bole as described above, giving the following formula:

$$V_a = \left[\frac{1}{2} (D_b + D_t) L_b \right] h_a$$

where the bole axis is assumed to be horizontal,

V_a = volume of alluvium extending to a height h_a , above top bole

h_a = height of alluvium starting at the upper elevation of bole's larger diameter and extending up

Using the power law function to describe the rapid taper that occurs in a tree trunk close to the ground, a tree's stump volume can be estimated. The stump or rootwad volume, V_r , refers to the portion of the tree extending from the base of its rootwad (corresponding to the tree's maximum diameter) to a height corresponding to D_b , after which it is assumed taper becomes linear (frustum model). The base of the rootwad is assumed to be flat.

$$V_r = \frac{\pi R_r^2 (x^{2t+1} - 1)}{(2t + 1)}$$

where t = taper exponent:

R_r = rootwad radius, with root end of tree set at $x=1$ (for power law taper).

$R(x)$ = tree radius at $x = R_r x^t$

x = location along bole axis (distance from $R_r + 1$).

$$t = \frac{\log(R(x) / R_r)}{\log(x)}$$

The tree's rootwad or stump area projected onto the horizontal plane, A_r , is two times the area beneath the curve $R(x) = R_r x^t$.

$$A_r = 2 \int_1^x R_r x^t dx$$

$$A_r = \frac{2R_r}{(t+1)} (x^{t+1} - 1)$$

Assuming alluvium buries the tree (lying horizontally) to the top of its rootwad, the volume of a tapered trapezoid that encompasses the rootwad is $V_{sr} = A_r R_r$, and the volume of alluvium, V_{ar} , is determined by subtracting one half the rootwad volume:

$$V_{ar} = V_{sr} - \frac{V_r}{2}$$

Anchors provide another analogy for examining snag stability. Anchors are rated based on their holding power which is equivalent to the ratio F_r/F_G defined earlier (Figure 3-10d). Since anchor weight is a limiting factor, anchor efficiency is based on increasing the resistance contributed by alluvium. Therefore, the single most important factor in anchor performance is its shape, not weight, as illustrated in Figure 3-14. Resultant forces due to the concentration of a tree's mass at its rootwad tend to drive roots into the bed in the downstream direction, similar to a plow share or anchor tip. Sediment displaced by rootwads that penetrate the bed will tend to accumulate on the downstream side of the rootwad, increasing the friction angle of the debris. If the tree begins to move downstream, the rootwad acts similar to a plow, piling additional sediment up downstream of the rootwad. Thus the shear stress necessary to maintain transport of a tree bole and rootwad can increase as the tree moves downstream. The ultimate size of the sediment pile downstream of the rootwad will depend on the rootwad's plow depth, size of rootwad and tree, scour occurring around the rootwad, and the angle of repose of the sediment. The process is summarized in Figure 3-15.

According to the model developed here, tree taper where the bole meets the root wad (i.e. buttressing) could theoretically influence resistance. Trees with gradual taper, such as Cedar, have more pronounced buttressing. Assuming two trees with equal diameter rootwads are each embedded to equal depths, the alluvial contribution to resistance is greatest for the tree with the most rapid taper. Drawing a potential analog using Pacific northwest trees, and assuming equivalent rootwad diameters and bed penetration, a Douglas fir, which has very little buttressing and rapid taper, will form a more effective plow, and thus encounter more resistance than a Red Cedar with strong buttressing and grounded taper. This difference in taper also results in different relative buoyancy at the same water depth. For water depths less than the trees rootwad radius, the Douglas fir will be less effected by buoyancy (Figure 3-7). The higher density of Douglas firs will further reduce buoyancy, indicating that Douglas firs are more likely to create stable snags than Cedars (assuming the trees are equivalent in length, rootwad diameter, and weight). But other size factors ultimately influence which trees form stable snags, principally the number of trees entering the river and the decay rate.

This rudimentary model for resistance due to anchor or plow effects and the hydrostatic analysis suggest that cedar snags in PNW streams may be less stable than similar sized snags of other species, such as Douglas fir or Black cottonwood. Cedar trees have a much more gradual or conical taper than other PNW species, whereas Douglas fir has a very pronounced, rapid taper very close to the ground. A Cedar thus has a smaller flow length ($R_1 - R_b$) than a Douglas fir with an identical rootwad radius. The Douglas fir will make a much more effective plow or bulldozer, and will require greater water depths to experience the same buoyant forces as the cedar. In addition, Western Red Cedars have the lowest specific gravity of PNW trees. Even though cedar trees may not be as stable as other PNW species, the huge sizes they attained in old-growth riparian forests, their affinity to low-lying floodplains of the western Cascades and their slow decay rate may, in part, explain why Western Red Cedar historically was one of the principal snag-forming trees in even some of the largest PNW rivers (Shoecraft 1875, Sedell and Frogatt 1984).

3.4 Stability in Small Channels: Strength Limited

The most common way in which the vast majority of wood debris (racked and loose members) deposit in small and large channels is by lodging up against channel margins or in-stream obstructions such as boulders and key member logs (Abbe and Montgomery 1996b, Diehl 1997a). When log length exceeds channel width a log can form a channel spanning flow obstruction. In steep headwater channels, these log steps can account for a significant percentage of the elevation loss (e.g., Keller and Tally 1979, Marston 1982, Thompson 1995). To create persistent, effective energy dissipaters, these logs must be capable of withstanding large-magnitude flow events. Is it reasonable to think a tree or log spanning a channel could withstand the impact and stresses of a debris flow? Is the size and species of tree representative of the channel being modeled? If so, and if these trees fall into the channel to form stable obstructions firmly lodged into either bank, then the log or tree is likely to trap a small amount of the debris flow mass, thus reducing the flow's momentum. Step bedforms created by these log dams would further contribute to dissipating debris flow momentum. Field observations suggest that debris flows were rapidly dissipated due to the abundance of large logs, since no debris flow deposits or run-out paths were found downstream of initiation points (slope failures).

A thorough analysis of standing trees broken by catastrophic debris flows associated with the 1980 eruption of Mt. St. Helens, and moving across a relatively low-gradient floodplain is presented by Wigmosta (1983). Coho and Burges (1994) found riparian tree diameter inversely proportional to the run-out distance or propagation of dam-break torrents, and observed that such events appear to be rare in old-growth forests. No one has presented a quantitative model to predict whether channel spanning logs, such as those observed in many forest channels (e.g. Marston 1982, O'Connor 1994, Haas 1996), are capable of withstanding debris flows. The ability of riparian trees in smaller, steeper, low-order channels to withstand dam-break flood torrents is addressed in a field study by Coho and Burges (1994).

3.4.1 Beam Model

Channel-spanning logs can be effective in retarding or dissipating debris flows (Swanston 1976). Assuming a channel-spanning tree bole or log is securely lodged into both banks and the wood is sound, under what conditions will it be able to withstand the forces delivered by catastrophic events (those events causing major alterations in channel form) such as a debris flow? The model presented here is applicable to debris flows or flood flows.

The abundance of WD obstructions in tributaries to the Queets River and the general absence of debris flow deposits and barren, scoured channels, led me to the hypothesis that WD obstructions are effective at dissipating catastrophic flows very quickly after their inception. By reducing both contributions of additional mass to the flows (i.e., trapping sediment and WD) and reducing the velocity of debris flows, WD obstructions could limit or decrease the flow's momentum and affect how far it travels downstream. To address the question of what type of log, if any, can withstand a debris flow when that log is securely wedged against either channel bank, I apply a simple beam model to estimate the forces necessary to rupture logs. Debris flows are assumed to represent the maximum probable flow events headwater channels will experience and thus provide a conservative estimate of the size of a stable log.

The channel-spanning log is roughly analogous to a beam subject to an external bending moment generated by the debris flow. When the external bending moment exceeds the log's strength or maximum internal bending moment, it will rupture. The maximum internal bending moment for a cylindrical log can be estimated using a modulus of rupture, \mathfrak{R} , assumed to be representative of the bole and the bole's diameter, D , assuming the bole approximates a cylinder this may be expressed as (Wigmosta 1983):

$$M_{i_{\max}} = \frac{\pi \mathfrak{R} D^3}{32}$$

Most estimates of the modulus of rupture for different woods are based on small, clear rectangular blocks. The shape, size, and presence of natural defects and variations in the wood's grain all tend to contribute to lower values for the modulus of rupture of tree boles. The modulus of rupture has been found to decrease as beam diameter increases (Garfinkel 1973). In addition, but also the modulus of rupture measured for beams with square x-sections should be multiplied by a factor of 1.18 to determine the value for a circular beam with the same cross-sectional area (Garfinkel 1973). Applying adjustments for circular cross-sectional and size effects, the corrected modulus of rupture, \mathfrak{R}_c is (Bohannan 1966, Wigmosta 1983):

$$\mathfrak{R}_c = K_r K_s \mathfrak{R}$$

where,

$K_r = 1.18$ = constant for converting shape factor of beam with square cross-section to beam with circular cross-section of diameter D .

$K_s = [2/35.1 * D]^{1/9}$ = shape factor for beam with square cross section $D * D$.

D = diameter of circular beam (log).

Wigmosta (1983) found that corrected modulus of rupture estimates for *Tsuga heterophylla* and *Picea situlansis* logs over-predicted the values determined from field tests (Tuomi 1979) by 24% and 11%, respectively.

A simple cylindrical beam of uniform diameter (Figure 3-16) is used to estimate the size and types of logs capable of forming channel spanning obstructions that could withstand extreme flows. The log is assumed to be a simple beam oriented normal to incident flow and securely fastened at either end. I calculated the maximum external moments for two different types of simple beams: (a) a beam fixed at both ends, and (b) a beam fixed at one end and pinned at the other end. Each of these two beam models was used to evaluate: (i) load uniformly distributed over the exposed log length, and (ii) a point impact at the channel center (Figures 3-16 and 3-17a-d). The maximum external moment each log beam model and loading condition are presented in Table 3-4.

The maximum internal moment of a cylindrical log represents the maximum moment it is capable of withstanding prior to rupture (Wigmosta 1983)

$$Mi_{\max} = \frac{\pi \mathfrak{R}_c D_c^3}{32}$$

where,

Mi_{\max} = maximum internal bending moment of cylindrical beam [Nm]

D_c = critical log diameter [m]

\mathfrak{R}_c = corrected modulus of rupture [KPa]

Thus a log beam would be stable for $Me_{\max} < Mi_{\max}$ and unstable for $Me_{\max} > Mi_{\max}$. The critical log diameter, D_c , can be derived and used to define a stability threshold between logs capable of withstanding a particular flow and those predicted to rupture. Rearranging the previous equations to solve for log diameter,

$$D_c^3 = \frac{4FL}{3\pi\mathfrak{R}}$$

The estimated critical diameter is thus:

$$D_c = \left(\frac{4FL^2}{3p\mathfrak{R}} \right)^{1/3}$$

where F = total force impacting log beam. Strength properties for common trees of the Pacific Northwest are presented in Table 3-5. The moments at either end of the log (resistance provided by channel walls), M_w , are assumed to always be greater than 0.5 Mi_{\max} (i.e., the sum of moments at each wall $> Mi_{\max}$). Under this assumption failure could only occur if the log breaks (i.e., rupture). The model does not predict whether a log could be torn from the bank.

The impact force for a debris flow uniformly distributed over a log's length, F_u , is:

$$F_u = C_D \rho D_b U^2 L$$

A boulder carried down in front of a debris flow will deliver a concentrated or point impact force proportional to the area of the log impacted. If the boulder strikes the center of the log, the impact force will be:

$$F_i = C_D \rho D_b U^2 D_i$$

where,

F_u = impact force of flow uniformly distributed over log length, [N]

F_p = impact force of boulder hitting center of log, [N]

D_b = diameter of log beam [m]

D_i = diameter of boulder coming in contact with log beam [m]

L = log length [m]

ρ = fluid density [kg/m³]

U = flow velocity [m/s]

C_D = drag coefficient of log obstruction

Substituting the force derivation into the solution for critical log diameter (i.e., setting $D = D_c$), the size of stable log beams can be estimated for particular flow conditions or impacts. The solution for log beams subjected to a uniformly distributed load across their length is thus:

$$D_c^3 = (\rho C_D D_i L U^2) \frac{32L}{\pi \mathfrak{R}_c} (k)$$

or

$$D_c = \left(k \frac{\rho C_D D_i 32}{\pi \mathfrak{R}_c} \right)^{1/3} U^{2/3} L^{2/3}$$

where,

$k = 1/12$ for a beam fixed at both ends

$k = 1/8$ for a beam fixed at one end and pinned at the other

D_i = log diameter (assumed constant over width of channel),

L = length of log spanning channel width.

Applying the same procedure to the case of a log beams subjected to a point load or impact yields the following solutions:

$$D_c^3 = (\rho C_D D_1 L U^2) \frac{32 w_i}{\pi R_c} (k)$$

or

$$D_c = \left(k \frac{\rho C_D D_1 L w_i 32}{\pi R_c} \right)^{1/3} U^{2/3}$$

where,

$k = 1/8$ for a beam fixed at both ends

$k = 3/16$ for a beam fixed at one end

w_i = width of object impacting log beam (length of log subjected to impact)

The four cases described above were evaluated for particular channel conditions to determine whether it is reasonable to assume that trees are capable of withstanding the impacts associated with the most severe conditions that can occur naturally. Predicted critical diameter for a channel spanning log beam (oriented at 90°) fixed at both ends is predicted for both a uniformly distributed load associated with a debris flow (Figure 3-17a) and a localized or point impact delivered by a boulder at the beam's center (Figure 3-17b). Critical diameters increase as a function of channel width. Identical predictions of critical diameter were done assuming a log beam fixed at one end and pinned at the other end (Figure 3-17c,d). Log strength is primarily a function of diameter and secondarily the tree species (assuming all other variables and condition of wood are similar). Within the size range of headwater channels (5-20 m), the beam model clearly indicates that only trees with diameters of approximately 0.5 m or more are capable of withstanding the drag imposed by a debris flow or boulder impact, and thus any probable flood event (which would have lower fluid density and velocity).

The model suggests that most mature and old-growth deciduous and coniferous forests where trees equal or greater than 0.5 m in diameter are common, fallen trees can be of sufficient size to form flow barriers that can dissipate the momentum of catastrophic flows and impacts. Channels in which logs are incapable of withstanding debris throws or

flood waves are scoured clean and left devoid of WD. This simple beam model may provide at least a partial explanation for the relatively high frequency of channel-spanning logs (i.e., logs steps) in old-growth forests of the Pacific Northwest where key logs commonly have diameters $\geq 0.5\text{m}$ (O'Connor 1994, Haas 1996 chapter 1). Little evidence of channel-scouring, catastrophic events was found in streams of the Queets River basin, where large in-stream log obstructions were ubiquitous (see Chapter 1).

3.5 Discussion

Several models have been presented to better understand the mechanics of stable wood debris in channels. This analysis was separated into two fundamentally different domains based on the channel boundary conditions: large alluvial channels where WD is unconstrained by channel banks and small channels where WD is constrained by channel banks. In large channels, WD stability depends on frictional resistance of the wood debris itself and its effect on flow conditions and bed morphology, primarily functions of its shape and weight. The effective weight of WD is a function of its rootwad and bole diameters, assuming the rootwad diameter is less than one-half the total length. This is reflected in observations of stable debris in large channels where $D_{\text{max}}/h_c \gg L_{\text{wd}}/w_c$, and frequently $w_c \gg L_{\text{wd}}$. Variables that influence a force balance analysis of in-stream wood debris stability are summarized in Table 3-6. Wood strength has relatively little effect on stability in these channels.

Wood debris stability in small, steep channels, primarily depends on resistance provided by pre-existing channel boundary conditions on which the WD becomes lodged. Thus debris size relative to the channel size is important, especially length. Since these pieces of wood tend to be firmly secured at fixed points (i.e., obstructions or banks), there can be significant unsupported sections of these boles where they extend into the channel or span obstructions. In these situations, wood strength can become extremely important. Strength is generally proportional to wood density, but wood samples undergoing decay have experienced significant reductions in strength despite negligible decreases in density (Bravery and Lavers 1971, Hardie 1980).

3.5.1 Stabilizing Factors Associated With A Root Mat

A rootwad concentrates most of the mass of a tree bole onto a relatively small area of a channel bed. Rootwads can act similar to an anchor or bulldozer blade. The resultant forces due to the weight of a tree are distributed over the tree's surface area that comes in contact with the bed. If part of the tree penetrates an unconsolidated bed, resistance can be increased significantly. When a tree first enters a channel its rootwad will still retain alluvium, bedrock or soil from where it had been growing. This material can increase the effective weight of the tree and shift the centroid even closer to the rootwad due to the high density of the alluvium relative to the wood.

Flow alteration associated with natural WD jams can result in substantial sedimentation on the downstream side of the structure (Abbe and Montgomery 1996b). When a rootwad or the debris accumulation raked against it is large, downstream sedimentation can form a floodplain island, burying the bole of the original snag. Deposition of additional WD or sediments provides surcharge to a pre-existing WD jam that increases the cumulative F_G , thus increasing the stability.

$$F_G = F_{wg} + F_{sg} - (F_{wb} + F_{sb})$$

where

F_G = net gravitational force acting on channel bed

F_{wg} = log weight

F_{wb} = buoyant force due to submerged log volume

F_{sg} = surcharge contributing to log weight (overlying sediment, trees, wood)

F_{sb} = buoyant force acting on surcharge (if any).

Reid (1981) compiled volume estimates of rootwad alluvium for fallen trees on hillslopes in the Queets watershed. The average volume was 4 m³, equivalent to adding about 6800-8000 kg per rootwad. The 55 samples were from trees with basal diameters ranging from 0.2 to 1.8 m (Reid 1981).

3.5.2 Physical Properties of Wood

The density of WD plays an important role in its stability. Density is dependent on the tree species, the part of the tree it came from, age of the tree, moisture content of the wood, mechanical damage or alteration of the wood and any decay. Trees are composed of three basic types of wood: bark, sapwood, and heartwood, which generally exhibit significant differences in density and permeability (i.e., drying and wetting rates) under dry, green, and saturated conditions. Dry wood will absorb atmospheric moisture through capillary action and is generally assumed to have a moisture content of approximately 12% with respect to the oven dry mass of the wood. Moisture contents are dependent on the wood's dry density, which vary between species (e.g., 0.10 for Balsa to 1.35 for some tropical hardwoods) and decay condition. The moisture content of living trees (i.e., green wood) is generally assumed to be about 30% and can be over 300% in saturated wood.

Throughout my investigation of WD stability thus far, I've assumed that density is constant throughout a given tree bole (doesn't vary with space), when in fact wood density can vary considerably within a single tree bole. Density can vary significantly between the heartwood, sapwood, bark of the tree trunk and branches. The actual solid organic matter of wood consists primarily of cellulose and some lignin, with a density of 1.46 – 1.52 g/cc (Lincoln 1986). As the porosity of wood approaches zero, its density approaches 1.5 g/cc. All wood has some porosity consisting of intercellular spaces which store water. Oven dried wood retains approximately 12% of its mass in water locked up within its cellular structure. Specific gravities of the world's woods range from 0.16 g/cc (*Balsa*, *Ochroma pyramidale*) to 1.30 g/cc (*Piratinera guianensis*); values for Pacific northwest woods range from 0.37 for Western Red Cedar (*Thuja plicata*) to 0.77 for Pacific Madrona (*Arbutus Menziesii*) (Lincoln 1986).

Dry wood expands as its moisture content (ratio of water mass to dry wood mass) increases; further expansion becomes negligible when moisture contents exceed 30%. Despite volume changes, saturated wood can have effective densities twice that of dry wood. Moisture content has a significant effect on the properties of wood. With respect to the stability of WD in a channel, the principal concern regards how moisture will influence

weight and strength. Live trees native to the Pacific Northwest have average moisture contents ranging from 30% to over 200% of the wood's dry weight. The specific density of tree cores taken from common trees found in western Washington was measured for oven dry and saturated conditions. Saturated specific densities commonly exceeded one, suggesting that some logs would likely sink when saturated (Figure 3-18). Seasonal changes in the moisture content of WD can either increase or decrease WD stability for the same hydraulic conditions (stream stage) at different times of the year. Seasonal variations in precipitation and stream discharge in Western Washington result in the driest conditions in the fall, so WD is most susceptible to transport at this time (Figure 19). Frequent rain, low evaporation rates and temperatures of the fall and winter increase the effective density of WD and increase its stability. Wood debris size also plays a role in the rate it absorbs or loses water. Drying (and wetting) rates are inversely proportional to wood size (Harmon and Sexton 1995).

Decay reduces the dry density and increases the permeability of wood. Water absorption rate is proportional to permeability so decayed wood will increase its weight more rapidly but have a saturated weight less than the same wood with less decay. The decay state may thus increase stability over short time scales but reduce the stability of both dry and saturated states. Wood lying at or below the base flow water table can remain saturated throughout the year, and experience lower rates of decay. Wood in anaerobic conditions (i.e., submerged) can remain sound for tens of thousands of years (Becker and Schmirer 1977, Nanson et al. 1995). Decay effectively reduces the size and strength of wood debris. Strength is generally proportional to wood density (Hardie 1980), but strength decreases more rapidly with time than wood mass (Figure 3-20). The two general models of wood debris stability describe (i) large low gradient channels, and (ii) small high gradient channels, and represent two fundamentally different situations. In large channels, WD stability is primarily a function of wood shape, size and weight. Wood strength has relatively little effect on stability in these channels.

Decay rates are a function of tree species, size, wood density, and fiber saturation (Mean et al. 1986, Ceylonese et al. 1987). Assuming decay proceeds uniformly from the

outer circumference of a cylindrical log, the effective log diameter some time after a given time interval can be estimated (Figure 3-21). This estimate of effective log diameter can then be used to assess possible changes in stability over time.

3.5.3 Additional Factors Affecting Stability

Field observations reveal that after a snag initially stabilizes in the channel, subsequent conditions can either decrease or increase the snag's stability. Change in channel bed elevation is one such condition. Channel incision, the lowering of the bed, can reduce the stability of both new WD and pre-existing snags. Incision confines high flows that previously may have spread out onto a floodplain and secondary channels, thereby increasing the depth, velocity and frequency of peak flows. Increased depths and velocities increase buoyancy and drag, both reducing WD stability. Incision also tends to result in a reduction of sinuosity which would diminish the probability of WD deposition. In contrast, channel aggradation tends to reduce flow depths and increase sinuosity and bar development, which contribute to increased WD stability.

Local scour and sedimentation around a snag can increase stability. In addition to the stabilizing effects of sediment deposition downstream of a snag's rootwad (previously discussed), the accumulation of WD upstream of the snag and vegetation growth above the snag can enhance stability. Debris accumulation upstream of a snag can decrease erosive flow moving through its rootwad and enlarge the flow separation envelope and sedimentation zone downstream (Figure 3-22). Vegetation colonizing the depositional surface created by a snag or debris jam contributes surcharge and root cohesion to further stabilize the debris. Vegetation also increases the hydraulic roughness of the bar surface, which promotes additional sedimentation (McKenney et al. 1995). Factors such as root cohesion and surcharge can be integrated into the weight and friction limited model to make long-term predictions of log jam stability.

3.6 Conclusion

Wood debris, and tree boles in particular, can form flow obstructions throughout a channel network. Tree boles firmly lodged in the beds of large channels or “snags” form stable obstructions that alter flow patterns and bed morphology, and accumulate flotsam that would have otherwise moved downstream. Snags were once a ubiquitous feature in rivers flowing through old growth forests of North America (Lyell 1830, Ruffner 1886, Veatch 1906, Russell 1909, Guardia 1927, 1933, Phillips and Holder 1991). The massive accumulation of debris often associated with snags and their geomorphic and hydrologic effects imposed significant impediments to river navigation and land development.

Recognition of the importance of WD on fluvial and riparian ecosystems has reversed some long-standing practices in river management, particularly the establishment of guidelines to re-introduce WD in streamside forests as opposed to aggressively removing them. Yet re-introduction of wood debris poses new, legitimate concerns regarding detrimental impacts to conveyance (flood protection), bridges, navigation and other infrastructure (e.g., Rankin 1980). A large gulf remains between those who consider wood debris a beneficial component of a stream and those who view wood debris as a hazard. In both perspectives there is an implicit acknowledgment that wood is significant, whether by its presence or absence. Thus it seems ironic that we have so much to learn about the mechanics of snags and their geomorphic consequences. Efforts to better understand these topics could be invaluable in moving past the current “log jam” between traditional river engineering and new strategies to rehabilitate fluvial environments.

I have examined some of the primary factors controlling WD stability and have developed a general quantitative framework for predicting the characteristics of stable WD or snags. The presence of a rootwad significantly influences the physics of WD stability and jam formation in large channels, thus providing a partial explanation of why many of the stable WD accumulations observed in the field appear to have initiated as a tree bole still attached to much of its rootwad (Abbe and Montgomery 1996b). A rootwad elevates a tree's centroid and increases its frictional resistance thereby reducing the return frequency of the flow necessary to move it downstream. The accumulation of sediment downstream

of a rootwad results in an anchoring effect that can contribute substantially to the stability of a tree bole.

This work may and has been used to help design stable WD structures to rehabilitate aquatic and riparian ecosystems, and provide effective alternatives to common river engineering problems such as bank erosion and bridge protection (Abbe et al. 1997). The procedures outlined here also offer a framework for evaluating the impacts of natural or anthropogenic disturbances that alter channel morphology, flow conditions, or the characteristics of trees entering the channel.

Notes to Chapter 3

1. The depth to which a tree bole penetrates the channel bed can be estimated using methods to predict soil stamp depth (Berstein 1913, Wiślicki 1969) or footing depth (Terzaghi 1944, 1953; Terzaghi and Peck 1967; Sounglent 1972).

$$p = (k_c + k_f) z_s^n$$

$$z_s = [p/(k_c + k_f)]^{1/n}$$

where:

p = specific pressure of stamp on soil which is equivalent to the normal stress imposed on the surficial contact strip (kg cm^{-2})

k_c = vertical soil deformation modulus due to soil cohesion ($\text{kg cm}^{-(n+1)}$)

k_f = vertical soil deformation modulus due to soil cohesion ($\text{kg cm}^{-(n+1)}$)

z_s = soil subsidence (cm)

n = dimensionless soil defining exponent

Bernstein R., Probleme Zur Experimentellen Motorpfugmechanik. Motorwaga, 1913.

2. General formula for estimating cumulative resistance of alluvium pushed by bulldozer presented by Wiślicki (1978).

$$W'_R = W_A \cos \delta + T \cos \nu + W_B + W_C \cos \nu \sin \nu$$

$$W'_R = \gamma_s b_{rw} \left\{ AB + R \left[\frac{R}{2} D + E \right] (F \tan \phi + G) F + H \right\} + I$$

$$A = \left[\lambda h^2 \vartheta \cos \phi \arcsin(2\vartheta^{-1})(\tan \phi + \tan \varphi) \right]$$

$$B = \left[\cos \delta \cos \psi \tan \phi \sin C \right]$$

$$C = \left(\frac{\alpha + \varphi + \phi}{2} \right)$$

$$D = \left(\frac{\Theta_c}{180^\circ} \right) - \sin \Theta_c$$

$$E = 2z \tan C \sin \left(\frac{\Theta_c}{2} \right)_{F=\sin C}$$

$$H = \frac{1}{2} (l_m - z \tan C)^2 \tan \beta \tan \phi_{l=c z b_1 \tan C}$$

b_l = wood (i.e., "bulldozer") blade width [cm]

C = sediment cohesion [kg cm²]

h = wood (i.e., "bulldozer") blade height [cm]

l_m = length of sediment mass in front of wood (i.e., "bulldozer") blade [cm]

z = stamp or cutting depth [cm]

W_R' = overall resistance due to cutting and pushing the disturbed alluvium in the horizontal plane, i.e., in the direction of the driving force (downstream) [kg]

W_A = resistance due to pushing the alluvium piled-up against the surface of rootwad plow area [kg]

W_B = resistance due to pushing disturbed sediment mass over undisturbed bed material [kg]

W_C = weight of pushed up sediment [kg]

$$= \gamma (V_1 + V_2) = \gamma [0.5 b_l R^2 \{(\Theta_c \pi/180^\circ) - \sin \Theta_c\} + 2 z b_l R \tan((\alpha + \varphi + \phi)/2)]$$

α = sediment cutting angle [degrees]

β = angle of repose of sediment pile in front of wood plow [degrees]

δ = inclination of force W_A to the horizontal [degrees]

ϕ = angle of internal friction of sediments [degrees]

γ = sediment bulk density [kg cm^{-3}]

φ = angle of friction between sediment and wood [degrees]

λ = coefficient allowing for difference between design and measured stresses ($\lambda = 1.2-1.4$) which is due to part of the excavated sediment being cast aside. Accepted value of $\lambda = 1.3$ (Wiślicki 1978).

s = normal stress in sediment [kg cm^{-2}]

τ = shear stress in sediment [kg cm^{-2}]

ν = inclination of shear plane with horizontal [degrees]

ψ = angle by which force W_A diverges from the perpendicular to the slip surface [degrees]

$\vartheta = R / h$

Θ_C = angle of subtending arc-length of plow blade formed by wood surface (i.e., rootwad) intersecting vertical plane [degrees]

R = radius of wood (i.e., "bulldozer") blade [cm]

T = tangential force to the shear plane ML occurring in the course of cutting and pushing disturbed sediment mass over wood surface (i.e., blade).

$$= \tau F = c F + \sigma F \tan \phi = c z b_l (\sin \nu)^{-1} + (W_A + W_C \cos \nu) \tan \phi$$

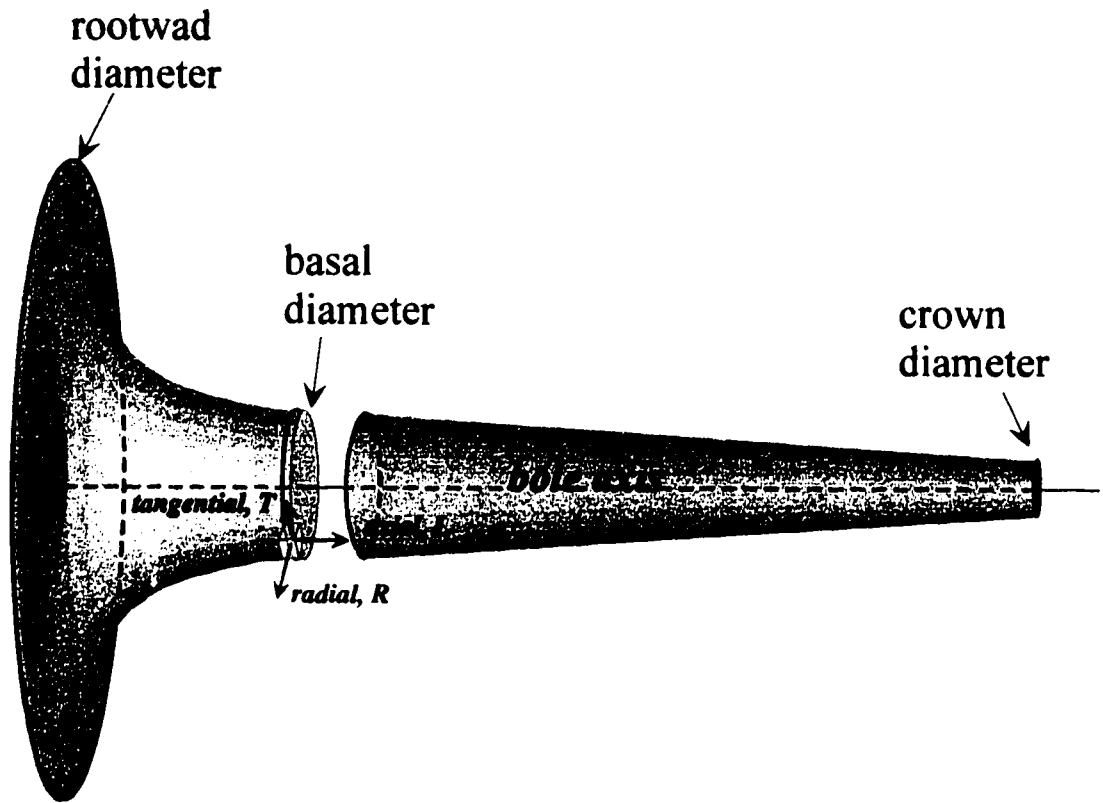


Figure 3-1 Basic Tree Bole Structure and Force Definitions

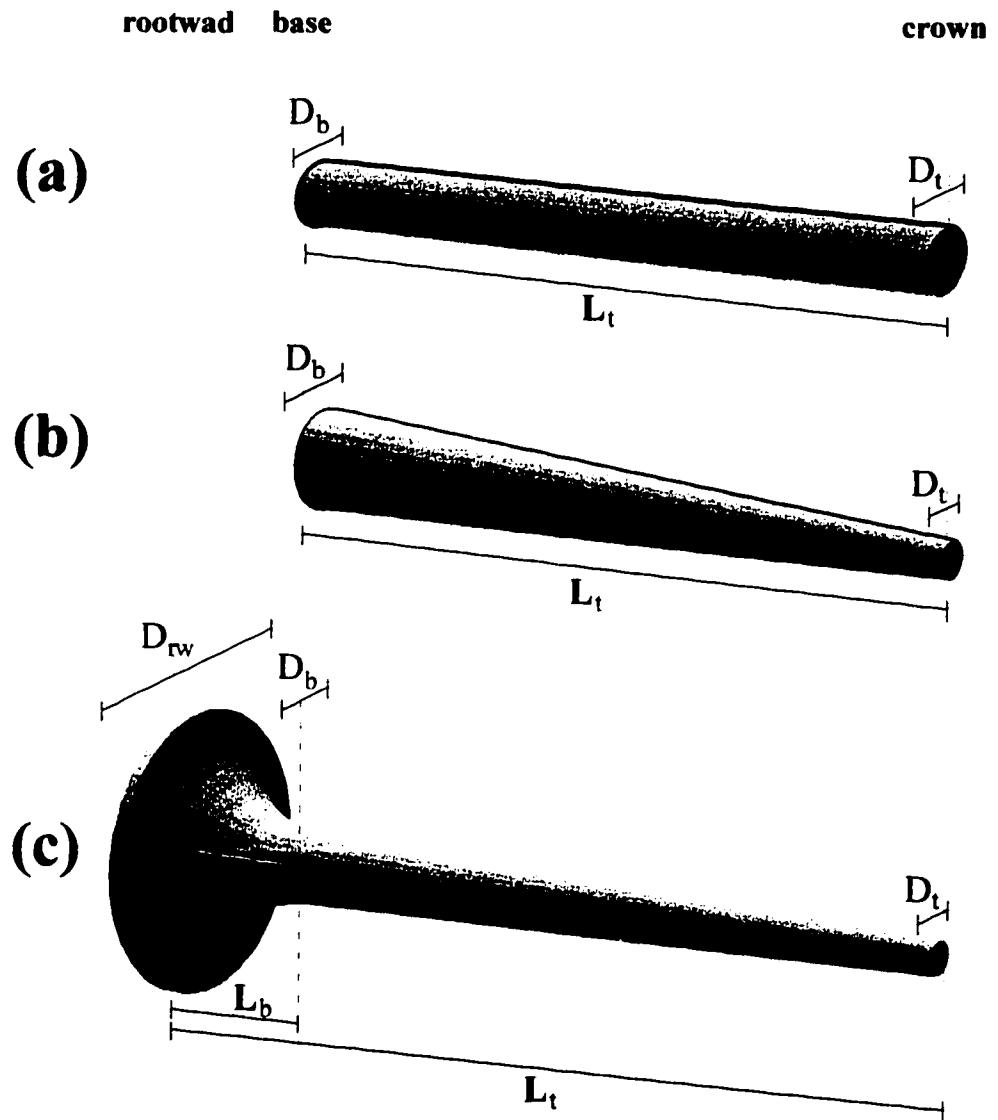


Figure 3-2 Simple Form Models of Tree Boles: Uniform Cylinder (a), Frustum (b), and Power-law Taper Model

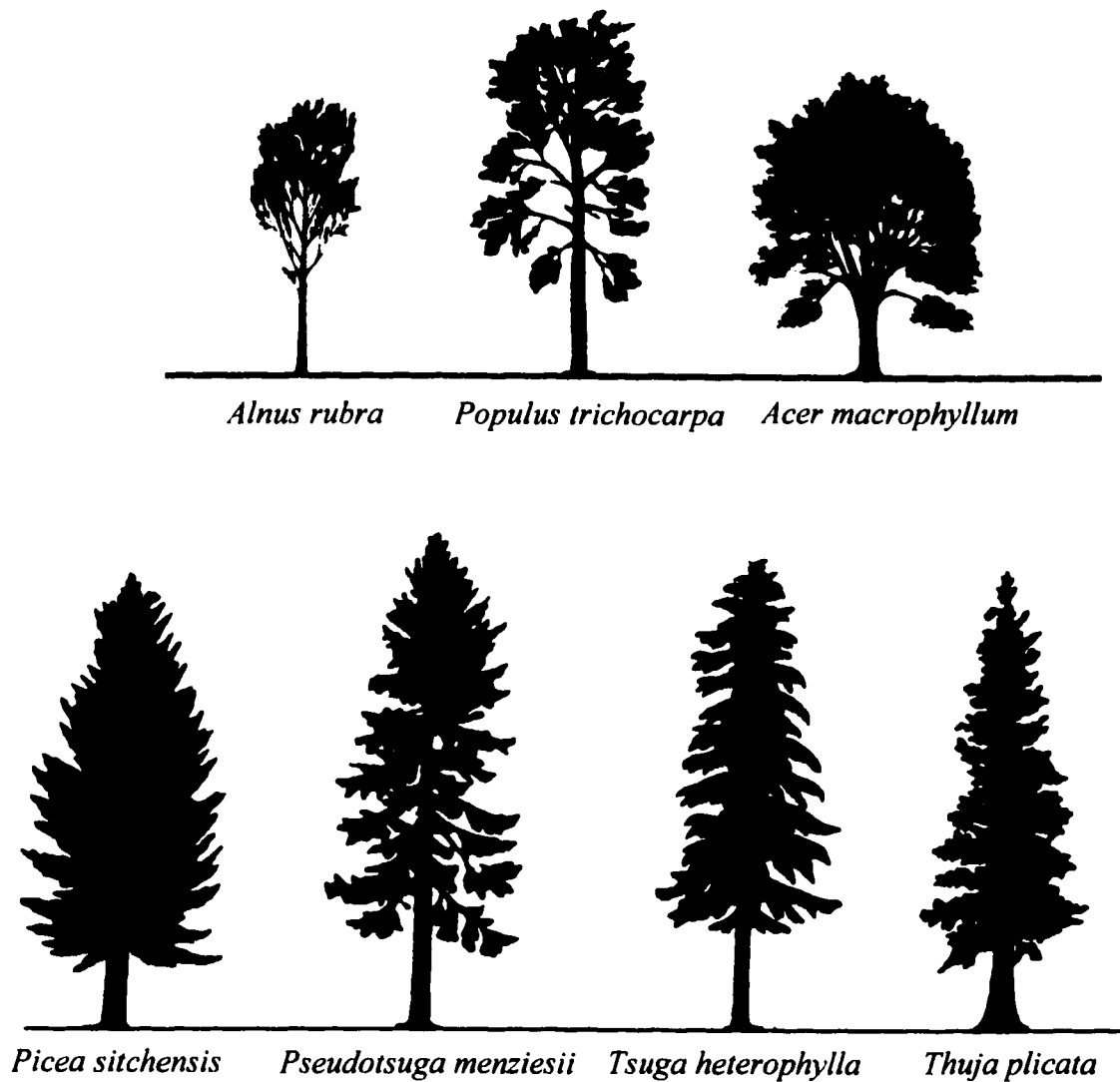
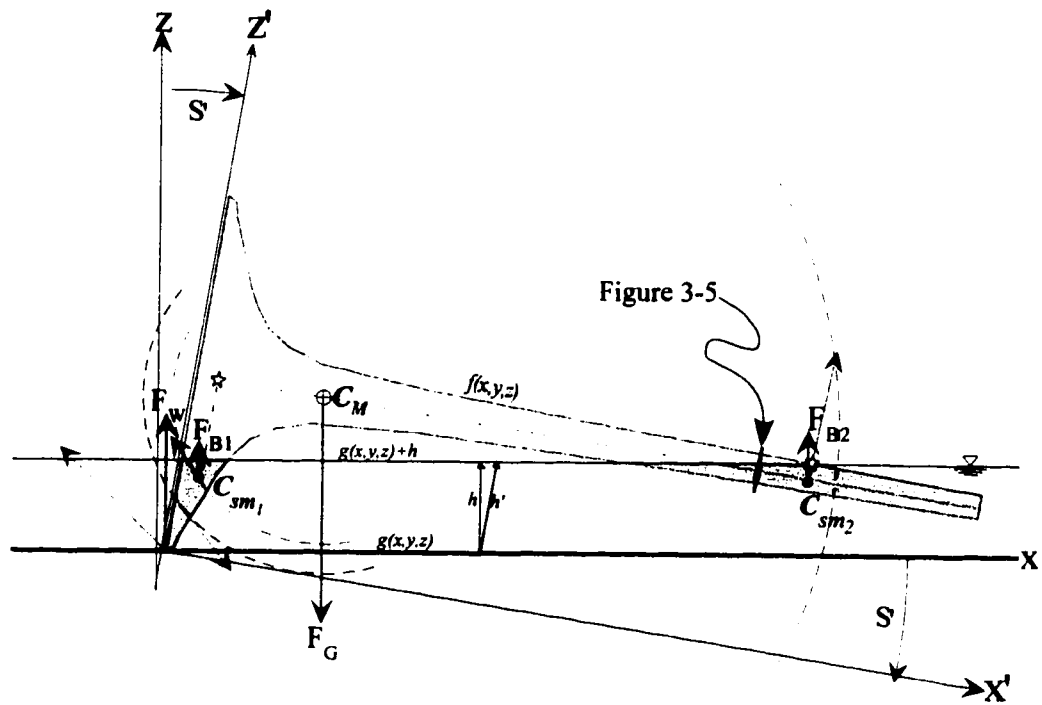


Figure 3-3 Bole and Canopy Form of Common Pacific Northwest Trees



- \rightarrow F_D drag force due to flow
- \uparrow F_w normal resistance provided by bed
- \uparrow $F_{n,z}$ buoyant forces of displacement (submerged volumes)
- \downarrow F_G weight of tree bole
- \curvearrowright moments acting about tree centroid, C_M
- $f(R)$ tree bole taper model
- $g(x,y,z)$ channel bed plane
- $g(x,y,z)+h'$ water surface plane
- h water depth
- x', z' transformed coordinates
- S' bed & water surface slope relative to tree bole axis (in model)

Figure 3-4 Free-body Diagram of Ideal Tree Bole Resting on Channel Bed

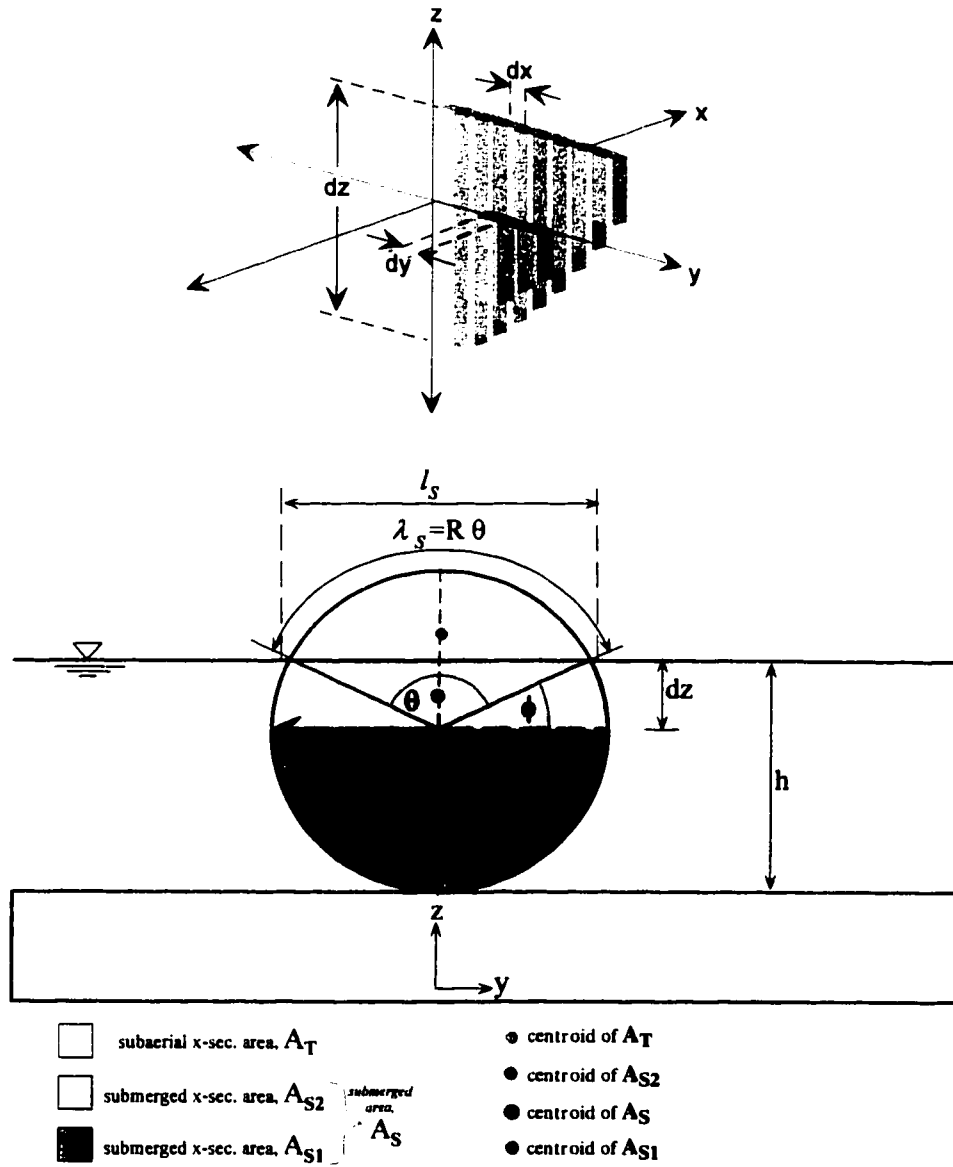


Figure 3-5 Centroids of Circle Segments

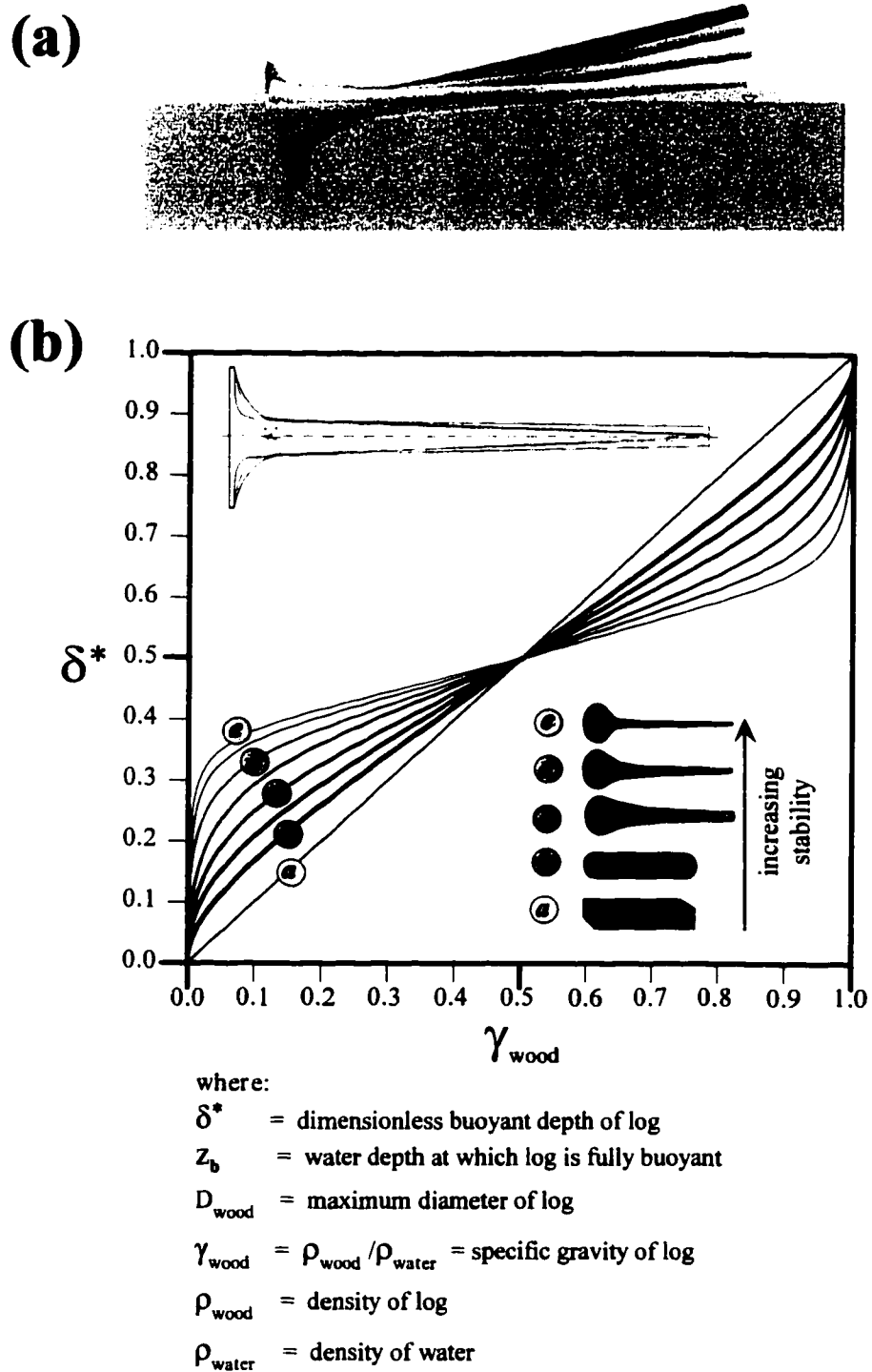


Figure 3-6 Effect of Bole Taper on Draft or Buoyant Depth (a), and Dimensionless Buoyant Depth as a Function of Specific Gravity and Bole Taper.

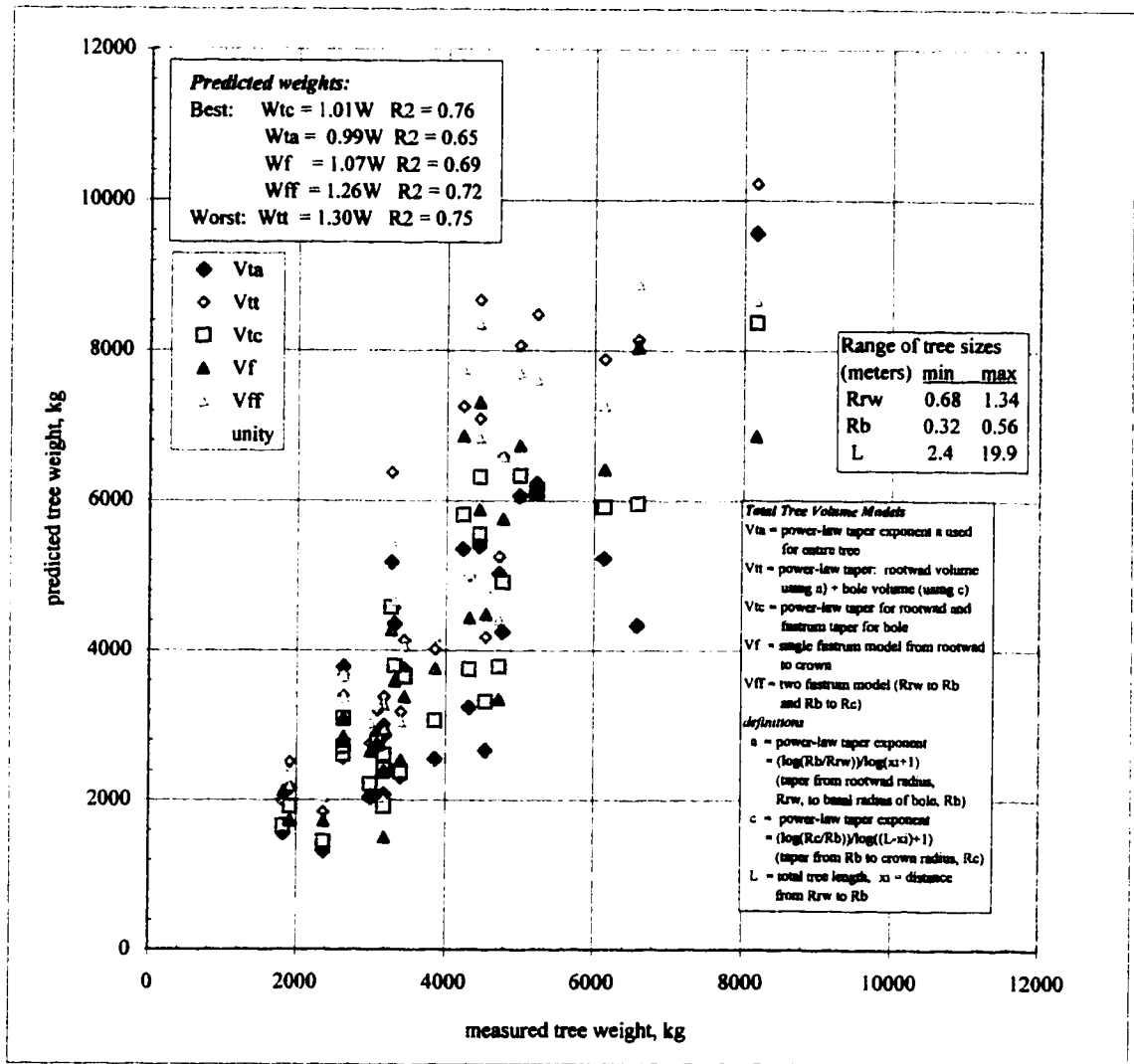


Figure 3-7 Comparison of tree geometry models to estimate weights of trees with measured weights. Field density of trees computed from tree cores.

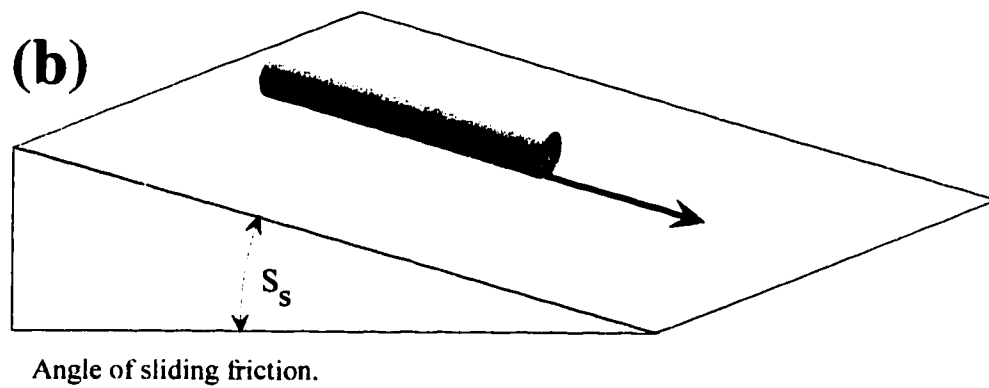
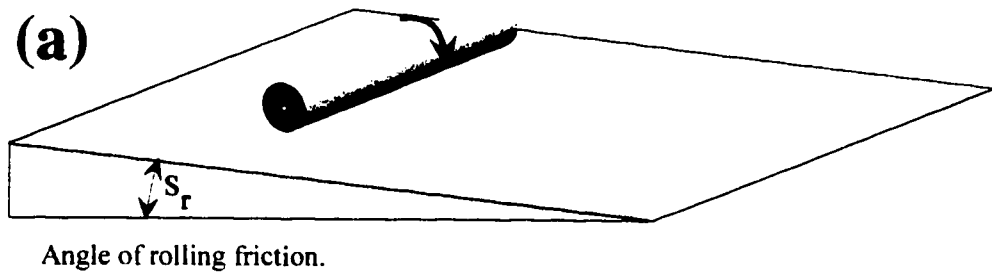


Figure 3-8 WD orientation with respect to ground surface slope and differences between rolling and sliding friction. Adapted from Onda and Matsuleura 1997.

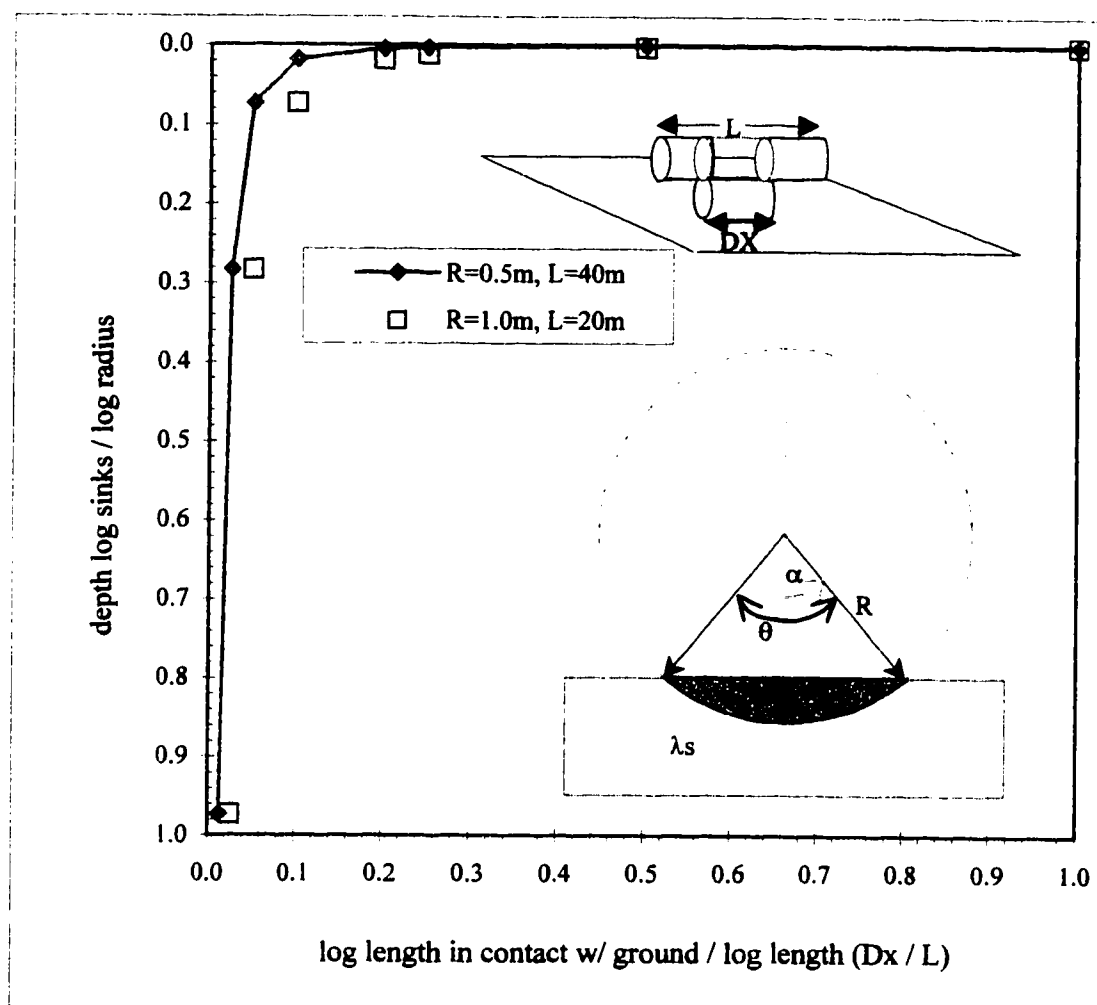


Figure 3-9a. Simple model of WD foot print and depth.

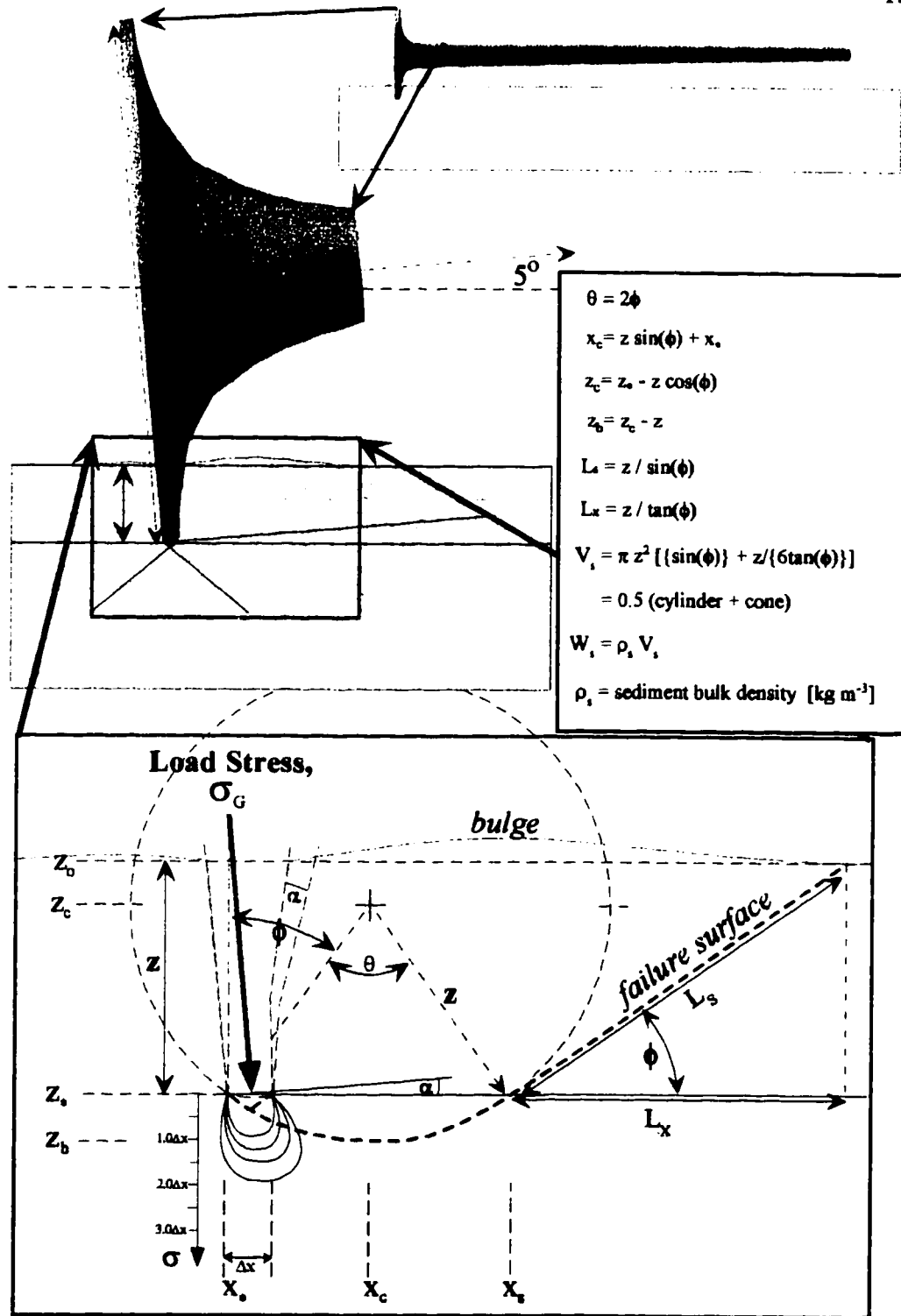


Figure 3-9b. Conical approximation for estimating sediment volume which must be overridden or plowed in profile.

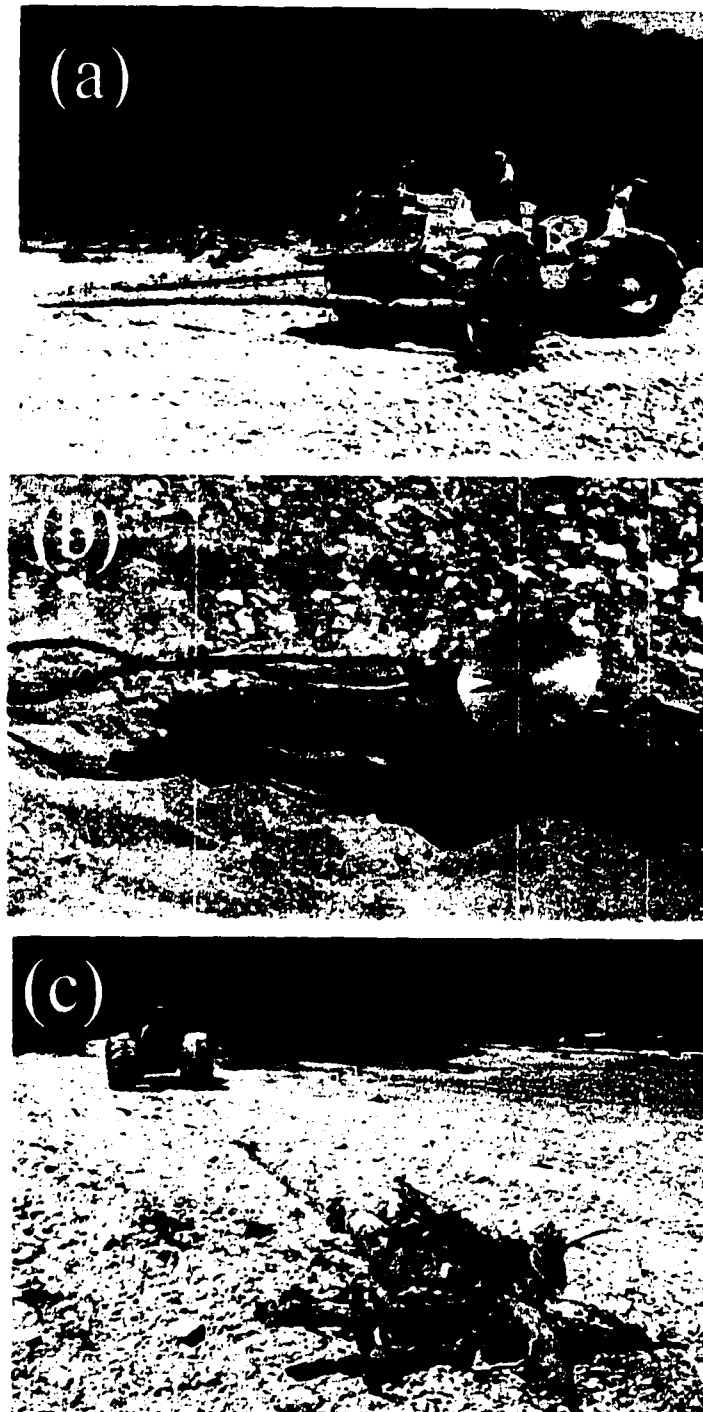


Figure 3-10 (a,b,c) Empirical estimates of static friction by dragging tree boles with and without rootwads across gravel bar. Tree boles were weighed (a), rigged up to drag with a scale between skidder and bole (b). The skidder slowly accelerated until the tree bole began to slide (c). The scale recorded the maximum force necessary to initiate sliding. Drag repeated at least 3 times for each orientation of tree bole and substrate composition. Tree boles were rotated to change the plow length and effective surface area in contact with the ground surface (i.e., normal stress).

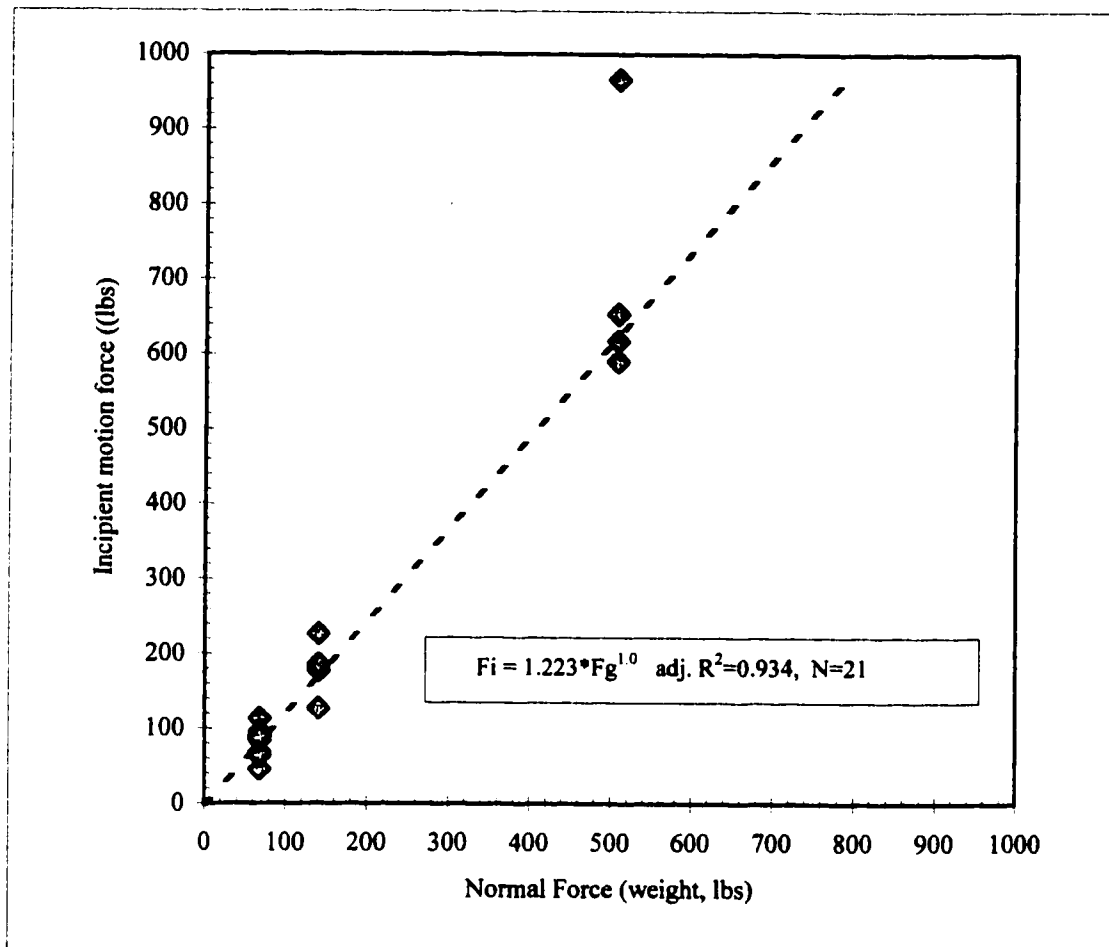
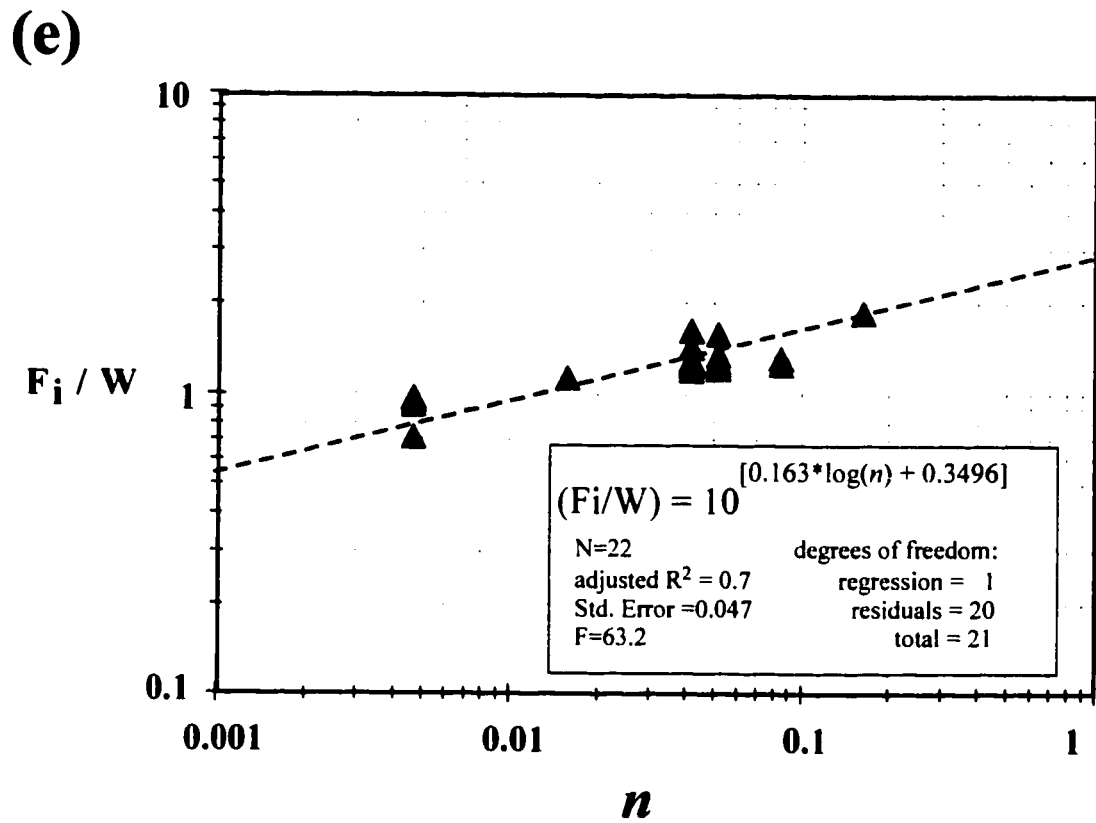


Figure 3-10 (d) Force necessary to initiate sliding plotted as a function of tree weight for different normal stresses. Regression excludes outlier point ($F_i = 1043$ kg) which occurred when the crown of one tree bole became embedded in the ground.



where, F_i = Force necessary to initiate motion
 W = tree weight
 n = plow length / tree length

Figure 3-10 (e) Incipient motion force as function of plow depth.

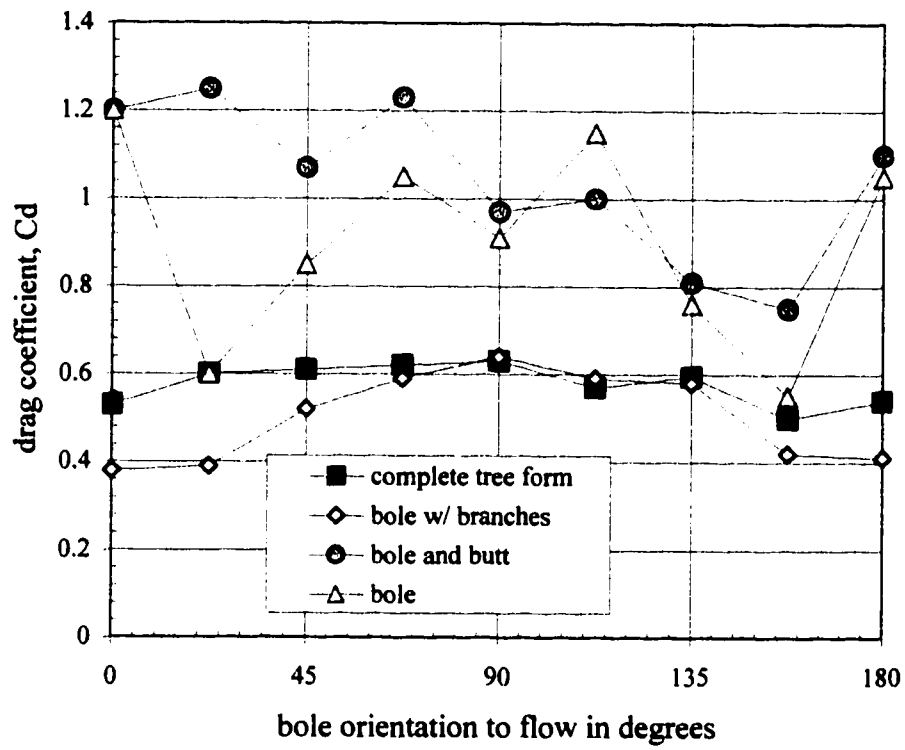


Figure 3-11 Drag coefficients derived by Gippel et al (1992) for different tree forms and orientations.

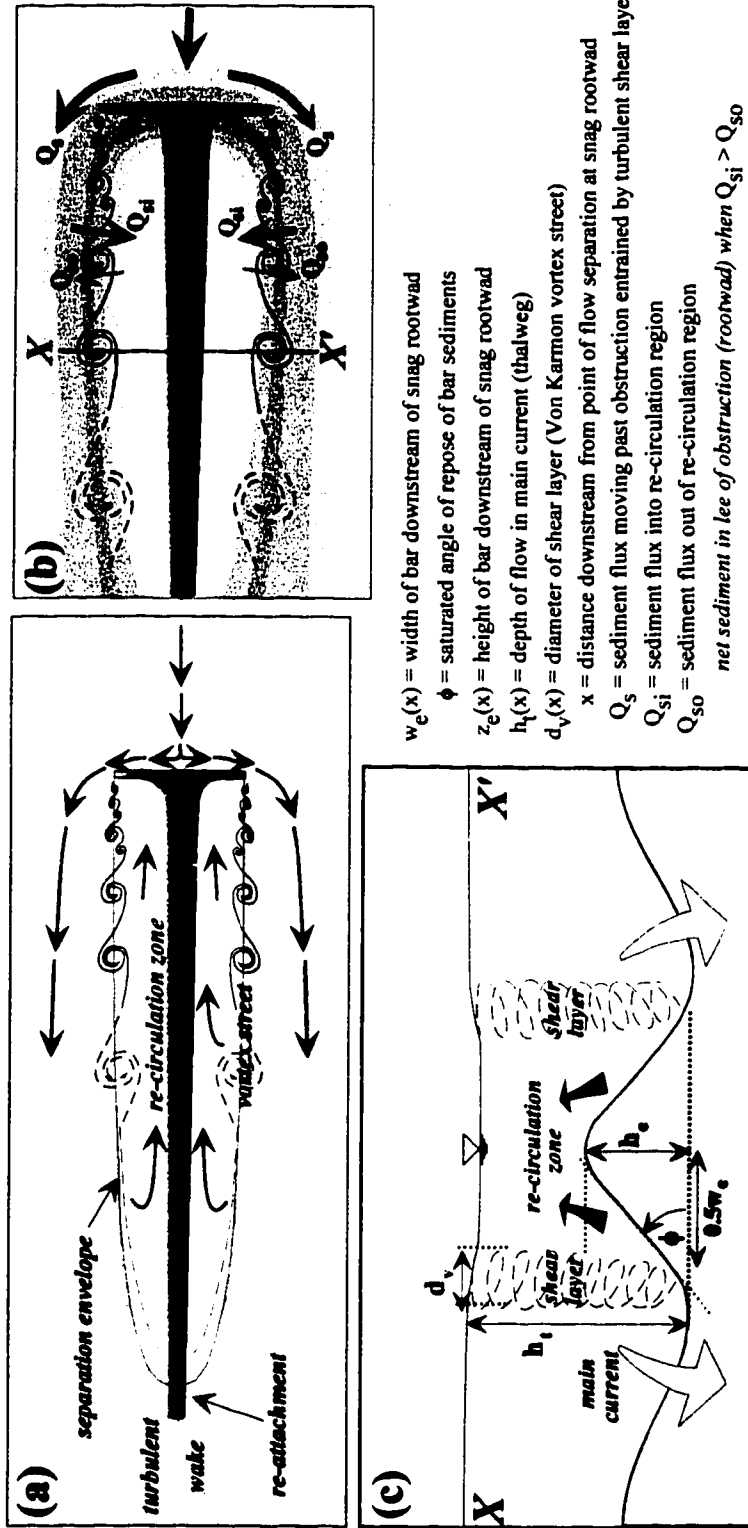


Figure 3-12 General flow structure around a bluff body and sediment accumulation within separation Envelope or eddy (a). Flow structure summary illustrating sediment flux into eddy region (b).

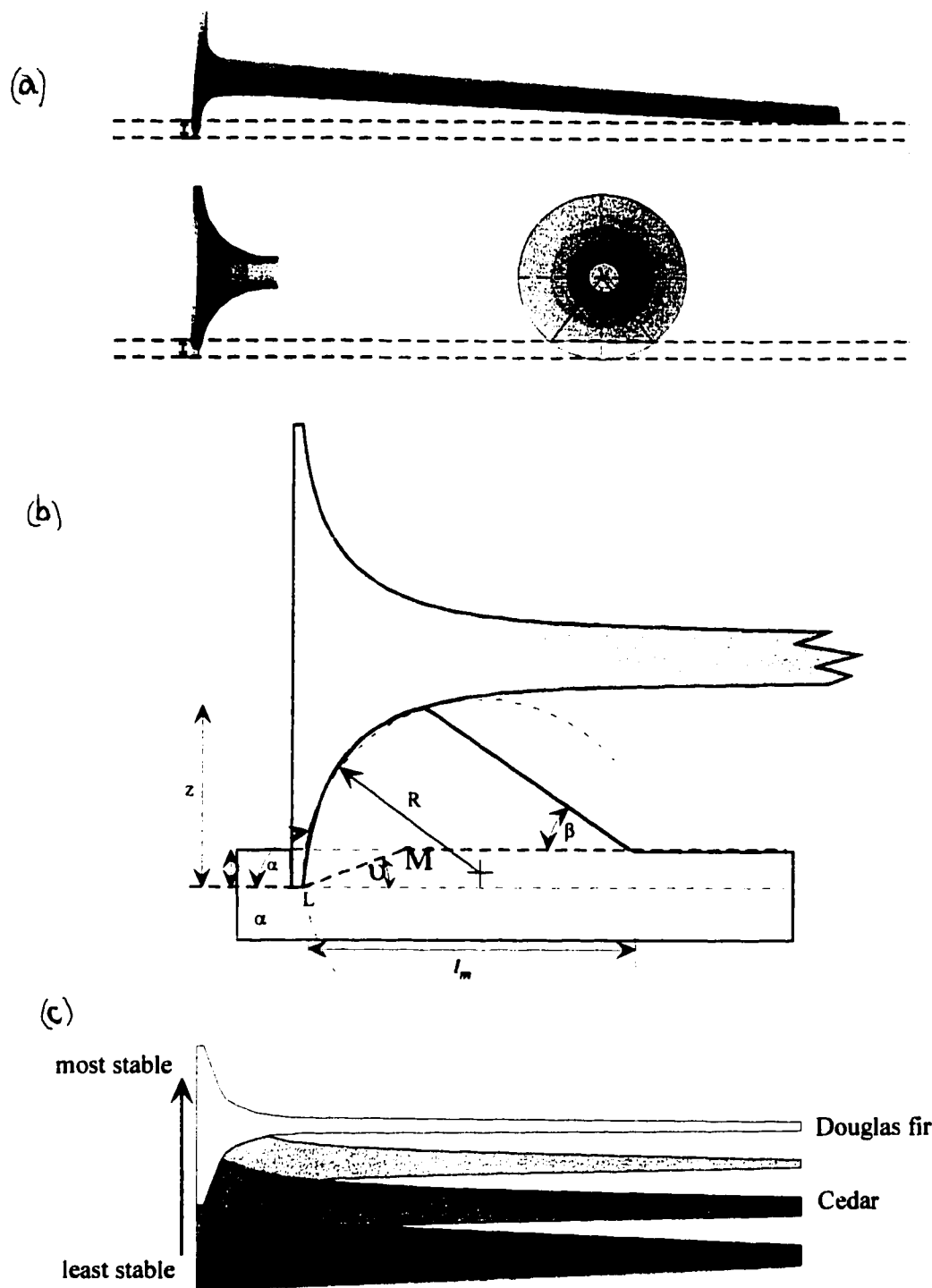


Figure 3-13 (a,b,c) Anchoring of a snag (tree bole) in an alluvial bed. Graphic description of tree bole with rootwad penetrating bed surface (a). Sediment buttrressing downstream of rootwad could result from either sedimentation in the lee of a stable snag or from sediment pushed up as a tree moves along the bed with its rootwad acting like a bulldozer blade (b). Tree bole taper will directly influence the relative magnitude of sediment buttrressing (c).

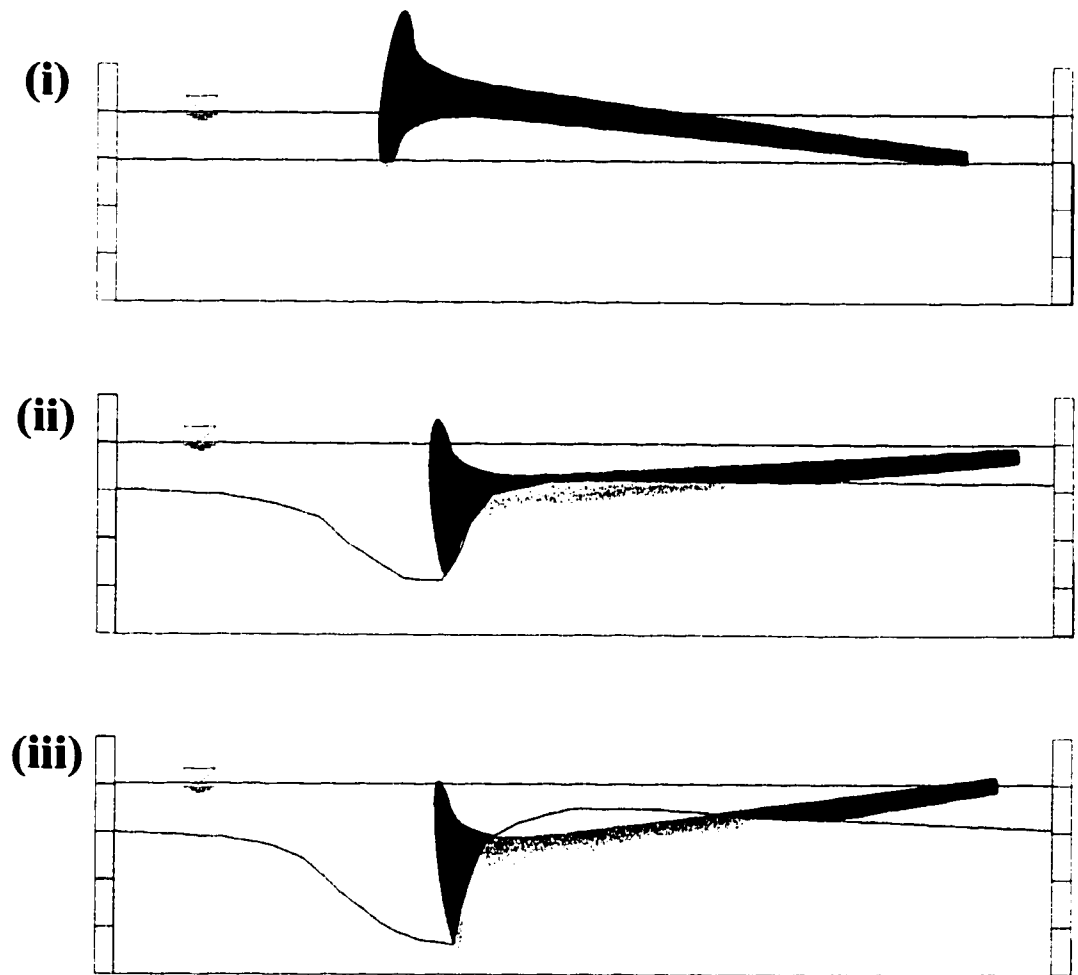


Figure 3-13 (d) Settling of bole associated with scour directly upstream and beside of rootwad and sediment buttressing downstream of rootwad (a).

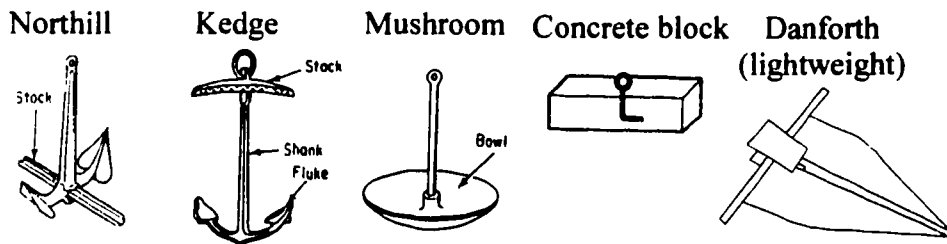
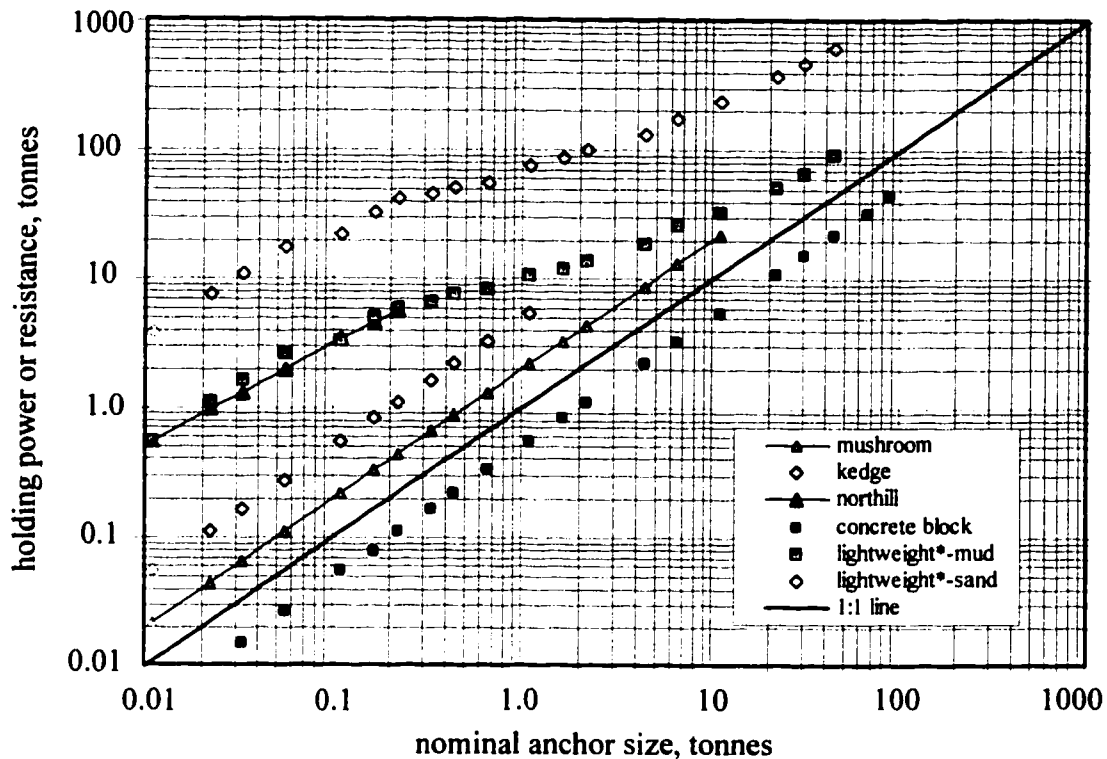


Figure 3-14 Anchor analogy for snag stability demonstrating the significance of shape on holding power (data from Myers et al., 1969)

In-stream Wood Debris Stability

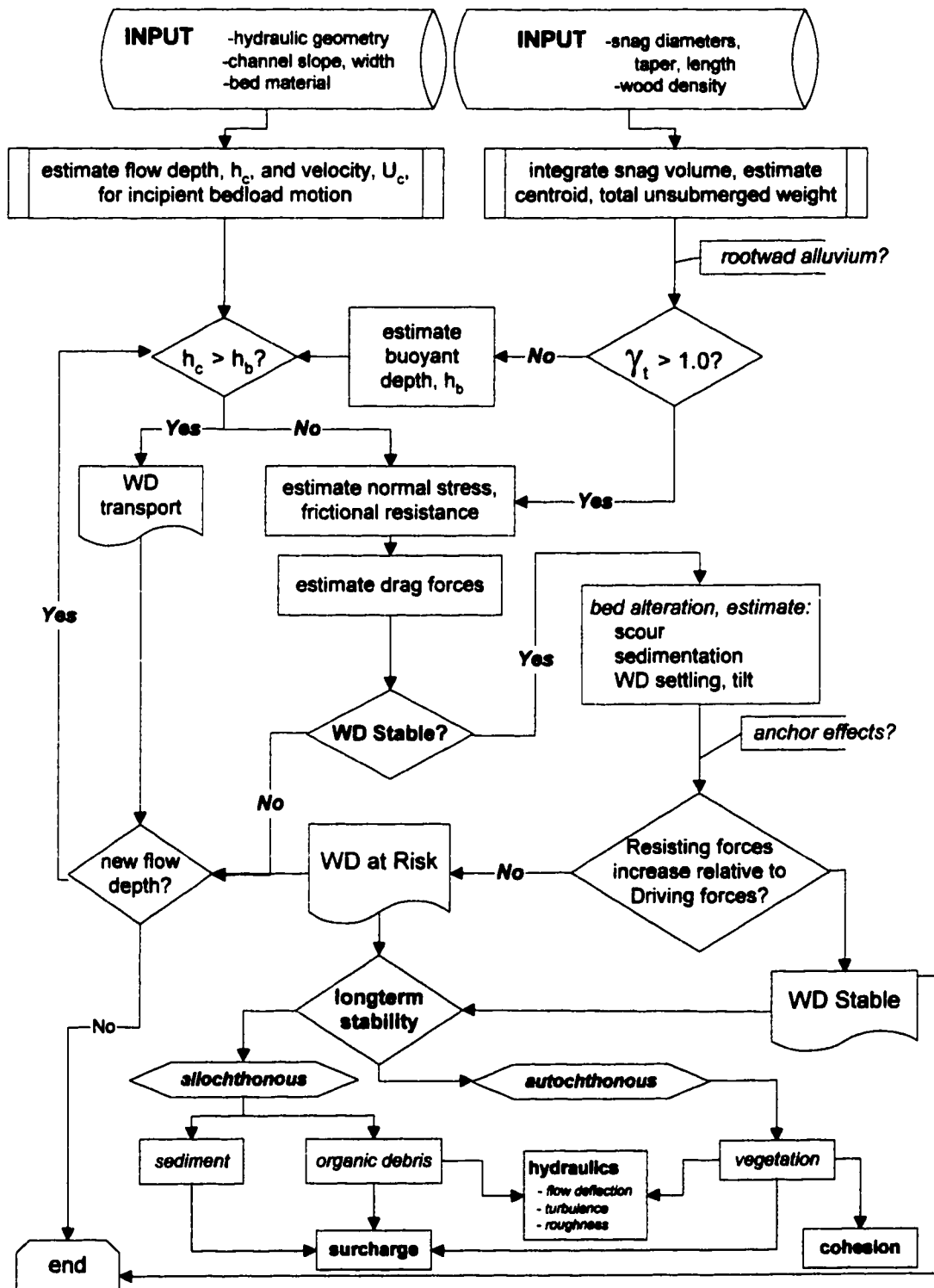


Figure 3-15 Flow chart presentation of factors and processes associated with wood debris stability in low-gradient channels.

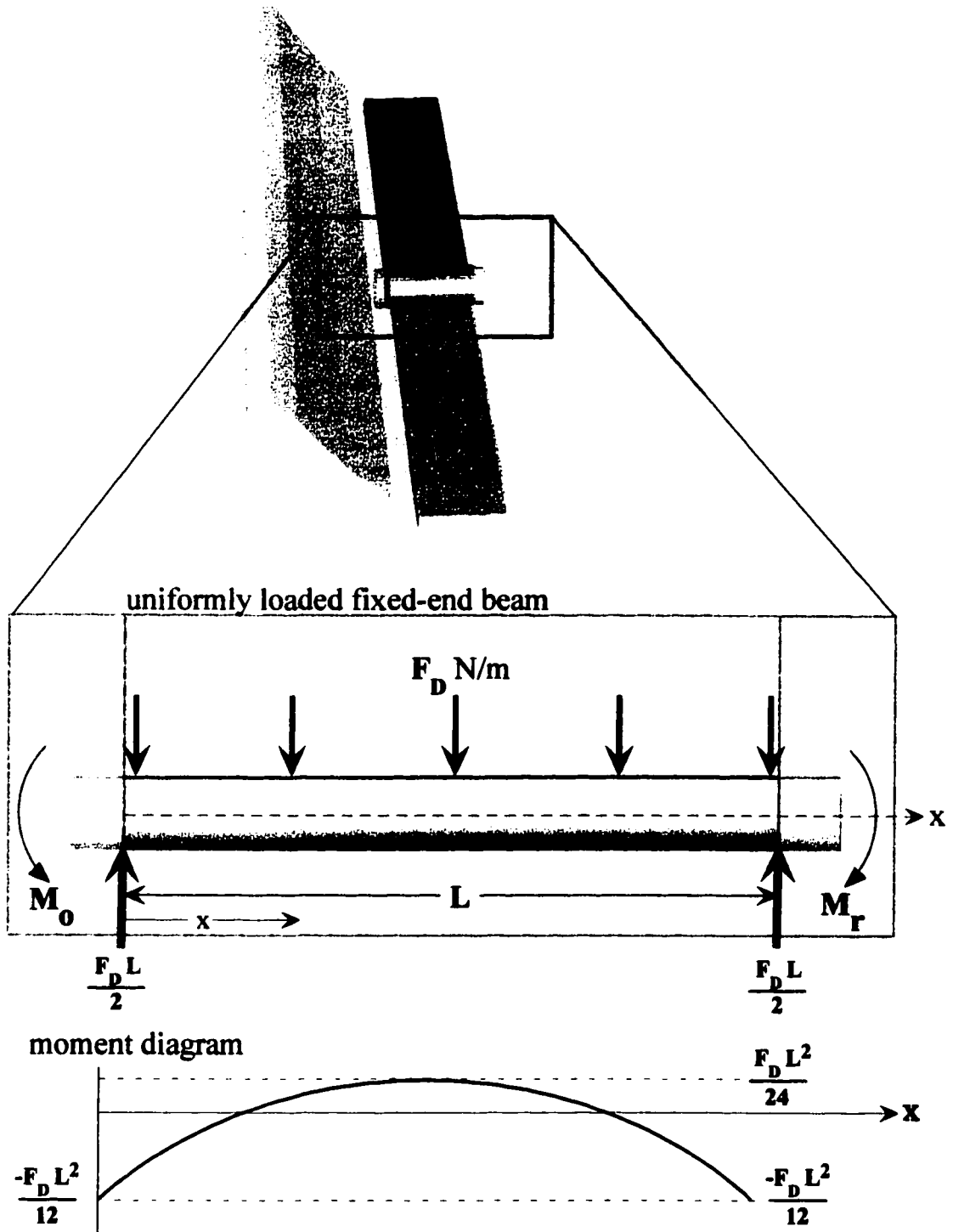


Figure 3-16 Definition sketch of simple beam model of log barriers or steps in low-order, steep headwater channels. Log is assumed to be a uniform cylinder (no taper) securely anchored on either end and oriented normal to flow.

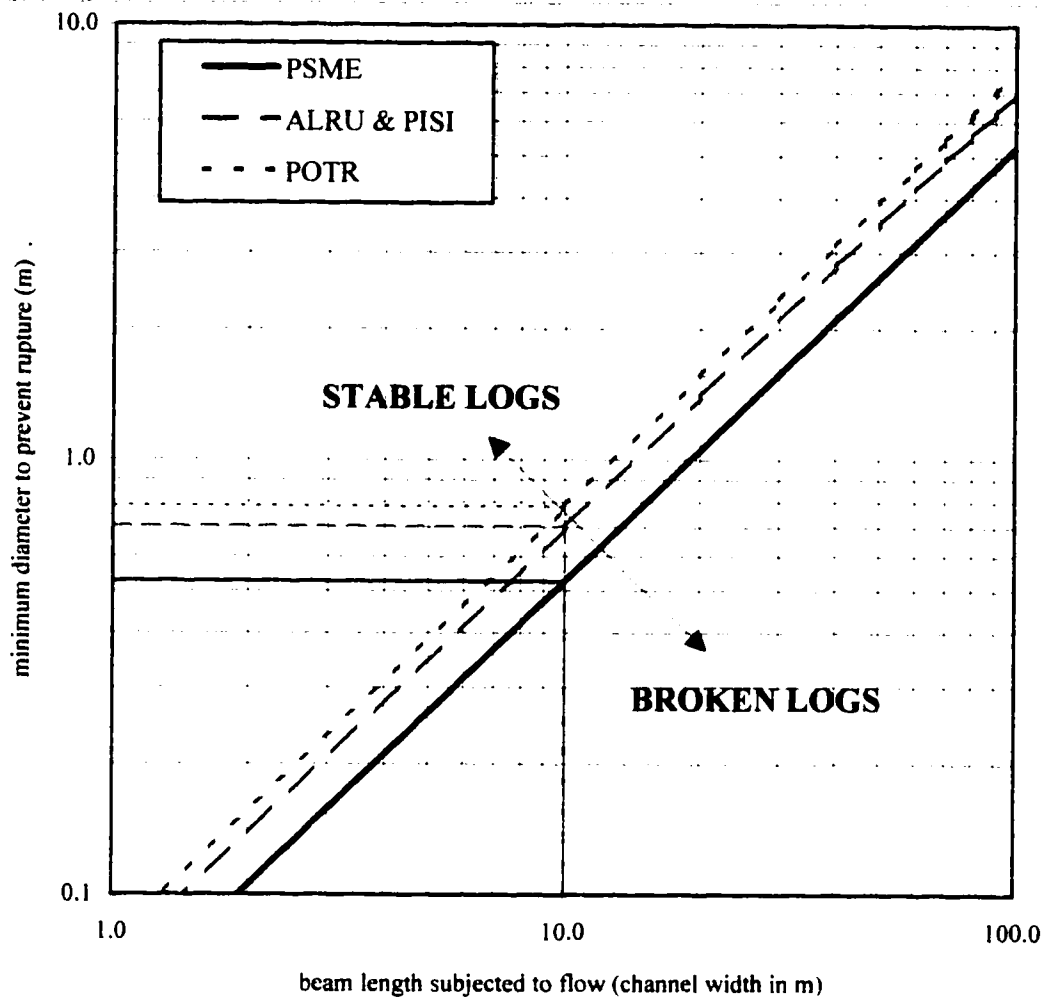


Figure 3-17 (a) Diameter of a log beam fixed at both ends necessary to withstand a uniformly distributed load due to a debris flow with a density of 2000 kg/m^3 and moving at 10 m/s , plotted as a function of channel width (assumed coincident with flow width). Critical diameters for *Pseudotsuga menziesii* (PSME), *Alnus rubra* (ALRU), *Picea sitchensis* (PISI), *Thuja plicata* (THPL), and *Populus trichocarpa* (POTR) are plotted as a function of channel width (assumed coincident with beam length).

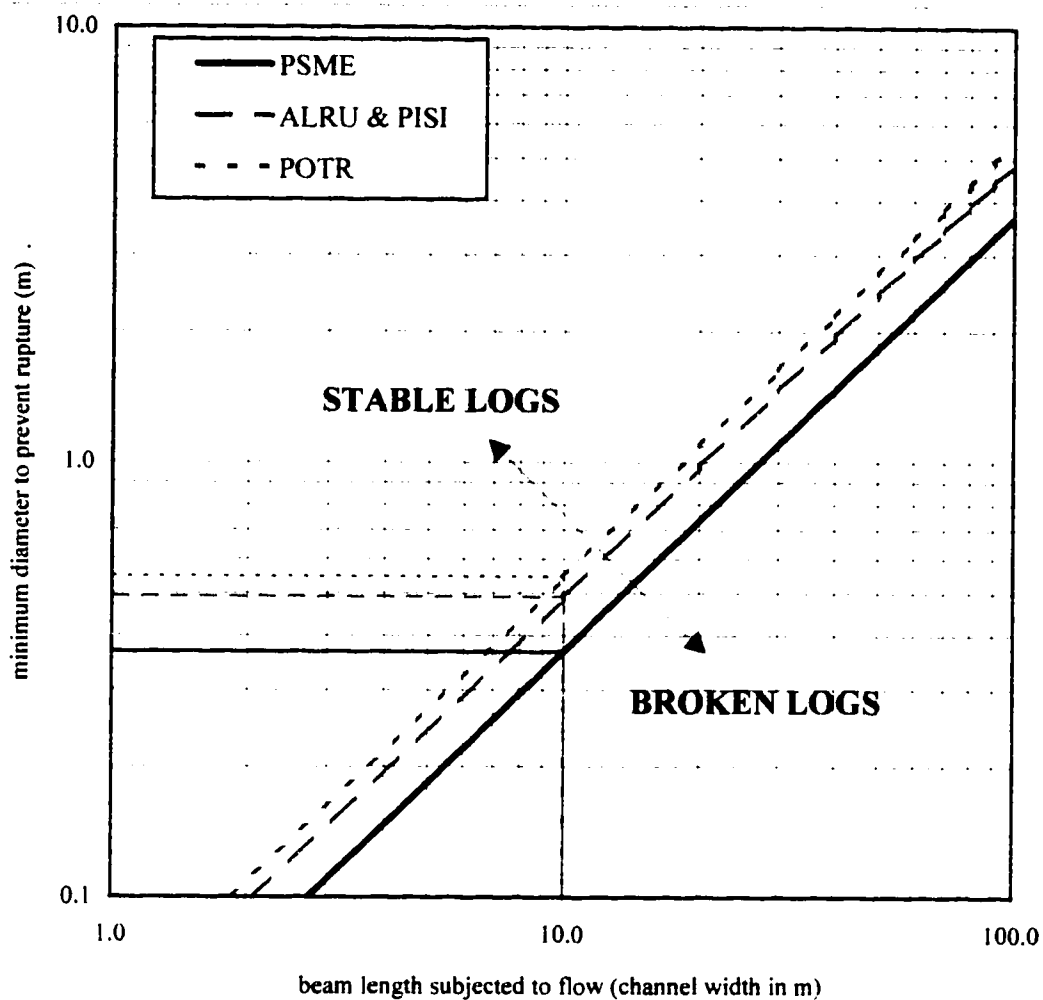


Figure 3-17 (b) Diameter of a log beam fixed at both ends necessary to withstand an impact by a boulder $1/4$ the beam's length (i.e., channel width). Boulder is assumed to have a density of 2600 kg/m^3 and moving at 10 m/s . Critical diameters for *Pseudotsuga menziesii* (PSME), *Alnus rubra* (ALRU), *Picea sitchensis* (PISI), *Thuja plicata* (THPL), and *Populus trichocarpa* (POTR) are plotted as a function of channel width (assumed coincident with beam length).

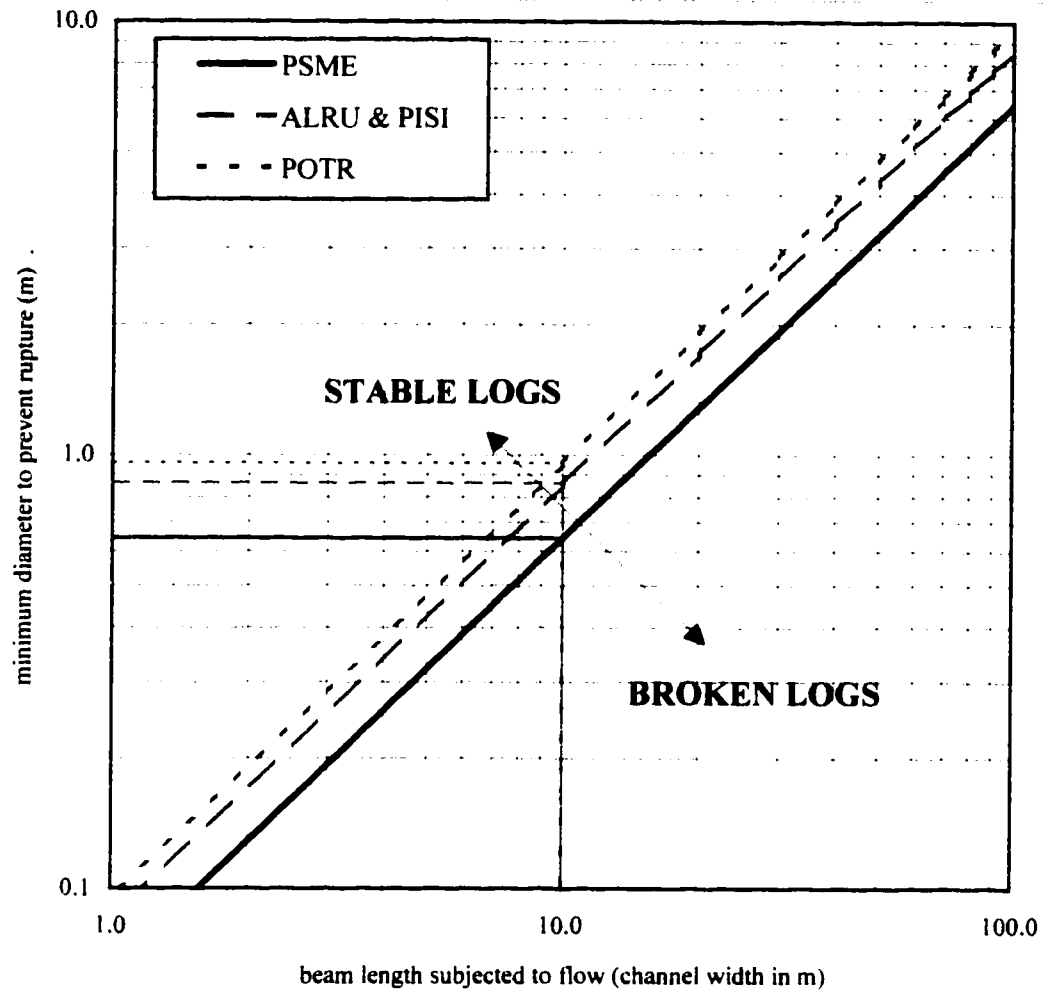


Figure 3-17 (c) Diameter of a log beam fixed at one end and pinned at the other end necessary to withstand a uniformly distributed load due to a debris flow with a density of 2000 kg/m^3 and moving at 10 m/s , plotted as a function of channel width (assumed coincident with flow width). Critical diameters for *Pseudotsuga menziesii* (PSME), *Alnus rubra* (ALRU), *Picea sitchensis* (PISI), *Thuja plicata* (THPL), and *Populus trichocarpa* (POTR) are plotted as a function of channel width (assumed coincident with beam length).

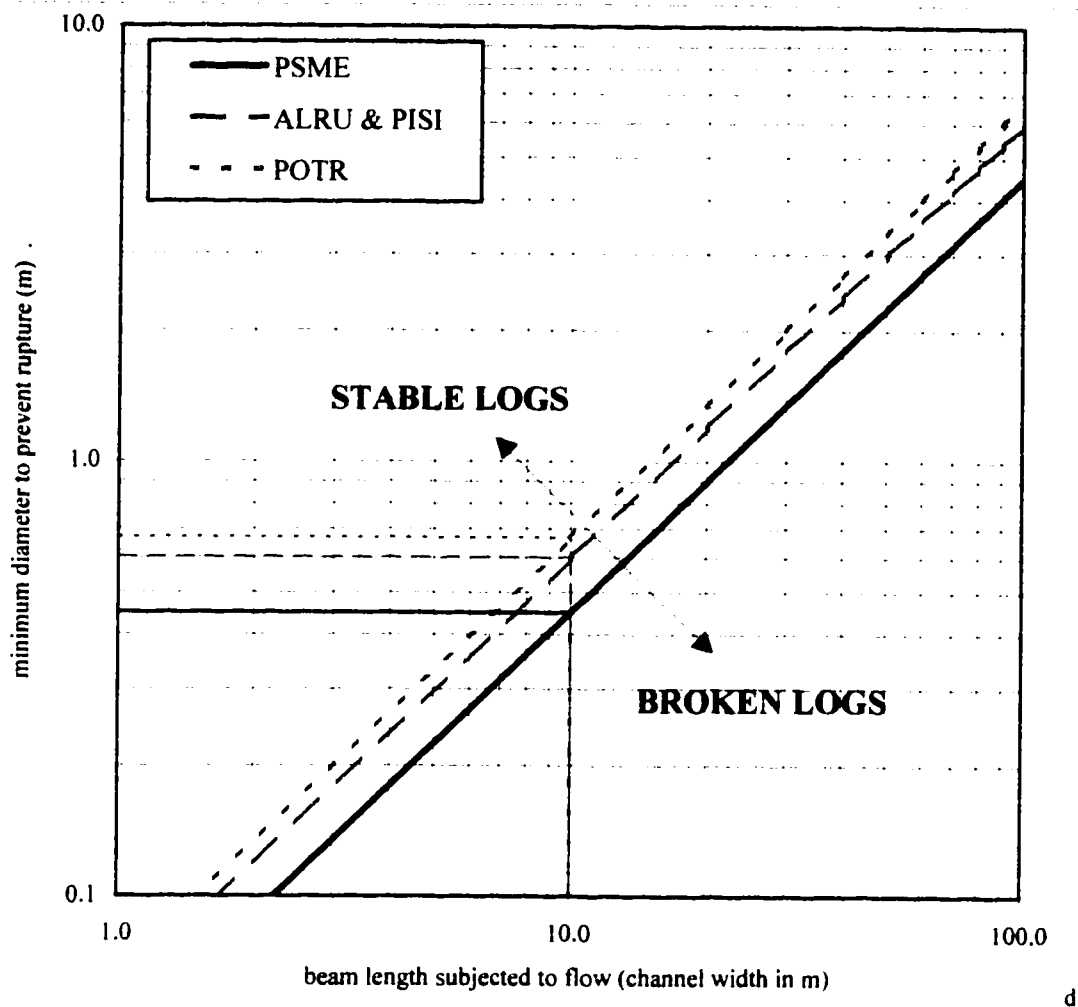


Figure 3-17 (d) Diameter of a log beam fixed at one end and pinned at the other end necessary to withstand an impact by a boulder $1/4$ the beam's length (i.e., channel width). Boulder is assumed to have a density of 2600 kg/m^3 and moving at 10 m/s . Critical diameters for *Pseudotsuga menziesii* (PSME), *Alnus rubra* (ALRU), *Picea sitchensis* (PISI), *Thuja plicata* (THPL), and *Populus trichocarpa* (POTR) are plotted as a function of channel width (assumed coincident with beam length).

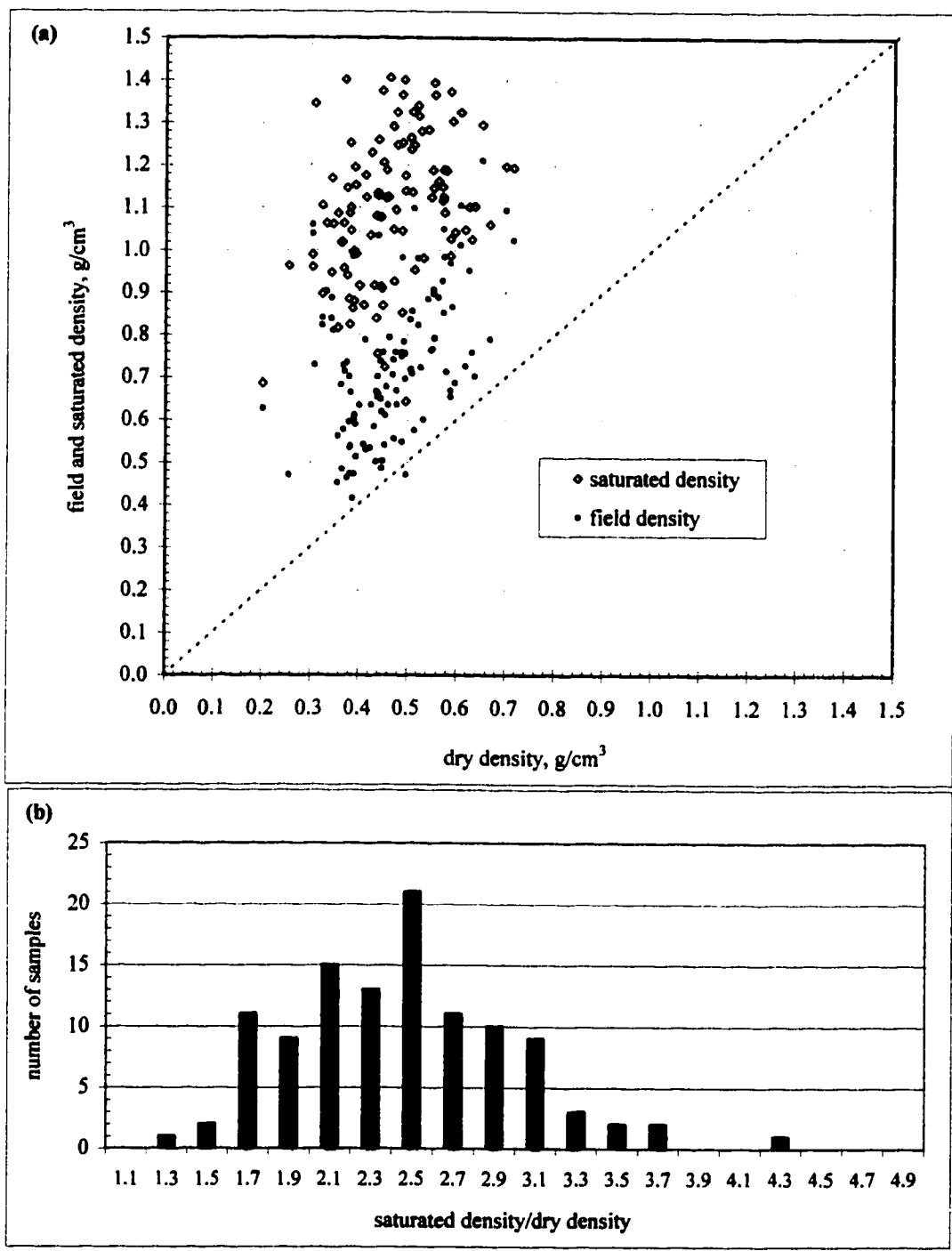


Figure 3-18 Plot illustrating the maximum range of wood densities found several species native to the Pacific Northwest. Note that once saturated, the specific gravity of wood debris can exceed unity. Even in regions where most of the trees have low densities, such as the PNW, it is not uncommon to find sunken log resting on the channel bottom.

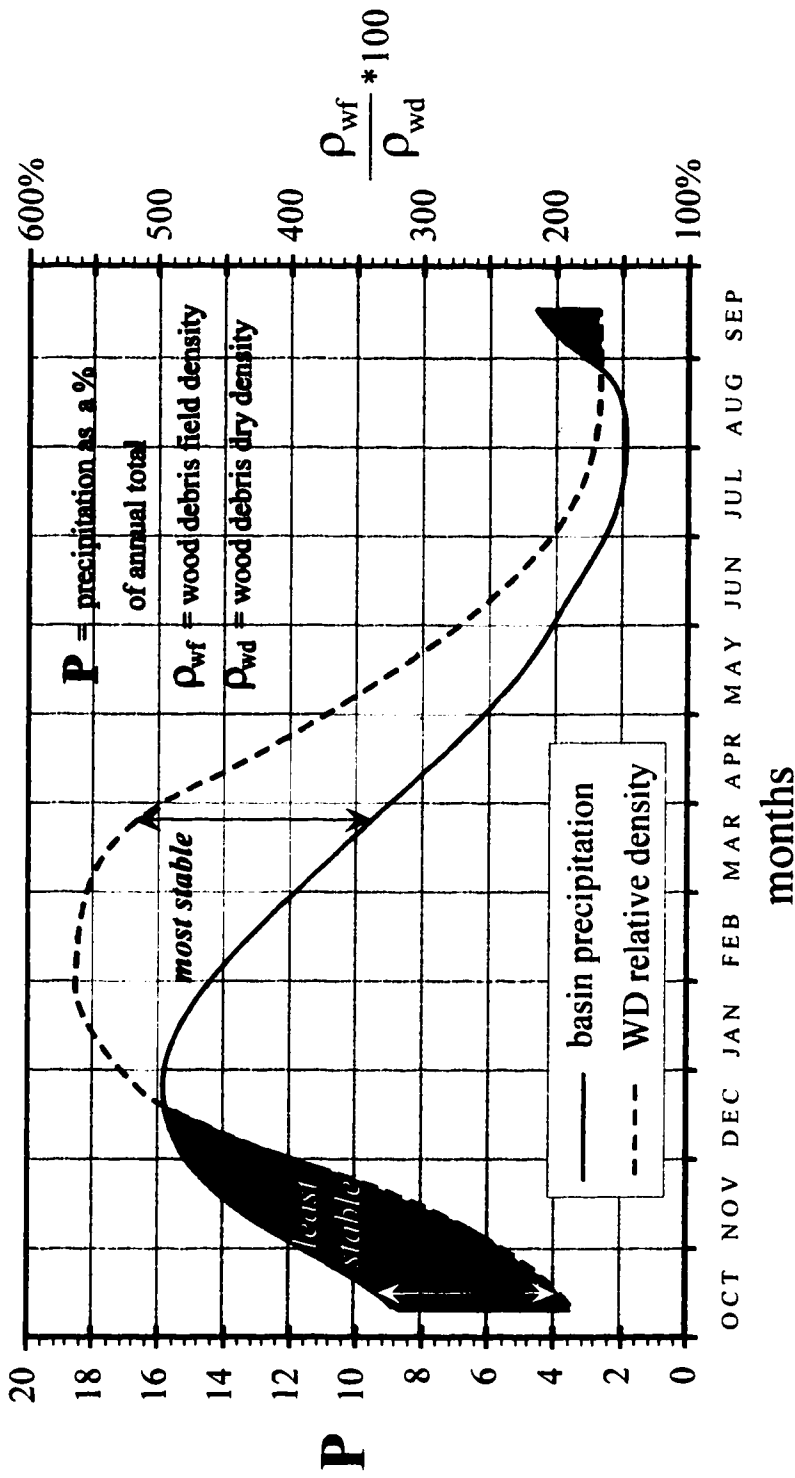


Figure 3-19 Hypothetical graph illustrating the effect of regional climates and seasonal precipitation on the stability of wood debris. In catchments on the west slope of the Cascade and Olympic mountains in Washington State, almost all of the annual precipitation occurs during the 9 months of Fall, Winter, and Spring. The summers are characterized by long, sunny, warm days and extremely low flows in streams and rivers. By the end of the summer, wood debris situated above the water table reaches its lowest moisture content of the year and its greatest potential buoyancy. Wood debris in this region will generally be most susceptible to transport early in the Fall. By November or December, wood moisture contents may be near saturation due to the frequent rain and high flows, low rates of evaporation, and short days. If two identical logs are placed in streams of similar size in two different climates and the logs subjected to identical flow conditions, the log in the more arid region will be the first to move, thus suggesting a lower frequency of stable wood debris accumulations in arid regions.

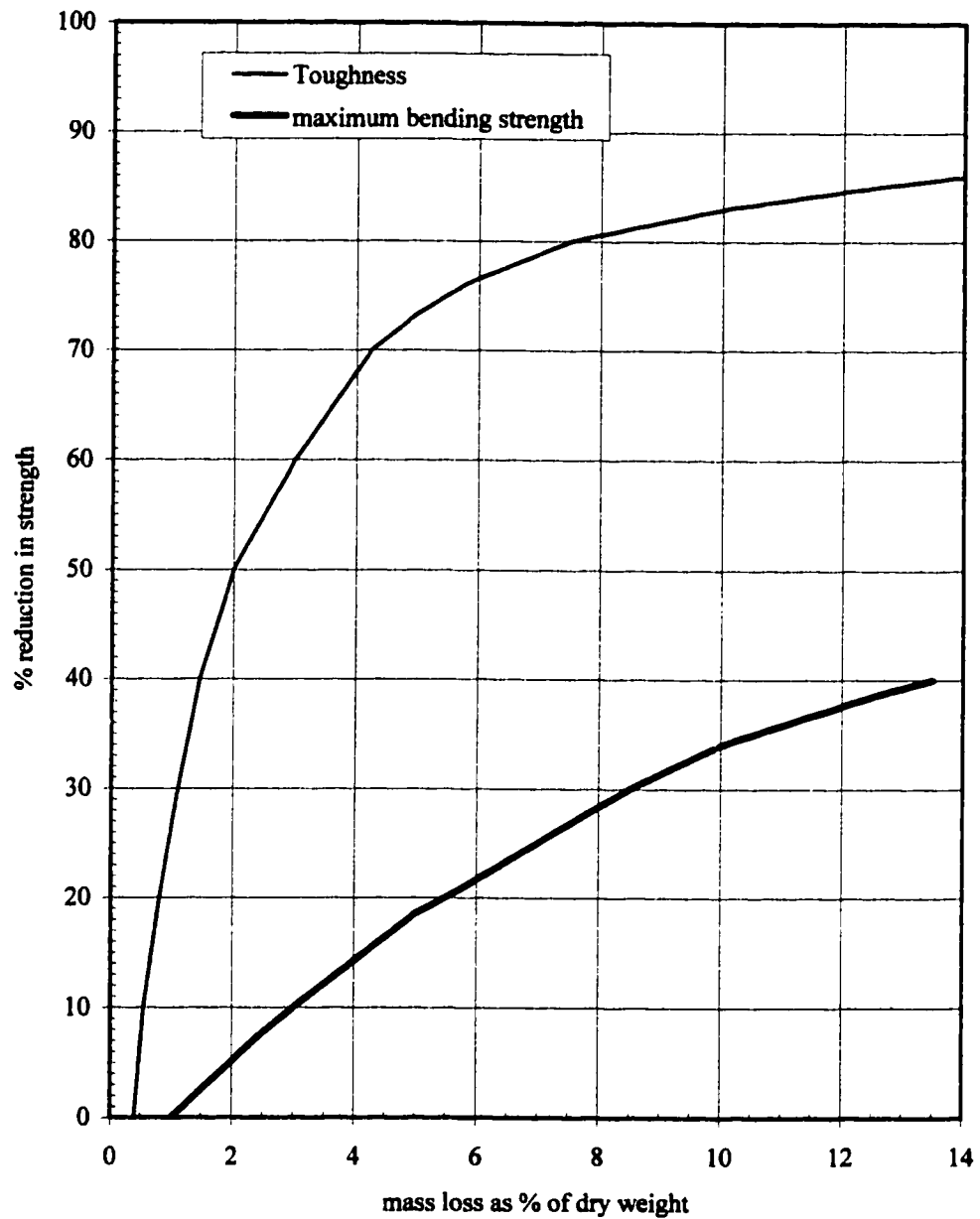
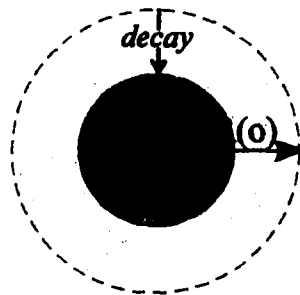
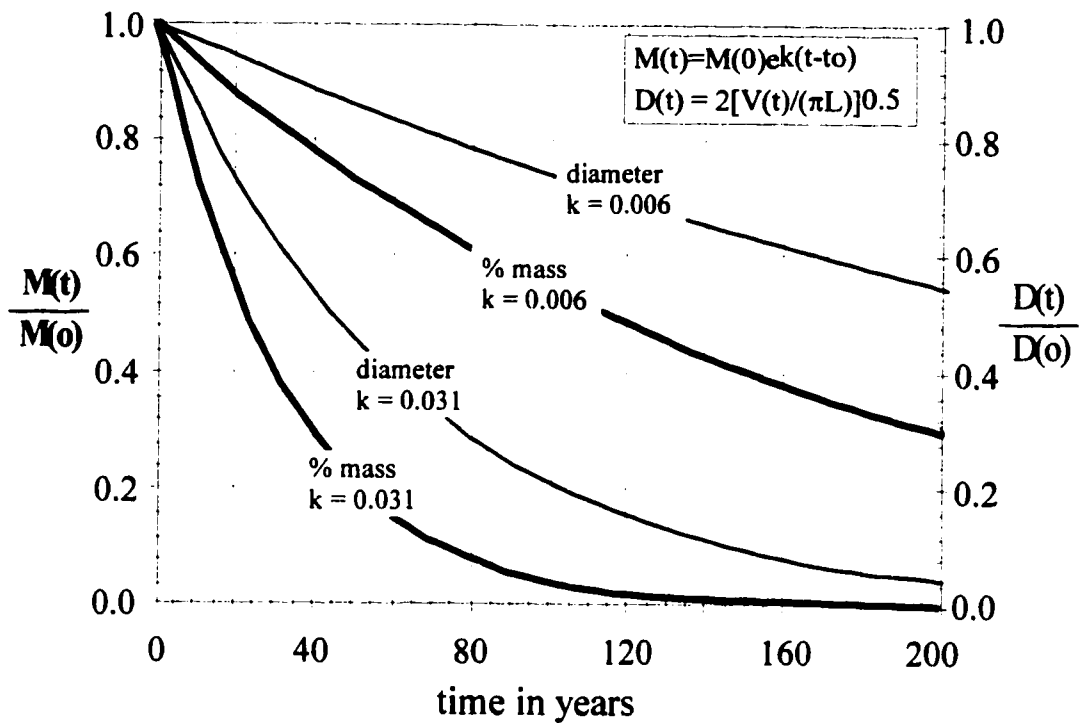


Figure 3-20 Effects of decay on wood strength. Bending strength and especially toughness, experience a rapid reduction with respect to mass loss. Based on effect of fungus *Chaetomium globosum* on bending strength and toughness of beech (*Fagus sylvatica*) (from Armstrong and Savory 1959).



- $R(o)$ = initial log radius
- $R(t)$ = log radius at time t
- $D(o)$ = initial log diameter
- $D(t)$ = log diameter at time t
- $M(o)$ = initial log mass
- $M(t)$ = log mass at time t

Figure 3-21 Application of simple decay model using decay constants of $k=0.006$ (old-growth conifers) and $k=0.031$ (black cottonwood) to estimate % mass remaining and diameter relative to initial diameter with time. Diameter predictions based on decay progressing from the perimeter of a cylinder to its center. Decay coefficients based on Sollins (1982), Means et al. (1986), Ceylonese et al. (1987), Hyatt (1998).

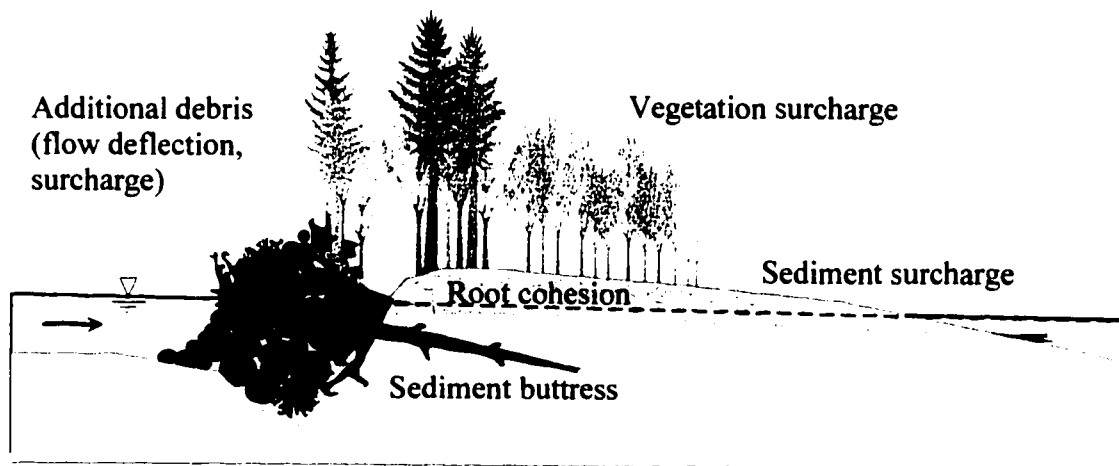


Figure 3-22 Illustration summarizing additional factors that influence debris stability: surcharge (alluvium and vegetation), additional debris accumulation (sealing and deflecting flow), root cohesion (adding cohesion to cohesionless sediments downstream and on top of debris); and overlying canopy (shade can reduce drying rates of wood, maintaining greater moisture contents but accelerating decay).

Table 3-1 Alluvial substrate bearing capacities		
Substrate	In-situ Consistency	Bearing Capacity (kg/m ²)
well-graded mixture of fine and coarse-grained soil: glacial till, hardpan, boulder clay	very compact	97,649
gravel, gravel-sand mixtures, boulder-gravel mixtures	very compact	68,354
	medium to compact	48,824
	loose	29,295
coarse to medium sand, sand with little gravel	very compact	39,059
	medium to compact	29,295
	loose	14,647
fine to medium sand, silty or clayey medium to coarse sand	very compact	29,295
	medium to compact	24,412
	loose	14,647
homogeneous inorganic clay, sandy or silty clay	very stiff to hard	39,059
	medium to stiff	15,530
	soft	4,882
inorganic silt, sandy or clayey silt, varved silt-clay-fine sand	very stiff to hard	29,295
	medium to stiff	14,647
	soft	4,882
compiled from Department of Navy 1982, Table 1, Chapter 4 and US Army Corps of Engineers 1993)		

TABLE 3-2				
Best-fit Empirical Models for Estimating Drag Coefficients (Gippel et al. 1996)				
form model	drag coefficient C_D (q = bole orientation in degrees)	std. error of est.	R^2	p
complete tree	$C'_D = 0.506 + \theta (1.82E-3)$	0.046	0.664	0.004
bole with branches	$C'_D = 0.357 - \theta (2.22E-4)$ $- \theta^2 (1.13E-4) - \theta^3 (7.93E-7)$	0.022	0.978	0.0001
bole only	$C'_D = 1.117 - \theta (5.28E-2)$ $+ \theta^2 (1.44E-3) - \theta^3 (9.77E-6)$	0.075	0.985	0.0007

TABLE 3-3 Bulk densities and friction angles as a function of grain size				
sediment (moderately to slightly rounded)	grain size, mm	dry bulk density, kg/m ³	saturated bulk density, kg/m ³	friction angles
coarse gravel, boulders	>192	2,100-2,200	1,300-1,400	43-46
coarse gravel	36-144	2,000-2,100	1,250-1,300	42-45
medium gravel	18-36	1,925-1,975	1,175-1,225	41-44
fine gravel	9-18	1,750-1,800	1,100-1,150	40-42
gravelly sand	4.5-9.0	1,700-1,750	1,050-1,100	38-41
coarse sand	1.0-4.5	1,600-1,650	1,000-1,050	33-39
medium sand	0.54-1.0	1,550-1,600	950-1,000	29-35
fine sand	0.06-0.54	1,450-1,500	900-950	22-30
compiled from Lane 1953 and U.S. Army Corps of Engineers 1993				

Table 3-4 Log Beam Maximum Moments		
Model	max.moment, $M e_{max}$	location on beam
1 Log beam fixed at both ends		
a) Load uniformly distributed over log length	$(F_u L) / 12$	ends at both banks
b) Point impact at center of log span*	$(F_i L) / 8$	both ends and center
2 Log beam fixed at one end and pinned at other end		
a) Load uniformly distributed over log length	$(F_u L) / 8$	bank with fixed end
b) Point impact at center of log span*	$3 (F_i L) / 16$	bank with fixed end
<p>* point impact is assumed to be delivered by entrained boulder F_u = total force uniformly distributed across log length [N] = $C_D \rho_f D_l U^2 L$ F_i = total force delivered as point impact at center of log [N] = $C_D \rho_b D_l U^2 D_b$ L = length of log spanning channel or flow width [m] C_D = drag coefficient of log, ρ_f = fluid density of flow [kg/m³], ρ_b = density of boulder impacting log [kg/m³], D_l = log beam diameter, D_b = boulder diameter, assumed to length of log subjected to impact U = flow velocity (boulder assumed to be moving at same velocity) [m/s]</p>		

TABLE 3-5
Specific Gravity, Modulus of Rupture and Modulus of Elasticity Values for Common Pacific Northwest Trees¹

Common Name	Genus:	Species:	Green Wood:: MC = 30			Dry Wood: MC = 12		
			Specific Gravity ²	Modulus of Rupture ³ , MR (N/m ²)	Modulus of Elasticity ME (N/m ²)	Specific Gravity ²	Modulus of Rupture ³ , MR (N/m ²)	Modulus of Elasticity ME (N/m ²)
Subalpine fir	<i>Abies</i>	<i>lasiocarpa</i>	0.31	3.40E+7	7.20E+6	0.32	5.90E+7	8.90E+6
Western Red Cedar	<i>Thuja</i>	<i>plicata</i>	0.31	3.59E+7	6.50E+6	0.32	5.17E+7	7.70E+6
Black Cottonwood	<i>Populus</i>	<i>trichocarpa</i>	0.31	3.40E+7	7.40E+6	0.35	5.90E+7	8.80E+6
Engelmann Spruce	<i>Picea</i>	<i>engelmannii</i>	0.33	3.20E+7	7.10E+6	0.35	6.40E+7	8.90E+6
Grand Fir	<i>Abies</i>	<i>grandis</i>	0.35	4.00E+7	8.60E+6	0.37	6.10E+7	1.08E+7
Sitka Spruce	<i>Picea</i>	<i>sitchensis</i>	0.37	3.90E+7	7.40E+6	0.40	7.00E+7	1.08E+7
Ponderosa	<i>Pinus</i>	<i>ponderosa</i>	0.38	3.50E+7	6.90E+6	0.40	6.50E+7	8.90E+6
Red Alder	<i>Alnus</i>	<i>rubra</i>	0.37	4.50E+7	8.10E+6	0.41	6.80E+7	9.50E+6
Silver Fir	<i>Abies</i>	<i>amabilis</i>	0.40	4.40E+7	9.80E+6	0.43	7.30E+7	1.19E+7
Yellow Cedar	<i>Chamaecyparis</i>	<i>nootkatensis</i>	0.42	4.40E+7	7.90E+6	0.44	7.70E+7	9.80E+6
Mountain Hemlock	<i>Tsuga</i>	<i>mertensiana</i>	0.42	4.30E+7	7.20E+6	0.45	7.90E+7	9.20E+6
Western Hemlock	<i>Tsuga</i>	<i>heterophylla</i>	0.42	4.30E+7	7.20E+6	0.45	7.90E+7	9.20E+6
Bigleaf Maple	<i>Acer</i>	<i>macrophyllum</i>	0.44	5.10E+7	7.60E+6	0.48	7.40E+7	1.00E+7
Douglas fir	<i>Pseudotsuga</i>	<i>menziesii</i>	0.45	5.30E+7	1.08E+7	0.48	8.50E+7	1.34E+7

¹ MR, ME: ASTM 1980. MRc: Bohannan 1966, Garfinkel 1973, Tuomi 1974, NFPA 1977, Wigmosta 1983.

² specific gravity computed from oven-dry mass (MC=0%) and volume at MC=12%. MC = moisture content in % of dry wood mass

³ MR values for small, clear rectangular samples. Corrected modulus of rupture, MRc, for logs (circular cross-section): $MRc = 1.18 \cdot MR \cdot [2 / (3.51 \cdot D)]^{1/3}$

Table 3-6 Variables influencing force balance analysis for in-stream wood debris		
Forces	Static	Dynamic
F_G Gravity Forces	WD size Wood density Wood saturation	Rate of water absorption Changes in Wood Characteristics <i>mechanical degradation</i> <i>biochemical degradation</i>
F_B Buoyant Force	Shape of wood Density distribution in WD Water depth	Effect of wood on local water level in: <i>straight reach (backwater);</i> <i>bend (super-elevation at bank)</i>
F_D Drag Force	Drag coefficient: <i>effective form</i> <i>shape of wood</i> <i>orientation</i> <i>blockage coefficient</i> <i>flow velocity</i> Bed topography at WD	Effect of WD of flow: <i>backwater effects</i> <i>elevated water surface directly</i> <i>upstream of WD</i> <i>eddy formation</i>
F_R Resistance to Sliding	Static friction coefficient: <i>bed material</i> <i>bed load capacity</i> <i>WD shape</i> surcharge: <i>alluvium</i> <i>vegetation</i> <i>root cohesion</i>	Dynamic friction coefficient: <i>bed bearing capacity</i> <i>plow effects</i> <i>draft of WD</i> <i>length of WD</i> <i>channel size and curvature</i>

CHAPTER 4: A NEW MECHANISM OF FLOODPLAIN AND TERRACE FORMATION IN FORESTED REGIONS

4.1 Introduction

The physical and ecological conditions of rivers throughout the world at the close of the twentieth century bear little resemblance to conditions that existed during the preceding millennium, leaving fluvial geomorphologists few places to apply Lyell's tenet that "the present provides a key to the past." Forests have existed for about 400 million years, covering over 30% of the earth's land surface during the Holocene. Forests deliver tremendous quantities of wood debris (WD) to rivers, and one of the widespread human impacts to rivers has been the loss of wood debris through channel clearing and destruction of riparian forests (Ruffner 1886, Sedell and Luchessa 1982, Sedell and Frugatt 1984, Swift 1984, Benke 1990).

Numerous studies have demonstrated that WD can have a significant effect on flow conditions and morphology of small channels (e.g., Zimmerman et al. 1967, Heede 1972, Swanson and Lienkaemper 1978, Keller and Tally 1979, Triska and Cromack 1980, Bisson et al. 1987, Kochel et al. 1987, Nakamura and Swanson 1993, Montgomery et al. 1995, Nanson et al. 1995, Beebe 1997, Bilby and Bisson 1998). But can in-stream WD affect fluvial processes enough to change the morphology of rivers and their floodplains? Although the few geomorphic studies of WD in large forest rivers do indicate that WD can influence large channels and their floodplains (e.g., Veatch 1906, Russell 1909, Guardia 1927, 1933, Triska 1984, Abbe and Montgomery 1996b, Gippel et al. 1996), WD has received little or no attention in fluvial geomorphology text books (e.g., Leopold et al. 1964, Morisawa 1968, Schumm 1977, Richards 1982, Mangelsdorf et al. 1989, Knighton 1998).

Existing models of floodplain and terrace formation imply distinct relationships between the age and elevation of alluvial surfaces. Scroll bar development associated with channel migration results in a lateral sequence of progressively younger surfaces. Overbank sedimentation on bars creates relatively smooth low-relief floodplain surfaces.

Changes in the external boundary conditions, such as climate or tectonics, that are sufficient to alter the river's discharge and sediment regime can lead to channel incision, floodplain abandonment, and terrace formation. Long-term incision can create a sequence of alluvial surfaces with gradients similar to the modern channel and that decrease in age with decreasing elevation. Forests developed on an active floodplain are expected to exhibit distinct lateral age gradients, whereas forests developed on terraces are expected to exhibit age structures that parallel the terrace ages until they become covered by mature forests. In contrast to these expectations, I found quite different patterns in the Queets basin. Here I present evidence for a new model of floodplain and terrace formation unique to forested valleys.

4.2 Study Site

Field surveys were conducted in the 1190 km² Queets River basin on the western slope of the Olympic Mountains to document the geomorphic effects of wood debris accumulation in a relatively pristine river system. The Queets and adjacent Hoh valleys experienced at least 6 alpine glacial advances with the most recent occurring 18,000 yrs BP (Thackray 1996). Glacial till, moraines, outwash and lacustrine sediment associated with these alpine glaciations form high terrace surfaces at least 30 m above the present floodplain (Thackray 1996). However, the west slope of the Olympics was not affected by the continental ice sheet that affected the eastern Olympics and the Puget Sound,

The west slope of the Olympic peninsula has remained forested for at least 17,000 years (Florer 1972, Heusser 1972, 1974, Buckingham et al. 1995, Whitlock 1992). The Queets basin extends from the Pacific Ocean to 2440 m over a distance of about 110 km. Elevations under 1200 m are mantled by dense coniferous forest. The western Olympics have a humid maritime climate and receive precipitation averaging 2.5 m near the Pacific and over 6 m in the headwaters, most of which falls as rain between November and June. The Queets River gaging station (USGS #12040500) is located at river kilometer (RK) 8 and has a catchment of 1153 km². The one-year recurrence peak flow is approximately

1189 cms (42,000 cfs). The maximum discharge on record (1931-1967, 1975-1997) was 3693 cms (130,400 cfs) and occurred on 1/22/31.

Olympic National Park (ONP) encompasses approximately 500 km² of the upper Queets watershed and the river valley to within 12 km of the Pacific Ocean (Figure 4-1). The forest conditions within ONP represent old-growth temperate rain forest unaffected by human disturbance (Henderson et al. 1989, Kirk and Franklin 1992, Buckingham et al. 1995) except for minor forest clearing that occurred in the Queets valley prior to inclusion in the park (Morgan 1955). Upland forest communities are dominated by Sitka Spruce (*Picea sitchensis*), Douglas Fir (*Pseudotsuga menziesii*), Western Hemlock (*Tsuga heterophylla*), and Western Red Cedar (*Thuja plicata*). Floodplain forests of the Queets River are dominated by deciduous hardwoods including Red Alder (*Alnus rubra*), Bigleaf Maple (*Acer macrophyllum*), and Black Cottonwood (*Populus trichocarpa*) less than 100 years old.

4.3 Methods

The mainstem Queets valley can be accessed by vehicles as far as RK 39 (Sam's Creek confluence). Access further upstream is possible only by foot. A trail maintained by ONP allowed rafts to be packed in as far as RK 64. Rafts were used to survey jam and pool frequency between RK 39-64, and to access specific study sites (RK 60-62, RK 54-56, RK 47-51, RK 45-47) along the mainstem river channel. Sites upstream of RK 64 were surveyed by foot. Canoes were used to survey downstream of RK 39. Profiles and cross-sections were surveyed in channels with gradients ranging from 0.001 to 0.25 m/m and widths from 2 to 200 m. Channel morphology ranged from bedrock and boulder-cascade to meandering pool-riffle gravel-bedded channels. The geomorphic effects of individual jams were documented with topographic and surface texture mapping.

Channel planform change and migration rates were investigated using historical and recent maps (GLO 1895, 1901, DNR 1985, 1990, USGS 1933, 1990) and aerial photographs. Maps and images were reproduced at identical scales (1:12,000) and registered to one another using transparent overlays. Changes in channel position from

1932 to 1985 (USGS 1933, 1990) were measured perpendicular to the valley axis at intervals corresponding to $\frac{1}{2}$ the channel's meander wavelength, and recorded with the distance upstream from the Pacific (RK) from recent maps. The difference between channel positions was then divided by the number of years to estimate minimum channel migration rates.

The width of the active channel migration zone within the Queets Valley was delineated using vegetation patterns reflective of fluvial disturbance and topography (map overlays on 1985, 1993, 1997 photos), measured at intervals similar to those used in measuring channel position. For each segment of the river, the recurrence interval for the channel to move across its migration zone was estimated by dividing the width of the active migration zone by the rate of channel migration.

Field observations and literature reviews were used to define different types of WD accumulations and to characterize the processes influencing their formation and geomorphic effects. Low altitude aerial photographs ($\sim 1:12,000$) taken in 1985 (black & white), 1993 (color IR), 1996 (normal color), and 1997 (color IR) were used to support field surveys. Wood debris mapping was done on mylar sheets overlain onto laminated 1993 photos. Jam frequency along the mainstem channel was mapped on 1:12,000 scale sheets with secondary or floodplain channels only mapped at specific sites. Mapping in tributaries and reach study sites were recorded on 1:6000 scale sheets. Numbered aluminum tags were nailed into trees to use as temporary benchmarks at several points along topographic transects so the surveys could be repeated in following years.

Buried WD was identified as part of a buried log jam if the WD was situated within channel deposits or bed material sediments, and therefore assumed to have formed within an active channel. In addition, three or more logs had be observed clearly racked on one another. Once identified, the site location was noted and stratigraphic conditions and log locations were sketched. A small saw was used to cut samples for ^{14}C dating. Samples were taken as small wedges from the log's perimeter to best ensure dates representative of the tree's death and provide a maximum age of when the log was deposited. These samples were then used to estimate a maximum age for the jam. The age of trees growing

above the buried jam was assumed to provide a minimum estimate of the jam's age. Tree age was estimated using standard tree-ring analysis (Phipps 1985). The age of trees too large to core was estimated using age-diameter curves developed from cut logs found along the Queets road and trail, and published age-diameter data for trees in the Queets basin (Van Pelt 1994, Huff 1995) and the adjacent Clearwater basin (Reid 1981). It was not possible to determine whether radiocarbon dates were taken from logs that were incorporated into the jam long after the jam formed or conversely, had already been in the river system long before the jam. To assess this uncertainty, multiple logs were dated for several of the buried jams. Radiocarbon dating of fifty samples was done at the University of Washington Quaternary Research Center Isotope Laboratory. Calibrated ^{14}C dates were estimated using Stuiver and Reimer (1993) and are reported relative to the 1950 NBS standard.

4.4 Floodplain Development

Valley bottoms can be described by the characteristics, or the absence, of three fluvial landforms: (i) unvegetated channel(s) occupying the lower elevations of the valley and frequently inundated, (ii) vegetated floodplain surfaces subject to episodic inundation, and (iii) surfaces above the floodplain, or terraces, that only rarely if ever experience inundation. The longitudinal profiles of these different surfaces are generally assumed to be parallel in a graded river (Mackin, 1948). Surfaces that are not parallel to one another will converge in one direction, a situation that is best illustrated by channels impounded by natural or artificial dams. Alluvial floodplain construction is generally explained by two principal processes: deposition of bars composed of bed load material by a laterally shifting channel, and overbank deposition consisting primarily of fine grained suspended load sediments (Wolman and Leopold 1957, Lewin 1978).

Channel migration analysis indicates the Queets River migrates across its active migration zone at least once every 200 years or less in 65% of the Queets River valley between RK 12-62 (Figure 4-2). Within these reaches, the median recurrence interval of floodplain disturbance is 90 years and the mean is 103 years. Using existing models of

floodplain development and disturbance these rates of channel migration would presumably preclude the development of old-growth forest patches.

Stable log jams create flow obstructions that re-direct flow lines and subsequently the course of a channel (Abbe and Montgomery 1996b). Through this simple process, log jams that may have initiated in the channel thalweg can end up along the channel's margins and eventually become incorporated into the river's floodplain, buried in point bars and mantled by overbank sedimentation and a dense forest cover.

Observations for the Queets River indicate that stable log jams form "hard points" within the channel migration zone, acting like natural revetments that protect patches of the floodplain and riparian forest from disturbance by channel migration. Examination of aerial photographs revealed several sites in the Queets where the river was observed crossing from one side of a jam to the other and back again in less than a decade. Channel migration exposes relic log jams in eroding banks, providing the principal means of finding and sampling log jams. The persistence of log jams was illustrated where relatively young jams remained intact after being re-exposed by the migrating channel and subjected to exceptional flow events.

Consider a bar apex jam formed at the confluence of Sam's River and the Queets shortly before 1975 (Figure 4-3). By deflecting flows around it, the jam quickly became incorporated into a new patch of floodplain mantled with *Alnus rubra*. In the winter of 1996, a peak flow with a recurrence interval of approximately 20 years occurred during which the channel moved from one side of the jam to the other. All trees were eradicated, except those growing on the jam's key member. The key member was unmoved by the flood (Figure 4-3). As a new floodplain forest began to form, the trees growing from this key member had a 20-year advantage.

When this process is repeated to produce different types, ages, and sizes of jams with differing longevities (resilience) within an actively migrating channel, the cumulative result is a complex mosaic of channel and floodplain forest patterns (Figure 4-4). Relict jams, particularly bar apex jams key members, provide a record of previous channel positions (Figure 4-6). The quantity of WD, both as individual tree boles and complete

jams deposited in the river channel can be better appreciated by examining recent floodplains (Figure 4-6). These jams eventually become completely buried in alluvium. Some may wash out when the channel reoccupies an old path, or they may last for centuries.

Fifty ^{14}C dates from wood found in buried jams beneath older forest patches showed that only one was modern; the oldest had a calibrated radio-carbon date of 1295 years BP (665 A.D.). The oldest trees growing on top of these jams were estimated to be about 400 years old (Figure 4-5). Stable WD “hard points” can last for centuries, and thus offer refugia for the development of old-growth forest patches. These old-growth forest patches provide a source of key members necessary to form stable jams. The persistence of these hard points increases the life expectancy of trees growing above them and in some cases leads to forest patches that are several hundred years older than the surrounding floodplain forest. This process is quite different from existing models of floodplain formation, which rely on external changes to the fluvial system to explain elevated surfaces such as rapid aggradation due to an increase in sediment supply, tectonic forcing or channel incision. Such explanations may not always apply in forested systems where WD accumulations alone are sufficient to explain channel and floodplain patterns and terrace development.

4.5 Terrace Development

Terraces form when a channel incises to the extent that it abandons its floodplain. Terraces are thought to form when external processes such as climate, tectonics, or human disturbance alter the fluvial regime sufficiently to initiate a period of either incision or aggradation. Terrace profiles usually parallel that of the river. Terraces with different elevations are generally assumed to be of different ages, with older terraces at higher elevations. Terrace profiles deviating from those of young surfaces usually are attributed to glacial features, major channel impoundments (upstream of moraines or landslides), or tectonic influences. I found both these assumptions to be incorrect when used to interpret alluvial terrace surfaces in the Queets basin.

Several unique aspects of alluvial terraces were found in the Queets system. Terrace surfaces consisted of both sand, typical of modern overbank deposition on floodplains of the Queets, and imbricated coarse gravel and cobbles representative of the active river bed. Historical analyses revealed some of these surfaces were quite recent, yet were located well above the present channel. The 1901 channel at RK 45 (RM 28) identified in Figure 4-6 is situated 2.5 m above the 1995 floodplain. Terrace-like surfaces are not confined to the margins of the Queets valley, but frequently occur as islands, often coincident with old growth forest patches. But since log jams periodically become so numerous or massive that they impound the entire river, new fill terraces are formed that can bury not only the active floodplain, but some terraces as well.

Recent channel aggradation upstream of a valley jam complex, (Queets RK 70, A = 98 km²) buried a 3000 m² patch of 200-300 (1.75-2.5 m DBH) year old *Picea sitchensis*, which I assumed had been growing on a floodplain or terrace. The trees were buried by 100-150 cm of coarse gravel that thinned upstream and was overlain by about 40 cm of sand. A small forest of snags was left protruding from a 15 year old forest of *Alnus rubra* that colonized the aggraded surface.

The stratigraphy of alluvial banks along the Queets is rarely continuous over more than a few hundred meters, consistent with the patchwork mosaic of floodplain development associated with log jams. The most consistent stratigraphy and sedimentology characteristics of alluvial banks along the Queets were deposits of imbricated gravels that thicken downstream, and are mantled by a relatively uniform deposit of sand. These deposits are identical to those from upstream of log jams, such as those surveyed in Alta Creek (Figure 4-7). These surface and subsurface dating and stratigraphic observations indicate that alluvial surfaces within 20 m of the active floodplain are Holocene fill-terraces.

I observed significant changes in channel profiles in just one year. Throughout the Queets River, channel beds aggraded upstream of large WD accumulations obstructing large portions of the channel. The effects of wood debris jams on channel aggradation were most dramatic in the steeper tributaries surveyed, where the valley jams formed

channel spanning obstructions. In confined reaches with gradients up to 0.24 m/m, valley jams elevated the channel up to 11 meters, transforming a reach from a boulder cascade-bedrock channel into a step-pool and pool-riffle channel.

When a valley jam forms in an alluvial channel, some of the flow is deflected into adjacent banks. Bank erosion introduces more trees to the channel along the axis of the jam (tree boles all tend to be perpendicular to channel). Through this process, a jam can grow to become several times the channel's original width, sometimes creating a massive WD structure extending the entire width of the valley bottom (i.e., "valley jam" described in chapter 1). These valley jams create large sediment and debris reservoirs and elevate large sections of the channel bed allowing relatively low magnitude flows to inundate terraces which previously were unlikely to be inundated. A terrace along Alta Creek was over 2 meters above the channel in 1993. In 1994 the bed was elevated to as much as one meter above the terrace surface, and bed material from the creek was actively being deposited on the terrace surface and burying the trunks of 200-400 year old trees (Figure 4-7).

Even in large alluvial pool-riffle channels, WD accumulations can obstruct enough of the valley floor to cause significant backwater that can also aggrade the channel. Aggradation rates of 1.5 m/year were documented at two sites along the mainstem Queets between 1993 and 1996. In particular, channel gradients changed from 0.031 to 0.0008, and 0.011 to 0.0006 along a 500 m profile at each site. At each of these mainstem sites, the river split into a system of distributary channels occupying a wider portion of the valley bottom that reached a maximum width coincident with maximum WD loading. Reductions in gradient and increases in roughness were sufficient to transform coarse cobble-bedded channels into sand-bedded channels. These valley jam complexes were composed of individual log jams that coalesced to form a complex up to 450 m in width, and 200 m in length. One mainstem valley jam complex consisted of a single large flow deflection jam and several bar apex jams. Another consisted of at least 6 small valley jams, each impounding distributary channels and several dozen bank input jams. Within and upstream of these valley jam complexes, I found large areas where established floodplain forests

were being buried. WD jam complexes affecting floodplain development were found as far downstream as the ONP boundary (RK 12.5-15.0, upstream of Clearwater River confluence), where the mainstem channel has an average bankfull width of about 110 m and depth of approximately 3.1 m. Reductions in gradient and increases in roughness were sufficient to transform coarse cobble-bedded channels into sand-bedded channels.

The most dramatic example of a fill terrace terminating above a buried log jam was found along the lower Queets (RK 26), with an upstream catchment area of 556 km². The buried jam was distributed through a 8m vertical section of imbricated gravel mantled by less than 10 cm of sand (Figure 4-8). The 1500 m² of terrace surface remaining at this site was horizontal, and covered with trees 250 to 300 years old (2-2.5 DBH). Calibrated ¹⁴C dates for five of the logs in this buried jam ranged from 600 to 900 years BP.

Existing models of terrace formation require a change in climate, baselevel (tectonic) or major disturbance such as landsliding or human actions. Terrace-like surfaces attributed to local disturbance in a watershed, such as large magnitude flood events or changes in sediment supply can occur, features referred to by Bull (1991) as dynamic response terraces. No exceptional peak flows occurred between 1993-1995 in the Queets. The channel aggradation illustrated in Figure 4-7 occurred between 10/93 and 7/94. The maximum peak flow at the Queets gaging station during this period had a recurrence interval of less than 2 years. It is possible forest fires may periodically increase sediment supply locally, but fires in the Queets basin have been small and infrequent throughout much of the Holocene (Huff 1995). Since over 90% of a tree's bole mass remains even after a catastrophic fire, any fire-related disturbance introducing large amounts of sediment to the channel are likely to also introduce large amounts of WD.

On longer time-scales, climate and forest cover of the Western Olympics has been stable throughout the Holocene (Crandell 1965, Florer 1972, Huesser 1972, 1974, Thackray 1996, Greenwald 1997). Interpretations that terrace surfaces approximately 20 m above the current channel are Late Pleistocene or early Holocene (Fonda 1974, Thackray 1996) conflict with evidence presented by Greenwald (1997) that a 20.7 m terrace along the Queets is no older than 5000 years. Descriptions of sediment core

stratigraphy and radiocarbon dating of alluvial surfaces within 8 m of the river found in this study are consistent with those of Greenwald (1997). Observations that terraces are currently forming in the Queets, sometimes at rates of several meters annually, show no relationship with either co-seismic subsidence or long-term uplift of the Olympic Peninsula.

Wood debris jams can episodically raise a channel and floodplain sufficiently to create fill terraces at least 10 m high, and possibly twice that height. In addition, terraces associated with WD jams tend to have lower gradients than the active channel. This process offers one explanation of why some terrace surfaces can have younger forests than lower lying alluvial surfaces.

4.6 Complementary Evidence of Historical Observation

Historical references describe the widespread occurrence of wood debris in rivers flowing through forest wilderness in very different physiographic regions of North America. Some scholars and naturalists of the late nineteenth and early twentieth centuries described or alluded to valley-scale alluvial landforms developing entirely due to the presence of wood debris accumulations (Veatch 1906, Russell 1909, Guardia 1927). Sediment storage behind WD accumulations was clearly illustrated in the channel and landscape changes that followed WD removal, such as incision of the Red River of Louisiana (Harvey et al. 1988) and the progradation of the Colorado River delta in Texas (Kanes 1970, Hartopo 1991). John Muir (1878) attributed the development of terraced wetlands and floodplains in steep headwater channels of the southern Sierra Nevada entirely to impoundments by fallen Sequoia trees (*Sequoia gigantea*). Early European settlers colonizing forested river valleys in western Washington reported that the frequency and magnitude of inundation was dramatically reduced simply by removing log jams, opening up thousands of square kilometers to settlement (Shoecraft 1875, Department of War 1883-84, 1898). In addition, the stratigraphy and sedimentology observed in the Queets is similar to fluvial sequences associated with uranium ores, in which fossilized deposits of channel logs thicken downstream terminating in large accumulations of logs and organics (McKelvey 1955).

During the last two hundred years, humans have dramatically reduced the quantity of wood debris in fluvial systems by direct removal of tens of thousands of snags (e.g. Ruffner 1886, Shields and Nunnally 1984, Sedell and Frogatt 1984, Gippel et al. 1996), and by eliminating both the recruitment processes (i.e., limiting channel migration) and the source of large riparian trees (e.g., Swift 1984, Mancini 1989, Malanson 1993, Goodwin et al. 1997). In the nineteenth and early twentieth centuries it was widely reported that wood debris played a principle role in the channel and floodplain development of some forest rivers (e.g., Lyell 1830, Davis 1901, Russell 1909). These interpretations may have been due to the ubiquitous and prodigious quantity of WD still found in North American rivers at the time, rather than detailed research, which was scarce at best (e.g. Veatch 1906, Guardia 1927, 1933). Conversely, the near-disappearance of WD from thousands of rivers in the last century may account for its absence in preeminent contemporary textbooks on fluvial geomorphology (e.g., Leopold et al. 1964, Schumm 1977, Richards 1982, Knighton 1998).

4.7 Conclusions

Observations of a relatively pristine forest river system offer compelling evidence that forests, by contributing large wood debris to the channel, can have fundamental effects on the development and morphology of the channel, floodplain, and floodplain forest. Stable log jams can create sites of floodplain refugia by providing an underlying foundation sufficient to withstand repeated assaults by the channel that erode and re-initiate the surrounding terrain. Natural log jams form alluvial "hard points" that allow the forest patches to attain ages otherwise improbable given the frequency with which the floodplain is recycled by channel migration. These patches of old growth in turn provide the large trees necessary to form stable log jams. Log jams can increase the distribution of ages, elevations, and patterns of alluvial surfaces and the overlying forest structure that form the floodplain.

The formation of stable in-stream wood debris accumulations can obstruct, retard and impound flow, thereby altering the planform and profile characteristics sufficiently to

influence floodplain and terrace development. Depositional surfaces arising from the presence of wood debris accumulations have lower slopes and diverge from the active floodplain surface as one moves downstream. A complex mosaic of alluvial surfaces differing in elevation greater than 10 m and with variable gradients can be created without any change in climate, base level, or sediment supply, but simply through temporal and spatial variations in the quantity and structure of wood debris within an active channel.

This new model demonstrates how WD can control floodplain and terrace formation, creating a complex mosaic of alluvial surfaces, channels, and forest patches that form a patchwork mosaic floodplain. In the Queets Valley, terrace-like landforms continue to form and be “re-activated;” they represent the magnitude of floodplain relief which can be attained in forested valleys due to wood loading in the channel. If the natural WD supply and its recruitment processes are not altered, these “terraces” may more accurately describe the magnitude to which floodplain surfaces can fluctuate in a forested environment. Human activities that reduce the size and number of trees that would otherwise enter a river system can result in irreversible incision and the loss of large areas of fluvial habitat.

These findings illustrate the need for care in interpreting the causal forces of alluvial terraces in forested environments, as well as in interpretations of fluvial sequences in the geologic record, particularly after forests first appeared in the Devonian, over 350 million years ago. Stratigraphic patterns observed in fluvial deposits that have been interpreted as climate fluctuations simply may be the result, in part, of logs jams.

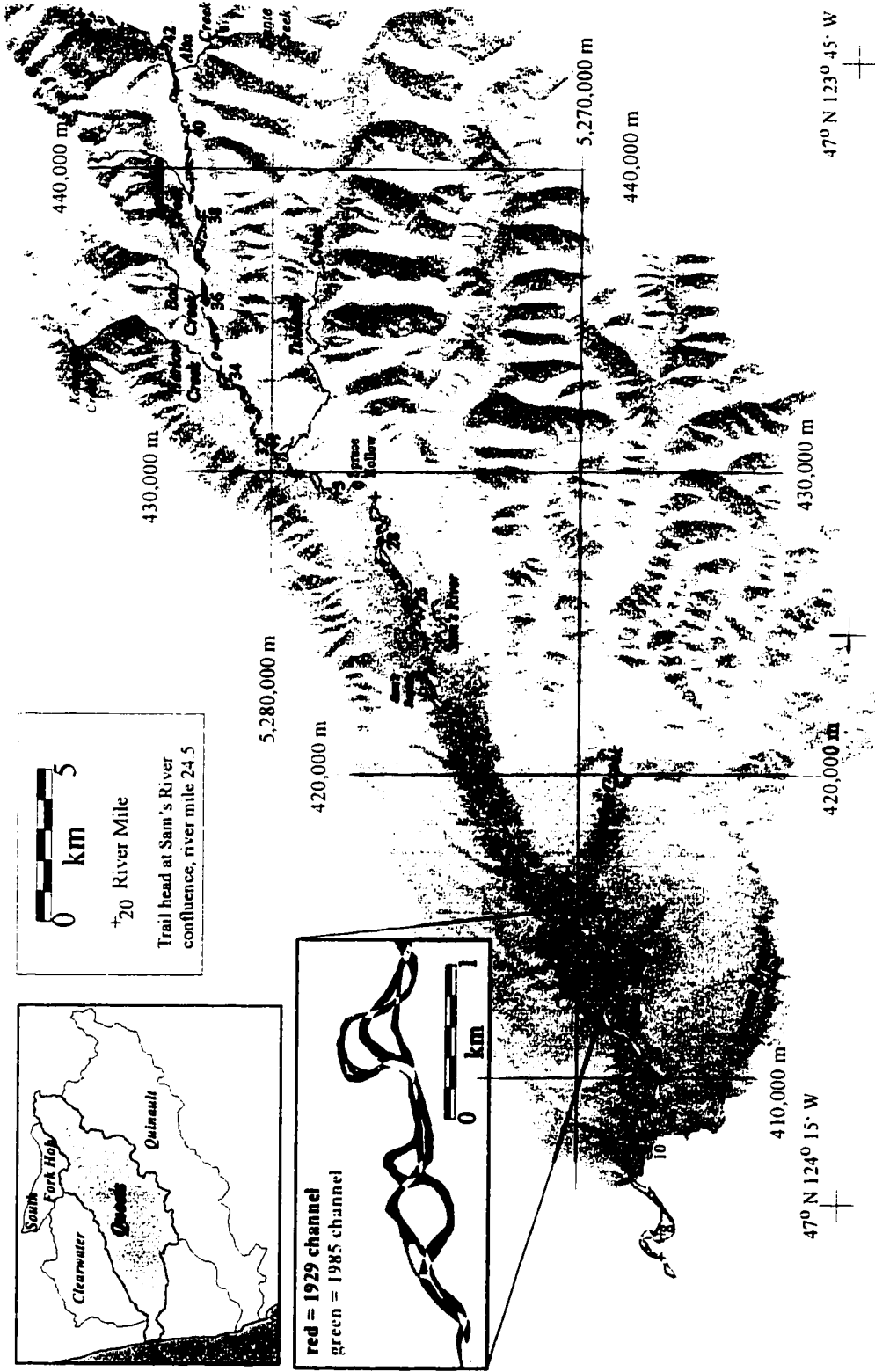


Figure 4-1. Drainage basins of Queets River drainage basin and adjacent catchments, southwestern portion of the Olympic Peninsula. Along the most of its length, the Queets River channel actively migrates across its valley, portrayed by the river's position in 1932 and 1985.

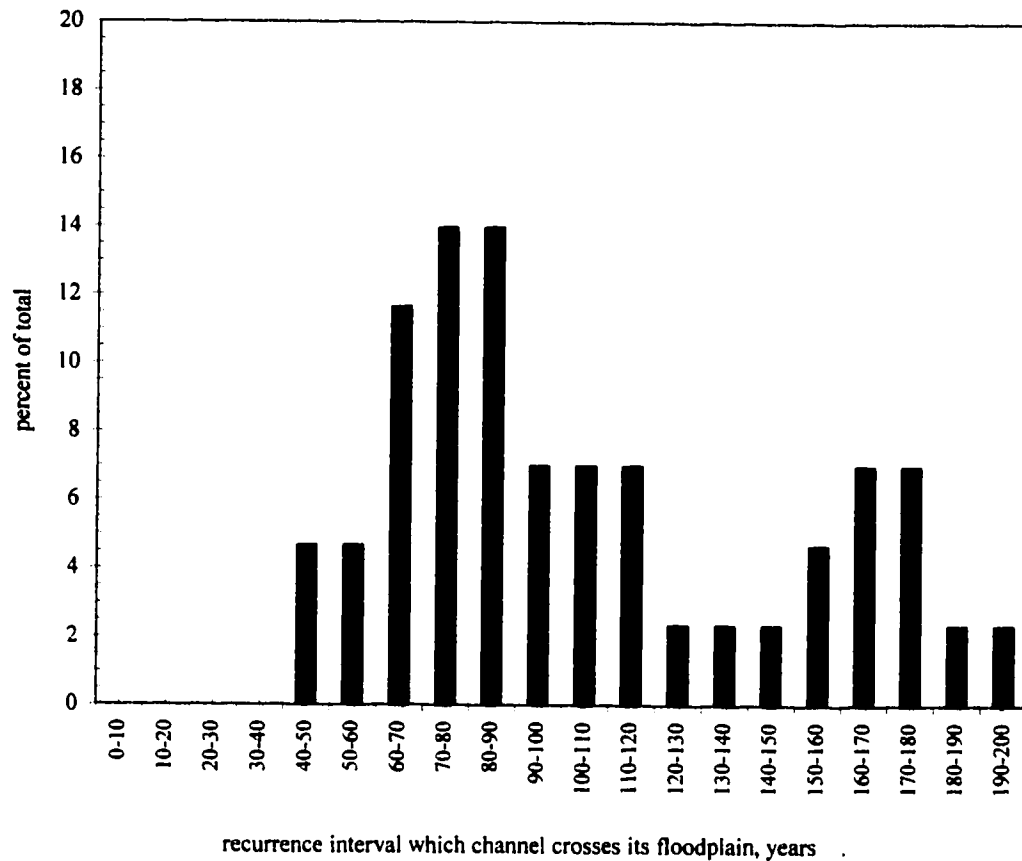


Figure 4-2. Distribution of recurrence intervals which the Queets River moves across its floodplain over approximately 65% of the river's length from RM 7.5 to 38.5 (RK 12- 62), drainage areas ranging from 673 to 137 km², respectively. Within these reaches, the Queets River moves across its floodplain in 200 years or less. The mean and median time it takes the river to recycle its floodplain within these reaches are 103 and 90 years, respectively.

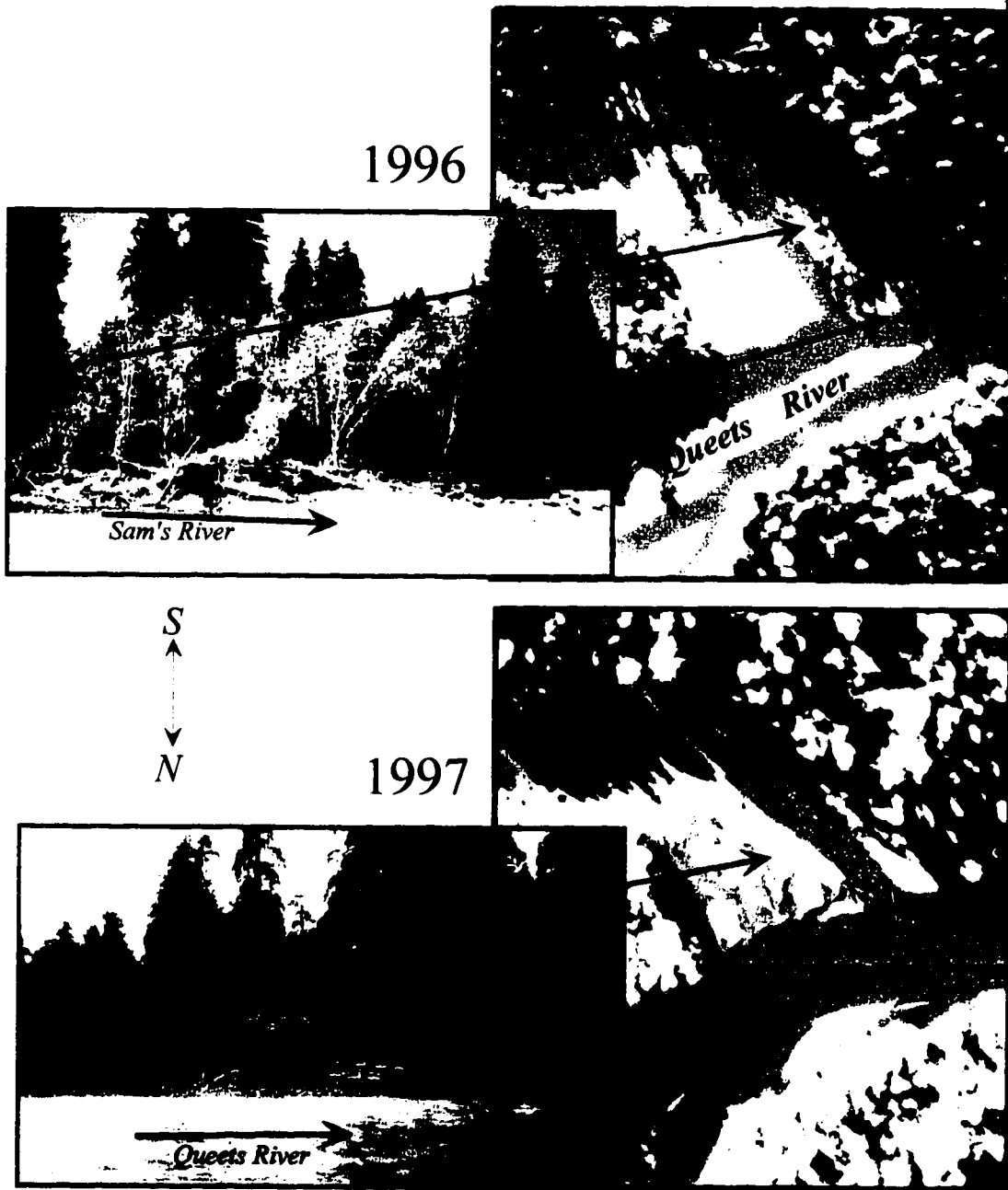


Figure 4-3. Bar Apex jam in Queets River at Sam's River confluence, Queets RM 24.6 (RK 39.6). Drainage area at site is 410 km².

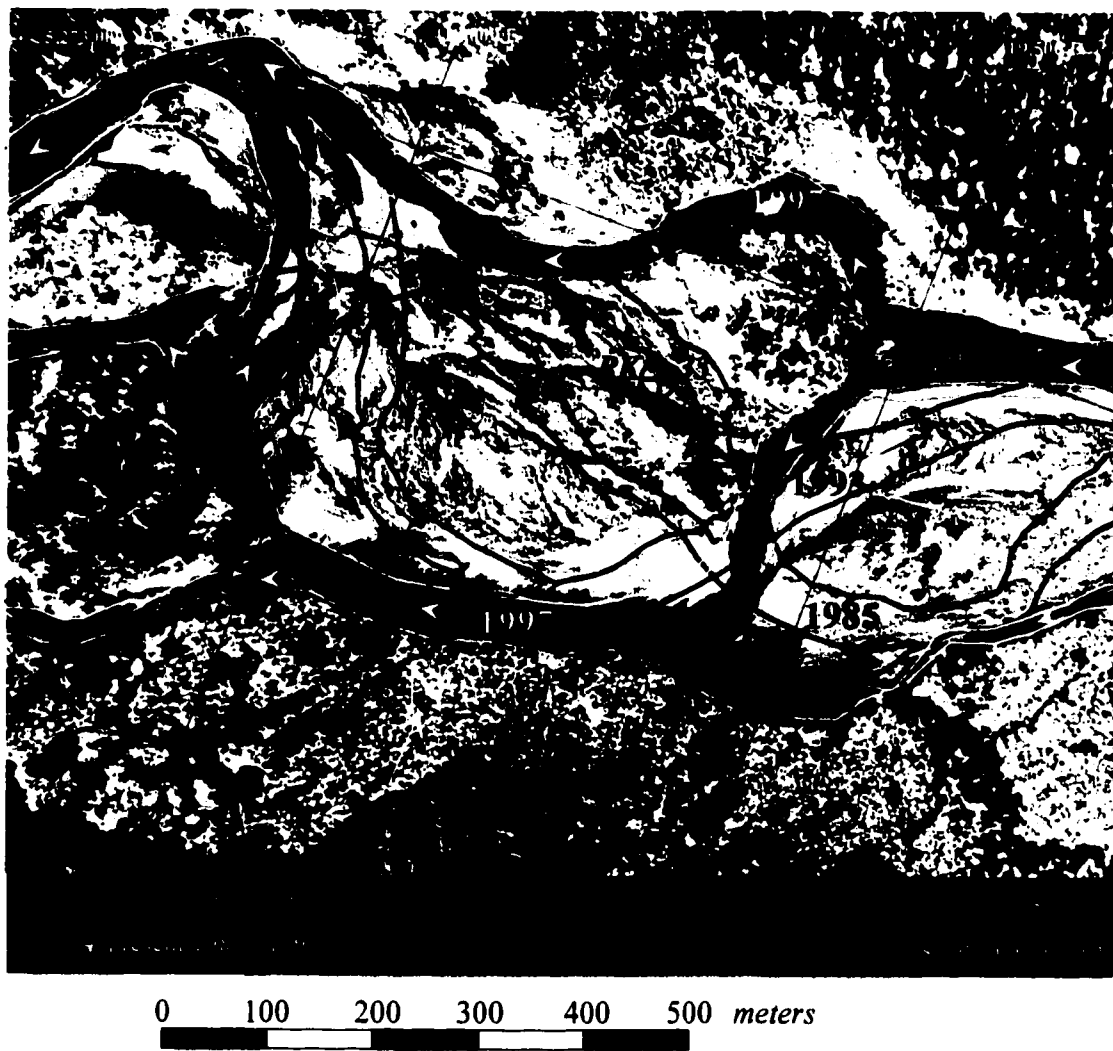


Figure 4-4. Floodplain channel and forest patch mosaic along Queets River mainstem channel, RM 20.2 (RK 32.5). Drainage area at site is approximately 435 km².

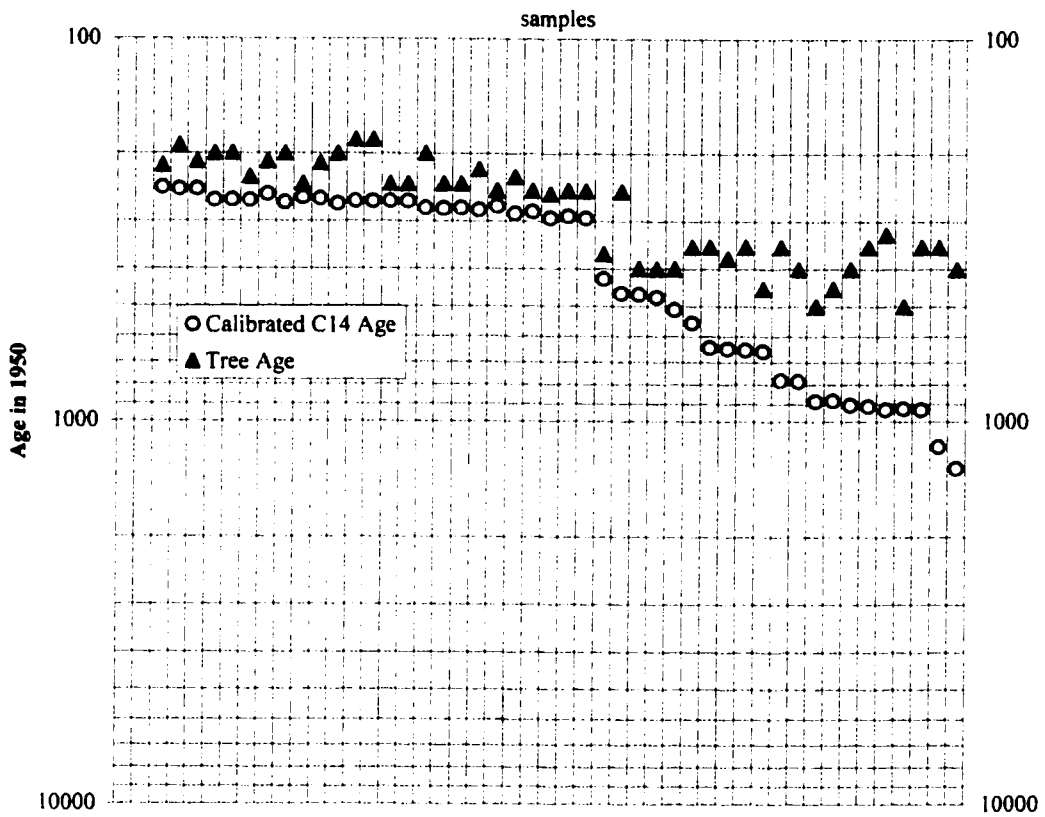


Figure 4-5. Calibrated radiocarbon dates and tree ages for buried jams distributed throughout the Queets River network.



Figure 4-6. Map illustrating positions of mainstem Queets River channel, recent wood debris accumulations, and relic jams in reach extending from RM 28.3-29.0 (RK 45.6-47). Coarse channel cobbles in abandoned positions of 1932 channel indicate the river bed was about 2.6-3.0 m higher than its current elevation. Note coincidence of old-growth forest patches above buried log jams, of which had wood over 1000 years old.

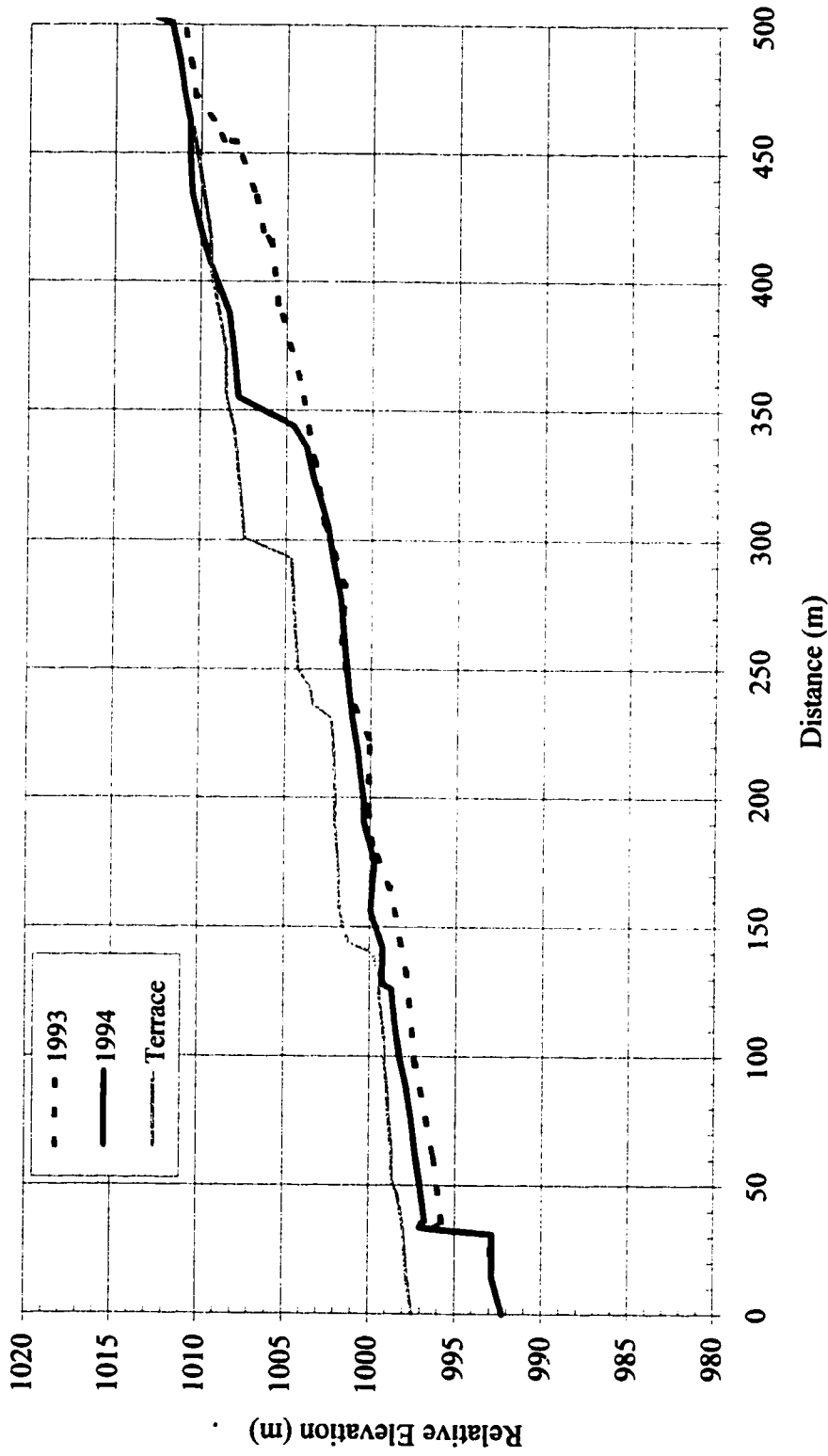
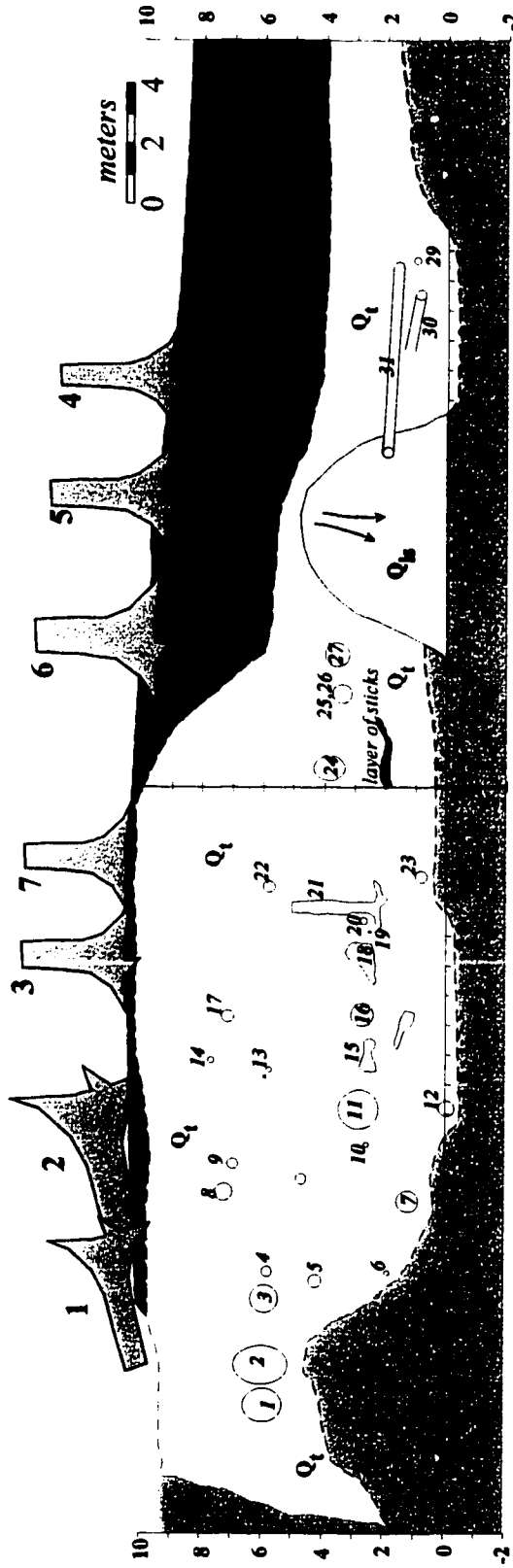


Figure 4-7. Channel profiles of Alta Creek in 1993 and 1994 showing aggradation upstream of valley jams. The profile of the terrace along the channel's eastern margin (river right bank) is also plotted (surveyed in 1994). Note the step-like form of the profiles created by the wood debris jams that results in surfaces that converge upstream and clearly evident in terrace profile. This profile morphology is most pronounced in smaller channels such as Alta (drainage area of about 23 km²), but identical patterns were found throughout the Queets River basin.

Minimum age of terrace surface trees approximately 250 yrs b.p.



Buried log jam, Queets River, River Km 25.76, river left (South) bank exposure September 1995.

	Calibrated 14C dates:	Trees growing on terrace:
	log # years b.p. log diameter (m)	tree # species diameter (m)
- recent landslide	8 = 642 yrs b.p. 0.58	1 <i>Tsuga heterophylla</i> 1.18
- imbricated gravels and cobbles	11 = 782 yrs b.p. 1.32	2 <i>Picea sitchensis</i> 2.05
- lacustrine clays (Pleistocene)	12 = 1161 yrs b.p. 0.52	3 <i>Tsuga heterophylla</i> 1.13
	23 = 912 yrs b.p. 0.40	4 <i>Tsuga heterophylla</i> 1.12
	26 = 931 yrs b.p. 0.63	5 <i>Pseudotsuga menziesii</i> 1.63
		6 <i>Picea sitchensis</i> 2.31
		7 <i>Picea sitchensis</i> 0.76

Figure 4-8. Large buried log jam beneath 8 m terrace adjacent to Queets River at RM 16 (RK 25.8). The remaining terrace surface had a slope of approximately 0.0003, compared to the active river's slope of 0.0025. Drainage area at site is approximately 552 km².

List of References

- Abbe, T.B. and D.R. Montgomery. 1996a. Flood-plain and terrace formation in forested landscapes. Geological Society of America Abstracts with Programs, Cordilleran Section 28(5), 41.
- Abbe, T.B. and D.R. Montgomery. 1996b. Large woody debris jams, channel hydraulics, and habitat formation in large rivers. *Regulated Rivers: Research and Management* 12, 201-221.
- Abbe, T.B., D.R. Montgomery, K. Fetherston, and E.M. McClure. 1993. A process-based classification of woody debris in a fluvial network: preliminary analysis of the Queets River, WA. *EOS, Transactions of the American Geophysical Union* 73(43), 296.
- Abbe, T.B., D.R. Montgomery, and C. Petroff. 1997. Design of stable in-channel wood debris structures for bank protection and habitat restoration: an example from the Cowlitz River, WA. In Wang, C.C., E.J. Langendoen, and F.D. Shields (Editors). *Proceedings of the Conference on Management of Landscapes Disturbed by Channel Incision*. Univ. of Mississippi. Oxford, MI. 809-814.
- Agee, J.K. 1988. *Streamside Man. Ripar. Wild. and For. Interaction*, Contrib. No.59, College For. Resources, Univ. WA, Seattle.
- Allen, J.R.L. 1985. *Principles of Physical Sedimentology*. Chapman & Hill. London.
- Armstrong, F.H. and J.G. Savory. 1959. The influence of fungal decay on the properties of timber. *Holzforschung* 13.
- Baker, C.J. 1979. The laminar horseshoe vortex. *Journal of Fluid Mechanics* 95, 347-367.
- Bearman, P.W. and T. Morel. 1984. Effect of free stream turbulence on the flow around bluff bodies. *Progress in Aerospace Science* 20, 97-123.
- Becker, B. and W. Schirmer. 1977. Palaeoecological study on the Holocene valley development of the River Main, southern Germany, *Boreas*, 4, 303-321.
- Beebe, J. T. 1997. Fluid patterns, sediment pathways and woody obstructions in the Pine River, Angus, Ontario. Unpubl. PhD. dissertation. Department of Geography and Environmental Studies, Wilfrid Laurier University. Waterloo, Ontario, Canada.
- Benda, L. 1990. The influence of debris flow on channels and valley floors in the Oregon Coast Range, U.S.A., *Earth Surface Processes and Landforms*, 15, 457-466.

- Benke, A.C. 1990. A perspective on America's vanishing streams. *Journal of North American Benthological Society* 9, 77-88.
- Best 1996. The fluid dynamics of small-scale alluvial bedforms. In Carling, P.A. and Dawson, M.R. (Editors). *Advances in Fluvial Dynamics and Stratigraphy*. John Wiley & Sons, New York, 67-126.
- Biging, G. S. 1984. Taper equations for second-growth mixed conifers of Northern California. *Forest Science* 30, 1103-1117.
- Bilby, R.E. 1979. The function and distribution of organic debris dams in forest stream ecosystems. Unpublished Ph.D. dissertation. Cornell Univ. Ithaca, NY.
- Bilby, R.E. and P.A. Bisson. 1998. Function and distribution of large woody debris. In R. Naiman and R.E. Bilby, Editors. *River Ecology and Management Lessons from the Pacific Coastal Ecoregion*. Springer-Verlag. New York, 324-346.
- Bilby, R.E. and J. W. Ward. 1989. Changes in characteristics and function of woody debris with increasing size of streams in Western Washington. *Transactions of the American Fisheries Society*, 118, 368-378.
- Bisson, P.A., R.E. Bilby, M.D. Bryant, C.A. Dolloff, G.B. Grette, R.A. House, M.L. Murphy, K.V. Koski, and J.R. Sedell. 1987. Large woody debris in forested streams in the Pacific Northwest: past, present, and future. In Salo, E.O. and T.W. Cundy (Eds.), *Streamside Management: Forestry and Fishery Interactions*. University of Washington Institute of Forest Resources Contribution No.57, Seattle, Washington, 143-190.
- Bohannon, B. 1966. Effect of size on bending strength of wood members. *Forest Products Laboratory. Research Paper FPL-56*. U.S. Department of Agriculture.
- Braudrick, C. , G. Grant, Y. Ishikawa, and H. Ikeda. 1997. Dynamics of wood transport in streams: a flume experiment. *Earth Surface Processes and Landforms*, 22, 669-683.
- Bravery, A. F. and G. H. Lavers. 1971. Strength properties of decayed softwood measured on miniature test beams. *International Biodeterioration Bulletin*, 7.
- Bruce, D. 1982. Butt log volume estimators. *Forest Science* 28, 489-503.
- Bruce, D., R. O. Curtis, and C. Vancoevering. 1968. Development of a system of taper and volume tables for Red Alder. *Forest Science* 14, 339-350.

- Bryant, M.D. 1980. Evolution of large, organic debris after timber harvest: Maybeso Creek, 1949 to 1978. General Technical Report PNW-101. U.S. D. A. Forest Service, Pacific Northwest Forest and Range Experiment Station, Portland, OR.
- Buckingham, N.M., J.E. Burger, T.N. Kaye, E.G. Schreiner, and E.L. Tisch. 1995. Flora of the Olympic Peninsula. Northwest Interpretive Association. Seattle, WA.
- Buffington, J.M. 1995. Effects of hydraulic roughness and sediment supply on surface textures of gravel-bedded rivers. Unpublished M.S. thesis. University of Washington, Seattle, Washington.
- Buffington, J.M. and D. R. Montgomery. 1997. A systematic analysis of eight decades of incipient motion studies, with special reference to gravel bedded rivers. *Water Resources Research* 33, 1993-2029.
- Bull, W.B. 1991. Geomorphic responses to climatic change. Oxford University Press. New York, NY. 326.
- CABO. 1989. CABO one and two family dwelling code. Council of American Building Officials. Falls Church, VA.
- Ceylonese, P., S.P. Cline, T. Veshoeven, D. Sachs, and G. Spycher. 1987. *Can. Journal. For. Res.* 17, 1585-1595.
- Chang, F.M. and H.W. Shen. 1979. Debris problems in the river environment. Federal Highway Administration Report No. FHWA-RD-79-62, 71.
- Chow, V.T. 1959. Open-Channel Hydraulics. McGraw-Hill. New York, New York.
- Church, M. 1992. Channel morphology and typology. In P. Calow and G.E. Petts, Editors. *The Rivers Handbook*. Blackwell Scientific Publications, Oxford, 126-143.
- Clay, C. 1949. The Colorado River Raft. *The Southwestern Historical Quarterly*, Vol. 102 (4), 400-426.
- Coho, C. and S.J. Burges. 1994. Dam-break floods in low order mountain channels of the Pacific Northwest. Water Resources Series Technical Report No.138. Department of Civil Engineering, University of Washington, Seattle, WA.
- Costa, J.E. and Schuster, R.L. 1988. The formation and failure of natural dams. *Geological Society of America Bulletin* 100, 1054-1068.

- Crandell, D.R. 1965. The glacial history of western Washington and Oregon. In Wright, H.E. Jr. and D.G. Frey (Eds.), *The Quaternary of the United States*. Princeton University Press, Princeton, New Jersey, 341-353.
- Dacy, G.H. 1921. Pulling the Mississippi's Teeth. *Scientific American*, Vol. 75(4), 60,70.
- D'Aoust, S.G. and R.G. Millar. 1999. Large woody debris fish habitat structure performance and ballasting requirements. Province of British Columbia, Ministry of Environment, Lands and Parks and Ministry of Forests. Watershed Restoration Management Report No.8.
- Davis, W.M. 1901. *Physical Geography*. Boston. Ginn & Company.
- Deane, W. 1888. A New Hampshire log-jam. *New England Magazine*, 30, 97-103.
- Department of War. 1883-84. Report of the Chief of Engineers, Vol.2, Part 1, in House Executive Documents, Vol.5, 2nd session, 48th Congress. U.S. Government Printing Office. Washington, D.C.
- Department of War. 1898. Survey of Skagit River from its mouth to Sedro, Washington. Letter from the Acting Secretary of War and Chief of Engineers, U.S. Army. United States House of Representatives Document No. 204. 55th Congress, 2nd Session. Washington D.C.
- Diehl, T. 1997a. Drift in channelized streams. In S.S.Y. Wang, E.J. Langendoen, and F.D. Shields, Jr., Editors. *Proceedings of the Conference on Management of landscapes disturbed by channel incision*. University of Mississippi, 139-143.
- Diehl, T. 1997b. Potential drift accumulation at bridges. Federal Highway Administration Report FHWA-RD-97-028. Washington D.C.
- Dorsey, F.L. 1941. *Master of the Mississippi*. The Riverside Press. Cambridge.
- Eckerle, W.A. and L.S. Langston. 1986. Horseshoe vortex formation around a cylinder. *American Society of Mechanical Engineering Paper No. 86-GT-246*.
- Everitt, B.L. 1968. Use of cottonwood in an investigation of the recent history of a flood plain, *Am. Jour. Science* 266, 417-439.
- Fahnestock, R. K. 1963. Morphology and hydrology of a glacial stream - White River, Mount Rainier, Washington. U.S. Geological Survey Professional Paper 422A.

- Ferguson, R. I., K. L. Prestegard, and P. J. Ashworth. 1989. Influence of sand or hydraulics and gravel transport in a braided gravel bed river. *Water Resources Research*, 25, 635-643.
- Ferro, V. and G. Giordano. 1992. Experimental study of flow resistance in gravel-bed rivers. *Journal of Hydraulic Engineering*, 117(10), 1239-1246.
- Fetherston, K. L., R.J. Naiman, and R.E. Bilby. 1995. Large woody debris, physical process, and riparian forest development in montane river networks of the Pacific Northwest. *Geomorphology* 13, 133-144
- Florer, L.E. 1972. Quaternary paleoecology and stratigraphy of the sea cliffs, western Olympic Peninsula, Washington. *Quaternary Research*, 2, 202-216.
- Fonda, R.W., 1974, Forest succession in relation to river terrace development in Olympic National Park, Washington, *Ecology*, 55(5), 927-942.
- Foreman, G. 1928. River navigation in the early southwest. *The Mississippi Valley Historical Review*, 15(1), 34-55.
- Franklin, J.F. and C.T. Dyrness. 1988. *The Natural Vegetation of Oregon and Washington*. Oregon State University Press, Corvallis, Oregon.
- Franklin, J.F. and M.A. Hemstrom. 1981. Aspects of succession in the coniferous forests of the Pacific Northwest. In D.C. West, H.H. Shugart, and D.B. Botkin, Editors. *Forest Succession: Concepts and Application*, Springer-Verlag, New York, 212-229.
- Franklin, J.F. and R.H. Waring. 1979. Distinctive features of the Northwest coniferous forest: development, structure, and function. In R.H. Waring, Editor. *Forests: Fresh Perspectives from Ecosystem Analysis*. Proceedings of the 40th Annual Biology Colloquium. Oregon State Univ. Press, Corvallis, OR, 59-85.
- French, R.H. 1985. *Open-Channel Hydraulics*. McGraw-Hill Book Co., New York.
- Garay, L. 1979. *A Tree Taper Model for the Entire Stem Profile Including Buttressing*. Institute of Forest Products. Tropical Forest Utilization System Research Report Contribution No. 36. University of Washington.
- Garfinkel, G. 1973. *Wood Engineering*. Southern Forest Products Association. New Orleans, LA. 201-209.

- Gillespie, Maj. G.L. 1881. Report of the Chief of Engineers, U.S. Army. Appendix OO 10, 2603-2605.
- Gippel, C.J., I.C. O'Neill and B.L. Finlayson. 1992. The Hydraulic Basis of Snag Management. Centre for Environmental Applied Hydrology, Department of Civil and Agricultural Engineering, University of Melbourne, Victoria, Australia.
- Gippel, C.J., I.C. O'Neill, and B.L. Finlayson. 1996. Distribution and hydraulic significance of large woody debris in a lowland Australian River. *Hydrobiologia*, 318, 179-194.
- Goodwin, C.N., Hawkins, C.P., and Kershner, J.L. 1997. Riparian restoration in the Western United States: overview and perspective. *Restoration Ecology* 5, 4-14.
- Gray, H. R. 1956. The Form and Taper of Forest Tree Stems. Imperial Forestry Institute Paper 32. Oxford University.
- Green, W.N. 1982. Midchannel islands: sedimentology, physiography, and effects on channel morphology in selected streams of the Great Bend Region of the Wabash Valley. Unpublished M.S. Thesis, Purdue University, Indiana.
- Greenwald, D.N. 1997. A 5,000 year record of disturbance and vegetation change in riparian forests of the Queets River, Washington. Unpubl. M.S. thesis. College of Forest Resources. University of Washington. Seattle, WA.
- Gregory, K.J. and R.J. Davis. 1992. Coarse woody debris in stream channels in relation to river channel management in woodland areas. *Regulated Rivers: Research & Management*, 7, 117-136.
- Gregory, K.J., A.M. Gurnell, and C.T. Hill. 1985. The permanence of debris dams related to river channel processes. *Journal of Hydrological Sciences*, 30, 371-381.
- Grette, G.B. 1985. The abundance and role of large organic debris in juvenile salmonid habitat streams in second growth and unlogged forests. M.S. thesis. University of Washington. Seattle, WA.
- Guardia, J. E. 1927. Successive human adjustments to raft conditions in lower Red River valley. Unpubl. M.S. thesis. University of Chicago. Chicago, Illinois.
- Guardia, J. E. 1933. Some results of the log jams in the Red River. *The Bulletin of the Geographical Society of Philadelphia* 31(3), 103-114.
- Gurnell, A. 1997. The hydrological and geomorphological significance of forested floodplains. *Global Ecology and Biogeography Letters* 6(3-4), 219-229.

- Haas, A.D. 1996. Coarse sediment storage by large woody debris in small, steep streams of the North Cascades. Unpublished Senior Thesis. University of Washington, Seattle, WA.
- Habersham, R. A. 1881. Report of the Chief of Engineers, U.S. Army. Appendix OO 10, 2605-2607. U.S. Government Publication Office, Washington D.C.
- Hardie, K. 1980. A review of strength testing as a measure of biodeterioration of wood and wood based materials. *International Biodeterioration Bulletin*, 16, 1-8.
- Harmon, M.F., J.F. Franklin, F.J. Swanson, P. Sollins, S.V. Gregory, J.D. Lattin, N.H. Anderson, S.P. Cine, N.G. Aumen, J.R. Sedell, G.W. Lienkaemper, K. Cromack, Jr., and K.W. Cummins. 1986. Ecology of coarse woody debris in temperate ecosystems. *Advances in Ecological Research*, 15, 133-302.
- Harmon, M. E. and J. Sexton. 1995. Water balance of conifer logs in early stages of decomposition. *Plant and Soil* 172, 141-152.
- Hartopo. 1991. The effect of raft removal and dam construction on the Lower Colorado River, Texas. Unpublished M.S. Thesis, Texas A & M Univ.
- Harvey, M.D, D.S. Biedenharn, and P. Combs. 1988. Adjustments of Red River following removal of the Great Raft in 1873 [abs.]. *EOS (Transactions of the American Geophysical Union)* 69(18), 567.
- Hedman, C.W. 1992. Southern Appalachian riparian zones: their vegetative composition and contributions of large woody debris to streams (*Rhododendron*, *Tsuga*, *Castanea Dentata*). Unpubl. PhD. Dissertation. Clemson University.
- Heede, B.H. 1972. Influences of a forest on the hydraulic geometry of two mountain streams. *Water Resources Bulletin*, 8, 523-530.
- Henderson, J., D. Peter, and R. Leshner. 1986. Preliminary plant associations of the Olympic National Forest. USDA, Forest Service, Pacific Northwest Region, Olympic National Forest.
- Henderson, J.A., D.H. Peter, R.D. Leshner, and D.C. Shaw. 1989. Forested plant associations of the Olympic National Forest. USDA Forest Service Technical Paper R6-ECOL-TP001-88.
- Heusser, C.J. 1972. Palynology and phytogeographical significance of a late-Pleistocene refugium near Kalaloch, Washington. *Quaternary Research*, 2, 189-201.

- Heusser, C.J. 1974. Quaternary vegetation, climate and glaciation of the Hoh River valley, Washington. *Geological Society of America Bulletin*, 85, 1547-1560.
- Hickin, E.J. 1984. Vegetation and river channel dynamics. *Canadian Geographer* 28. 111-126.
- Hoerner, S.F. 1951. *Fluid Dynamic Drag*. Published by the author. Trenton, NJ.
- Hoerner, S.F. 1965. *Fluid-Dynamic Drag*. Published by the author. Midland Park, New Jersey.
- Hogan, D.L. 1987. The influence of large organic debris on channel recovery in the Queen Charlotte Islands, British Columbia, Canada. In R.L. Beschta, T. Blinn, G.E. Grant, F.J. Swanson, and G.G. Ice, editors, *Erosion and Sedimentation in the Pacific Rim*. IAHS Publication No.165, 343-353.
- Hogan, D.L., S.A. Bird, and M. Hassan. 1995. Spatial and temporal evolution of small coastal gravel-bed streams: the influence of forest management on channel morphology and fish habitats. Paper presented at Gravel-Bed Rivers IV Symposium. Gold Bar, WA (unpublished manuscript).
- Huff, M.A. 1995. Forest age structure and development following wildfires in the western Olympic Mountains, Washington. *Ecological Applications* 5, 471-483.
- Hupp, C.R. 1999. Relations among riparian vegetation, channel incision processes and forms, and large woody debris. In S.E. Darby and A. Simon, editors. *Incised river channels; processes, forms, engineering and management*. John Wiley & Sons. Chichester, UK, 219-245.
- Ishikawa, Y. 1989. Studies on disasters caused by debris flows carrying floating logs down mountain streams. Unpublished draft report. Kyoto University. Kyoto, Japan.
- Johnson, A.C. 1991. Effects of Landslide-Dam-Break Floods on Channel Morphology. M.S. Thesis. College of Forest Resources, Univ. of Washington, Seattle.
- Kanes, W.H. 1970. Facies and development of the Colorado River Delta in Texas. In J.P. Morgan and R.H. Shaver, Editors. *Deltaic Sedimentation Modern and Ancient*. Special Publication No.15. Society of Economic Paleontologists and Mineralogists. Tulsa, OK, 78-106.
- Keller, E.A. and F.J. Swanson. 1979. Effects of large organic material on channel form and fluvial processes. *Earth Surface Processes*, 4, 361-380.

- Keller, E.A. and T. Tally. 1979. Effects of large organic debris on channel form and fluvial processes in the coastal Redwood environment. In D.D. Rhodes and G.P. Williams, Editors, *Adjustments of the Fluvial System, Proceedings of the 10th Annual Binghamton Geomorphology Symposium*. Kendall-Hunt, Dubuque, IA, 169-197.
- Kennedy, J.F. 1969. The formation of sediment ripples, dunes, and antidunes. In W.R. Sears, Editor, *Annual Review of Fluid Mechanics, Vol.1, Annual Reviews, Inc.* Palo Alto, CA. 147-168.
- Kirk, R. and J.F. Franklin. 1992. *The Olympic Rainforests: an ecological web*. University of Washington Press, Seattle, Washington, 128.
- Knighton, D. 1998. *Fluvial forms & processes: a new perspective*. Arnold. London, UK.
- Kochel, R.C., D.F. Ritter, and J. Miller. 1987. Role of tree dams in the construction of pseudo-terraces and variable geomorphic response to floods in Little River valley, Virginia. *Geology* 15, 718-721.
- Komar, P.D. 1987. Selective grain entrainment and the empirical evaluation of flow competence. *Sedimentology*, 34, 1165-1176.
- Kwan, R.T.F. and B.W. Melville. 1994. Local scour and flow measurements at bridge abutments. *Journal of Hydraulic Research*, 32, 661-673.
- Lai, K.Y.M. and A.H. Makomaski. 1989. Three-dimensional flow pattern upstream of a surface-mounted rectangular obstruction. *Journal of Fluids Engineering (ASME)*, 111, 449-456.
- Laursen, E.M. 1963. Analysis of relief bridge scour. *Proceedings of the American Society of Civil Engineers*, 89(HY3), 93-118.
- Leopold, L.B., M.G. Wolman, and J.P. Miller. 1964. *Fluvial Processes in Geomorphology*. San Francisco, CA. W. H. Freeman.
- Lewin, J. 1978. Floodplain geomorphology. *Progress in Physical Geography* 2, 408-437.
- Lienkaemper, G. W. and F. J. Swanson. 1987. Dynamics of large woody debris in streams in old-growth Douglas-fir forests. *Canadian Journal of Forest Research*, 17, 150-156.
- Limerinos, J.T. 1970. Determination of the Mannings coefficient from measured bed roughness in natural channels. *US Geological Survey Water Supply Paper 1898-B*.

- Lincoln, W.A. 1986. *World Woods in Color*. Linden Publishing Inc. Resno, CA.
- Lisle, T.E. 1986. Stabilization of a gravel channel by large streamside obstructions and bedrock bends, Jacoby Creek, northwestern California. *Geological Society of America Bulletin*, 97, 999-1011.
- Lisle, T.E. 1989. Using 'residual depths' to monitor pool depths independently of discharge. USDA For. Serv. Res. note PSW-394, Pacific Southwest Exp. Station, Berkeley, CA.
- Liu, H.K., K.M. Chang, and M.M. Skinner. 1961. Effect of bridge constriction in scour and backwater. Colorado State University Engineering Research Center Report CER60HKL22, Fort Collins, Colorado.
- Lowrey, W.M. 1968. The Red, In Davis, E.A., *The Rivers and Bayous of Louisiana*, Louisiana Education Research Association, Baton Rouge, LA, 53-73.
- Lyell, C. 1830. *Principles of Geology, Volume I*. John Murray London, UK (published in 1990 by University of Chicago Press. Chicago, IL.
- Mackin, J.H. 1948. Concept of the graded river. *Geological Society of America Bulletin* 59, 463-512.
- Malanson, G.P. 1993. *Riparian Landscapes*. Cambridge University Press. Cambridge, UK.
- Malanson, G.P. and D.R. Butler. 1990. Woody debris, sediment, and riparian vegetation of a subalpine river, Montana, U.S.A. *Arctic and Alpine Res.* 22(2), 183-194.
- Manci, K.M. 1989. Riparian ecosystem creation and restoration: a literature summary. U.S. Fish and Wildlife Service Biological Report 89(20), 59.
- Mangelsdorf, J., K. Scheurmann, and F. Weiss. 1989. *River morphology: a guide for geoscientists and engineers*. Berlin. Springer-Verlag.
- Marston, R.A. 1982. The geomorphic significance of log steps in forested streams. *Annals of the Association of American Geographers* 72, 99-108.
- McCall, E. 1984. *Conquering the Rivers*. Louisiana State Univ. Press. Baton Rouge, LA.
- McDade, M.H., F.J. Swanson, W.A. McKee, J.F. Franklin, and J. Van Sickle. 1990. Source distances for coarse woody debris entering small streams in western Oregon and Washington. *Canadian Journal of Forest Research* 20, 326-330.

- McKee, A., G. LaRoi, and J.F. Franklin, 1984, Structure, composition, and reproductive behavior of terrace forests, South Fork Hoh River, Olympic National Park. In Starkey, E.E., J.F. Franklin, and J.W. Matthews, Editors, *Ecological Research in National Parks of the Pacific Northwest*. Oregon State Univ. Forest Res. Lab. Publ., Corvallis, OR, 22-29.
- McKenney, R., R.B. Jaconson, and R.C. Wertheimer. 1995. Woody Vegetation and Channel Morphogenesis in Low-gradient, Gravel-bed Streams in the Ozark Plateaus, Missouri and Arkansas. *Geomorphology* 13. 175-198.
- Mean, J.E., K Cromack Jr., and P.C. MacMillan. 1986. Comparison of decomposition models using wood density of Douglas Fir logs. *Canadian Journal of Forest Research* 15, 1092-1098.
- Miller, A.J. 1995. Valley morphology and boundary conditions influencing spatial patterns of flood flow. In: J.E. Costa, A.J. Miller, K.W. Potter, and P.R. Wilcock (Editors). *Natural and Anthropogenic Influences in Fluvial Geomorphology*. American Geophysical Union Geophysical Monograph 89, 57-81.
- Montgomery, D.R., T.B. Abbe, J.M. Buffington, N.P. Peterson, K.M. Schmidt, and J.D. Stock. 1996. Distribution of bedrock and alluvial channels in forested mountain drainage basins, *Nature*, 381, 587-589.
- Montgomery, D.R. and J.M. Buffington. 1993. Channel classification, prediction of channel response, and assessment of channel condition. Washington State Department of Natural Resources Report TFW-SH10-93-002, Olympia, Washington.
- Montgomery, D.R. and J.M. Buffington. 1997. Channel reach morphology in mountain drainage basins. *Geological Society of America Bulletin*, 109, 596-611.
- Montgomery, D.R., J.M. Buffington, R.D. Smith, K.M. Schmidt, and G.R. Pess. 1995. Pool frequency in forest channels. *Water Resources Research*, 31, 1097-1105.
- Morgan, M.C. 1955. *The Last Wilderness*. University of Washington Press. Seattle, WA.
- Morisawa, M. 1968. *Streams; their dynamics and morphology*. New York, NY. McGraw-Hill.
- Muir, J. 1878. The new sequoia forests of California. *Harpers New Monthly Magazine* 57, 813-827.

- Myers, J. J., C. H. Holm, and R. F. McAllister. 1969. *Handbook of Ocean and Underwater Engineering*. Under auspices of the North American Rockwell Corporation. McGraw-Hill. New York.
- Nakamura, F. and F.J. Swanson. 1993. Effects of coarse woody debris on morphology and sediment storage of mountain stream system in western Oregon. *Earth Surface Processes and Landforms*, 18, 43-61.
- Nakamura, F. and F.J. Swanson. 1994. Distribution of coarse woody debris in a mountain stream, western Cascade Range, Oregon. *Canadian Journal of Forest Research*, 24, 2395-2403.
- Nanson, G.C. 1981. New evidence of scroll-bar formation on the Beatton River. *Sedimentology*, 28, 889-891.
- Nanson, G.C., Barbetti, M., and Taylor, G. 1995. River stabilization due to changing climate and vegetation during the late Quaternary in western Tasmania, Australia. *Geomorphology* 13, 145-158.
- National Research Council. 1992. *Restoration of Aquatic Ecosystems*. National Academy Press, Washington, D.C.
- Newnham, R.M. 1965. Stem Form and the Variation of Taper With Age and Thinning Regime. *Forestry* 38(2), 218-224.
- Nichols, H.L.Jr. 1976. *Moving the Earth: The Workbook of Excavation*. North Castle Books. Greenwich, CT.
- Nikuradse, J. 1933. *Laws for flows in rough pipes (translated from German)*. NACA Technical Memo.1292.
- NOAA (National Oceanic and Atmospheric Administration). 1978. *Climate of Washington*. *Climatology of the United States* No. 60. Washington D.C.
- Norse, E.A. 1990. *Ancient Forests of the Pacific Northwest*. Island Press. Covelo, CA.
- O'Connor, M.D. 1994. *Sediment transport in steep tributary streams and the influence of large organic debris*. Unpubl. Ph.D. dissertation. University of Washington. Seattle, WA.
- Onda, Y. and Y. Matsukura. 1997. Mechanism for the instability of slopes composed of granular materials. *Earth Surface Processes and Landforms*, 22, 401-411.

- Outwater, A. 1996. *Water, A Natural History*. Harper Collins Publishers, Inc. New York, 212 p.
- Pacific Meridian Resources. 1997. *Vegetation and Landform Database Development* (based on digital Landsat Thematic Mapper (TM) satellite imagery and field surveys). Final report submitted to Pacific Northwest Region of the U.S. National Park Service. Seattle, WA. Courtesy of Roger Hoffman, Olympic National Park, Port Angeles, WA.
- Parker, G. and P.C. Klingeman. 1982. On why gravel-bed streams are paved. *Water Resources Research*, 18, 1409-1423.
- Petryk, S. and G. Bosmajian. 1975. Analysis of flow through vegetation. *Journal of the Hydraulics Division, Proceedings of the American Society of Civil Engineers*, H7, 871-884.
- Philips, E.L. and W.R. Donaldson. 1972. Washington climate for these counties: Clallam, Grays Harbor, Jefferson, Pacific and Wahkiakum. Cooperative Extension Service Publication EM 3708. Washington State University, Pullman, WA.
- Phillips, J.D. and G.R. Holder. 1991. Large organic debris in the lower Tar River, North Carolina, 1879-1900. *Southeastern Geographer*, Vol. 31(2), 55-66.
- Phipps, R.L. 1985. Collecting, preparing, crossdating, and measuring tree increment cores. U.S. Water Resources Investigations Report 85-4148. Washington D.C.
- Pitlick, J. 1992. Flow resistance under conditions of intense gravel transport. *Water Resources Research*, 28, 891-903.
- Putz, F.E., P.D. Coley, K. Lu, A. Montalvo, and A. Aiello. 1983. Uprooting and snapping of trees: structural determinants and ecological consequences. *Canadian Journal of Forest Research*, 13, 1011-1020.
- Ramamurthy, A.S. and C.P. Ng. 1973. Effect of blockage on steady force coefficients. *Journal of the Engineering Mechanics Division, Proceedings of the American Society of Civil Engineers*, 99, 755-772.
- Rankin, D. 1980. Tress and Rivers. *Journal of the Soil conservation Service of New South Wales* 36, 129-133.
- Raudkivi, A.J. 1990. *Loose Boundary Hydraulics*. Pergamon Press, Oxford.

- Raudkivi, A.J. and R. Ettema. 1977. Effect of sediment gradation on clear water scour. *Proceedings of the American Society of Civil Engineering*, 103(HY10), 1209-1213.
- Reid, L. 1981. Sediment production from gravel-surfaced forest roads, Clearwater Basin, Washington. Report FRI-UW-8108. Fisheries Research Institute. University of Washington, Seattle, WA.
- Rice, S. 1994. Towards a model of changes in bed material texture at the drainage basin scale. In Kirkby, M.J., Editor. *Process Models and Theoretical Geomorphology*. John Wiley & Co, Inc., 159-172.
- Richards, K.S. 1982. *Rivers, form and process in alluvial channels*. London, UK. Methuen.
- Richmond, A.D. 1994. *Characteristics and Function of Large Woody Debris in Mountain Streams of Northern Colorado*. Unpublished Master Thesis, Department of Fishery and Wildlife Biology, Colorado State Univ., Fort Collins, CO.
- Roberts, B.W. 1980. Drag and pressure distribution on a family of porous, slotted disks. *Journal of Aircraft*, 17, 393-401.
- Roshko, A. 1993. Perspectives on bluff-body aerodynamics. *Journal of Wind Engineering and Industrial Aerodynamics* 49, 79-100.
- Rouse, H. 1946. *Elementary Mechanics of Fluids*. John Wiley & Sons, London.
- Ruffner, E.H. 1886. *The practice of the improvement of the non-tidal rivers of the United States, with an examination of the results thereof*. John Wiley & Sons. New York.
- Russell, I.C. 1909. *Rivers of North America*. G.P. Putnam's Sons, New York.
- Schumm, S.A. 1977. *The fluvial system*. New York, NY. Wiley.
- Sedell, J.R., P.A. Bisson, F.T. Swanson, and S.V. Gregory. 1988. What we know about trees that fall into streams and rivers. In Maser, C., R.F. Tarrant, J.M. Trappe, and J.F. Franklin (Eds.), *From the forest to the sea: story of fallen trees*, USDA For. Serv. Gen. Tech. Report PNW-GTR-229, Pacific Northwest Forest and Range Exp. Station, Portland, Oregon.

- Sedell, J.R. and J.L. Frogatt. 1984. Importance of streamside forests to large rivers: the isolation of the Willamette River, Oregon, U.S.A., from its floodplain by snagging and streamside forest removal. *Verhandlungen-Internationale Vereinigung für Theoretische und Angewandte Limnologie*, 22, 1828-1834.
- Sedell, J.R. and K.J. Luchessa. 1982. Using the historical record as an aid to salmonid habitat enhancement. In Armantrout, N.B. (Ed.), *Acquisition and utilization of aquatic habitat inventory information, Proceedings of a Symposium October 28-30, 1981*, The Hague Publishing, Billings, Montana, 222-245.
- Sedell, J.R., F.J. Swanson, and S.V. Gregory. 1984. Evaluating fish response to woody debris. In Hassler, T.J. (Ed.), *Proceedings of the Pacific Northwest Streams Habitat Management Workshop, American Fisheries Society, Humbolt State University, Arcata, California*, 191-221.
- Seno, K., T. Mizuyama, A. Ohba, and S. Uehara. 1984. Movement of logs in debris flow and log-traps. *Civil Engineering Journal*, 26, 9-13.
- Shepard, F.P. and D.G. Moore. 1960. Bays of central Texas coast. In F.P. Shepard, F.B. Phleger, and T.H. VanAndel, Editors. *Recent Sediments, Northwest Gulf of Mexico* American Association of Petroleum Geologists, 117-152.
- Shields, A. 1936. *Anwendung der Ähnlichkeitsmechanik und der Turbulenzforschung auf die Geschiebebewegung*. Translated by W.P. Ott and J.C. van Uchelen, California Institute of Technology, Pasadena, California.
- Shields, F.D. and N.R. Nunnally. 1984. Environmental aspects of clearing and snagging, *Journal of Environmental Engineering*, 110, 152-165.
- Shoecraft, R.P. 1875. Map of Township No. 31 North, Range No. 5 East, Willamette Meridian, Washington Territory. U.S. Bureau of Land Management, Plates of Washington Territory.
- Smith, R.D. 1990. Stream flow and bedload transport in an obstruction - affected, gravel-bed stream. Unpubl. Ph.D. thesis. Oregon State University. Corvallis, OR.
- Southard, J.B. 1971. Representation of bed configurations in depth-velocity-size diagrams. *Journal of Sedimentary Petrology* 41, 903-915.
- Stuiver, M. and P.J. Reimer. 1993. Extended ^{14}C data base and revised CALIB ^{14}C age calibration program. *Radiocarbon* 35, 215-230.

- Swanson, F.J. and G.W. Lienkaemper. 1978. Physical consequences of large organic debris in Pacific Northwest streams. USDA For. Serv. Gen. Tech. Report PNW-69, Pacific Northwest Forest and Range Exp. Station, Portland, Oregon.
- Swanson, F.J. and G.W. Lienkaemper. 1980. Interactions among fluvial processes, forest vegetation, and aquatic ecosystems, South Fork Hoh River, Olympic National Park, Washington. In Proceedings of the Second Conference on Scientific Research in the National Parks, 1979. U.S. Department of the Interior PB81-100083, Washington D.C., 23-34.
- Swanson, F.J. and G.W. Lienkaemper. 1984. Interactions among fluvial processes, forest vegetation, and aquatic ecosystems, South Fork Hoh River, Olympic National Park. In E.E. Starkey, J.F. Franklin, and J.W. Matthews, Editors. Proceedings of the second conference on scientific research in the National Parks. Oregon State Univ. Forest Research Lab. Publ., Corvallis, OR. 30-34.
- Swanston, D.N. 1991. Natural processes. In W.R. Meehan, Editor, Influences of Forest and Rangeland Management on Salmonid Fishes and Their Habitats. American Fisheries Society Special Publication 19, Bethesda, MD, 139-179.
- Swift, B.L. 1984. Status of riparian ecosystems in the United States. Water Resources Bulletin 20, 223-228.
- Tabor, R.W. 1987. Geology of Olympic National Park. Pacific Northwest Parks & Forests Association, Seattle, Washington.
- Tabor, R.W. and W.M. Cady. 1978. Geologic Map of the Olympic Peninsula. U.S. Geological Survey Miscellaneous Investigations Series Map I-994. Scale 1:125,000.
- Tally, T. 1980. The effects of geology and large organic debris on stream channel morphology and process for streams flowing through old-growth Redwood forests in Northwestern California. Unpublished Ph.D. dissertation. University of California. Santa Barbara, CA.
- Tarzwel, C.M. 1934. The purpose and value of stream improvement method. Stream Improvement Bulletin R-4. Presented at the Annual Meeting of the American Fisheries Society. Ogden, Utah.
- Tey, C.B. 1984. Local scour at bridge abutments. Master of Engineering Thesis, Department of Civil Engineering Report No.329. University of Auckland, New Zealand.

- Thackray, G.D. 1996. Glaciation and neotectonic deformation on the western Olympic Peninsula, Washington. Unpubl. Ph.D. thesis. Department of Geological Sciences. University of Washington. Seattle, WA.
- Thackray, G.D. and F.J. Pazzaglia. 1994. Quaternary stratigraphy, tectonic geomorphology, and fluvial evolution of the western Olympic Peninsula, Washington. In D.A. Swanson and R.A. Haugerud, editors. *Geologic Field Trips in the Pacific Northwest*. Geological Society of America. Denver, CO, 2A1 - 2A30.
- Thompson, D. 1995. The effects of large organic debris on sediment processes and stream morphology in Vermont. *Geomorphology* 11, 235-244.
- Toews, D.A. and Moore, M.K. 1982. The effects of streamside logging on large organic debris in Carnation Creek. Land Management Report 11, Ministry of Forests, Province of British Columbia, Victoria, British Columbia.
- Triska, F.J. 1984. Role of wood debris in modifying channel morphology and riparian areas of a large lowland river under pristine conditions: a historical case study. *Verhandlungen-Internationale Vereinigung für Theoretische und Angewandte Limnologie* 22, 1876-1892.
- Triska, F.J. and K.Jr. Cromack. 1979. The role of wood debris in forests and streams. In R.H. Waring, *Forests: Fresh Perspectives from Ecosystem Analysis, Proceedings of the 40th Annual Biology Colloquium*. Oregon State Univ. Press, Corvallis, OR, 171-190.
- Triska, F.J. and K. Cromack. 1980. The role of wood debris in forests and streams. In R.H. Waring, Editor. *Fresh Perspectives in Ecosystem Analysis*. Oregon State University Press. Corvallis, OR, 171-190.
- Tuomi, R. L., R. W. Wolfe, R. C. Moody, and F. W. Muchmore. 1979. Bending strength of large Alaska Sitka Spruce and Western Hemlock log bridge stringers. Forest Products Laboratory Research Paper FPL 341. U.S. Department of Agriculture.
- U.S. Army. 1947. Normal Annual Isohyetal Map, Olympic and Cascade Drainage Basins, Washington. 1:500,000. Army Corps of Engineers, Seattle District. Seattle, WA. File No. D-11-13-16.1.
- USGS. 1990. 7.5' Topographic Quadrangles: Queets, WA. Salmon River West, Salmon River East, Klochman Rock, Kimta Peak. US Geological Survey. Reston, VA.

- USGS. 1933. Topographic map and profile of the Queets River to determine possible dam sites. US Geological Survey. Washington D.C. 3 Plates.
- Van Pelt, R. 1994. Washington big tree program. College of Forest Resources. University of Washington. Seattle, WA.
- Van Sickle, J. and S.V. Gregory. 1990. Modeling inputs of large woody debris to streams from falling trees. *Canadian Journal of Forest Research*, 20, 1593-1601.
- Vannotte, R.L., G.W. Minshall, K.W. Cummins, J.R. Sedell, and C.E. Cushing. 1980. The river continuum concept. *Canadian Journal of Fisheries and Aquatic Science*, 37, 130-137.
- Veatch, A. C. 1906. Geology and underground water resources of Northern Louisiana and Southern Arkansas. Washington D.C. United States Geological Survey Professional Paper 46.
- Wallerstein, N., C.R. Thorne, and M.W. Doyle. 1997. Spatial distribution and impact of large woody debris in Northern Mississippi. In Wang, C.C., E.J. Langendoen, and F.D. Shields (Editors). *Proceedings of the Conference on Management of Landscapes Disturbed by Channel Incision*. Univ. of Mississippi. Oxford, MI, 145-150.
- Weigand, J., A. Mitchell, and D. Morgan. 1992. Coastal temperate rainforests: ecological characteristics, status and distribution worldwide. *Ecotrust Occasional Paper Series No.1*. Ecotrust. Portland, OR.
- Whiting, P. J. and W.E. Dietrich. 1990. Boundary shear stress and roughness over mobile alluvial beds. *Journal of Hydraulic Engineering*, 116(12), 1495-1511.
- Whitlock, C. 1992. Vegetational and climatic history of the Pacific Northwest during the last 20,000 years: implications for understanding present-day biodiversity. *The Northwest Environmental Journal* 8, 5-28.
- Wiberg, P.L. and J.D. Smith. 1987. Calculations of the critical shear stress for motion of uniform and heterogeneous sediment. *Water Resources Research*, 23, 1471-1480.
- Wigmosta, M. S. 1983. Rheology and flow dynamics of the Toutle debris flows from Mt. St. Helens. Unpubl. M.S. thesis. Department of Geological Sciences, University of Washington. Seattle.
- Williamson, C.H.K., Wu, J., and Sheridan, J. 1995. Scaling of streamwise vortices in wakes. *Physics of Fluids* 7, 2307-2309.

- Wiślicki, A. 1969. The Bulldozer-Tracklayer-Soil system (Współzależność parametrów lemieszka I zespołu jezdnego spycharki oraz warunków gruntowych). Institute for Organization and Mechanization of the Building Industry. Warszawa (Warsaw), Poland. 85p. English translation by Jerzy Bachrach published by the Foreign Scientific Publications Department of the National Center for Scientific, Technical and Economic Information. U.S. Department Commerce. National Technical Information Service No. TT 77-54048. Springfield, VA.
- Wolff H. H. 1916. The design of a drift barrier across the White River, near Auburn, Washington. Transactions of the American Society of Civil Engineers 16, 2061-2085.
- Wolman, M.G. 1954. A method of sampling coarse river-bed material. EOS, Transactions of the American Geophysical Union, 35, 951-956.
- Wolman, M.G. and Leopold, L.B. 1957. River flood plains: some observations on their formation. Washington D.C. U.S. Geological Survey Professional Paper 282-C.
- Zimmerman, R.C., J.C. Goodlett, and G.H. Comer, 1967. The influence of vegetation on channel form of small streams, Symposium on River Morphology, Inter. Assoc. Scien. Hydrology Publication, Gentbrugge, Belgium 75, 255-275.
- Zimmermann, M.H. and C.L. Brown. 1971. Tress, Structure and Function. Springer-Verlag. New York.

Vita

Timothy B. Abbe

Ph.D., Department of Geological Sciences, University of Washington, Seattle, WA 1998.

Dissertation title: Patterns, Mechanics and Geomorphic Effects of Wood Debris Accumulations in a Forest River System.

M.S., Geology Department, Portland State University, Portland, OR. 1989. Thesis title:

Sediment dynamics on the shore slopes of the Puget Island Reach of the Lower Columbia River, Oregon and Washington.

B.S., Geology Department, University of Vermont, Burlington, VT. 1984.

Other publications

Abbe, T.B., Montgomery, D.R., and Petroff, C. 1997. Design of stable in-channel wood debris structures for bank protection and habitat restoration: an example from the Cowlitz River, WA. Wang, C.C.Y., Langendoen, E.J., and Shields, F.D. (Eds.), *Proceedings of the Conference on Management of Landscapes Disturbed by Channel Incision.*, Center for Computational Hydroscience and Engineering, University of Mississippi, pp.409-414.

Abbe, T.B. and D.R. Montgomery. 1996. Floodplain and terrace formation in forested landscapes. *GSA Abstracts and Program*, Annual Cordilleran Meeting, Portland, OR. April 23. p.41.

Abbe, T.B. and Montgomery, D.R. 1996. Large Woody Debris Jams, Channel Hydraulics, and Habitat Formation in Large Rivers. *Regulated Rivers Research and Management*, Vol. 12, pp. 201-221.

Abbe, T., E.Andrews, and P. Faber, 1991. The physical evolution of a wetland restoration. ASCE Coastal Zone 91 Conference Proceedings. Paper No. 244. Long Beach, CA.

Abbe, T., P. Goodwin, and P.B. Williams. 1991. Marsh erosion by wave action. ASCE Coastal Zone 91 Conference Proceedings, Paper No. 245. Long Beach, CA.

Abbe, T. and K. Eriksen. 1989. Shallow water sand transport by ship waves. Coastal 89 Proc., ASCE, Charleston, SC, no.226.